

# Perturbative and non-perturbative aspects of RG flows in quantum field theory

THÈSE N° 7189 (2016)

PRÉSENTÉE LE 21 SEPTEMBRE 2016  
À LA FACULTÉ DES SCIENCES DE BASE  
LABORATOIRE DE PHYSIQUE THÉORIQUE DES PARTICULES  
PROGRAMME DOCTORAL EN PHYSIQUE

ÉCOLE POLYTECHNIQUE FÉDÉRALE DE LAUSANNE

POUR L'OBTENTION DU GRADE DE DOCTEUR ÈS SCIENCES

PAR

Lorenzo VITALE

acceptée sur proposition du jury:

Prof. V. Savona, président du jury  
Prof. R. Rattazzi, Prof. V. Rychkov, directeurs de thèse  
Prof. A. Schwimmer, rapporteur  
Prof. Z. Bajnok, rapporteur  
Prof. J. Penedones, rapporteur



ÉCOLE POLYTECHNIQUE  
FÉDÉRALE DE LAUSANNE

Suisse  
2016



# Acknowledgements

I would like to thank my supervisor Riccardo Rattazzi, not only for directing my thesis work, but also for genuinely caring about my personal development as a scientist.

I am extremely grateful to my co-supervisor Slava Rychkov, to whom I owe a significant part of what I learned during the last three years, for proposing me to work on the interesting topic of numerical methods in quantum field theory, and for mentoring me throughout our collaboration.

My period in Lausanne has been not so terrible, thanks to all the wonderful friends, PhD students, and postdocs I met here, whom I cannot mention in full. Among them, I cannot thank enough Giorgos, my friend, colleague and roommate, for being always supportive and ready to listen any time I needed it. The same goes for Davide, with whom I could share the ups and downs of the Ph.D. My special thanks go also to Boaz, David S., Javier, Matteo, Elodie, Rakhi, Themos, Marcella, Bernardo and Lea, who, I feel, had a particular influence on me, in a way or another. I also thank my old friends from Bari and Padova, Ciccio, Luca, Andrea, Pietro and Daniele.

Finally, I thank my family for the unconditional love they continue to give me, despite the distance that separates us.



# Abstract

This thesis explores two aspects of the renormalization group (RG) in quantum field theory (QFT).

In the first part we study the structure of RG flows in general Poincaré-invariant, unitary QFTs, and in particular the irreversibility properties and the relation between scale and conformal invariance. Within the formalism of the local Callan–Symanzik equation, we derive a series of results in four and six-dimensional QFTs. Specifically, in the four dimensional case we revisit and complete existing proofs of the  $a$ -theorem and of the equivalence between scale and conformal invariance in perturbation theory. We then present an original derivation of similar results in six-dimensional QFTs.

In the second part we present the Hamiltonian Truncation method and study its applicability to the numerical solution of non-perturbative RG flows. We test the method in the  $\lambda\phi^4$  model in two dimensions and show how it can be used to make quantitative predictions for the low-energy observables. In particular, we calculate the numerical spectrum and estimate the critical coupling at which the theory becomes conformal. We also compare our results to previous estimates. The main original ingredient of our analysis is an analytic renormalization procedure used to improve the numerical convergence.

We then adapt the method in order to treat the strongly-coupled regime of the model where the  $\mathbb{Z}_2$  symmetry is spontaneously broken. We reproduce perturbative and non-perturbative observables and compare our results with analytical predictions.

This thesis is based on the results presented in Refs. [1, 2, 3, 4].

**Keywords:** Quantum field theory, Renormalization group,  $a$ -theorem, Weyl anomaly, local Callan–Symanzik equation, Hamiltonian truncation



# Riassunto

In questa tesi si esaminano due aspetti del gruppo di rinormalizzazione in teoria quantistica di campo (QFT).

Nella prima parte si studia la struttura dei flussi di rinormalizzazione in generiche teorie di campo unitarie e invarianti di Poincaré, e nello specifico le proprietà di irreversibilità e la relazione tra invarianza di scala e conforme. Usando il formalismo dell'equazione di Callan–Symanzik locale, si derivano una serie di risultati sulle teorie quantistiche di campo in quattro e in sei dimensioni. In particolare, nel caso quadridimensionale si riesaminano e completano delle dimostrazioni esistenti del teorema “*a*” e dell'equivalenza tra invarianza di scala e conforme. Infine, viene presentata una dimostrazione originale di risultati analoghi in teorie di campo quantistiche in sei dimensioni.

Nella seconda parte viene introdotto il metodo di Troncamento Hamiltoniano, e si studia la sua applicabilità alla soluzione numerica di flussi di rinormalizzazione fortemente accoppiati. Il metodo viene testato sul modello  $\lambda\phi^4$  in due dimensioni e si dimostra la sua capacità di fare predizioni accurate per le osservabili di bassa energia. In particolare, si calcola lo spettro numerico e viene stimato l'accoppiamento critico tale che la teoria diventa conforme. Inoltre, i risultati numerici ottenuti vengono confrontati con stime precedenti. La novità principale della nostra analisi consiste in una procedura di rinormalizzazione analitica, che permette di migliorare la convergenza numerica.

Infine, si adatta il metodo allo studio del regime fortemente accoppiato dello modello  $\lambda\phi^4$ , dove la simmetria  $\mathbb{Z}_2$  è rotta spontaneamente. Vengono riprodotte osservabili perturbative e non perturbative, che si confrontano con predizioni analitiche.

Questa tesi si basa sui risultati ottenuti in [1, 2, 3, 4].

**Parole chiave:** Teoria quantistica di campo, Gruppo di rinormalizzazione, teorema “*a*”, anomalia di Weyl, equazione di Callan–Symanzik locale, Troncamento Hamiltoniano





# Contents

Acknowledgements	i
Abstract (English/Italiano)	iii
List of figures	xi
Introduction	1
<b>I The structure of RG flows</b>	<b>5</b>
1 Preliminaries	7
<b>2 The local Callan–Symanzik equation</b>	<b>13</b>
2.1 Introduction . . . . .	13
2.2 The local Callan–Symanzik equation . . . . .	16
2.2.1 General set-up . . . . .	16
2.2.2 The structure of Weyl symmetry . . . . .	19
2.2.3 The structure of the Weyl anomaly . . . . .	30
2.3 Weyl consistency conditions and gradient flows . . . . .	35
<b>3 Constraining RG flows in four dimensions</b>	<b>39</b>
3.1 Correlation functions of $T$ off-criticality . . . . .	39
3.1.1 The dilaton effective action . . . . .	39
3.1.2 Computation of $\Gamma_{local}$ . . . . .	43
3.1.3 Computation of $\Gamma_{non-local}$ . . . . .	44
3.1.4 Correlators of $T$ and the constraints on the RG flow . . . . .	46
3.2 Discussion . . . . .	51
<b>4 Constraining RG flows in six dimensions</b>	<b>55</b>
4.1 Introduction . . . . .	55
4.2 Wess–Zumino consistency conditions . . . . .	56
4.3 Irreversibility . . . . .	58
4.4 Discussion . . . . .	60

<b>II</b>	<b>Exact diagonalization methods</b>	<b>63</b>
<b>5</b>	<b>Hamiltonian truncation</b>	<b>65</b>
5.1	Introduction . . . . .	65
5.2	The problem and the method . . . . .	67
5.2.1	Hamiltonian . . . . .	67
5.2.2	Truncation . . . . .	70
5.3	UV cutoff dependence and renormalization . . . . .	72
5.3.1	General remarks . . . . .	72
5.3.2	Computation of $\Delta H$ . . . . .	74
5.3.3	Renormalization procedures . . . . .	79
5.3.4	A test for the $\phi^2$ perturbation . . . . .	82
5.4	Study of the $\phi^4$ theory . . . . .	84
5.4.1	Varying $g$ . . . . .	85
5.4.2	The critical point . . . . .	87
5.4.3	$L$ dependence . . . . .	89
5.4.4	$E_{\max}$ dependence . . . . .	92
5.4.5	Comparison to the TCSA methods . . . . .	94
5.5	Comparison with prior work . . . . .	95
5.5.1	DLCQ . . . . .	96
5.5.2	QSE diagonalization . . . . .	97
5.5.3	DMRG . . . . .	97
5.5.4	Lattice Monte Carlo . . . . .	98
5.5.5	Uniform matrix product states . . . . .	101
<b>6</b>	<b>Hamiltonian truncation in the <math>\mathbb{Z}_2</math>-broken phase</b>	<b>103</b>
6.1	The Chang duality . . . . .	103
6.1.1	Formulation and consequences . . . . .	103
6.1.2	Review of the derivation . . . . .	105
6.1.3	Numerical check of the duality . . . . .	106
6.2	The $\mathbb{Z}_2$ -broken phase . . . . .	108
6.2.1	Modified zero mode treatment . . . . .	108
6.2.2	Varying the normal-ordering mass . . . . .	110
6.2.3	Results . . . . .	112
6.3	Conclusions . . . . .	116
<b>7</b>	<b>Discussion and outlook</b>	<b>119</b>
<b>III</b>	<b>Appendix</b>	<b>121</b>
<b>A</b>	<b>Local CS equation in <math>d = 4</math></b>	<b>123</b>
A.1	Definitions and useful equations . . . . .	123
A.1.1	Notations . . . . .	123

A.1.2	Lie derivatives . . . . .	124
A.1.3	Gravitational terms and their Weyl variations . . . . .	125
A.1.4	Weyl Variations of dimensionful functions of the sources . . . . .	125
A.2	Weyl symmetry in a regulated theory . . . . .	125
A.2.1	The variation of $\lambda^I$ . . . . .	127
A.2.2	The variation of $A_\mu^A$ . . . . .	128
A.2.3	Dim 2 operators . . . . .	129
A.2.4	Consistency conditions for the anomaly coefficients . . . . .	129
A.3	Unitarity and anomalous dimensions of currents . . . . .	130
A.4	The consistency conditions for the Weyl anomaly . . . . .	132
<b>B</b>	<b>Local CS equation in <math>d = 6</math></b>	<b>135</b>
B.1	Derivation of the consistency conditions . . . . .	135
B.2	Conventions and basis for the anomaly . . . . .	135
<b>C</b>	<b>Perturbative checks of Hamiltonian truncation</b>	<b>139</b>
C.1	$\mathbb{Z}_2$ -unbroken phase . . . . .	139
C.2	$\mathbb{Z}_2$ -broken phase . . . . .	140
<b>D</b>	<b>Computational details for the Hamiltonian truncation</b>	<b>143</b>
D.1	Speeding up the Hamiltonian matrix computation . . . . .	143
D.2	Renormalization in the $\mathbb{Z}_2$ -broken phase . . . . .	145
<b>E</b>	<b>Semiclassical ground state splitting</b>	<b>149</b>
E.1	Ground state splitting . . . . .	149
<b>Bibliography</b>		<b>161</b>



# List of Figures

1	Illustration of RG flows . . . . .	2
2.1	Illustration of perturbative RG flow . . . . .	16
3.1	The contour $C$ in the complex $s$ plane. . . . .	49
3.2	The 2-2 and 3-1 cuts of the on-shell dilaton scattering amplitude. . . . .	49
3.3	The different configurations for the diagrams with 2-2 cut. . . . .	50
5.1	Test of the $M(E)$ asymptotics. . . . .	79
5.2	Ground state energy for the $\phi^2$ perturbation . . . . .	84
5.3	Spectra of excitations for the $\phi^2$ perturbation . . . . .	84
5.4	Numerical spectra as function of $g$ . . . . .	85
5.5	Numerical spectrum as a function of $g$ and fit of the critical coupling . . . . .	87
5.6	Comparison with the CFT spectrum; see the text. . . . .	88
5.7	Vacuum energy density and excitation spectrum for $g = 1$ , as a function of $L$ . . . . .	90
5.8	Vacuum energy density and excitation spectrum for $g = 2.97$ , as a function of $L$ . . . . .	93
5.9	Dependence of the spectrum on $E_{\max}$ for $g = 1$ . . . . .	93
5.10	Dependence of the spectrum on $E_{\max}$ for $g = 3$ . . . . .	93
5.11	Comparison with QSE . . . . .	98
5.12	Matching between lattice and continuum descriptions . . . . .	99
6.1	Solutions of the duality transformation in the $\phi^4$ theory . . . . .	104
6.2	Numerical spectra for the direct and dual theories as a function of $g$ . . . . .	107
6.3	Dependence on $g$ of the vacuum energy and spectrum for $L = 12$ . . . . .	113
6.4	Dependence on $g$ of the vacuum energy and spectrum for $L = 20$ . . . . .	114
6.5	Dependence on $L$ of the vacuum energy and spectrum for $g = 0.1$ . . . . .	114
6.6	Dependence on $L$ of the spectrum for $g = 0.05$ . . . . .	114
6.7	Ground state splitting as a function of $L$ for $g = 0.05$ . . . . .	116
6.8	Kink mass as a function of $g$ . . . . .	116
C.1	Comparison of perturbative and numerical spectra in the symmetric phase . . . . .	140
C.2	Comparison of perturbative and numerical spectra in the broken phase . . . . .	142
E.1	Finite volume correction to the vacuum energy splitting . . . . .	152



# Introduction

Quantum field theory (QFT) is a framework describing a plethora of physical systems, ranging from statistical mechanics and condensed matter physics to particle physics.

Typically, these contain an infinite or very large number of degrees of freedom. A simple example is provided by the scalar theory with  $\mathbb{Z}_2$  symmetry in  $d$  dimensions, whose dynamics is described by a Lagrangian for a field  $\phi$ ,

$$\mathcal{L} = \frac{1}{2} \partial_\mu \phi \partial^\mu \phi + \lambda_2 \phi^2 + \lambda_4 \phi^4 + \lambda_6 \phi^6 + \dots, \quad (1)$$

where the dots denote an infinite series of terms with increasing powers of  $\phi$  and/or its derivatives  $\partial_\mu \phi$ . This theory is used to model, among others, ferromagnets near the Curie temperature and fluctuations of the Higgs field in the Standard Model (SM) of particle physics. The field  $\phi$  can fluctuate over a wide range of energy scales, from the ultraviolet (UV) cutoff  $\Lambda$  (such as the Planck mass in the SM) down to the infrared (IR) observable scales. Therefore, it would seem not feasible to make predictions using QFT, as there are an infinite number of coupled degrees of freedom.

This difficulty can be tackled via the renormalization group (RG) approach.<sup>1</sup> The RG originates from the fact that the effect of high-energy degrees of freedom on low-energy observables can be accounted for by an effective theory. Concretely, from (1) one can write an effective Lagrangian only for the field modes  $\phi'$  with momenta  $k \leq \Lambda'$ , after the modes with momenta  $\Lambda' < k < \Lambda$  are integrated out in the path integral,

$$\mathcal{L}_{eff} = \frac{1}{2} \partial_\mu \phi' \partial^\mu \phi' + \lambda_2(\Lambda') \phi'^2 + \lambda_4(\Lambda') \phi'^4 + \lambda_6(\Lambda') \phi'^6 + \dots,$$

where the “running” couplings  $\lambda_n$  depend on the cutoff  $\Lambda'$ . The evolution of the running couplings with the cutoff is called RG flow.

A particularly interesting case is encountered when  $\frac{d}{d\Lambda} \lambda_n(\Lambda) = 0$ , i.e. when the running couplings are constant. In this case, the theory sits at a scale-invariant fixed point, where the observables are independent of the momentum scale and fluctuations are correlated at any distance.<sup>2</sup> This scenario is relevant for systems close to phase transitions, such as water

---

<sup>1</sup>See [5] for a classic review on the renormalization group.

<sup>2</sup>See [6] for a pedagogic exposition on the renormalization group approach to critical phenomena.

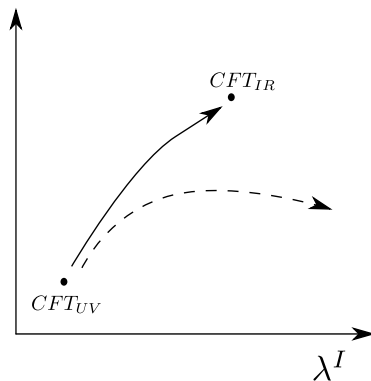


Figure 1: Example of RG flows in the abstract space of coupling constants  $\lambda^I$ . The solid trajectory starts close the original fixed point and ends towards another infrared fixed point. The dashed trajectory instead goes to a gapped phase.

at the liquid-vapor critical point. As it turns out, in most cases of interest, scale invariance at the fixed points is enhanced to a larger symmetry represented by the conformal group.<sup>3</sup> We will henceforth assume that the fixed points are described by conformally invariant field theories (CFTs). [7]

In this thesis we will be concerned with deformations of CFTs. The general problem we are interested in is the following. What can we say about the RG flow and the low-energy phase of a QFT, based on its microscopic description? As an example, in the UV, QCD is a theory of weakly-interacting quarks and gluons, whose parameters are known from measurements performed at high-energy experiments. However, at energies of order  $\Lambda_{\text{QCD}} \sim 1\text{GeV}$  the physics changes completely and in the IR we have an effective description in terms of pions and hadrons. Is it possible to match quantitatively the low-energy and high-energy observables?

Formally, the general framework we will be working with entails a UV CFT, whose dynamics is usually encoded in a conformally invariant action  $S_{\text{CFT}}$ , deformed by a set of local scalar operators  $\mathcal{O}_I$ ,

$$S = S_{\text{CFT}} + \int d^d x \lambda^I \mathcal{O}_I(x),$$

which at large distances can drive the system away from the original fixed point, towards another fixed point or to a gapped phase. This situation is illustrated pictorially in figure 1.

We would like to stress that in this setup, the UV CFT need not necessarily be a fundamental description of the system under study up to arbitrarily high energy. Whenever there is a large separation of mass scales in a theory, say  $\Lambda_1 \ll \Lambda_2$ , at intermediate energies  $\Lambda_1 \ll E \ll \Lambda_2$  the system is approximately scale-invariant. For instance, in a model of particle physics,  $\Lambda_2$  can be the mass of a weakly-interacting heavy particle, while  $\Lambda_1$  can represent the mass of another light particle or a non-perturbatively generated scale, such as  $\Lambda_{\text{QCD}}$ .

It is in general difficult to solve renormalization group flows exactly. However, when the

---

<sup>3</sup>This important aspect will be discussed in more depth in Part I of this thesis.



---

dynamics is weakly-coupled, it is possible to solve perturbatively for the running couplings,

$$\Lambda \frac{d}{d\Lambda} \lambda^I = \beta^I,$$

where the  $\beta^I$  are expressed as a power expansion in the  $\lambda^I$ . This is the situation we will mostly consider in Part I of this thesis.

On the contrary, if the interactions are strong, a perturbative approach is not available and it is sometimes necessary to resort to non-analytic, numerical methods to predict the IR physics from the UV data. The lattice Monte Carlo method [8] has set the standard for numerical approaches to QFT in the last decades. However, it has some drawbacks as it is affected by statistical errors and requires a significant amount of computational resources. In Part II of this thesis we will explore an alternative approach to solve the RG flow of QFTs numerically.

## I. The structure of RG flows

In the first part we study model-independent properties of RG flows which apply to a broad class of theories, given by Poincaré-invariant QFTs in even space-time dimensions. One of the questions we want to address is under what conditions the scale invariance at the fixed point is enhanced to full conformal invariance. Additionally, we are interested in studying monotonicity constraints on the RG flow. In particular an important results, named “*a*-theorem”, states that there exists a function of the energy scale which decreases monotonically along the RG flow from the UV to the IR, and which is unambiguously defined at the fixed points.

We refer the reader to Chapter 1 for a more detailed and technical introduction to the subject. There, we also review a series of exact results in two space-time dimensions.

In Chapters 2,3,4 we will discuss renormalization in curved space time, using the formalism of the local Callan–Symanzik equation, with the goal to derive constraints on RG flows in higher dimensions.

Some important definitions and auxiliary results are contained in appendices A, B.

## II. Exact diagonalization methods

In Part II we explore the Hamiltonian Truncation (HT) method, a representative of exact diagonalization techniques in QFT, which can be used to solve numerically strongly-coupled RG flows in any dimensions.

The HT method can be considered as a generalization of the Rayleigh–Ritz method in quantum mechanics. Take for instance the simple anharmonic oscillator.

$$H = H_0 + V, \quad H_0 = \frac{1}{2}p^2 + \frac{1}{2}\omega^2 x^2, \quad V = \lambda x^4.$$

## Introduction

---

We can choose as a basis of the Hilbert space the set of eigenstates of the free part of the Hamiltonian  $H_0$ ,

$$H_0|n\rangle = \omega \left( n + \frac{1}{2} \right) |n\rangle, \quad n = 0, 1, \dots .$$

We can then compute the matrix element of  $H$  over a finite subspace of states  $|0\rangle, |1\rangle, \dots, |n_{\max}\rangle$  and diagonalize the full, non-perturbative Hamiltonian over this subspace. The low-energy spectrum of eigenvalues will converge as the cutoff  $n_{\max}$  is taken to infinity.

The procedure used in the HT method is similar. The QFT is regulated both in the IR and in the UV, by putting it in finite volume and by imposing a cutoff on the space of states. This prescription results in a finite-dimensional, discrete Hamiltonian which can be diagonalized exactly on a computer to find the low-energy spectrum of excitations. In this way, the non-perturbative IR dynamics is solved numerically, while the high-energy degrees of freedom decouple from the low-energy spectrum as the UV cutoff is taken to infinity. The main original ingredient of our study will be an analytic renormalization procedure used to “integrate out” the high-energy states and improve the predictions of the low-energy Hamiltonian.

In Chapter 5, after a more detailed introduction on the HT method, we will apply it to the study of the  $\phi^4$  theory in two dimensions, focusing on the region where the  $\mathbb{Z}_2$  symmetry of the model,  $\phi \rightarrow -\phi$ , is preserved. Furthermore, we will discuss the renormalization procedure and show how it improves the numerical convergence.

In Chapter 6, we will adapt the method to analyze the regime where the  $\mathbb{Z}_2$  symmetry of the model is spontaneously broken, and study both the topologically-trivial and non-trivial spectra of excitations.

Technical details are relegated to appendices C, D, E.

## Part I

# The structure of RG flows



# Chapter 1

## Preliminaries

In the first part of this thesis we discuss the physical consequences of Poincaré invariance, unitarity and locality<sup>1</sup> for general even-dimensional QFTs, without reference to the UV details of the theory.

One of the most prominent results is concerned with the irreversibility of RG flows. According to the Wilsonian picture of renormalization, which involves a coarse-graining of degrees of freedom, it is expected that at low energies there should be less excitations with respect to high energies. Let us provide a simple perturbative example.

Suppose we have a  $U(1)$ -invariant theory for a complex scalar field  $\Phi$  in  $d = 3$  dimensions, with a negative mass squared term and a small quartic interaction,

$$\mathcal{L} = \partial_\mu \Phi^* \partial^\mu \Phi - m^2 \Phi^* \Phi + \lambda (\Phi^* \Phi)^2, \quad \lambda^2 \ll m^2. \quad (1.1)$$

Since both the quadratic and quartic operators in (1.1) are relevant,<sup>2</sup> in the UV the spectrum is composed by two weakly-interacting scalar degrees of freedom (the real and imaginary parts of  $\Phi$ ).

Below energy scales of order  $v = \frac{m^2}{\lambda}$ , the  $U(1)$  symmetry is spontaneously broken, and we end up with an effective theory for the  $U(1)$  Goldstone boson  $\pi$ ,

$$\mathcal{L}_{\text{eff}} = \frac{1}{2} \partial_\mu \pi \partial^\mu \pi + \frac{c_4}{v^4} (\partial_\mu \pi \partial^\mu \pi)^2 + \dots, \quad (1.2)$$

where the omitted terms are suppressed by increasing powers of  $E/v$ .

We just showed a perturbative example of a UV-complete QFT where the number of degrees of freedom decreases along the RG flow. This picture was borne out in general two-dimensional QFTs in the seminal paper by Zamolodchikov [9], who specified a positive-definite function

---

<sup>1</sup>By locality we mean the existence of the energy-momentum tensor  $T_{\mu\nu}$ , i.e. a local primary spin-2 tensor generating the space-time symmetries.

<sup>2</sup>CFT operators are classified into relevant, marginal or irrelevant according to whether their scaling dimension is smaller, equal to or larger than  $d$  respectively.

of the energy scale which monotonically decreases along the RG flow, thereby providing an effective “counting” of degrees of freedom.

Let us review Zamolodchikov’s argument.<sup>3</sup> Working in the Euclidean signature, we define the functions

$$\begin{aligned} F(|x|^2) &\equiv z^4 \langle T(z, \bar{z}) T(0) \rangle, \\ G(|x|^2) &\equiv z^3 \bar{z} \langle \Theta(z, \bar{z}) T(0) \rangle, \\ H(|x|^2) &\equiv z^2 \bar{z}^2 \langle \Theta(z, \bar{z}) \Theta(0) \rangle, \end{aligned}$$

where  $z, \bar{z}$  are the complex coordinates  $z = x_1 + ix_2$ ,  $\bar{z} = x_1 - ix_2$ , while  $T$  and  $\Theta$  are defined as the components of the energy-momentum (EM) tensor:  $T \equiv T_{zz}$  and  $\Theta \equiv T^\mu_\mu$ . The conservation of the EM tensor reads

$$\partial_{\bar{z}} T + 4\partial_z \Theta = 0. \tag{1.3}$$

Next, let us define the  $C$ -function,

$$C = 2 \left( F - \frac{1}{2} G - \frac{3}{16} H \right), \tag{1.4}$$

which depends explicitly on the length scale  $|x|$  via  $\log(\mu|x|)$ , where  $\mu$  is a typical mass scale of the problem.<sup>4</sup> By using the conservation equation (1.3) it is possible to prove that

$$\frac{dC}{d \log|x|^2} = -\frac{3}{4} H \leq 0, \tag{1.5}$$

where the positivity of  $H$  in Euclidean signature is enforced by unitarity. This is the celebrated  $c$ -theorem.

Now, suppose that the UV and IR fixed points are described by CFTs, in which  $\Theta = 0$ . When  $\log|x| \rightarrow \pm\infty$ , corresponding to the IR and UV asymptotics respectively,  $C$  is simply proportional to the central charge  $c$ , as in a two-dimensional CFT<sup>5</sup>

$$\langle T(z, \bar{z}) T(0) \rangle = \frac{1}{2(2\pi)^2} \frac{c}{z^4}. \tag{1.6}$$

Therefore, a straightforward corollary of (1.5) is that  $c_{\text{UV}} > c_{\text{IR}}$  for any two CFTs connected by an RG flow.

Another very important issue regards the nature of the fixed points at the ends of RG flows. By construction, fixed points are scale invariant (or trivial) theories, and it is usually assumed their space-time symmetry group is enhanced to the full conformal group. This assumption is crucial in many physical applications, as conformal invariance imposes many more constraints

---

<sup>3</sup>Here we follow the exposition given in [10].

<sup>4</sup>For instance,  $\mu$  can correspond to the mass  $M$  in the Lagrangian (1.1). At this energy scale the heavy field decouples from the spectrum.

<sup>5</sup>See [7] for a comprehensive review on two-dimensional conformal field theory

---

on the dynamics of the fixed points. For instance, the conformal bootstrap approach, which has recently been used to determine the critical exponents of the three-dimensional critical Ising model to unprecedented precision [11, 12, 13], heavily relies on the conformal symmetry of the correlators of the theory.

In two space-time dimensions, the equivalence SFT=CFT was proved by Polchinsky [14] by extending Zamolodchikov’s proof. Let us sketch the argument. Suppose that  $T_{\mu\nu}$  has canonical scaling, i.e.

$$i[S, T_{\mu\nu}] = x^\alpha \partial_\alpha T_{\mu\nu} + dT_{\mu\nu}, \quad (1.7)$$

where  $d$  is the space-time dimension and  $S$  is the generator of scale transformations. In this case the  $C$  function defined in (1.4) does not depend on  $|x|$ . Therefore, from (1.5), the two-point function of  $\Theta$  vanishes. In  $d \geq 2$  this implies that the theory is conformally invariant [14]. Thus, the only step to complete the argument is to prove (1.7). In general, in a scale-invariant field theory,  $T_{\mu\nu}$  obeys the following scaling law

$$i[S, T_{\mu\nu}] = x^\alpha \partial_\alpha T_{\mu\nu} + dT_{\mu\nu} + \partial^\rho \partial^\sigma \tilde{Y}_{\mu\rho\nu\sigma}, \quad (1.8)$$

where  $\tilde{Y}$  is an operator with the symmetries of the Riemann tensor.<sup>6</sup> It is then possible to show that the additional term in (1.8) can be eliminated by improving the EM tensor, under the assumption that the spectrum of operators above the identity is discrete and their scaling dimensions are strictly greater than 0.

Given the importance of the  $c$ -theorem and of the relation between scale and conformal invariance for quantum field theories, it is of great interest to generalize these studies to higher dimensions. In Part I of this thesis we discuss constraints on the RG flows in even dimensions greater than two, in particular four and six.<sup>7</sup>

What prevents a simple generalization of Zamolodchikov’s argument to higher dimensions is that in  $d > 2$  there are multiple tensor structures in the two-point function of  $T_{\mu\nu}$ , and it is impossible to directly derive an equation like (1.5). Nevertheless, Cardy [20] conjectured that a version of the  $c$ -theorem should hold in four dimensions as well. Let us review his proposal. In  $d = 2$ , the central charge  $c$  appears in the Weyl anomaly [21], which represents the Weyl variation of the effective action of the CFT in curved background:

$$2g^{\mu\nu} \frac{\partial}{\partial g^{\mu\nu}} \mathcal{W}[g_{\mu\nu}] = -\frac{c}{12} R, \quad (1.9)$$

---

<sup>6</sup>It corresponds to an additive logarithmic renormalization of the EM tensor, which can be seen as adding a counterterm of the form  $R^{\alpha\beta\mu\nu} Y_{\alpha\beta\mu\nu}$  to the effective action in curved background.

<sup>7</sup>In odd dimensions  $d$  there is evidence for the “ $F$ -theorem”, stating that the logarithm of the Euclidean partition function on the sphere  $S_d$  is monotonically decreasing [15, 16, 17]. In [18] it was shown that this quantity is proportional to the universal term of the entanglement entropy across the sphere  $S_{d-2}$ , for which independent arguments for its monotonicity exist [19]. We won’t have anything more to say about constraints on odd-dimensional RG flows in this thesis.

where  $R$  is the Ricci scalar. In four dimensions, the Weyl anomaly reads

$$2g^{\mu\nu} \frac{\partial}{\partial g^{\mu\nu}} \mathcal{W}[g_{\mu\nu}] = -aE_4 + cW^2, \quad (1.10)$$

where  $W^2$  is the Weyl tensor squared and  $E_4$  is the Euler density, whose integral is a topological invariant (like  $R$  in two dimensions). We are going to introduce and discuss the Weyl anomaly extensively in Chapter 2.

Cardy's conjecture (named  $a$ -theorem) states that  $a$  decreases monotonically along the RG flow.

It is instructive to give an example application of the  $a$ -theorem, as presented in [20]. Consider an asymptotically-free  $SU(N_c)$  gauge theory with  $N_f$  flavors. The degrees of freedom of this theory in the UV are represented by  $N_f \times N_c$  free fermions and  $N_c^2 - 1$  free bosons. Rescaling the anomaly so that  $a = 1$  for a massless scalar, we find  $a = 62$  for a massless boson and  $a = 11$  for a free fermion. We then have

$$\lim_{g \rightarrow 0} a(g) \sim 62 \left( N_c^2 - 1 \right) + 11N_c N_f. \quad (1.11)$$

Conversely, in the IR we have a strongly-coupled theory and we expect the chiral symmetry to be spontaneously broken, resulting in  $N_f^2 - 1$  Goldstone bosons. Therefore

$$\lim_{g \rightarrow \infty} a(g) = N_f^2 - 1. \quad (1.12)$$

Thus, the  $a$ -theorem corresponds to the following constraint in this class of theories

$$62 \left( N_c^2 - 1 \right) + 11N_c N_f > N_f^2 - 1, \quad (1.13)$$

which is violated for  $N_f$  sufficiently large. However, in this particular example there is no contradiction because asymptotic freedom is lost for  $N_f$  smaller than the bound given by (1.13) [22]. Nevertheless, a similar logic could be used to constrain scenarios of dynamical symmetry breaking in strongly coupled theories beyond the Standard Model.

Recently, a non-perturbative proof of the  $a$ -theorem in  $d = 4$  has been presented by Komargodski and Schwimmer in [23], using dispersion relations for certain dilaton scattering amplitudes, which are related to correlators of the trace of the EM tensor  $T$ . The technique behind this proof is reminiscent of the 't Hooft anomaly matching condition [24], stating that the anomaly of an internal symmetry should be the same both at low and high energy. Even though the Weyl symmetry is explicitly broken by the RG flow, the change in the anomaly can be accounted for by the introduction of a spurion (the dilaton) restoring the symmetry. The ideas presented in [23] laid the foundation for demonstrating the equivalence SFT=CFT in four dimensions [25] within perturbation theory.

In Part I of this thesis we employ instead the approach pioneered by Osborn [26] to discuss constraints on RG flows in even-dimensional QFTs. This approach, named local Callan-



---

Symanzik (CS) equation, treats the couplings and background metric as sources for the local operators of the theory and generalizes the CS equation in the presence of space-time dependent sources. It will be discussed extensively in Chapter 2.

In Chapter 3, we use the local CS equation to calculate systematically the dilaton effective action around a fixed point. This will be used to fill in some gaps in the proof of the equivalence SFT=CFT of [25]. Also, we will show the connection between the proof of the  $a$ -theorem using the dilaton scattering amplitudes and the constraints on the RG flow derived from the local CS equation.

In Chapter 4, we apply the local CS equation to study constraints on RG flows in six-dimensional unitary QFTs. Under some assumptions, we establish the  $a$ -theorem in this class of theories and prove the equivalence SFT=CFT.



## Chapter 2

# The local Callan–Symanzik equation

### 2.1 Introduction

The source method is a well established tool for probing the structure of Quantum Field Theory (QFT). The basic idea is to promote the Lagrangian parameters (coupling constants and masses) to local background fields and to exploit the resulting (possibly local) symmetries to constrain the form of the effective action. Moreover, the use of local sources allows to control the correlators of the associated composite operators, and, in particular, allows to map the behavior of some operators across strongly coupled regimes. Prominent examples of the use of the source method are given by the chiral Lagrangian of low-energy hadrodynamics [27] and by exact results for holomorphic quantities in supersymmetric gauge theories [28]. Another playground where to usefully apply the method is given by softly broken supersymmetry, in perturbation theory [29] and beyond [30].

A crucial aspect of any given QFT is its behavior under renormalization group (RG) evolution. Technically, RG evolution corresponds to the change of the dynamics under a dilation. In view of that, it seems natural, in order to try and explore the structure of the RG flow, to formally promote the explicitly broken dilation invariance to an exact Weyl symmetry. Of course, in order to be able to do that, one must promote the Lagrangian parameters to local fields with definite transformation property under Weyl symmetry. In particular the flat Minkowski metric  $\eta_{\mu\nu}$  must be upgraded to a generic curved metric  $g_{\mu\nu}$ . This program was carried out to a very significant extent about two decades ago in a series of interesting papers by Jack and Osborn [31, 32, 26]. One first basic result is that the Weyl variation of the quantum effective action  $\mathcal{W}$  in the presence of sources is given by an anomaly equation<sup>1</sup>

$$\left(2g^{\mu\nu}\frac{\delta}{\delta g^{\mu\nu}(x)} - \beta^I(\lambda)\frac{\delta}{\delta\lambda^I(x)} + \dots\right)\mathcal{W}[g, \lambda, \dots] = \mathcal{A}(x) \quad (2.1)$$

---

<sup>1</sup>An earlier version of this equation was introduced already in 1979 by Drummond and Shore [33].

where  $\lambda^I$  are the external sources, and  $\mathcal{A}$  is a local scalar function of these sources and the metric. In the case of a conformal field theory (CFT), by turning off all the sources apart from the metric,  $\mathcal{A}$  reduces to the well known expression for the Weyl anomaly [34]. On the other hand, away from criticality, where  $\beta \neq 0$ , this equation can be interpreted as a local generalization of the Callan–Symanzik (CS) equation. Now, a second, perhaps more interesting set of results follows from the request of integrability of  $\mathcal{A}$ . This request can be enforced along two equivalent routes. One is to directly derive  $\mathcal{A}$  from the bare Lagrangian in a given renormalization scheme, for instance dimensional regularization [32]. The other is to require  $\mathcal{A}$  satisfies a Wess–Zumino consistency condition, regardless of details concerning the renormalization scheme [26]. The result is a set of non-trivial constraints involving the  $\beta$ -functions and the anomaly coefficients. The latter can also be interpreted as the short distance singularities in different correlators involving the energy momentum tensor and composite scalars and vectors. It is indeed according to that interpretation that some of these results had earlier been derived in works by Brown and Collins [35] and by Hathrell [36]. However, concerning 4D QFT, the most remarkable result of refs. [32, 26] is a relation involving the  $\beta$ -function and a quantity  $\tilde{a}$  that coincides with the anomaly coefficient  $a$  at critical points<sup>2</sup>

$$\frac{\partial \tilde{a}}{\partial \lambda^I} = (\chi_{IJ} + \xi_{IJ})\beta^J \quad (2.2)$$

where  $\chi$  and  $\xi$  are respectively symmetric and antisymmetric covariant tensors over the space of couplings. Indeed, in the '70's, a relation of this form had been proved at finite loop order, and for specific models, through a laborious diagrammatic analysis [37]. However the use of the local CS equation offers both a deeper viewpoint and a more systematic approach. Moreover, as  $\tilde{a}$  only depends on the RG scale via its dependence on the running couplings, a corollary of the Eq. (2.2) is

$$\mu \frac{d\tilde{a}}{d\mu} = \beta^I \frac{\partial \tilde{a}}{\partial \lambda^I} = \chi_{IJ} \beta^J \beta^I. \quad (2.3)$$

This equation is fully analogous to the perturbative incarnation of Zamolodchikov's  $c$ -theorem [9] for 2D QFT, with  $\chi_{IJ}$  interpreted as a *metric* in the space of couplings. Indeed the  $c$ -theorem itself can be shown to coincide with the Wess–Zumino consistency condition associated with the 2D anomaly off-criticality. More precisely, in the 2D case, as proved in ref. [26], there exists a choice of scheme where a quantity  $\tilde{c}$ , coinciding with  $c$  at criticality, evolves according to the analogue of Eq. (2.3), with a positive definite metric. Concerning the 4D case, although in ref. [32, 26] the positivity of  $\chi_{IJ}$  could be established at leading order in perturbation theory, a robust non perturbative picture was missing. Perhaps because of this obstacle, no attempt to draw conclusions on the structure of 4D flows, in particular on their irreversibility, was made in those works.

Even in the absence of a proof, Eq. (2.3), Cardy's conjecture [20] and direct evidence from exact results in supersymmetric gauge theories [38] had led to the belief that an irreversibility

---

<sup>2</sup> $a$  is the coefficient of the Euler density term in the Weyl anomaly in 4 dimensions.

argument for  $a$ , an  $a$ -theorem, should have existed in the 4D case as well. But a complete proof only arrived in 2011, in the work of Komargodski and Schwimmer (KS) [23, 39], who showed that, in any flow between two CFTs, the end points of the flow satisfy the inequality  $a_{UV} > a_{IR}$ , where  $a_{UV}$  ( $a_{IR}$ ) is the value of the  $a$  coefficient in the UV (IR) fixed point. With the wisdom of hindsight, it is now rather clear why the 4D proof took so much longer: while for the  $c$ -theorem in 2D it suffices to study the 2-point function of  $T_{\mu\nu}$ , the 4D analogue requires a study of higher point correlators. This necessity had already been noticed by Osborn [26], but within the local CS methodology there was no concrete guideline onto how to proceed. KS instead found a guideline in the form of an external background dilaton field, the component of the background metric that couples to the trace  $T$  of the energy momentum tensor. The on-shell dilaton scattering amplitude just happens to package the right combination of 2-, 3- and 4-point functions of  $T$  that is directly sensitive to the RG flow of the anomaly coefficient  $a$ . Using a dispersion relation for the scattering amplitude and using unitarity, KS could then compare the value of  $a$  at the UV and IR asymptotics and prove  $a_{UV} > a_{IR}$ .

The  $a$ -theorem represents a non-perturbative constraints on the RG flow under the assumption that the end points are described by conformal field theories. However the same methodology introduced by KS gives a guideline to obtain further constraints on the structure of the flow, very much like it happens in 2D. A further step in this direction was given in ref. [25], where the finiteness of the amplitude was used to exclude anomalous asymptotic behaviors for perturbative RG flows.<sup>3</sup> In a sense, the ingredients for this proof already existed in [32, 26], but the usage of the dilaton amplitude and dispersion relations made the connection to the asymptotics of the theory more transparent. Ref. [25] provided a synthetic derivation relying on the minimal set of ingredients needed in a perturbative computation. In particular, no detailed discussion of the structure and the role of multiple insertions of  $T$  was given. Moreover, issues like scheme dependence, operator mixing and the role of explicitly broken global symmetries were not analyzed in full detail. Similarly the connection between the dilaton amplitude trick and Eq. (2.3) was not fully explored.

In this and in the following Chapter we illustrate all these details and we present a systematic method for computing correlation functions of  $T$  off-criticality, by studying and applying the local Callan-Symanzik equation. A by-product of this study is a new understanding of the structure of the Weyl anomaly. In practice we have shown that the anomaly can be written in a manifestly consistent manner up to the very few terms related to the  $a$  coefficient.

This Chapter consists of a detailed analysis of the local Callan-Symanzik equation and is largely based on the original work by Osborn [26]. In particular, in section 2.2.1 we present the equation and give a simple description of its derivation (a more detailed discussion based on dimensional regularization is given in appendix A.2). Section 2.2.2 focuses on the generator of Weyl transformations, and subtle issues involving its dependence on the scheme, choice of improvement and ambiguities in the presence of global symmetries. We also introduce new

---

<sup>3</sup>That result was confirmed by an explicit study in weakly coupled gauge theories in ref. [40]. As concerns ruling out anomalous asymptotics beyond perturbation theory, the specific case of scale invariant field theory without conformal invariance was cornered in ref. [25] and even more significantly so in ref. [41, 42].

terminology and notations which are essential for the discussion in the following sections. Next, in section 2.2.3 we study the anomaly, which is parameterized by 25 unknown tensor coefficients related by  $\sim 10$  differential consistency conditions. We show that most of these conditions can be explicitly solved and that the anomaly can be reformulated in a manifestly consistent form, with only 3 non-trivial consistency conditions remaining. One combination of these is the famous equation (2.2), while two others, involve anomalies related to external gauge fields. We then apply these results to the study of gradient flow formulas for the  $\beta$ -functions in section 2.3.

## 2.2 The local Callan–Symanzik equation

### 2.2.1 General set-up

Our main goal is to study the properties of the RG flow in the neighborhood of a conformally invariant fixed point. The basic idea, as sketched in fig. 2.1, is to turn on all the possible marginal deformations of the CFT, which we describe by a set of independent couplings  $\lambda^I$ ,  $I = 1, \dots, N$ , such that  $\lambda^I = 0$  corresponds to the unperturbed CFT. These couplings are associated with scalar operators  $\mathcal{O}_I$ , corresponding, at the fixed point, to primaries with dimension equal to 4. We shall moreover assume the original fixed point is endowed with an exact flavor symmetry  $G_F$ , which is in general explicitly broken at  $\lambda^I \neq 0$ . One relevant

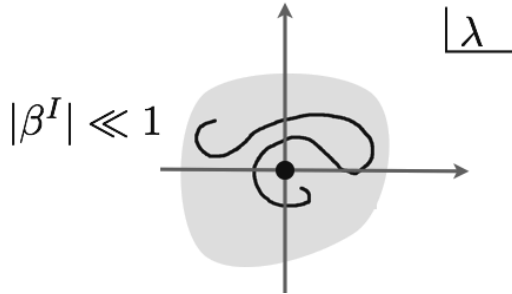


Figure 2.1: Our discussion concerns RG flows in the vicinity of a conformal fixed point, where the  $\beta$ -function and the anomalous dimensions can be treated as small perturbations.

question, originally addressed in ref. [25], is to ask which flows are possible and which are not, under the assumption that the asymptotics lie perturbatively close to the original fixed point. An example to which our assumption applies is given by weakly coupled renormalizable gauge theories with scalars and fermions. In that case the original fixed point corresponds to free field theory. In particular it can be applied to the study of the flows in large  $N$  theories where one plays Banks-Zaks tricks [43, 44] to obtain novel fixed points or, possibly anomalous flows, such as SFTs (theories with scale but not conformal invariance) or limit cycles<sup>4</sup>. However, our analysis also applies to the case where the original CFT represents a strongly coupled non-perturbative fixed point endowed with its own marginal deformations, like they are known

<sup>4</sup>As we already mentioned these exotic possibilities are now ruled out by the analysis in ref. [25], which, among other things, we will here reproduce with extra details.

---

## 2.2. The local Callan–Symanzik equation

to exist in supersymmetry. Indeed, as we shall be able argue later on, our discussion applies to the more general case in which there exists an extended region of  $\lambda$  space, where, even though the  $\lambda^I$  may not be treated as small perturbations, the  $\beta$ -function can still be treated as small. Examples of this more general case can be found in QFTs with manifolds of fixed points (see for instance [45]). While we do not know of any explicit examples in theories without supersymmetry, we believe consideration of this possibility, even if merely conceptual, better illustrates what are the necessary ingredients in our study.

In QFT the trace of the energy momentum tensor  $T \equiv T_\mu^\mu$  is known to correspond to the divergence of the naive dilation current. The change of the dynamics under (naive) dilations is thus controlled by correlators involving  $T$ . In order to make the properties of these correlators more explicit, we need to expand  $T$  in a complete basis of scalar operators of dimension 4. This basis surely includes the scalar deformations  $\mathcal{O}_I$  that generate the flow, but in principle there could also appear divergences of the flavor currents  $\partial_\mu J_A^\mu$  and operators of the form  $\nabla^2 \mathcal{O}_a$  where, at the fixed point,  $\mathcal{O}_a$ , are primary scalars of dimension 2. It is therefore crucial to have a convenient method to control the properties of these operators. Now, the standard methodology to define composite operators and their correlators is to introduce the associated space-time dependent sources. For instance, the energy momentum tensor  $T^{\mu\nu}$  will have as its source a local background metric  $g_{\mu\nu}(x)$ , while  $\mathcal{O}_I$  will have as its source a space-time dependent coupling  $\lambda^I(x)$ . Along the same line, in order to source the currents  $J_A^\mu$ , we shall turn on background vector fields  $A_\mu^A(x)$  gauging the flavor group  $G_F$ , while the dimension 2 operators  $\mathcal{O}_a$  will be sourced by scalar fields  $m^a(x)$ . We shall collectively indicate the set of local sources by  $\mathcal{J} \equiv (g^{\mu\nu}, \lambda^I, A_\mu^A, m^a)$ . The renormalized partition function in the source background

$$Z[\mathcal{J}] \equiv e^{i\mathcal{W}[\mathcal{J}]} = \int \mathcal{D}\Phi e^{iS[\Phi, \mathcal{J}]} \quad (2.4)$$

acts as the generator of the correlators for the associated renormalized composite operators. The same information is more efficiently encapsulated in the quantum effective action  $\mathcal{W}$ , which generates the connected correlators. When acting on  $\mathcal{W}$  the functional derivative with respect to a source coincides with the insertion of the corresponding operator in a connected correlator

$$\begin{aligned} \frac{2}{\sqrt{-g}} \frac{\delta}{\delta g^{\mu\nu}(x)} &\equiv [T_{\mu\nu}(x)] & \frac{1}{\sqrt{-g}} \frac{\delta}{\delta \lambda^I(x)} &\equiv [\mathcal{O}_I(x)] \\ \frac{1}{\sqrt{-g}} \frac{\delta}{\delta A_\mu^A(x)} &\equiv [J_\mu^A(x)] & \frac{1}{\sqrt{-g}} \frac{\delta}{\delta m^a(x)} &\equiv [\mathcal{O}_a(x)] . \end{aligned} \quad (2.5)$$

Time ordered  $n$ -point correlators are obtained by first taking  $n$  derivatives of  $\mathcal{W}$  and then setting the sources to “zero”,

$$g^{\mu\nu}(x) \rightarrow \eta^{\mu\nu}, \quad \lambda^I(x) \rightarrow \lambda^I = \text{const}, \quad A_\mu^A = 0, \quad m^a(x) \rightarrow m^a = \text{const}. \quad (2.6)$$

We will use the following convention:

$$\begin{aligned} \langle \mathbf{T} \{ \mathcal{O}_{I_1}(x_1) \dots \mathcal{O}_{I_n}(x_n) \} \rangle &= \frac{(-i)^{n-1}}{\sqrt{-g(x_1)} \dots \sqrt{-g(x_n)}} \frac{\delta}{\delta \lambda^{I_n}(x_n)} \dots \frac{\delta}{\delta \lambda^{I_1}(x_1)} \mathcal{W} \Big| \\ \langle \mathbf{T} \{ T(x_1) \dots T(x_n) \} \rangle &= \frac{(-i)^{n-1} 2^n}{\sqrt{-g(x_1)} \dots \sqrt{-g(x_n)}} g^{\mu_n \nu_n} \frac{\delta}{\delta g^{\mu_n \nu_n}(x_n)} \dots g^{\mu_1 \nu_1} \frac{\delta}{\delta g^{\mu_1 \nu_1}(x_1)} \mathcal{W} \Big|. \end{aligned} \quad (2.7)$$

where the symbol  $\Big|$  denotes that the functional derivatives are evaluated in the background (2.6). Notice that our definition of the  $n$ -point correlator of  $T$  coincides with the standard one

$$\langle \mathbf{T} \{ T(x_1) \dots T(x_n) \} \rangle_S = \frac{(-i)^{n-1} 2^n}{\sqrt{-g(x_1)} \dots \sqrt{-g(x_n)}} g^{\mu_n \nu_n} \dots g^{\mu_1 \nu_1} \frac{\delta}{\delta g^{\mu_n \nu_n}(x_n)} \dots \frac{\delta}{\delta g^{\mu_1 \nu_1}(x_1)} \mathcal{W} \Big| \quad (2.8)$$

up to contact terms.

A standard property of effective actions for sources is to formally respect extended symmetries, up to anomalies. As concerns diffeomorphisms and  $G_F$  transformations, in this work we shall make the simplifying assumptions that they are anomaly free. Indeed most of our discussion shall focus on the case of parity invariant theories, for which  $\text{diff} \times G_F$  are not anomalous.<sup>5</sup> The other crucial symmetry is given by Weyl transformations under which the metric transforms as

$$g^{\mu\nu}(x) \rightarrow e^{2\sigma(x)} g^{\mu\nu}(x) \quad \delta_\sigma g^{\mu\nu}(x) = 2\sigma(x) g^{\mu\nu}(x) \quad (2.9)$$

and whose anomaly is the centerpiece of our study. The origin of the Weyl anomaly is discussed in more detail in the appendix, focusing on dimensional regularization. Here we shall limit ourselves to the basic story, which goes as follows. As a function of the sources  $\mathcal{J} \equiv (g^{\mu\nu}, \lambda^I, A_\mu^A, m^a)$  and of the dynamical fields the bare action can be in general split as

$$S = S^{(1)}[\Phi, \mathcal{J}] + S^{(2)}[\mathcal{J}] \quad (2.10)$$

where  $S^{(1)}$  involves only terms that non-trivially depend on the dynamical fields, while  $S^{(2)}$  contains, instead, purely source dependent terms such as  $(\nabla^2 \lambda)^2$ ,  $R(\nabla \lambda)^2$ ,  $R_{\mu\nu} R^{\mu\nu}$ , etc.. The addition of  $S^{(2)}$  is necessary in order to obtain a finite quantum effective action after renormalization. In dimensional regularization  $S^{(2)}$  can be chosen to be a series of pure poles in  $1/\epsilon$ . Now, given that  $\mathcal{J}$  represent the complete set of sources for the operators that can appear in the expansion of  $T$ , it is basically by definition that there must exist a choice of Weyl transformation  $\delta_\sigma \mathcal{J}$  such that  $S^{(1)}$  is invariant. Once again, as we show in the appendix, in dimensionally regulated weakly coupled gauge theories, this fact is pretty obvious. On the other end, once  $\delta_\sigma \mathcal{J}$  is picked that way, it is clear that  $S^{(2)}$  will in general not be invariant.<sup>6</sup> Since  $S^{(2)}$  has no dependence on the dynamical fields, its variation will directly control the

<sup>5</sup>The effect of anomalies has been studied in Ref. [46].

<sup>6</sup>Unless new sources, coupling to pure functions of  $\mathcal{J}$  are introduced, in such such a way that their variation compensates for  $\delta_\sigma S^{(2)}$ .



variation of the quantum effective action. We thus have

$$\int d^4x \delta_\sigma \mathcal{J} \frac{\delta}{\delta \mathcal{J}} \mathcal{W} = \int d^4x \delta_\sigma \mathcal{J} \frac{\delta}{\delta \mathcal{J}} S^{(2)} \equiv \int d^4x \mathcal{A}_\sigma \quad (2.11)$$

where the locality of  $S^{(2)}$  dictates  $\mathcal{A}_\sigma$  must be a local function of the sources. Notice moreover that, even though  $S^{(2)}$  is a series of counterterms that diverge with the cut-off, by Eq. (2.11), its variation  $\int \mathcal{A}_\sigma$  equals the variation of the renormalized action with respect to the renormalized sources, and must therefore be finite.  $\mathcal{A}_\sigma$  represents an anomaly for the Weyl symmetry. Eq. (2.11) is the local Callan-Symanzik equation we sketched in Eq. (2.1).

### 2.2.2 The structure of Weyl symmetry

In this section we analyze in detail the Weyl transformation of the sources. The discussion is based mainly on [26], but we shall highlight properties which we repute relevant to the study of the anomaly and to the computation of the dilaton effective action.<sup>7</sup>

Let us recall once more the role of our sources. The dimensionless sources  $\lambda^I(x)$ , associated with quasi marginal operators  $\mathcal{O}_I(x)$ , are local versions of the couplings  $\lambda^I$  that produce the RG flow we want to study. The CFT fixed point we are expanding around corresponds to  $\lambda^I = 0$ . This fixed point respects a flavor symmetry  $G_F$ , which is in general explicitly broken at  $\lambda^I \neq 0$ . The vectors  $A_\mu^A$ , with the index  $A$  running in the adjoint of  $G_F$ , are background fields gauging  $G_F$ . They act as sources for the currents  $J_A^\mu$ . By the scalars  $m^a(x)$ , we indicate the sources of scalar operators  $\mathcal{O}_a$  with dimension equaling 2 at the fixed point. Notice that  $m^a$  have mass dimension two, in spite of the perhaps misleading notation (which we adopted from ref. [26]). The CFT may also possess relevant scalar deformations of dimension  $\neq 2$ . For instance, in weakly coupled gauge theories these are given by fermion masses and scalar trilinears, that are associated with dimension 3 operators. In the limit where the corresponding mass deformations vanish the appearance of these operators in the expansion of  $T$  is forbidden by Lorentz invariance. We shall thus neglect them in the course of our discussion. Finally notice that, although we do not indicate it, the sources and the corresponding composite operators in Eq. (2.5) are defined at some renormalization scale  $\mu$ .

The discussion in this section is not affected by the assumption of parity conservation. As it will be clear from Eq. (2.14), that is simply because, by dimensional analysis, the Levi-Civita tensor  $\epsilon^{\mu\nu\rho\sigma}$  cannot appear in the Weyl transformation of the sources. The situation is however different for the Weyl anomaly discussed in section 2.3. Notice that for parity invariant theories,  $G_F$  should be thought as a (maximal) vector subgroup of the full flavor group.

The Weyl symmetry generator is the sum of the variations of the complete set of sources  $\mathcal{J} = (g^{\mu\nu}, \lambda^I, A_\mu^A, m^a)$

$$\delta_\sigma \mathcal{J} \frac{\delta}{\delta \mathcal{J}} \equiv \Delta_\sigma = \Delta_\sigma^g - \Delta_\sigma^\beta \quad (2.12)$$

---

<sup>7</sup>As further reading material we recommend [47, 48].

where

$$\begin{aligned}\Delta_\sigma^g &= \int d^4x \, 2\sigma g^{\mu\nu} \frac{\delta}{\delta g^{\mu\nu}} \\ \Delta_\sigma^\beta &= - \int d^4x \left( \delta_\sigma \lambda \cdot \frac{\delta}{\delta \lambda} + \delta_\sigma A_\mu \cdot \frac{\delta}{\delta A_\mu} + \delta_\sigma m \cdot \frac{\delta}{\delta m} \right).\end{aligned}\quad (2.13)$$

The Weyl variation of the sources will have the most general form compatible with dimensional analysis (power counting) and symmetry (diffeomorphisms and  $G_F$ ). That is:

$$\begin{aligned}\delta_\sigma \lambda^I &= -\sigma \beta^I \\ \delta_\sigma A_\mu^A &= -\sigma \rho_I^A \nabla_\mu \lambda^I + \partial_\mu \sigma S^A \\ \delta_\sigma m^a &= \sigma \left( m^b (2\delta_b^a - \bar{\gamma}_b^a) + C^a R + D_I^a \nabla^2 \lambda^I + \frac{1}{2} E_{IJ}^a \nabla_\mu \lambda^I \nabla^\mu \lambda^J \right) - \partial_\mu \sigma \theta_I^a \nabla^\mu \lambda^I + \nabla^2 \sigma \eta^a\end{aligned}\quad (2.14)$$

where  $\nabla$  denotes the  $G_F$  covariant derivative

$$\nabla_\mu \lambda^I = \partial_\mu \lambda^I + A_\mu^A (T_A \lambda)^I \quad (2.15)$$

and  $T_A$  is a generator of  $G_F$ . By dimensional analysis, the various coefficients  $\beta^I, \rho_I^A, \dots, \eta^a$  in Eq. (2.14) are functions of the marginal couplings  $\lambda^I$ . Moreover, as the Weyl symmetry commutes with  $G_F$ , these coefficients should be covariant functions. It would be straightforward to add to this setup the sources  $\tilde{m}^\alpha$  of relevant scalar deformations having dimension  $\neq 2$  at the original fixed point. By dimensional analysis the transformation would simply reduce to

$$\delta_\sigma \tilde{m}^\alpha = \sigma D_\beta^\alpha \tilde{m}^\beta \quad (2.16)$$

with  $D_\beta^\alpha$  a  $\lambda$ -dependent matrix whose eigenvalues differ from 2 in the whole neighborhood of the fixed point we are studying. Notice that unlike for the case of  $m^a$  in Eq. (2.14), the dimensionality of  $\tilde{m}^\alpha$  forbids the presence of terms involving  $R(g)$  or derivatives of  $\sigma$  and  $\lambda$ .

The local Callan-Symanzik can thus be written as

$$\Delta_\sigma \mathcal{W} = (\Delta_\sigma^g - \Delta_\sigma^\beta) \mathcal{W} = \int d^4x \mathcal{A}_\sigma. \quad (2.17)$$

We shall now study the Weyl generator  $\Delta_\sigma$  in detail, focusing on properties that will help clarify the structure of the anomaly and also help compute the matrix elements of  $T$ .

### The global CS equation, dilations and conformal transformations

It is important to relate the Weyl symmetry generator  $\Delta_\sigma$  to the other incarnations of dilations. First we must relate it to RG transformations, which are obtained as follows. Consider first all the classically dimensionful parameters appearing in  $\mathcal{W}$ . In our case these are just the renormalization scale  $\mu$  and the dimension two sources  $m^a$ . Accounting for the fact that

## 2.2. The local Callan–Symanzik equation

lengths are purely controlled by  $g_{\mu\nu}$ , we have then the obvious identity

$$\Delta^\mu \mathcal{W} \equiv \left[ \mu \frac{\partial}{\partial \mu} + \int d^4x \left( 2m^a(x) \frac{\delta}{\delta m^a(x)} + 2g^{\mu\nu}(x) \frac{\delta}{\delta g^{\mu\nu}(x)} \right) \right] \mathcal{W} = 0. \quad (2.18)$$

By combining the above operator with a Weyl generator with constant parameter  $\sigma = -1$ , in such a way as to eliminate the derivative with respect to the metric, we obtain

$$\Delta^{RG} \equiv \Delta^\mu + \Delta_{\sigma=-1} = \mu \frac{\partial}{\partial \mu} + \int d^4x \left( \beta^I \frac{\delta}{\delta \lambda^I(x)} + \bar{\gamma}_b^a m^b(x) \frac{\delta}{\delta m^a(x)} + \dots \right) \quad (2.19)$$

which corresponds to the ordinary Callan-Symanzik operator generalized to the case of local sources. The RG transformation of the effective action,  $\Delta^{RG}\mathcal{W}$ , is simply the integral of the Weyl anomaly for constant  $\sigma$ . This result establishes a direct connection between the terms in the anomaly and the explicit dependence on  $\ln \mu$  of  $\mathcal{W}$ . This dependence is associated with logarithmic UV divergences. We shall further discuss this connection in section 2.2.3.

The other important incarnations are global dilations and special conformal transformations. They correspond to those particular combinations of a diffeomorphism and a Weyl transformation that leave the flat metric  $\eta_{\mu\nu}$  invariant. The generator of infinitesimal diffeomorphisms is defined by

$$\begin{aligned} \Delta_\xi^{Diff} &= \int d^4x \left( (\nabla_\rho \xi^\mu g^{\rho\nu} + \nabla_\rho \xi^\nu g^{\mu\rho}) \frac{\delta}{\delta g^{\mu\nu}} - \nabla_\mu \xi^\nu A_\nu^A \frac{\delta}{\delta A_\mu^A} \right) \\ &\quad - \int d^4x \xi^\rho \left( \nabla_\rho \lambda^I \frac{\delta}{\delta \lambda^I} + \nabla_\rho A_\nu^A \frac{\delta}{\delta A_\nu^A} + \nabla_\rho m^a \frac{\delta}{\delta m^a} \right). \end{aligned} \quad (2.20)$$

Our assumption that diffeomorphism are non-anomalous corresponds to  $\Delta_\xi^{Diff}\mathcal{W} = 0$  for any  $\xi$ . An infinitesimal dilation is given by the following combination of a diffeomorphism and a Weyl transformation

$$\xi^\mu = cx^\mu \quad \sigma = -c \quad (2.21)$$

The corresponding generator is

$$\begin{aligned} \Delta_c^D &\equiv \Delta_{\xi=cx}^{Diff} + \Delta_{\sigma=-c} \\ &= c \int d^4x \left( \beta^I \frac{\delta}{\delta \lambda^I} + (\rho_I^A \nabla_\mu \lambda^I - A_\mu^A) \frac{\delta}{\delta A_\mu^A} \right) \\ &\quad - c \int d^4x \left( m^b (2\delta_b^a - \bar{\gamma}_b^a) + C^a R + D_I^a \nabla^2 \lambda^I + \frac{1}{2} E_{IJ}^a \nabla_\mu \lambda^I \nabla^\mu \lambda^J \right) \frac{\delta}{\delta m^a} \\ &\quad - c \int d^4x x^\rho \left( \nabla_\rho \lambda^I \frac{\delta}{\delta \lambda^I} + \nabla_\rho A_\nu^A \frac{\delta}{\delta A_\nu^A} + \nabla_\rho m^a \frac{\delta}{\delta m^a} \right) \end{aligned} \quad (2.22)$$

Infinitesimal special conformal transformations are instead given by

$$\xi^\mu = 2(b \cdot x)x^\mu - x^2 b^\mu \quad \sigma = -2b \cdot x \quad (2.23)$$

so that the corresponding generator is

$$\begin{aligned}
\Delta_b^K &\equiv \Delta_{\xi=(2(b \cdot x)x^\mu - x^2 b^\mu)}^{Diff} + \Delta_{\sigma=-2b \cdot x} \\
&= 2b_\mu \int d^4x \left( x^\mu \beta^I \frac{\delta}{\delta \lambda^I} + \left( x^\mu \left( \rho_I^A \nabla_\nu \lambda^I - A_\nu^A \right) - \delta_\nu^\mu S^A \right) \frac{\delta}{\delta A_\nu^A} \right) \\
&\quad - 2b_\mu \int d^4x \left( x^\mu \left( m^b (2\delta_b^a - \bar{\gamma}_b^a) + C^a R + D_I^a \nabla^2 \lambda^I + \frac{1}{2} E_{IJ}^a \nabla_\mu \lambda^I \nabla^\mu \lambda^J \right) - \theta_I^a \nabla^\mu \lambda^I \right) \frac{\delta}{\delta m^a} \\
&\quad - \int d^4x \left( 2(b \cdot x)x^\rho - x^2 b^\rho \right) \left( \nabla_\rho \lambda^I \frac{\delta}{\delta \lambda^I} + \nabla_\rho A_\nu^A \frac{\delta}{\delta A_\nu^A} + \nabla_\rho m^a \frac{\delta}{\delta m^a} \right). \tag{2.24}
\end{aligned}$$

QFTs that are invariant under dilations (and conformal transformations) correspond to points in source space that are left invariant by the action of  $\Delta^D$  (and  $\Delta^K$ ). As expected, a point  $\lambda^I = \lambda_*^I = const$ , such that  $\beta^I = 0$ , with also  $g_{\mu\nu} = \eta_{\mu\nu}$ ,  $A_\mu^A = m^a = 0$  satisfies dilation invariance. On the other hand, from the explicit form of  $\Delta^K$ , one sees that the condition for conformal invariance is a different one. In particular, if  $\beta = 0$  while  $S^A \neq 0$  we have an SFT, that is a QFT with scale invariance but without conformal invariance.

### The local CS equation and the operator algebra

Equation (2.17) encapsulates the relation between  $T$  and the other composite operators. By iterating the equation we find this relation for any number of insertions of  $T$ . We can consider the following distinct cases:

- When none of the points in the time ordered correlator coincide, then by Eq. (2.17) we can write

$$\langle \mathbf{T} \{ T(x) \dots \} \rangle \supset \beta^I \langle \mathbf{T} \{ \mathcal{O}_I(x) \dots \} \rangle + S^A \langle \mathbf{T} \{ \partial_\mu J_A^\mu(x) \dots \} \rangle - \eta^a \langle \mathbf{T} \{ \square \mathcal{O}_a(x) \dots \} \rangle \tag{2.25}$$

This can be understood as an operator equation for  $T$ :

$$T = \beta^I [\mathcal{O}_I] + S^A \partial_\mu [J_A^\mu] - \eta^a \square [\mathcal{O}_a]. \tag{2.26}$$

The coefficients  $\beta^I$ ,  $S^A$  and  $-\eta^a$  are the coordinates of  $T$  in the space of dimension 4 composite operators.

- When two, or more, points coincide, we find contact terms proportional to variations of the coefficients in the Weyl generator, e.g.

$$\begin{aligned}
\langle \mathbf{T} \{ T(x) \mathcal{O}_I(y) \dots \} \rangle &\supset -i\delta(x-y) \left( \partial_I \beta^J \langle \mathbf{T} \{ \mathcal{O}_J(x) \dots \} \rangle - \rho_I^A \langle \mathbf{T} \{ \partial_\mu J_A^\mu(x) \dots \} \rangle \right. \\
&\quad \left. - D_I^a \langle \mathbf{T} \{ \square \mathcal{O}_a(x) \dots \} \rangle \right) \\
\langle \mathbf{T} \{ T(x) \mathcal{O}_I(y) \mathcal{O}_J(z) \dots \} \rangle &\supset -\delta(x-y)\delta(x-z) E_{IJ}^a \langle \mathbf{T} \{ \mathcal{O}_a(x) \dots \} \rangle \tag{2.27}
\end{aligned}$$

- When all points coincide, there are additional ultra-local contributions encoded by the

Weyl anomaly. These will be discussed in section 2.2.3.

It is also interesting to consider the field operator interpretation of the commutators of the source differential operators with  $\Delta^{RG}$ ,  $\Delta^D$  and  $\Delta^K$  defined in the previous section. In particular the commutators with  $\Delta^{RG}$  control the renormalization scale dependence of the corresponding renormalized composite operators. For instance we have

$$\left[ \Delta^{RG}, \frac{\delta}{\delta \lambda^I(x)} \right] = -\partial_I \beta^J \frac{\delta}{\delta \lambda^J(x)} + \dots \quad \rightarrow \quad \mu \frac{d}{d\mu} \mathcal{O}_I = -\partial_I \beta^J \mathcal{O}_J + \dots \quad (2.28)$$

The commutators with  $\Delta^D$  and  $\Delta^K$  control the transformation of the composite operators in the Ward identities for the corresponding (generally explicitly broken) symmetries. At the special symmetry preserving points in parameter space these can be interpreted as the commutator with the corresponding conserved charges  $D$  and  $K^\mu$ . The explicit computation of the commutators among the various functional differential operators leads to the following results

$$\mu \frac{d}{d\mu} \begin{pmatrix} T \\ O_a \\ J_A^\mu \\ O_I \end{pmatrix} = \begin{pmatrix} 0 & 6C^b \square & 0 & 0 \\ 0 & -\bar{\gamma}_a^b & 0 & 0 \\ 0 & D_K^b (T_A \lambda)^K \partial^\mu & -\rho_K^B (T_A \lambda)^K & 0 \\ 0 & D_I^b \square & \rho_I^B \partial_\mu & -\partial_I \beta^J \end{pmatrix} \begin{pmatrix} T \\ O_b \\ J_B^\mu \\ O_J \end{pmatrix} \quad (2.29)$$

$$D \begin{pmatrix} T \\ O_a \\ J_A^\mu \\ O_I \end{pmatrix} = \begin{pmatrix} 4 & -6C^b \square & 0 & 0 \\ 0 & 2\delta_a^b + \bar{\gamma}_a^b & 0 & 0 \\ 0 & -D_K^b (T_A \lambda)^K \partial^\mu & 3\delta_A^B + \rho_K^B (T_A \lambda)^K & 0 \\ 0 & -D_I^b \square & -\rho_I^B \partial_\mu & 4\delta_I^J + \partial_I \beta^J \end{pmatrix} \begin{pmatrix} T \\ O_b \\ J_B^\mu \\ O_J \end{pmatrix} \quad (2.30)$$

$$K^\mu \begin{pmatrix} T \\ O_a \\ J_A^\nu \\ O_I \end{pmatrix} = 2 \begin{pmatrix} 0 & 6C^b \partial^\mu & 0 & 0 \\ 0 & 0 & 0 & 0 \\ 0 & -(D_K^b + \theta_K^b) (T_A \lambda)^K g^{\mu\nu} & 0 & 0 \\ 0 & (2D_I^b + \theta_I^b) \partial^\mu & \rho_I^B + \partial_I S^B & 0 \end{pmatrix} \begin{pmatrix} T \\ O_b \\ J_B^\mu \\ O_J \end{pmatrix} \quad (2.31)$$

Focusing on fixed points, we shall later comment on the consistency of the above results with the algebra of unitary conformal field theory.

### Ward identities and ambiguities

The basis of renormalized operators used to write  $T$  in Eq. (2.26) is redundant in the presence of symmetries. Indeed, by the equations of motion,  $\nabla_\mu J_A^\mu$  equals the  $G_F$  variation of the Lagrangian and can thus be expressed in terms of a combination of  $\mathcal{O}_I$  and  $\mathcal{O}_a$ . In the background source approach this is viewed by considering the  $G_F$  Ward identity ( $\alpha^A(x)$  are

the Lie parameters of  $G_F$ )

$$\Delta_\alpha^F \mathcal{W} \equiv \int d^4x \left[ \alpha^A \left( (T_A \lambda)^I \frac{\delta}{\delta \lambda^I(x)} + (T_A m)^a \frac{\delta}{\delta m^a(x)} \right) - \nabla_\mu \alpha^A \left( \frac{\delta}{\delta A_\mu^A(x)} \right) \right] \mathcal{W} = 0 \quad (2.32)$$

which simply translates into the operator equation

$$(T_A \lambda)^I \mathcal{O}_I + (T_A m)^a \mathcal{O}_a + \nabla_\mu J_A^\mu = 0. \quad (2.33)$$

An alternative procedure is to define a new Weyl generator by combining the original  $\Delta_\sigma$  with an infinitesimal  $G_F$  transformation with Lie parameter  $\alpha^A(x) = -\sigma(x)\omega^A(\lambda)$

$$\Delta_\sigma \rightarrow \Delta'_\sigma \equiv \Delta_\sigma + \Delta_{-\sigma\omega}^F \quad (2.34)$$

Provided  $\omega^A(\lambda)$  is chosen to be a covariant (but otherwise arbitrary) function of the  $\lambda$ 's, the redefined Weyl symmetry still commutes with  $G_F$ . Eq. (2.34) corresponds to the following redefinition of the coefficients of the local CS operator:

$$\begin{aligned} \beta^I &\rightarrow \beta^I + (\omega^A T_A \lambda)^I & \bar{\gamma}_b^a &\rightarrow \bar{\gamma}_b^a + (\omega^A T_A)_b^a \\ S^A &\rightarrow S^A + \omega^A & \rho_I^A &\rightarrow \rho_I^A - \partial_I \omega^A. \end{aligned} \quad (2.35)$$

Notice that this is an ambiguity inherent in the definition of the  $\beta$ -function and of the anomalous dimensions [26, 49]. When carrying out the renormalization procedure this ambiguity corresponds to the freedom in defining the wave function renormalization matrix relating bare and renormalized fields [25].

The redundancy in the definition of  $\Delta_\sigma$  is quite analogous to a gauge symmetry. Like for gauge symmetry, unambiguous physical information is carried by the invariants, which in our case are given by

$$\begin{aligned} B^I &= \beta^I - (S^A T_A \lambda)^I \\ P_I^A &= \rho_I^A + \partial_I S^A \\ \gamma_b^a &= \bar{\gamma}_b^a - (S^A T_A)_b^a. \end{aligned} \quad (2.36)$$

These are the quantities that unambiguously describe the RG flow. Indeed they correspond to fixing the “gauge” by choosing  $\omega^A = -S^A$  in Eq. (2.35) so that the redefined  $S^A$  vanishes. Correspondingly, by solving for  $\nabla_\mu J_A^\mu$  in Eq. (2.33), at  $m_a = 0$ ,  $T$  in Eq. (2.26) reads

$$T = B^I [\mathcal{O}_I] - \eta^a \square [\mathcal{O}_a]. \quad (2.37)$$

Notice that by the change in Eq. (2.34) also the  $\Delta^{RG}$  acquires an extra flavor rotation term. Making the choice  $\omega^A = -S^A$  and using Eq. (2.33), the RG transformation of the renormalized

## 2.2. The local Callan–Symanzik equation

operators becomes then (disregarding the contribution from  $\mathcal{O}_a$ )

$$\mu \frac{d}{d\mu} \begin{pmatrix} J_A^\mu \\ O_I \end{pmatrix} = \begin{pmatrix} -P_K^B(T_A\lambda)^K & 0 \\ 0 & -(\partial_I B^J + P_I^C(T_C\lambda)^J) \end{pmatrix} \begin{pmatrix} J_B^\mu \\ O_J \end{pmatrix} \quad (2.38)$$

With this definition, we can identify the following matrices as the anomalous dimensions of the composite operators

$$\begin{aligned} \gamma_I^J &= \partial_I B^J + P_I^A(T_A\lambda)^J \\ \gamma_A^B &= P_K^B(T_A\lambda)^K. \end{aligned} \quad (2.39)$$

### Lie derivatives

A recurrent object that will appear in the analysis is a variant of the Lie derivative, which describes the Weyl transformation of covariant tensors

$$\begin{aligned} \mathcal{L}[Y_{IAa\dots}^{JBb\dots}] &= B^K \partial_K Y_{IAa\dots}^{JBb\dots} + \gamma_I^K Y_{K Aa\dots}^{JBb\dots} + \gamma_A^C Y_{I C a\dots}^{JBb\dots} + \gamma_a^c Y_{I A c\dots}^{JBb\dots} \\ &\quad - \gamma_K^J Y_{I A a\dots}^{K B b\dots} - \gamma_C^B Y_{I A a\dots}^{J C b\dots} - \gamma_c^b Y_{I A a\dots}^{J B c\dots} + \dots \end{aligned} \quad (2.40)$$

where the different  $\gamma$  matrices were defined in (2.36) and (2.39). The operator  $\mathcal{L}$  so defined satisfies the distributive property of derivatives when considering products of tensors, including contractions of covariant and contravariant indices. Schematically one has

$$\mathcal{L}[Y \cdot Z] = Y \cdot \mathcal{L}[Z] + \mathcal{L}[Y] \cdot Z. \quad (2.41)$$

For instance one has  $\mathcal{L}[Y_A^I \cdot Z^A] = Y_A^I \mathcal{L}[Z^A] + \mathcal{L}[Y_A^I] Z^A$ . Moreover one can easily check that the tensor  $v_A^I \equiv (T_A\lambda)^I$  satisfies  $\mathcal{L}[v_A^I] = 0$  and can thus be carried freely in and out of the  $\mathcal{L}$  symbol. The latter property depends crucially on Eq. (2.39) which relates the anomalous dimensions for scalars and currents. The Lie derivative appears, for example, in the Weyl variation of space-time derivatives of the sources

$$\begin{aligned} \Delta_\sigma(Y_I \nabla^\mu \lambda^I) &= \sigma(-\mathcal{L}[Y_I] \nabla_\mu \lambda^I) + \partial_\mu \sigma(-B^I Y_I) \\ \Delta_\sigma(Y_I \nabla^2 \lambda^I) &= \sigma(2Y_I \nabla^2 \lambda^I - \mathcal{L}[Y_I] \nabla^2 \lambda^I - Y_I U_J^I \gamma_{KL}^J \nabla_\mu \lambda^K \nabla^\mu \lambda^L) \\ &\quad + \partial_\mu \sigma(-2Y_I U_J^I \nabla^\mu \lambda^J) + \nabla^2 \sigma(-B^I Y_I) \end{aligned} \quad (2.42)$$

where  $Y_I$  is an arbitrary covariant function, and where we also defined the following tensors

$$\begin{aligned} U_I^J &= \delta_I^J + \partial_I B^J + \frac{1}{2} P_I^A(T_A\lambda)^J \\ \gamma_{JK}^I &= (U^{-1})_L^I (\partial_{(J} \gamma_{K)}^L + P_{(J}^A(T_A)_K^L) \end{aligned} \quad (2.43)$$

Notice that in the specific example of Eq. (2.42) the Weyl operator acts on  $G_F$  singlets. Therefore the result is automatically dependent only on the invariant coefficient functions  $B$  and  $P$ . In the case of the Weyl variation of tensors of  $G_F$  there would appear an additional

$G_F$  rotation with Lie parameter  $S^A$ . In the course of our study we shall however mostly encounter the action on  $G_F$  singlets.

### Source reparametrization and the form of $\Delta_\sigma$

The choice of parametrization of the sources is of course subject to some freedom. A change of parametrization leads to a change in the definition of the renormalized composite operators and in the form of the Weyl operator  $\Delta_\sigma$ . Compatibly with dimensionality, one can consider the reparametrization

$$\begin{aligned}\lambda^{I'} &= \lambda^I + f^I \\ A_\mu^{A'} &= A_\mu^A + f_I^A \nabla_\mu \lambda^I \\ m^{a'} &= m^a + f_b^a m^b + \frac{1}{6} f^a R + f_I^a \nabla^2 \lambda^I + \frac{1}{2} f_{IJ}^a \nabla_\mu \lambda^I \nabla^\mu \lambda^J .\end{aligned}\quad (2.44)$$

Provided the various coefficients  $f_I, f_I^A, \dots$  respect  $G_F$  covariance, the new parameters  $\lambda^{I'}, A_\mu^{A'}, m^{a'}$  transform as the corresponding original ones under  $G_F$ . The effective action changes form but its value is unaffected:

$$\mathcal{W}'[g, \lambda', A', m'] \equiv \mathcal{W}[g, \lambda, A, m]. \quad (2.45)$$

The form of the Weyl operator in the new coordinates is straightforwardly derived by applying the chain rule. One finds the following relation for the coefficients in the new coordinate system:

$$\begin{aligned}\beta^{I'} &= \beta^I + \beta^J \partial_J f^I \\ \rho_I^{A'} &= \rho_I^A + \mathcal{L}[f_I^A] \\ S^{A'} &= S^A - B^I f_I^A \\ C^{a'} &= C^a - \frac{1}{6} \mathcal{L}[f^a] \\ D_I^{a'} &= D_I^a - \mathcal{L}[f_I^a] \\ E_{IJ}^{a'} &= E_{IJ}^a - \mathcal{L}[f_{IJ}^a] - 2U_L^K \gamma_{IJ}^L f_K^a \\ \theta_I^{a'} &= \theta_I^a + B^J f_{JI}^a + 2U_I^J f_J^a \\ \eta^{a'} &= \eta^a + f^a - B^I f_I^a\end{aligned}\quad (2.46)$$

where we used the Lie derivative and the matrix  $U_I^J$  introduced in the previous section.

The most important remark concerning the above equation is that by a suitable choice of  $f^a$  and  $f_I^a$ , the tensor coefficients  $\eta^a$  and  $\theta_I^a$  can both be set to zero. As suggested by Eq. (2.37), and as further clarified in section 2.2.2, the choice  $\eta^a = 0$  corresponds to an “improved” energy momentum tensor.

As we said, the change of coordinates corresponds to a redefinition of the renormalized operators. It is possible, however to find linear combinations of operators that are invariant under the



## 2.2. The local Callan–Symanzik equation

change of basis. Consider, for example, the change of coordinates  $m^a \rightarrow m^{a'} = m^a + f_I^a \nabla^2 \lambda^I$ . Focusing on the scalars for simplicity, the operators in the new basis are related to the original ones via

$$\begin{aligned} [\mathcal{O}_I] &= [\mathcal{O}_I]' + f_I^a \square [\mathcal{O}_a]' \\ [\mathcal{O}_a] &= [\mathcal{O}_a]' \end{aligned} \quad (2.47)$$

Combining this with Eq. (2.46) we find that the operator

$$[\tilde{\mathcal{O}}_I] = [\mathcal{O}_I] + \frac{1}{2} (U^{-1})_I^J \theta_J^a \square [\mathcal{O}_a] \quad (2.48)$$

is scheme independent. This definition will be useful in section 3.1.4.

### Consistency conditions

The abelian nature of the Weyl symmetry imposes constraints on the form of the generator  $\Delta_\sigma$ . The vanishing of the commutator

$$[\Delta_{\sigma_2}, \Delta_{\sigma_1}] = 0 \quad (2.49)$$

leads to a set of equations relating the different coefficients appearing in (2.14):

$$\begin{aligned} B^I P_I^A &= 0 \\ B^I D_I^a &= \mathcal{L}[\eta^a] + 6C^a \\ B^J E_{JI}^a &= -\mathcal{L}[\theta_I^a] - 2U_I^J D_J^a. \end{aligned} \quad (2.50)$$

Notice that these consistency conditions are independent of the choice of gauge discussed in section 2.2.2. Alternatively, as shown in appendix A.2, these conditions can be derived by directly computing the coefficients of  $\Delta_\sigma$  from a dimensionally regulated action. According to that derivation the abelian nature of Weyl invariance, as realized on the bare sources in Eq. (A.13), is just an explicit fact, which need not be imposed.

One can easily check that the consistency condition  $P_I^A B^I = 0$  implies  $\mathcal{L}[B^I] = 0$ . Together with  $\mathcal{L}[(T_A \lambda)^I] = 0$  we thus have

$$\begin{aligned} B^I \mathcal{L}[Y_{IJ\dots}] &= \mathcal{L}[B^I Y_{IJ\dots}] \\ (T_B \lambda)^I \mathcal{L}[Y_{AI\dots}] &= \mathcal{L}[(T_B \lambda)^I Y_{AI\dots}] \end{aligned} \quad (2.51)$$

What role is played by Eq. (2.50)? For instance, at a point where  $B = 0$ , the second equation ensures that, once the choice  $\eta^a = 0$  is made,  $C^a$  must also vanish. Eq. (2.29) then implies that if  $T$  is improved so as to vanish at a given RG scale then it automatically vanishes at all scales. The first equation, as we shall see in section 3, ensures the absence of currents in the short distance singularities of correlators with multiple insertions of  $T$ . This significantly

simplifies the derivations of constraints on the structure of RG flows.

### Dimension 2 covariant functions

In general, the Weyl transformation of dimensionful functions of the sources contains derivatives of  $\sigma$  (see Eq. (2.42)). However, it is possible to find linear combinations of dimension 2 functions which transform “covariantly” under this symmetry:

$$\begin{aligned}\Pi^{IJ} &= \nabla_\mu \lambda^I \nabla^\mu \lambda^J - B^{(I} \Lambda^{J)} \\ \Pi^a &= m^a - \eta^a \frac{R}{6} - \frac{1}{2} \theta_I^a \Lambda^I\end{aligned}\tag{2.52}$$

where we defined the function

$$\Lambda^I = (U^{-1})^I_J \left( \nabla^2 \lambda^J + \frac{1}{6} B^J R \right).\tag{2.53}$$

The variations of  $\Pi^{IJ}$  and  $\Pi^a$  contain no derivatives of  $\sigma$ . In the “gauge”  $S^A = 0$  they are

$$\begin{aligned}\Delta_\sigma \Pi^{IJ} &= \sigma \left( 2\Pi^{IJ} - \gamma_K^I \Pi^{KJ} - \gamma_K^J \Pi^{IK} + \gamma_{KL}^{IJ} \Pi^{KL} \right) \\ \Delta_\sigma \Pi^a &= \sigma \left( 2\Pi^a - \gamma_b^a \Pi^b + \gamma_{IJ}^a \Pi^{IJ} \right)\end{aligned}\tag{2.54}$$

where we defined the tensors

$$\begin{aligned}\gamma_{KL}^{IJ} &= B^{(I} \gamma_{KL}^{J)} \\ \gamma_{IJ}^a &= \frac{1}{2} \left( E_{IJ}^a + \theta_K^a \gamma_{IJ}^K \right).\end{aligned}\tag{2.55}$$

In computing the transformation property of  $\Pi^a$  we imposed the consistency conditions (2.50).  $\Pi^{IJ}$  and  $\Pi^a$  will play an important role in the rest of this Chapter.

### Limiting cases

It is interesting to consider various limiting ‘fixed points’. Focusing on  $T$  in Eq. (2.26), we can basically consider three cases:

1. When both  $\eta^a$  and  $B^I \equiv \beta^I - S^A (T_A \lambda)^I$  are zero the operator  $T$  vanishes, corresponding to a conformal fixed point. Notice that conformality is signaled by the vanishing of  $B^I$  and not of any other choice of  $\beta$ -function. Conformal theories with non-vanishing  $\beta$ -functions were discovered in [40].

It is interesting to consider the conformal transformations in Eq. (2.31) in this limit. Choosing a parametrization where  $\theta_I^a = 0$ , the consistency conditions Eq. (2.50) imply  $D_I^a = C^a = 0$ , so that all entries in Eq. (2.31) vanish, apart from one. In particular one finds  $K^\mu \mathcal{O}^a = K^\mu J_A^\mu = 0$ , consistent with these operators being primaries, but also  $K^\mu \mathcal{O}_I = -P_I^A J_A^\mu$ , indicating that some of the  $\mathcal{O}^I$  are descendants of the currents. This

## 2.2. The local Callan–Symanzik equation

result is indeed expected because of Eq. (2.33). In appendix A.3 we study this in detail showing there exists an operator basis where each broken symmetry current is associated to a unique scalar descendant. In this basis all the remaining scalar operators are annihilated by the generator of special conformal transformations and all the remaining currents are conserved and have vanishing anomalous dimension.

2. The case  $B^I = 0$  and  $\eta^a \neq 0$  corresponds to a fixed point whose energy-momentum tensor is not improved

$$T(x) = -\eta^a \square [\mathcal{O}_a] . \quad (2.56)$$

This possibility is relevant when considering a QFT flowing to different CFTs in the UV and in the IR. Adjusting the coupling to the background metric such that the energy momentum tensor is improved at one asymptotic does not imply improvement at the other.

3. Another type of conceivable fixed point is an SFT, corresponding to the existence of a scheme where  $\beta^I = 0$  but  $S_A \neq 0$  so that  $B^I \neq 0$ . As noticed below (2.24), such point in coupling space is invariant under dilation but not under conformal transformations. In this case (2.26) becomes

$$T = -\partial_\mu [V^\mu] \quad (2.57)$$

where  $V^\mu = S^A J_A^\mu + \eta^a \partial^\mu \mathcal{O}_a$  is referred to as the virial current. By Eq. (2.37), since  $B^I \neq 0$  and since  $\mathcal{O}_I$  and  $\mathcal{O}_a$  are independent operators, we have also that  $T = -\partial_\mu V^\mu \neq 0$ , with no possibility of improvement to make  $T = 0$ . The fact that  $T$  vanishes only up to a total derivative is another way to see that the theory is endowed with global scale invariance, but not with conformal invariance (local scale invariance). Perturbative unitary SFTs are ruled out by the argument in ref. [25], which we shall revisit in section 3.1.4.

Notice that in the case of an SFT, one can consistently consider a reduced set of sources by freezing  $\lambda^I = \lambda_*^I = \text{const}$  such that  $\beta^I = 0$  and by reducing  $A_\mu^A$  to a one dimensional subspace:  $A_\mu^A \equiv S^A C_\mu$ . One can then easily check that the Weyl transformation of  $A_\mu^A$  in Eq. (2.14), simply reduces to  $\delta_\sigma C_\mu = \partial_\mu \sigma$ . The relation  $B^I P_I^A = 0$  is essential to obtain this result. The source  $C_\mu$  so defined thus corresponds to the virial current gauge field of ref. [25]. Notice also that the inhomogeneous terms in  $\delta_\sigma m^a$ , at  $\eta^a = \theta_I^a = 0$ , package into a term proportional to  $\tilde{R} \equiv R + 6\partial^\mu C_\mu - 6C^\mu C_\mu$ . Similarly the quantities  $\Pi^{IJ}$  reduce to constant coefficients times  $\tilde{R}$ . The quantity  $\tilde{R}$  on the reduced set of sources  $g_{\mu\nu}, C_\mu$  satisfies  $\delta_\sigma \tilde{R} = 2\sigma \tilde{R}$  and plays an important role in the structure of the anomaly in a SFT, as we shall comment later.

### 2.2.3 The structure of the Weyl anomaly

We will now discuss the structure of the anomaly appearing in the local CS equation

$$\Delta_\sigma \mathcal{W}[g, \lambda, m, A] = \int d^4x \mathcal{A}_\sigma \quad (2.58)$$

First, let us review the anomaly at an improved conformal fixed point ( $B^I = \eta^a = 0$ ). This case corresponds to freezing all the sources apart from the metric ( $\lambda^I = \lambda_*^I = \text{const}$ , such that  $B^I(\lambda_*) = 0$  and  $A_\mu^A = m^a = 0$ ). The Weyl generator  $\Delta_\sigma$  thus reduces to the metric variation  $\Delta_\sigma^g$ . The anomaly  $\mathcal{A}_\sigma$  is a linear combination of all the dimension 4 scalars that can be constructed from the metric and its derivatives [34, 50]

$$\frac{1}{\sqrt{-g}} \mathcal{A}_\sigma = \sigma \left( aE_4 - bR^2 - cW^2 \right) - \nabla^2 \sigma dR. \quad (2.59)$$

where  $R$  is the scalar curvature,  $W^2$  is the Weyl tensor squared, and  $E_4$  is the 4-dimensional Euler density.

The anomaly is constrained by a Wess-Zumino integrability condition [51]: since the Weyl symmetry is abelian, one must have

$$\Delta_{\sigma_2}^g \left( \int dx_1 \mathcal{A}_{\sigma_1} \right) - \Delta_{\sigma_1}^g \left( \int dx_2 \mathcal{A}_{\sigma_2} \right) = [\Delta_{\sigma_2}^g, \Delta_{\sigma_1}^g] \mathcal{W} = 0. \quad (2.60)$$

This condition is satisfied by all terms in Eq. (2.59) apart from  $R^2$ . At a CFT fixed point, the anomaly coefficient  $b$  must therefore vanish.

Deser and Schwimmer classified the conformal anomalies into three types [52]:

- Contributions that equal the variation of a local functional. Such contributions can be eliminated by adding to the action a suitable local functional. They must, therefore, not be considered as genuine anomalies. In the present case,  $\nabla^2 \sigma R$  corresponds to such a removable term, as it equals the Weyl variation of  $\sqrt{g}R^2$ .
- Type “A”: Anomalies that vanish when integrated over space-time with a constant  $\sigma$ . An equivalent characterization of these anomalies is that they do not contribute to

$$\mu \frac{d}{d\mu} \mathcal{W} \equiv \Delta^{RG} \mathcal{W}. \quad (2.61)$$

Therefore type “A” anomalies are not associated with additional (logarithmic) UV divergences arising in the presence of space-time dependent sources. The Euler density anomaly is such an anomaly because its integral vanishes on topologically trivial spaces, such as Minkowski space. In practice this is because  $\sqrt{g}E_4$  can be locally written as a total derivative (of a non covariant quantity).

- Type “B”: Anomalies that do not vanish when integrated over space-time. Equivalently, by the previous argument involving  $\Delta^{RG}$ , these anomalies are associated with an explicit

## 2.2. The local Callan–Symanzik equation

In  $\mu$  dependence in the effective action. In 4D CFTs the corresponding anomaly is  $W^2$ . An example of the associated  $\ln \mu$  dependence is given by the two point function of  $T_{\mu\nu}$  which in Fourier space reads

$$\langle T_{\mu\nu} T_{\rho\sigma} \rangle = c \Pi_{\mu\nu\rho\sigma}^{(2)} p^4 \ln p^2 / \mu^2, \quad (2.62)$$

where  $\Pi_{\mu\nu\rho\sigma}^{(2)}$  is the projector on transverse traceless 2-index tensors.

Strictly speaking, also the  $E_4$  can give rise to a  $\ln \mu$  dependence, but only when the CFT is embedded in a space with non trivial topology, like for instance the sphere  $S_4$ . In any case, the logarithmic divergences associated with  $E_4$  do not affect local quantities, such as correlators.

Let us now consider the anomaly in the presence of all the external sources, and see what becomes of the properties we just discussed. Up to terms involving  $e^{\mu\nu\rho\sigma}$ , the most general form, first given in [26], is

$$\begin{aligned} \frac{1}{\sqrt{-g}} \mathcal{A}_\sigma &= \sigma \left( \beta_a W^2 + \beta_b E_4 + \frac{1}{9} \beta_c R^2 \right) - \nabla^2 \sigma \left( \frac{1}{3} dR \right) \\ &+ \sigma \left( \frac{1}{3} \chi_I^e \nabla_\mu \lambda^I \nabla^\mu R + \frac{1}{6} \chi_{IJ}^f \nabla_\mu \lambda^I \nabla^\mu \lambda^J R + \frac{1}{2} \chi_{IJ}^g G^{\mu\nu} \nabla_\mu \lambda^I \nabla_\nu \lambda^J \right. \\ &\quad \left. + \frac{1}{2} \chi_{IJ}^a \nabla^2 \lambda^I \nabla^2 \lambda^J + \frac{1}{2} \chi_{JK}^b \nabla_\mu \lambda^I \nabla^\mu \lambda^J \nabla^2 \lambda^K + \frac{1}{4} \chi_{IJKL}^c \nabla_\mu \lambda^I \nabla^\mu \lambda^J \nabla_\nu \lambda^K \nabla^\nu \lambda^L \right. \\ &+ \partial^\mu \sigma \left( G_{\mu\nu} w_I \nabla^\nu \lambda^I + \frac{1}{3} R Y_I \nabla_\mu \lambda^I + \tilde{S}_{IJ} \nabla_\mu \lambda^I (U^{-1})_K^J \nabla^2 \lambda^K + \frac{1}{2} T_{IJK} \nabla_\nu \lambda^I \nabla^\nu \lambda^J \nabla_\mu \lambda^K \right) \\ &- \nabla^2 \sigma \left( U_I \nabla^2 \lambda^I + \frac{1}{2} V_{IJ} \nabla_\nu \lambda^I \nabla^\nu \lambda^J \right) \\ &+ \sigma \left( \frac{1}{2} p_{ab} \hat{m}^a \hat{m}^b + \hat{m}^a \left( \frac{1}{3} q_a R + r_{aI} \nabla^2 \lambda^I + \frac{1}{2} s_{aIJ} \nabla_\mu \lambda^I \nabla^\mu \lambda^J \right) \right) \\ &+ \partial_\mu \sigma \left( \hat{m}^a j_{aI} \nabla^\mu \lambda^I \right) - \nabla^2 \sigma \left( \hat{m}^a k_a \right) \\ &+ \sigma \left( \frac{1}{4} \kappa_{AB} F_{\mu\nu}^A F^{B\mu\nu} + \frac{1}{2} \zeta_{AIJ} F_{\mu\nu}^A \nabla^\mu \lambda^I \nabla^\nu \lambda^J \right) + \partial^\mu \sigma \left( \eta_{AI} F_{\mu\nu}^A \nabla^\nu \lambda^I \right) \end{aligned} \quad (2.63)$$

where  $G_{\mu\nu}$  is the Einstein tensor,  $F_{\mu\nu}^A$  is the field strength associated with the background field  $A_\mu^A$  and  $\hat{m}^a = m^a - \frac{1}{6} \eta^a R$ . As in the CFT limit,  $\mathcal{A}_\sigma$  is redundant, in that it is only defined modulo the variation of a local functional  $F$  of the sources:  $\mathcal{A}_\sigma \sim \mathcal{A}_\sigma + \Delta_\sigma F$ . This redundancy corresponds to the freedom in choosing a renormalization procedure. At the same time  $\mathcal{A}_\sigma$  is subject to the Wess-Zumino consistency condition, now given by the analogue of Eq. (2.60) with  $\Delta_\sigma$  instead of  $\Delta_\sigma^g$ ,

$$\Delta_{\sigma_2} \left( \int dx_1 \mathcal{A}_{\sigma_1} \right) - \Delta_{\sigma_1} \left( \int dx_2 \mathcal{A}_{\sigma_2} \right) = [\Delta_{\sigma_2}, \Delta_{\sigma_1}] \mathcal{W} = 0. \quad (2.64)$$

This condition translates [26] into  $\sim 10$  differential equations involving the 25 tensor coefficients appearing in  $\mathcal{A}_\sigma$ .

A new result, which we present here, is a reformulation of the anomaly, in which most of the consistency equations are explicitly solved, leaving only three non-trivial constraints. One

of these is the equation discovered in [32, 26] and describing the flow of the coefficient  $a$ . The other two equations involve instead the anomaly coefficients associated with the flavor gauge fields. One key observation in our analysis is that, by eliminating a suitable set of scheme dependent terms, most of the consistency equations become algebraic. They can thus be readily solved and substituted back into the anomaly. The consistency equations in this suitable scheme choice appear in appendix A.4.

According to our analysis the general anomaly in Eq. (2.63) can be written as a sum of five terms which we indicate using an analogy with the Weyl anomaly of a CFT (Eq. (2.59)):

$$\mathcal{A}_\sigma = \mathcal{A}_\sigma^{\nabla^2 R} + \mathcal{A}_\sigma^{R^2} + \mathcal{A}_\sigma^{W^2} + \mathcal{A}_\sigma^{E_4} + \mathcal{A}_\sigma^{F^2} . \quad (2.65)$$

The different parts of the anomaly are:

1. Generalized  $\nabla^2 R$  anomaly

The generalized  $\nabla^2 R$  anomaly represents the terms that can be written as  $\Delta_\sigma F$  and can thus be eliminated by a choice of scheme. By a proper choice of local terms, that is specified in the appendix, the coefficients  $d, U_I, V_{IJ}, \tilde{S}_{(IJ)}, T_{IJK}, k_a, j_{aI}$  can be set to zero.

2. Generalized  $R^2$  anomaly

The terms associated with  $\beta_c, Y_I, \chi_I^e, \chi_{IJ}^f, \chi_{IJ}^a, \chi_{IJK}^b, q_a, r_{aI}$  can be rewritten using the consistency equations in the following compact form:

$$\frac{1}{\sqrt{-g}} \mathcal{A}_\sigma^{R^2} = \sigma \left( \frac{1}{2} b_{ab} \Pi^a \Pi^b + \frac{1}{2} b_{aIJ} \Pi^a \Pi^{IJ} + \frac{1}{4} b_{IJKL} \Pi^{IJ} \Pi^{KL} \right) \quad (2.66)$$

This part of the anomaly is simply the most general bilinear scalar constructed from the covariant objects  $\Pi^{IJ}$  and  $\Pi^a$  which were defined in (2.52). Since the variation of the  $\Pi$ 's does not contain derivatives of  $\sigma$ , the above term is manifestly consistent.

We refer to this anomaly as the generalized  $R^2$  anomaly because in the limit where  $\nabla\lambda = m = 0$  the only term remaining from this anomaly is proportional to  $R^2$ . The definitions of the coefficients appearing here, in terms of the original parameterization of the anomaly, are given in the appendix.

3. Generalized  $W^2$  anomaly

$$\frac{1}{\sqrt{-g}} \mathcal{A}_\sigma^{W^2} = -\sigma c W^2 \quad (2.67)$$

The form of the  $W^2$  anomaly is unchanged off criticality. The only difference is that the  $c$  coefficient is replaced by a function of the sources  $\lambda^I$ , but the anomaly remains manifestly consistent.

4. Generalized  $E_4$  anomaly

## 2.2. The local Callan–Symanzik equation

As in the case of the  $W^2$  anomaly, away from the fixed point, the coefficient of the  $E_4$  anomaly is a function of the  $\lambda$ 's, and is thus space-time dependent. However, since the Weyl variation of  $E_4$  contains two derivatives of  $\sigma$ , the consistency condition involves (after integration by parts) terms proportional to  $\nabla_\mu a$ , which are not present at the fixed point where  $a(\lambda)$  is a numerical constant. The result is that the  $E_4$  anomaly is no longer automatically consistent away from criticality: additional terms must exist in order to restore consistency. We find that a consistent anomaly containing  $E_4$  must have the following structure:

$$\begin{aligned} \frac{1}{\sqrt{-g}} \mathcal{A}_\sigma^{E_4} &= \sigma \left( a E_4 + \chi_{IJ}^g \left( \frac{1}{2} \Gamma_{\mu\nu} \nabla^\mu \lambda^I \nabla^\nu \lambda^J - \frac{1}{4} U_K^I \Lambda^K \Lambda^J \right) + \frac{1}{2} \bar{\chi}_{IJK}^g \Omega^{IJK} \right) \\ &\quad + \partial^\mu \sigma \left( w_I G_{\mu\nu} \nabla^\nu \lambda^I \right) - \frac{1}{2} \partial_{[J} w_{I]} \Xi_\sigma^{IJ} \end{aligned} \quad (2.68)$$

where  $\chi_{IJ}^g$  and  $w_I$  are functions of  $\lambda$ , introduced in Eq. (2.63), and where we used the notations defined in sec. 2.2.2 plus the definitions

$$\begin{aligned} \Gamma_{\mu\nu} &= G_{\mu\nu} + \frac{R}{6} g_{\mu\nu} \\ \Omega^{IJK} &= \left( \Pi^{IJ} + \frac{1}{2} B^{(I} \Lambda^{J)} \right) \Lambda^K \\ \Xi_\sigma^{IJ} &= \Lambda^I \left( 2 \partial_\mu \sigma \nabla^\mu \lambda^J - \sigma \gamma_{KL}^J \Pi^{KL} \right). \end{aligned} \quad (2.69)$$

and

$$\bar{\chi}_{IJK}^g = -\partial_{(J} \chi_{KI)}^g + \frac{1}{2} \partial_K \chi_{IJ}^g. \quad (2.70)$$

Notice that, even though it involves several terms, this anomaly is described by just three tensor functions  $a, w_I, \chi_{IJ}^g$ . Moreover, Wess-Zumino consistency implies the following constraint

$$\mathcal{L}[w_I] = -8 \partial_I a + \chi_{IJ}^g B^J \quad (2.71)$$

### 5. Generalized $F^2$ anomaly

The generalized  $F^2$  anomaly depends on three coefficients,  $\kappa_{AB}, \zeta_{AIJ}$  and  $\eta_{AI}$ , and takes the form

$$\begin{aligned} \frac{1}{\sqrt{-g}} \sigma \mathcal{A}_\sigma^{F^2} &= \sigma \left( \frac{1}{4} \kappa_{AB} F_{\mu\nu}^A F^{B\mu\nu} + \frac{1}{2} \zeta_{AIJ} F_{\mu\nu}^A \nabla^\mu \lambda^I \nabla^\nu \lambda^J \right. \\ &\quad \left. + \left( \frac{1}{2} P_I^A \zeta_{AJK} + \eta_{AI} \partial_{[J} P_{K]}^A \right) \Omega^{IJK} \right) \\ &\quad + \partial^\mu \sigma \left( \eta_{AI} F_{\mu\nu}^A \nabla^\nu \lambda^I \right) - \frac{1}{2} \eta_{A[I} P_{J]}^A \Xi_\sigma^{IJ} \end{aligned} \quad (2.72)$$

The three coefficients appearing in this anomaly are related to one another and to the

coefficients of the generalized  $E_4$  anomaly via 2 consistency conditions<sup>8</sup>

$$\begin{aligned}\mathcal{L}[\eta_{AI}] &= \kappa_{AB}P_I^B + \zeta_{AIJ}B^J - \chi_{IJ}^g(T_A\lambda)^J \\ 0 &= \eta_{AI}B^I + w_I(T_A\lambda)^I\end{aligned}\tag{2.73}$$

In the end we find that the anomaly can be described by 10 physical scheme independent tensorial coefficients, constrained by the 3 consistency conditions in Eqs.(2.71,2.73). Note however that the second constraint in (2.73) is not fully independent from the other two. Indeed, the vanishing of the Lie derivative of this constraint is automatic once the other two constraints are enforced.

### Comments on the $R^2$ anomaly

Some comment on the  $\mathcal{A}_\sigma^{R^2}$  anomaly are in order, as it represents a novelty compared to the well known CFT limit. We will show that it is associated with logarithmic divergences in CFTs that can be “unimproved” when scalar operators of dimension exactly equal to two are present. We will also show that the components associated with operators with non-zero anomalous dimensions can be eliminated by a choice of scheme.

The coefficients  $b_{ab}$ ,  $b_{aIJ}$  and  $b_{IJKL}$  are associated with the short distance singularities in respectively  $\langle\mathcal{O}_a\mathcal{O}_b\rangle$ ,  $\langle\mathcal{O}_a\mathcal{O}_I\mathcal{O}_J\rangle$  and  $\langle\mathcal{O}_I\mathcal{O}_J\mathcal{O}_K\mathcal{O}_L\rangle$ . To see this, let us perform analytic continuation to work with Euclidean signature, and follow an argument similar to the one presented, for instance, in [53]. Consider the action of the RG flow operator  $\Delta^{RG}$  on the correlator  $G_{ab}(x) \equiv \langle\mathcal{O}_a(x)\mathcal{O}_b(0)\rangle$ ,

$$\mu\frac{d}{d\mu}G_{ab}(x) = \Delta^{RG}\frac{\delta}{\delta m_a(x)}\frac{\delta}{\delta m_b(0)}\mathcal{W}\tag{2.74}$$

$$= \left[\Delta^{RG}, \frac{\delta}{\delta m_a(x)}\frac{\delta}{\delta m_b(0)}\right]\mathcal{W} + \frac{\delta}{\delta m_a(x)}\frac{\delta}{\delta m_b(0)}\mathcal{A}_{-1}\tag{2.75}$$

$$= -\gamma_a^c G_{cb}(x) - \gamma_b^c G_{ac}(x) - b_{ab}\delta^4(x).\tag{2.76}$$

At the fixed point, where  $\gamma_a^b, B^I = 0$  and  $b_{ab} = b_{ab}^{(0)} = \text{const}$ , by conformal invariance  $G_{ab}(x)$  takes the form

$$G_{ab}(x) = C_{ab}\mathcal{R}\frac{1}{(x^2)^2} = -C_{ab}\frac{1}{4}\square\frac{\log x^2\mu^2}{x^2},\tag{2.77}$$

where the function  $1/(x^2)^2$  is regulated (via differential regularization [54]) due to the presence of the non-integrable singularity in  $x = 0$ , and  $C_{ab}$  is positive-definite by unitarity. Taking the RG derivative of (2.77),

$$\mu\frac{d}{d\mu}G_{ab}(x) = 2\pi^3 C_{ab}\delta^4(x).\tag{2.78}$$

---

<sup>8</sup>Indeed the  $E_4$  anomaly is not fully consistent on its own in the presence of a non-vanishing field strength background  $F_{\mu\nu}^A$ . Terms involving the field strength in the Weyl variation of the  $E_4$  anomaly go along with similar terms from the  $F^2$  anomaly, and thus appear in the  $F^2$  consistency condition in Eq. (2.73).



### 2.3. Weyl consistency conditions and gradient flows

By comparing equations (2.78) and (2.76), we conclude that  $b_{ab}^{(0)}$  must be negative definite. Considering the expression for  $\Pi^a$  in Eq. (2.52) at the original fixed point  $\lambda^I = 0$ , the anomaly associated with  $b_{ab}^{(0)}$  reduces to

$$b_{ab}^{(0)} \left( m^a - \frac{\eta^a}{6} R \right) \left( m^b - \frac{\eta^b}{6} R \right). \quad (2.79)$$

By Eq. (2.78) this result is readily interpreted as due to a deformation of the CFT by the coupling  $(m^a - \eta^a R/6)\mathcal{O}_a$ . This is also consistent with the interpretation of  $\eta^a$  as a parameter describing the “unimprovement” of the CFT. We stress, although it is obvious, that compared to the standard CFT anomaly in Eq. (2.59), where  $R^2$  is inconsistent, Eq. (2.79) is made consistent by the Weyl transformation of an extra source,  $m^a$ . A related discussion of this issue is found in sect. 2.3 in ref. [25].

Notice that the coefficients  $b_{ab}$ ,  $b_{aIJ}$  and  $b_{IJKL}$  can be modified by the addition of local counterterms of the same form:

$$\begin{aligned} \delta\mathcal{W} &= \int d^4x \sqrt{-g} \left( \frac{1}{2} c_{ab} \Pi^a \Pi^b + \frac{1}{2} c_{aIJ} \Pi^a \Pi^{IJ} + \frac{1}{4} c_{IJKL} \Pi^{IJ} \Pi^{KL} \right) \\ \delta b_{ab} &= -\mathcal{L}[c_{ab}] \\ \delta b_{aIJ} &= -\mathcal{L}[c_{aIJ}] + \gamma_{IJ}^{KL} c_{aKL} + 2\gamma_{IJ}^b c_{ab} \\ \delta b_{IJKL} &= -\mathcal{L}[c_{IJKL}] + \gamma_{IJ}^{MN} c_{MNKL} + \gamma_{KL}^{MN} c_{IJMN} + \gamma_{KL}^a c_{aIJ} + \gamma_{IJ}^a c_{aKL}. \end{aligned} \quad (2.80)$$

In particular, at a CFT fixed point  $\delta b_{ab} = \gamma_a^c c_{cb} + \gamma_b^c c_{ac}$ , so that all the entries in  $b_{ab}$  can be eliminated apart from those associated with operators of dimension exactly equal to 2. This makes sense because only for those entries does  $G_{ab}(p^2)$  involve a logarithm, corresponding to an ineliminable  $\ln \mu$  dependence in  $\mathcal{W}$ . The same remark applies to  $b_{aIJ}$  and  $b_{IJKL}$ : around a CFT fixed point the only genuine anomalies, the ones that cannot be removed by local counterterms, correspond to 3- and 4-point functions of fields, such that the sum of their anomalous dimensions vanishes.

It is also interesting to consider what would become of these anomalies in the limit of an SFT. Limiting the set of sources to just  $g^{\mu\nu}$  and the virial gauge field  $A_\mu^A = S^A C_\mu$ , and improving the theory by the choice  $\eta^a = 0$ , the anomaly reduces to a term proportional to  $\tilde{R}^2$  (see sec. 2.2.2). This is the SFT anomaly discussed in ref. [25]. As this anomaly coefficient controls the  $J = 0$  component of the energy momentum 2-point function, one easily deduces that the coefficient must be positive in a unitary theory.

### 2.3 Weyl consistency conditions and gradient flows

If one considers the quantity [32, 26]

$$\tilde{a} = a + \frac{1}{8} w_I B^I \quad (2.81)$$

then Eq. (2.71) together with the second constraint in Eq. (2.73) implies the famous gradient flow equation

$$8\partial_I \tilde{a} = \left( \chi_{IJ}^g + \partial_I w_J - \partial_J w_I + P_I^A \eta_{AJ} \right) B^J. \quad (2.82)$$

The gradient flow equation is one major result in the work of Jack and Osborn [32]. To our knowledge, however, in the general case involving global symmetries, it was not cast in the form of Eq. (2.82) until recently in [55] (see for instance section 3.6 of ref.[25]). Notice indeed that, in order to obtain Eq. (2.82), Eq. (2.73) is crucial, in that it implies that a seemingly spurious term  $P_I^A w_J (T_A \lambda)^J$  is indeed proportional to the  $B^I$ 's. Eq. (2.82) gives rather non-trivial relations among perturbative expansion coefficients of the  $\beta$ -function and of the other quantities in the right hand side. Indeed, as pointed out in [32] and further demonstrated in [55], there arise relations purely involving the  $\beta$ -functions of different couplings at different perturbative orders. For instance, in weakly coupled gauge theories with scalars, one can relate the leading contribution of the scalar quartic coupling to the gauge  $\beta$ -function, which comes at 3-loops, to the 1-loop  $\beta$ -function for the scalar quartic itself.

Another implication of Eq. (2.82) is that  $\tilde{a}$  is stationary at a conformally invariant fixed point, where  $B^I = 0$ . Notice that at a CFT  $\tilde{a}$  and  $a$  have the same value, though  $a$  is in general not stationary. However, since at a CFT  $\partial_I a = -w_J \partial_I B^J / 8$ , we have that  $a$  is still stationary with respect to marginal perturbations, that is perturbations associated with vanishing eigenvalues of  $\partial_I B^J$ . A corollary of this result is that  $a$  must be constant on any manifold of fixed points. Moreover, since in a CFT  $a$  is the coefficient of one of the three structures describing the 3-point function of  $T_{\mu\nu}$  [56], our result implies the vanishing of the tensor structure corresponding to  $a$  in

$$\int d^4x \langle \mathcal{O}(x) T_{\mu\nu}(y) T_{\rho\sigma}(z) T_{\tau\chi}(w) \rangle. \quad (2.83)$$

Although we have not studied that, this result should also be obtained by using the constraints imposed by conformal symmetry on the correlators. A corresponding result applies in 2D CFTs for the correlator  $\int d^2x \langle \mathcal{O}(x) T_{\mu\nu}(y) T_{\rho\sigma}(z) \rangle$ . Though in that case it trivially follows from the vanishing of correlators involving  $n$  insertions of  $T$  and one insertion of another primary, which is a consequence of the Virasoro algebra.

However, the most interesting consequence of Eq. (2.82) is obtained by contracting it with  $B^I$

$$8\mu \frac{d\tilde{a}}{d\mu} \equiv 8B^I \partial_I \tilde{a} = \chi_{IJ}^g B^I B^J, \quad (2.84)$$

where the relation  $B^I P_I^A = 0$  was used. The relevance of this result lies in the positivity property of the matrix  $\chi_{IJ}^g$ , as for  $\chi_{IJ}^g > 0$  it implies  $\tilde{a}$  is a monotonically evolving function of the couplings. Moreover, in an SFT, one would have that  $B^I \partial_I = -S^A (T_A \lambda)^I \partial_I$  is just a  $G_F$  rotation. Then the  $G_F$  covariance of  $\tilde{a}$  would imply  $\chi_{IJ}^g B^I B^J = 0$ . For a positive definite  $\chi_{IJ}^g$  one would conclude that  $B^I = 0$ , and that therefore the theory must be a CFT.

Indeed, as noted already in [32], unitarity guarantees the positivity of  $\chi_{IJ}^g$  in a neighborhood

### 2.3. Weyl consistency conditions and gradient flows

of the original CFT where all  $\beta$ -functions and anomalous dimensions remain small. This proof is based on the following relation between  $\chi_{IJ}^g$  and the anomaly coefficient  $\chi_{IJ}^a$  (see Eq. (2.63)):

$$\chi_{IJ}^g = -2\chi_{IJ}^a + O(B, \partial B, P) \quad (2.85)$$

This relation can be derived from the Wess-Zumino consistency condition of the original anomaly. When  $B, \partial B, P$  can be treated as perturbations, then all anomalous dimensions are small and the positivity of  $\chi_{IJ}^g$  coincides with negativity of  $\chi_{IJ}^a$ . We will now describe a proof for the negativity of this matrix in unitary theories. In section 3.1.4 we will present an alternative argument for the positivity of  $\chi_{IJ}^g$  based on the dilaton scattering amplitude.

The negativity of  $\chi_{IJ}^a$  can be established as follows: by the same considerations used in the discussion around Eq. (2.76) and by the use of Eq. (2.63), we have that the Euclidean two point function  $G_{IJ} \equiv \langle \mathcal{O}_I(x) \mathcal{O}_J(0) \rangle$  satisfies the RG equation

$$\mu \frac{d}{d\mu} G_{IJ} + \gamma_I^K G_{KJ} + \gamma_J^K G_{IK} = -\chi_{IJ}^a \square \square \delta^4(x). \quad (2.86)$$

At the conformal fixed point in differential regularization  $G_{IJ}$  takes the form [53]:

$$G_{IJ}(x) = C_{IJ} \mathcal{R} \frac{1}{(x^2)^4} = -\frac{1}{3 \times 4^4} C_{IJ} \square^3 \frac{\log x^2 \mu^2}{x^2} \quad (2.87)$$

where  $C_{IJ}$  is Zamolodchikov metric, which is positive definite in unitary theories. From the above equations it follows that, up to corrections controlled by the anomalous dimensions and  $\beta$ -functions, unitarity implies  $\chi_{IJ}^a < 0$  and thus, by the previous discussion,  $\chi_{IJ}^g$  must be positive. Notice that this conclusion is not affected by changes of scheme generated by the addition of local counterterms to the action. Indeed under these additions one has  $\chi_{IJ}^a \rightarrow \chi_{IJ}^a + \mathcal{L}[c_{IJ}]$ , with  $c_{IJ}$  a covariant function of the couplings: the change in  $\chi_{IJ}^a$  is again controlled by anomalous dimensions and  $\beta$ -functions, which are small under our hypothesis. Let us stress again our conclusion: in a neighborhood of the original fixed point (see fig. 1) where the  $\beta$ -function and the anomalous dimensions of  $\mathcal{O}_I, \mathcal{O}_a, J_A^\mu$  can be treated as small perturbations, unitarity implies the positivity of  $\chi_{IJ}^g$ . We should also emphasize that this result does not rely on the perturbativity of  $\lambda^I$ . Indeed  $\chi_{IJ}^g$  may differ significantly by its value at the fixed point, but under our assumptions of small  $\beta$  and small anomalous dimensions, unitarity nails  $\chi_{IJ}^g$  to be positive. Nonetheless, we understand that the generic situation is one where the smallness of  $\beta$  and of the anomalous dimensions is controlled by the size of the couplings  $\lambda^I$  themselves.

Now, the integral of Eq. (2.84)

$$\tilde{a}(\lambda(\mu_2)) - \tilde{a}(\lambda(\mu_1)) = \frac{1}{8} \int_{\mu_1}^{\mu_2} \chi_{IJ}^g(\lambda(\mu)) B^I(\lambda(\mu)) B^J(\lambda(\mu)) d \ln \mu \quad (2.88)$$

gives a straightforward bound on the asymptotics of the RG flow. As long as the RG trajectory is in the neighborhood of the original fixed point, the left-hand side of Eq. (2.88) is finite, since as  $\tilde{a}$  is a finite function of the renormalized couplings. Then, if the RG trajectory remains in

## Chapter 2. The local Callan–Symanzik equation

---

this neighborhood asymptotically,  $\ln \mu \rightarrow \pm\infty$ , the positive integrand at the right hand side must vanish in the corresponding asymptotics

$$\lim_{\ln \mu \rightarrow \pm\infty} \chi_{IJ}^g(\lambda(\mu)) B^I(\lambda(\mu)) B^J(\lambda(\mu)) = 0. \quad (2.89)$$

This can only happen if either  $B^I \rightarrow 0$  or if  $\chi_{IJ}^g$  asymptotes a matrix with null eigenvalues. In the latter case, the operators corresponding to such eigenvalues would vanish in the limit where  $\beta$ -functions and anomalous dimensions are neglected: so they must vanish for real otherwise our hypothesis of negligible  $\beta$ -functions and anomalous dimensions is violated. We conclude that within our hypothesis, one must have  $B^I \rightarrow 0$  asymptotically for all non-null operators. The asymptotics must therefore be CFTs. A particular case satisfying our hypothesis is that of Banks-Zaks type theories: the only possible asymptotics in a neighborhood of the original free field theory must as well be CFTs.

## Chapter 3

# Constraining RG flows in four dimensions

In section 2.3 we reviewed the consistency condition approach of [26] to derive a gradient flow equation.

In this Chapter we present a method for computing the  $n$ -point correlators of  $T$ , which we package in terms of an effective dilaton action. We show how to express these correlators as the sum of a local term related to the anomaly (section 3.1.2) and correlators of composite scalar operators (section 3.1.3). Finally, in section 3.1.4 we use this machinery to revisit the results of ref. [25]. We also connect the dilaton based approach of ref. [25] to the consistency condition approach of ref. [26]. As a by-product we show that there exists a scheme where the metric  $\chi_{IJ}^g$  essentially coincides with a manifestly positive definite metric constructed in terms of combinations of matrix elements of composite operators. That is the analogue of what done in ref. [26] for the 2D case. In section 3.2 we draw our conclusions.

### 3.1 Correlation functions of $T$ off-criticality

#### 3.1.1 The dilaton effective action

In this section we shall use the local Callan-Symanzik equation to write the correlators of  $T$  in terms of the correlators of the other composite operators, plus local terms associated with the anomaly. For this purpose we will introduce the dilaton field  $\tau(x)$ , and define the dilaton effective action  $\Gamma[\bar{g}, \tau]$  as the quantum effective action  $\mathcal{W}$  evaluated in the background<sup>1</sup>

$$\mathcal{J}_1(\bar{g}, \tau) \equiv (g^{\mu\nu} = e^{2\tau} \bar{g}^{\mu\nu}, \lambda^I = \lambda^I(\mu) = \text{const}, A_\mu^A = 0, m^a = 0). \quad (3.1)$$

---

<sup>1</sup>We keep a non-trivial background metric in order to allow in principle to control matrix elements of  $T_{\mu\nu}$ . But we shall eventually focus on the flat case  $\bar{g}_{\mu\nu} = \eta_{\mu\nu}$ .

This effective action can be written as an expansion in powers of  $\tau$

$$\Gamma[\bar{g}, \tau] = \mathcal{W}[\mathcal{J}_1] = \exp\{\Delta_\tau^g\} \mathcal{W}[\mathcal{J}] \Big|_{\mathcal{J}=\mathcal{J}_0} = \sum_{n=0}^{\infty} \frac{1}{n!} \underbrace{\Delta_\tau^g \dots \Delta_\tau^g}_n \mathcal{W}[\mathcal{J}] \Big|_{\mathcal{J}=\mathcal{J}_0} \quad (3.2)$$

where we used the operator  $\Delta_\tau^g$  defined in (2.13), and defined the background  $\mathcal{J}_0$  as

$$\mathcal{J}_0(\bar{g}) \equiv (g^{\mu\nu} = \bar{g}^{\mu\nu}, \lambda^I = \lambda^I(\mu) = \text{const}, A_\mu^A = 0, m^a = 0). \quad (3.3)$$

Using the definition (2.7), we see that the coefficient of the  $\tau(x_1) \dots \tau(x_n)$  term in  $\Gamma[\bar{g}, \tau]$ , evaluated with a flat metric  $\bar{g}^{\mu\nu} = \eta^{\mu\nu}$ , corresponds to the  $n$ -point correlator for  $T$

$$\Gamma[\eta, \tau] = \sum_{n=0}^{\infty} \frac{i^{n-1}}{n!} \int d^4x_n \dots \int d^4x_1 \tau(x_n) \dots \tau(x_1) \langle \mathbf{T} \{T(x_1) \dots T(x_n)\} \rangle. \quad (3.4)$$

In order to write the correlators of  $T$  in terms of those of the other composite operators we need to consider the quantum action for the Weyl transformed sources

$$\mathcal{J}_2(\bar{g}, \tau) \equiv \exp\{-\Delta_\tau\} \mathcal{J} \Big|_{\mathcal{J}=\mathcal{J}_1} = (\bar{g}^{\mu\nu}, \lambda^I[\tau], A_\mu^A[\tau], m^a[\tau]), \quad (3.5)$$

for which the  $\tau$  dependence is transferred to  $\lambda^I, A_\mu^A, m^a$ . We shall discuss below the form of the Weyl transformed sources  $\lambda^I[\tau], A_\mu^A[\tau], m^a[\tau]$ . The effective action for  $\tau$  can then be conveniently written as the sum of two contributions

$$\Gamma[\bar{g}, \tau] = \left\{ \mathcal{W}[\mathcal{J}_1] - \mathcal{W}[\mathcal{J}_2] \right\} + \mathcal{W}[\mathcal{J}_2] \equiv \Gamma_{local}[\tau] + \Gamma_{non-local}[\tau] \quad (3.6)$$

where the term in curly brackets  $\equiv \Gamma_{local}$  is clearly local, as it corresponds to a finite Weyl variation of the action. The second term  $\Gamma_{non-local}$  is a functional where  $\lambda^I[\tau], A_\mu^A[\tau], m^a[\tau]$  act as sources for respectively  $\mathcal{O}_I, J_A^\mu, \mathcal{O}_a$ . When focusing on an order by order expansion in  $\tau$ , it is also convenient to write Eq. (3.6) as

$$\begin{aligned} \Gamma[\bar{g}, \tau] &= \exp\{\Delta_\tau^g\} (1 - \exp\{-\Delta_\tau\}) \mathcal{W} \Big|_{\mathcal{J}_0} + \exp\{\Delta_\tau^g\} \exp\{\Delta_\tau^\beta - \Delta_\tau^g\} \mathcal{W} \Big|_{\mathcal{J}_0} \\ &= \exp\{\Delta_\tau^g\} (1 - \exp\{-\Delta_\tau\}) \mathcal{W} \Big|_{\mathcal{J}_0} + \exp\left\{ \Delta_\tau^\beta + \frac{1}{2} [\Delta_\tau^g, \Delta_\tau^\beta - \Delta_\tau^g] + \dots \right\} \mathcal{W} \Big|_{\mathcal{J}_0} \\ &\equiv \Gamma_{local}[\tau] + \Gamma_{non-local}[\tau]. \end{aligned} \quad (3.7)$$

where in the second term we made use of  $-\Delta_\tau = \Delta_\tau^\beta - \Delta_\tau^g$ . In principle, the dots in the second line can be completed using the Baker-Campbell-Hausdorff (BCH) formula. Again, the first term is manifestly local because all the terms in it involve at least one power of  $\Delta_\tau$  acting on  $\mathcal{W}$ , which gives the anomaly  $\mathcal{A}$ . The second expression is a series of terms involving derivatives of  $\mathcal{W}$  with respect to the sources, that is a series of correlation functions of composite operators. Notice that in the absence of dimension 2 operators, all the commutators in the BCH formula vanish, and the computation simplifies significantly.

### 3.1. Correlation functions of $T$ off-criticality

In principle, the effective action can be obtained by working out the exponentials in Eq. (3.7) order by order in  $\tau$ . A perhaps more direct way to get a hold of the result is to consider the source

$$\mathcal{J}_{1+y}(\bar{g}, \tau) \equiv \exp\{-y\Delta_\tau\} \mathcal{J} \Big|_{\mathcal{J}=\mathcal{J}_1} = (\bar{g}^{\mu\nu} e^{2(1-y)\tau}, \lambda^I[\tau, y], A_\mu^A[\tau, y], m^a[\tau, y]), \quad (3.8)$$

which interpolates between  $\mathcal{J}_1$  at  $y = 0$  and  $\mathcal{J}_2$  at  $y = 1$ . The advantage of using this interpolating source is readily seen when considering  $\Gamma_{local}[\tau]$ . One can indeed write

$$\Gamma_{local}[\tau] = \mathcal{W}[\mathcal{J}_1] - \mathcal{W}[\mathcal{J}_2] = - \int_0^1 dy \frac{d}{dy} \mathcal{W}[\mathcal{J}_{1+y}] = \int d^4x \int_0^1 dy \mathcal{A}_\tau(\mathcal{J}_{1+y}) \quad (3.9)$$

where  $\mathcal{A}_\tau(\mathcal{J}_{1+y})$  is just the Weyl anomaly of Eq. (2.63) computed for Lie parameter  $\sigma = \tau$  on the background  $\mathcal{J}_{1+y}$ . To compute both pieces in  $\Gamma[\bar{g}, \tau]$  we must then first find  $\mathcal{J}_{1+y}$ . This is done by solving a set of differential equations. Indeed, by its definition,  $\mathcal{J}_{1+y}$  satisfies

$$\frac{d}{dy} \mathcal{J}_{1+y} = -\Delta_\tau \mathcal{J}_{1+y} \quad (3.10)$$

which corresponds to a set of first order differential equations for its components. Given Eq. (2.14) the solution is found by considering  $\lambda^I$  first,  $A_\mu^A$  second and  $m^a$  third. We have

$$\frac{d}{dy} \lambda^I[\tau, y] = \tau B^I(\lambda[\tau, y]) \quad (3.11)$$

which, with initial condition  $\lambda^I[\tau, 0] = \lambda^I(\mu)$ , has solution

$$\lambda^I[\tau, y] = \lambda^I(\mu e^{y\tau}) \quad (3.12)$$

This result is obvious given the definition of  $\lambda^I[\tau, y]$  in Eq. (3.8), but for the other sources the result will be less obvious. Consider now the vector field. One has

$$\frac{d}{dy} A_\mu^A[\tau, y] = \tau y B^I P_I^A \partial_\mu \tau - \tau P_I^A (T_B \lambda)^I A_\mu^B[\tau, y] \quad (3.13)$$

where  $\lambda^I \equiv \lambda^I(\mu e^{y\tau})$  is understood everywhere. Notice moreover that by the relation  $B^I P_I^A = 0$  only the homogeneous term survives. Thus, given the initial condition  $A_\mu^A[\tau, 0] = 0$ , the unique solution is  $A_\mu[\tau, y] = 0$ . This is an interesting and non-trivial result. It implies that  $\Gamma_{local}$  is not affected by anomaly terms involving the field strength of the external gauge fields, while  $\Gamma_{non-local}$  is independent of the correlation functions of the Noether currents  $J_\mu^A$ . We stress that this result depends on the choice  $S^A = 0$  and would not hold otherwise. As we saw in section 2.2.2, setting  $S^A = 0$  amounts to using the Ward identity Eq. (2.33) to eliminate  $\partial_\mu J_A^\mu$  in the expansion of  $T$  in Eq. (2.26). What our present argument shows, is that  $J_A^\mu$  is eliminated altogether, including the general case where operators are inserted at coinciding points and contact terms must be taken into consideration.

Consider finally  $m^a$ . Its Weyl transformation is somewhat intricate, and so is the differential equation for  $m^a[\tau, y]$ . The computation is considerably simplified by focusing instead on

the ‘‘covariant’’ quantity  $\Pi^a[\tau, y]$ . This is simply related to  $m^a[\tau, y]$  (see Eq. (2.52)) via the sources we already computed, the metric  $g^{\mu\nu}[\tau, y] \equiv \bar{g}^{\mu\nu} e^{2(1-y)\tau}$  and  $\lambda^I[\tau, y]$ . By Eq. (2.54) the equation it satisfies is

$$\frac{\delta}{\delta y} \Pi^a[\tau, y] = -\tau \left\{ (2 - \gamma)_b^a \Pi^b[\tau, y] + \gamma_{IJ}^a \Pi^{IJ}[\tau, y] \right\} \quad (3.14)$$

$$= -\tau \left\{ (2 - \gamma)_b^a \Pi^b[\tau, y] + e^{2\tau y} (6C^a + \mathcal{L}[\tilde{\eta}^a]) \left( \frac{1}{6} \bar{R} + \nabla^2 \tau - (\nabla \tau)^2 \right) \right\} \quad (3.15)$$

where  $\tilde{\eta}^a = \eta^a + \frac{1}{2} \theta_I^a (U^{-1})^I_B B^J$  and where, as before,  $\lambda^I \equiv \lambda^I(\mu e^{y\tau})$  is understood everywhere. In the second line we have used the explicit expression for  $\gamma_{IJ}^a \Pi^{IJ}[\tau, y]$ , which is readily computed as this quantity purely depends on  $\lambda^I$  and on the metric. Furthermore we have used its definition and the consistency conditions to rewrite the coefficient  $\gamma_{IJ}^a$ . This is a standard differential equation whose solution is formally written in terms of integrals involving the known functions on the right-hand side. The dependence on  $\tau$  can then be made explicit by expanding the formal solution in a Taylor series in  $\tau$ .

The structure of  $\Pi^a$  is the main source of complication in the computation of  $\Gamma[\bar{g}, \tau]$  for general  $\tau$ . Here we shall focus on the specific dilaton field configurations respecting the ‘‘on-shell condition’’<sup>2</sup>

$$R(\bar{g}^{\mu\nu} e^{2\tau}) = e^{2\tau} \left( \bar{R} + 6 \left[ \nabla^2 \tau - (\nabla \tau)^2 \right] \right) = e^{2\tau} \left( \bar{R} - 6e^\tau \nabla^2 e^{-\tau} \right) = 0 \quad (3.16)$$

which for the flat background  $\bar{g}^{\mu\nu} = \eta^{\mu\nu}$  reduces to the massless Klein-Gordon equation for the ‘‘canonical’’ dilaton  $1 + \phi \equiv e^{-\tau}$ . The effective action for a dilaton satisfying the on-shell condition very roughly generates the correlators of  $T$  for light-like external momenta, though the relation is more involved because of contact terms. These configurations are interesting because they are precisely those that help constraining the structure of the RG flow [25]. Now, in the case of an on-shell dilaton, a remarkable simplification takes place:  $\Pi^a[\tau, y] = \Pi^{IJ}[\tau, y] = 0$ . Indeed one readily checks that for on-shell configurations the boundary condition is  $\Pi^a[\tau, 0] = \Pi^{IJ}[\tau, 0] = 0$ . Then, since the system of  $\Pi[\tau, y]$ ’s satisfies a homogeneous differential equation (see Eq.(2.54)), the solution vanishes identically. By the explicit form of  $\Pi^a$  we thus have that on-shell and for a flat metric

$$\Pi^a[\tau, y] = 0 \quad \longrightarrow \quad m^a[\tau, y] = e^{2(1-y)\tau} \left[ y(1-y)\eta^a + y^2 \frac{\theta_I^a}{2} B^I \right] \nabla^2 \tau \quad (3.17)$$

where again all coefficients implicitly depend on  $\tau$  and  $y$  via  $\lambda^I \equiv \lambda^I(\mu e^{y\tau})$ . Notice that for  $y = 1$ , relevant for the computation of  $\Gamma_{non-local}$ , the above result further simplifies to (all  $\tau$  dependence now explicit)

$$m^a[\tau, 1] = \frac{\theta_I^a(\lambda(\mu e^\tau))}{2} B^I(\lambda(\mu e^\tau)) \nabla^2 \tau. \quad (3.18)$$

We have now all the ingredients to quickly evaluate the dilaton effective action in the on-shell

---

<sup>2</sup>In the Appendix of [1] we give more details about the general case.



case. We shall consider the local and non-local contributions separately.

### 3.1.2 Computation of $\Gamma_{local}$

From Eq. (3.9) we see that  $\Gamma_{local}$  is linear in the anomaly. It thus consist of the addition of 5 terms, one for each of the contributions in Eq. (2.65).

$$\Gamma_{local} = \Gamma^{\nabla^2 R} + \Gamma^{R^2} + \Gamma^{W^2} + \Gamma^{E_4} + \Gamma^{F^2} \quad (3.19)$$

#### 1. $\Gamma^{\nabla^2 R}$

This local contribution can be obtained by dividing the generating functional into two pieces

$$\mathcal{W} = \mathcal{W}' - \mathcal{F}_{\nabla^2 R} \quad (3.20)$$

where

$$-\Delta_\sigma \mathcal{F}_{\nabla^2 R} = \int d^4x \mathcal{A}_\sigma^{\nabla^2 R}. \quad (3.21)$$

while  $\mathcal{W}'$  is a modified action whose anomaly has the canonical form  $\mathcal{A}^{R^2} + \mathcal{A}^{W^2} + \mathcal{A}^{E_4} + \mathcal{A}^{F^2}$ . The explicit expression for  $\mathcal{F}_{\nabla^2 R}$  is given in (A.47). By the definition Eq. (3.2), and by using Eq. (A.47) we then simply have

$$\Gamma^{\nabla^2 R}[\bar{g}, \tau] = -\mathcal{F}_{\nabla^2 R}[\mathcal{J}_1] = - \int d^4x \sqrt{-\bar{g}} \tilde{d} \left( \frac{R[\bar{g}]}{6} + \nabla^2 \tau - (\nabla \tau)^2 \right)^2 \quad (3.22)$$

where  $\tilde{d}$  is given by

$$\tilde{d} = d + \frac{1}{2} B^I U_I + \frac{1}{4} \tilde{S}_{(IJ)} B^I \tilde{B}^J - \eta^a k_a - \frac{1}{2} \eta^a j_{aI} \tilde{B}^I \quad (3.23)$$

and we introduced the notation  $\tilde{B}^I = (U^{-1})^I_J B^J$ . It is important that once we have extracted this piece from the generating functional, the remaining terms must be evaluated using  $\mathcal{W}'$ , namely in a scheme where the generalized  $\nabla^2 R$  anomaly vanishes.

The main result here is that  $\Gamma^{\nabla^2 R}$  vanishes for dilaton configurations satisfying Eq. (3.16). As such this contribution does not affect the discussion on the RG flow structure: that makes sense, since the local functional  $\mathcal{F}_{\nabla^2 R}$  is arbitrary.

#### 2. $\Gamma^{R^2}$

This contribution is given by the integral of a quadratic form in the  $\Pi$ 's. It is therefore proportional to the square of  $\bar{R} + 6 [\nabla^2 \tau - (\nabla \tau)^2]$ , and therefore trivially vanishes for on-shell dilaton configurations.

#### 3. $\Gamma^{W^2}$

The contribution from  $\mathcal{A}^{W^2}$  is easily integrated:  $\sqrt{g}W^2$  is Weyl invariant, so that the only dependence on  $\tau$  and  $y$  comes from the coefficient function  $c(\lambda)$ . We find

$$\Gamma^{W^2}[\bar{g}, \tau] = - \int dx \sqrt{-\bar{g}} C(\lambda(\mu), \tau) W^2[\bar{g}] \quad (3.24)$$

where  $C(\lambda(\mu), \tau) = \int_{\mu}^{\mu e^{\tau}} c(\lambda(\bar{\mu})) d \ln \bar{\mu}$ . This contribution vanishes in a flat metric background.

#### 4. $\Gamma^{E_4} + \Gamma^{F^2}$

We group these two contributions, since  $\mathcal{A}^{E_4}$  and  $\mathcal{A}^{F^2}$  are related by the Wess-Zumino consistency condition. Notice however that since  $A_{\mu}^A[\tau, y] = 0$ , the gauge field strength vanishes and  $\mathcal{A}^{F^2}$  reduces to the terms proportional to  $P_I^A$ . We find

$$\begin{aligned} \Gamma^{E_4}[\bar{g}, \tau] = & \int d^4x \sqrt{-\bar{g}} \left( A(\lambda(\mu), \tau) E_4[\bar{g}] \right. \\ & + \tilde{a}(\lambda(e^{\tau}\mu)) \left( 4G^{\mu\nu}[\bar{g}] \partial_{\mu}\tau \partial_{\nu}\tau - 4\nabla^2\tau \partial_{\mu}\tau \partial^{\mu}\tau + 2(\partial_{\mu}\tau \partial^{\mu}\tau)^2 \right) \\ & \left. - \mathcal{L}[\tilde{a}](\lambda(e^{\tau}\mu)) (\partial_{\mu}\tau \partial^{\mu}\tau)^2 + \dots \right) \end{aligned} \quad (3.25)$$

where  $A(\lambda(\mu), \tau) = \int_{\mu}^{\mu e^{\tau}} a(\lambda(\bar{\mu})) d \ln \bar{\mu}$ , while the dots stand for additional terms of order  $O(B)^2$  and proportional to  $\bar{R} + 6[\nabla^2\tau - (\nabla\tau)^2]$ . These additional terms therefore vanish on-shell.

Notice that Eq. (2.84) implies  $8\mathcal{L}[\tilde{a}] = \chi_{IJ}^g B^I B^J = O(B^2)$ . Therefore, close to the fixed point, where we can use  $B^I$  as a small expansion parameter, and focusing on a flat metric, the above formula reduces to

$$\Gamma^{E_4}[\eta, \tau] = \tilde{a} \int d^4x \left( -4\nabla^2\tau \partial_{\mu}\tau \partial^{\mu}\tau + 2(\partial_{\mu}\tau \partial^{\mu}\tau)^2 \right) + O(B^2) \quad (3.26)$$

This has precisely the form of the Wess-Zumino term at the fixed point [23]: the non-trivial result is that the corrections begin only at order  $(B^I)^2$ .

Let us summarize: for flat background metric  $\bar{g}^{\mu\nu} = \eta^{\mu\nu}$  and for  $\tau$  satisfying the on-shell condition  $\nabla^2 e^{-\tau} = 0$ , the local contribution to the effective action is controlled by the anomaly coefficient  $\tilde{a}$  and reduces to the second and third lines of Eq. (3.25).

### 3.1.3 Computation of $\Gamma_{non-local}$

As long as we are not interested in correlators involving  $T_{\mu\nu}$  we can set  $\bar{g}^{\mu\nu} = \eta^{\mu\nu}$ . Using the results in section 3.1.1, we have

$$\Gamma_{non-local} = \mathcal{W}[\mathcal{J}_2] = \mathcal{W}[\lambda[\tau, 1], m[\tau, 1]] \quad (3.27)$$

### 3.1. Correlation functions of $T$ off-criticality

where, with a slight abuse of notation, we have dropped the metric and gauge field as one is flat and the other vanishes. By writing

$$\begin{aligned} & \mathcal{W}[\lambda[\tau, 1], m[\tau, 1]] = \\ & \exp \left\{ \int d^4x \left[ (\lambda[\tau, 1] - \lambda^I(\mu)) \frac{\delta}{\delta \bar{\lambda}^I(x)} + m^a[\tau, 1] \frac{\delta}{\delta \bar{m}^a(x)} \right] \right\} \mathcal{W}[\bar{\lambda}, \bar{m}] \Big|_{\bar{\lambda}=\lambda(\mu), \bar{m}=0} \end{aligned} \quad (3.28)$$

and by using the functional correspondence between derivatives and operators, they have that the  $\tau$  dependence of  $\Gamma_{non-local}$  is effectively generated by adding to the Lagrangian of the QFT an effective interaction (we use  $[\lambda[\tau, 1] = \lambda(\mu e^\tau)$ )

$$\mathcal{L}_{eff} = (\lambda^I(\mu e^\tau) - \lambda^I(\mu)) \mathcal{O}_I + (m^a[\tau, 1]) \mathcal{O}_a. \quad (3.29)$$

In the case of an on-shell dilaton the explicit result is

$$\mathcal{L}_{eff} = (\lambda^I(\mu e^\tau) - \lambda^I(\mu)) \mathcal{O}_I + \frac{\theta_I^a(\lambda(\mu e^\tau))}{2} B^I(\lambda(\mu e^\tau)) \nabla^2 \tau \mathcal{O}_a. \quad (3.30)$$

where of course the composite operators are also renormalized at the scale  $\mu$ . Because of the piece proportional to  $\theta_I^a$ , this result corrects the naive expectation according to which in a QFT with purely marginal deformations the effective coupling to a background dilaton is simply obtained by promoting  $\lambda(\mu)$  to  $\lambda(\mu e^\tau)$ . That would for instance be automatically true in the absence of dimension 2 scalars. However, we have seen before that even in the presence of dimension 2 operators a scheme to define composite operators exists where  $\theta_I^a = 0$ . In such a scheme the form of the effective dilaton interaction would respect the naive expectation. Notice that the operator redefinition generated by the source reparametrization in Eq. (2.44), reduces to a simple operator shift, as described in Eq. (2.47), only when operators are inserted at separated points. When considering insertions at coinciding points the operator mapping is made more involved by the presence of contact terms. In view of that, one should not be worried if the second term in Eq. (3.30) cannot be naively absorbed by the first through a simple operator shift.

We should however stress that the simple result in Eq. (3.30) relies on two other ingredients. First, it relies on the choice  $S^A = 0$  to fix the freedom in defining the RG flow. This choice is equivalent to using the Ward identity to rewrite  $\partial_\mu J_A^\mu$  in terms of  $\mathcal{O}_I$  and  $\mathcal{O}_a$ . Secondly, and more importantly, Eq. (3.30) is only valid for on-shell dilatons. Without that assumption there would be new genuine contributions basically related to the existence of the additional non-minimal operators  $\sqrt{g}R(g)\mathcal{O}_a$  coupling the QFT to gravity.

For the purpose of the discussion in the next section, it is useful to write the lowest order contributions to  $\Gamma_{non-local}$  in an expansion in the canonical dilaton  $\phi$

$$e^{-\tau} = 1 + \phi. \quad (3.31)$$

for which the on-shell condition is  $\nabla^2 \phi = 0$ . Using the expansions  $\tau = -\phi + \frac{1}{2}\phi^2 - \dots$  and

$\nabla^2\tau = -(1-\phi)\nabla^2\phi + (\nabla\phi)^2 + \dots$  we find

$$\Gamma_{non-local}[\eta, \phi] = : \exp \left\{ \int d^4x \left( -\phi B^I \frac{\delta}{\delta\lambda^I(x)} + \frac{\phi^2}{2} \left( B^J (\delta_J^I + \partial_J B^I) \frac{\delta}{\delta\lambda^I(x)} + \frac{1}{2} B^J \theta_J^a \nabla^2 \frac{\delta}{\delta m^a(x)} \right) + O(\phi^3) \right) \right\} : \mathcal{W} | \quad (3.32)$$

where by the  $:$  we mean that the functional derivatives do not act on their coefficients. As a check of the consistency of our result notice that the term proportional to  $\phi^2$  is given by

$$\int d^4x \frac{\phi^2}{2} B^J (\delta_J^I + \partial_J B^I) [\tilde{\mathcal{O}}_I] \quad (3.33)$$

where  $\tilde{\mathcal{O}}_I$  is the scheme independent dimension 4 operator defined in Eq. (2.48). Also consistently with that: thanks to  $\nabla^2\phi = 0$ ,  $\mathcal{O}_I$  and  $\tilde{\mathcal{O}}_I$  make no difference in the term linear in  $\phi$ .

### 3.1.4 Correlators of $T$ and the constraints on the RG flow

The constraint on the RG flow asymptotics discussed in section (2.3) can be alternatively derived by studying the specific combination of correlators of  $T$  that corresponds to the  $2 \rightarrow 2$  scattering amplitude of a background on-shell dilaton. This approach is at the basis of the proof of the  $a$ -theorem in ref [23] and was already followed in ref. [25] to constrain the RG flow asymptotics. This section has a twofold aim. On one hand we would like to use the results of the previous section to fill in some details that were not fully developed in ref. [25]. These concern the role of multiple insertions of  $T$ , and the issues of scheme dependence and operator mixing. In the end these issues affect only subleading contributions and so they do not alter the proof in ref. [25] as, under the assumption of perturbativity, that only relies on the leading order scattering amplitude. However, with a complete control of the scattering amplitude, the relation with the consistency condition approach of refs.[31, 32, 26] will be more clear. That is our second aim.

The idea is to study specific combinations of correlators of  $T$  that can be directly interpreted as the  $2 \rightarrow 2$  scattering amplitude of the background dilaton field  $\phi$  defined in Eq. (3.31)

$$(2\pi)^4 \delta(p_1 + \dots + p_4) A(p_1, p_2, p_3, p_4) = \frac{\delta}{\delta\phi(p_1)} \frac{\delta}{\delta\phi(p_2)} \frac{\delta}{\delta\phi(p_3)} \frac{\delta}{\delta\phi(p_4)} \mathcal{W}[\mathcal{J}_1] \Big|_{\bar{g}=\eta, \phi=0} \quad (3.34)$$

Notice that since

$$\frac{\delta}{\delta\phi} = -e^\tau \frac{\delta}{\delta\tau} \quad (3.35)$$

### 3.1. Correlation functions of $T$ off-criticality

the amplitude is a combination of 4-, 3- and 2-point functions

$$\begin{aligned}
A(p_1, \dots, p_4) &= -i \langle \mathbf{T} \{ T(p_1) T(p_2) T(p_3) T(p_4) \} \rangle \\
&\quad - (\langle \mathbf{T} \{ T(p_1 + p_2) T(p_3) T(p_4) \} \rangle + \text{permutations}) \\
&\quad + i (\langle \mathbf{T} \{ T(p_1 + p_2) T(p_3 + p_4) \} \rangle + \text{permutations}) \\
&\quad + i (\langle \mathbf{T} \{ T(p_1 + p_2 + p_3) T(p_4) \} \rangle + \text{permutations}) . \tag{3.36}
\end{aligned}$$

Notice that, for generic kinematics, the correlators of  $T$  require renormalization. As a result of that, these correlators are generically  $\mu$  dependent. An equivalent statement is that the dilaton effective action for a generic  $\phi$  is  $\mu$  dependent. As discussed in section 2.2.1 this dependence is fully controlled by the integral of the anomaly for a constant variation parameter  $\sigma = \text{const}$ . Now, it turns out that, for a pure dilaton background  $g_{\mu\nu} = \eta_{\mu\nu}(1 + \phi)^2$  satisfying the “on-shell” condition

$$R(e^{-2\tau}\eta_{\mu\nu}) = e^{3\tau}\nabla^2 e^{-\tau} = (1 + \phi)^{-3}\nabla^2\phi = 0 \tag{3.37}$$

the anomaly of Eq. (2.63) integrates to zero. Indeed, in a pure dilaton background ( $\lambda^I = \text{const}$ ,  $A_\mu^A = m^a = 0$ ) the only terms to consider are those involving just the metric:  $E_4$  integrates to zero over asymptotically flat space,  $\sqrt{-g}W^2(g)$  vanishes for conformally flat metrics, while the on-shell condition (3.37) eliminates the  $R^2$  term. The scattering amplitudes for on-shell dilatons are thus automatically finite, that is they are RG independent.

The same conclusion can be obtained from the power counting analysis in ref. [25], from which one deduces that for an on-shell dilaton background all counterterms vanish except for a cosmological constant term  $\frac{\Lambda}{4!}(1 + \phi)^4$ . For  $m^a \neq 0$  the cosmological term would logarithmically depend on  $\mu$ . This dependence is associated with the  $\Pi^a\Pi^b$  terms in the anomaly. However, for the case  $m^a = 0$  we are interested in there is just a quartic divergence:  $\Lambda$  is a  $\mu$  independent constant, that we may in principle even set to zero. Indeed Eq. (2.63) corresponds to the choice  $\Lambda = 0$ .

As a consequence of the above discussion, on dimensional grounds, the scattering amplitude, takes the form

$$A(s, t) = s^2 F(s/\mu^2, t/\mu^2, \lambda(\mu)) + \Lambda \tag{3.38}$$

with  $F$  an RG invariant function

$$\left( \mu \frac{\partial}{\partial \mu} + B^I \frac{\partial}{\partial \lambda^I} \right) F(s/\mu^2, t/\mu^2, \lambda(\mu)) = 0. \tag{3.39}$$

Notice that, since the dilaton is a flavor singlet source,  $F$  must be invariant under the background  $G_F$ : in Eq. (3.39) we can equally well use  $B^I$  or  $\beta^I$ .

The constraint on the flow is obtained by considering a dispersion relation for the forward scattering amplitude  $A(s, t = 0)$  [23, 25]. In principle, given the kinematics ( $p_i^2 = 0, t = 0$ ), one may be concerned about the IR finiteness of the amplitude. While we believe it should

be possible to carefully study the conditions for IR finiteness by performing an operator expansion analysis, in the present study we shall content ourselves by assuming the amplitude is finite. There are different reasons to believe that must be the case. One is that, as it will become clear below,  $A(s, t = 0)$  appears to provide a concrete “on-shell” scheme to define the quantity  $\tilde{a}$  that emerged from the study of the consistency conditions. It seems hard to believe that happens just by chance. Another, maybe weaker, indication is associated with the explicit form of  $A(s, t = 0)$ , when expanded in powers of the  $\beta$ -function. As we shall discuss below, at the leading  $\beta^2$  order, the amplitude is determined by the two point functions of operators  $\tilde{O}_I$  with dimension near 4, and is manifestly IR finite. The next-to-leading order  $\sim \beta^3$  is determined by 3-point functions of such operators, which at lowest order in  $\beta$  can be computed in the original unperturbed CFT. Here again, the explicit computations of CFT 3-point in momentum space [57], allows to rule out IR singularities. According to this reasoning IR singularities could only arise beyond the order  $\beta^4$ . While this seems difficult to believe, a dedicated analysis seems to be needed to rule out this possibility. We leave such analysis for future work.

Let us now go back to the forward amplitude. It is useful to parametrize it as

$$A(s, 0) = s^2 F(s/\mu^2, 0, \lambda(\mu)) + \Lambda \equiv -8s^2 \alpha(s) + \Lambda \quad (3.40)$$

such that the positivity constraint imposed by unitarity becomes

$$\text{Im}A(s, 0) \geq 0 \quad \implies \quad \text{Im}\alpha \leq 0 \quad (3.41)$$

Notice that, by the results of sections 3.1.2-3.1.3, Eq. (3.25) in particular, at a conformally invariant fixed point,  $\alpha$  coincides with the anomaly coefficient  $a$ . Away from criticality, using the  $\mu$  independence of  $A$ , we can also write

$$-8\alpha(s) = F(1, 0, \lambda(\sqrt{s})), \quad (3.42)$$

a finite function of the running couplings. The dispersion relation corresponds to the Cauchy integral relation

$$\oint_C \frac{A(s, 0)}{s^3} ds = 0 \quad (3.43)$$

for the contour  $C$  shown in figure 3.1. By using crossing  $A(s, 0) = A(-s, 0)$  and “hermiticity”  $A(s, 0)^* = A(s^*, 0)$ , and by defining the “average” amplitude

$$\bar{\alpha}(s) = \frac{1}{\pi} \int_0^\pi \alpha(se^{i\theta}) d\theta \quad (3.44)$$

Eq. (3.43) becomes [25]

$$\bar{\alpha}(s_2) - \bar{\alpha}(s_1) = \frac{2}{\pi} \int_{s_1}^{s_2} \frac{ds}{s} (-\text{Im}\alpha(s)) \geq 0 \quad (3.45)$$

Notice that by crossing and hermiticity,  $\bar{\alpha}$  is a real quantity. Notice also that the cosmological term, being analytic over the whole complex plane automatically gives no contribution to the

dispersion relation.

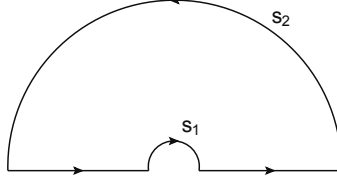


Figure 3.1: The contour  $C$  in the complex  $s$  plane.

We can now use the results from our study of the local Callan-Symanzik equation to elucidate both sides of Eq. (3.45). Consider the left-hand side first. The split of the dilaton effective action into a local and non-local contribution corresponds to a similar splitting for the dilaton amplitude  $\alpha = \alpha_{loc} + \alpha_{non-loc}$ . The results of the two previous sections imply

$$\alpha_{loc} = \tilde{a}(\lambda(\mu)) + O(B^2) \quad \alpha_{non-loc} = O(B^2) \quad (3.46)$$

from which, using the  $\mu$  independence of  $\alpha$ , we deduce  $\bar{\alpha}$  satisfies

$$\bar{\alpha}(s) = \tilde{a}(\lambda(\sqrt{s})) + O(B^2) \quad (3.47)$$

This relation is sufficient to conclude that there exists a choice of scheme where  $\bar{\alpha}(s) = \tilde{a}(\lambda(\sqrt{s}))$ . Indeed adding to  $\mathcal{W}$  the local term

$$\frac{c_{IJ}}{2} \sqrt{g} G^{\mu\nu} \nabla_\mu \lambda^I \nabla_\nu \lambda^J \quad (3.48)$$

does not affect the dilaton amplitude, as that is computed at  $\nabla_\mu \lambda^I = 0$ , but modifies  $\tilde{a}$  and  $\chi_{IJ}^g$  according to

$$\tilde{a} \rightarrow \tilde{a} + B^I B^J c_{IJ} \quad \chi_{IJ}^g \rightarrow \chi_{IJ}^g + \mathcal{L}(c_{IJ}). \quad (3.49)$$

The first equation, together with Eq. (3.47), implies a  $c_{IJ}$  with regular dependence on  $\lambda^I$  can be chosen such that  $\bar{\alpha}(s) = \tilde{a}(\lambda(\sqrt{s}))$ . Consider now the right-hand side of Eq. (3.45).

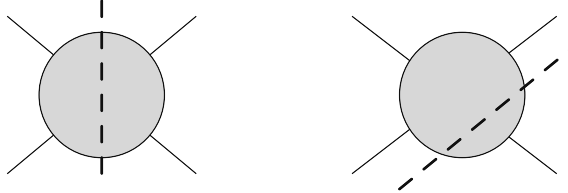


Figure 3.2: The 2-2 and 3-1 cuts of the on-shell dilaton scattering amplitude.

The imaginary part of the amplitude is obviously only affected by the non-local part of the dilaton action. We must thus expand  $\Gamma_{non-loc}$  to fourth order in  $\phi$ . Notice first of all, as it may also seem obvious, that only 2-2 cuts contribute<sup>3</sup> if the amplitude is assumed to be

<sup>3</sup>Indeed this is necessary to establish Eq.(3.41), as 2-2 cuts are manifestly positive while 3-1 cuts are not

finite for external momenta on the light cone: 3-1 cuts would expectedly be associated with singularities at  $p_i^2 = 0$ . The absence of 3-1 cuts physically corresponds to the fact that a background massless dilaton cannot decay to QFT states. This last statement can also be checked by noticing that the contribution from  $\Gamma_{non-local}$  to the dilaton 2-point function vanishes on-shell.

Now, since only 2-2 cuts contribute to the imaginary part, we must consider terms where at most two  $\phi$ 's are at coinciding point, as shown in the fig. (3.3). The contributions with at

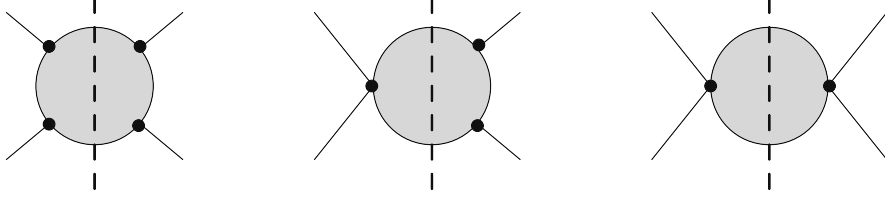


Figure 3.3: The different configurations for the diagrams with 2-2 cut.

most two coinciding  $\phi$ 's are determined by the  $O(\phi^4)$  term in the expansion of Eq. (3.32). These contributions can be written in terms of ‘‘Feynman rules’’ where the building blocks are 2- 3- and 4- point correlators of  $\mathcal{O}_I$  and  $\mathcal{O}_a$ . Inserting a complete set of states  $|\Psi\rangle$  in the cut, the imaginary part is conveniently written as

$$-\text{Im } \alpha(s) = \frac{1}{16s^2} \sum_{\Psi} (2\pi)^4 \delta^4(p_{\Psi} - p_1 - p_2) B^I B^J \mathcal{M}_J(\Psi)^* \mathcal{M}_I(\Psi) \quad (3.50)$$

with the matrix elements defined as

$$B^I \mathcal{M}_I(\Psi) \equiv B^I \langle \Psi | \left[ (\delta_I^K + \partial_I B^K) \tilde{\mathcal{O}}_K(0) + B^K \mathcal{O}_{IK}(p_1 - p_2) \right] | 0 \rangle \quad (3.51)$$

where we used the ‘‘scheme independent’’ dimension 4 operator  $\tilde{\mathcal{O}}_I$  defined in Eq. (2.48), and defined

$$\mathcal{O}_{IK}(p_1 - p_2) \equiv \int d^4 y e^{-i(p_1 - p_2)y/2} \mathbf{T}(\mathcal{O}_I(y) \mathcal{O}_K(-y)) . \quad (3.52)$$

$p_1$  and  $p_2$  are the momenta of the two incoming dilatons, so that  $(p_1 + p_2)^2 = s$ . The matrix element  $B^I \mathcal{M}_I(\Psi)$  describes the probability amplitude for two incoming dilatons to be converted into the state  $|\Psi\rangle$ . The first two terms in Eq. (3.51) correspond to two dilatons absorbed at coinciding points (pure  $\ell = 0$ -wave) while the third corresponds to insertions at non-coinciding points, and thus involves all higher partial waves  $\ell \geq 0$ .

One can thus define a positive metric  $G_{IJ}$  such that

$$-\text{Im } \alpha(s) = B^I B^J G_{IJ} \quad (3.53)$$

$$G_{IJ} = \frac{1}{16s^2} \sum_{\Psi} (2\pi)^4 \delta^4(p_{\Psi} - p_1 - p_2) \mathcal{M}_J(\Psi)^* \mathcal{M}_I(\Psi) \quad (3.54)$$

---

manifestly positive.



In the above equation, by the  $\mu$  independence of the amplitude, the couplings and the composite operators can be conveniently renormalized at  $\mu = \sqrt{s}$ . Plugging this result into Eq. (3.45) and comparing to Eq. (2.88) one concludes that, in the scheme where  $\tilde{a}(\lambda(\sqrt{s})) = \bar{\alpha}(s)$ ,

$$\chi_{IJ}^g = \frac{32}{\pi} G_{IJ} + \Delta_{IJ} \quad (3.55)$$

where  $\Delta_{IJ}$  satisfies  $B^I B^J \Delta_{IJ} = 0$ , while  $G_{IJ}$  is manifestly positive definite. The positive matrix  $G_{IJ}$  can be viewed as the 4D analogue of Zamolodchikov's metric for 2D RG flows

$$G_{IJ}^{2D} \equiv \frac{1}{p^2} \sum_{\Psi} (2\pi)^2 \delta^2(p_{\Psi} - p) \langle 0 | \mathcal{O}_I(0) | \Psi \rangle \langle \Psi | \mathcal{O}_J(0) | 0 \rangle. \quad (3.56)$$

With the benefit of hindsight we can now better appreciate the difference between the 2D and 4D cases. In the first case the RG flow is controlled by the 2-point correlator of  $T$ , while in the second a specific combination of 2-, 3-, and 4-point correlators is the relevant object. Without the dilaton scattering amplitude as a guideline it would not have been obvious how to assemble these correlators in order to construct  $G_{IJ}$ . Of course the approach we followed in this Chapter is bound to the study of near marginal deformations where both  $B^I$  and  $\partial_I B^J$  are treated as small perturbations. In that case  $G_{IJ}$  is dominated by the first term in Eq. (3.51) and takes the same 2-point function structure for the 2D case. That is the result discussed in ref. [25]. Ideally one could however conceive of extending Eq. (3.51) beyond perturbation theory including all scalar operators in the theory [58]. Unitarity would then dictate the evolution of  $\bar{\alpha}$  with energy is controlled by an infinite dimensional positive metric constructed in analogy with  $G_{IJ}$ .

We want to conclude with a comment concerning parity violation and  $\epsilon^{\mu\nu\rho\sigma}$  terms in the anomaly. In this Chapter we have disregarded them in order to simplify the discussion on the structure of the anomaly. However it is rather clear that their presence does not affect the derivation of the effective action for the dilaton, and the discussion about RG flow based on it. This is readily seen by considering in turn  $\Gamma_{local}$  and  $\Gamma_{non-local}$ . The former is a local action involving 4 derivatives and any power of a scalar field  $\tau$ : by Bose symmetry it is evident that one cannot write down any term involving  $\epsilon^{\mu\nu\rho\sigma}$ . The latter is totally determined by the Weyl transformation properties of the sources, which as we noticed in section 2.2.2, is not affected by parity violation. Therefore the discussion of RG flow asymptotics is not affected by parity violation and, consequently, by mixed flavor-gravity anomalies.

## 3.2 Discussion

Osborn's original paper [26] on the local RG outlined a beautiful formalism to shed light on the structure of RG flows, independent of details of the underlying theory. Chapter 2 can be largely considered as a corollary to that classic paper, where we obtained the following results:

- We introduced the ‘‘covariant’’ objects  $\Pi^a$  and  $\Pi^{IJ}$  whose Weyl variations do not involve derivatives of the Lie parameter. These objects are essential in all applications of

the local RG, from the construction of manifestly consistent Weyl anomalies to the computation of the effective action for a background dilaton.

- We showed that most of the consistency conditions for the Weyl anomaly can be explicitly solved and that the anomaly can be reformulated in a manifestly consistent form, with only 3 non-trivial consistency conditions remaining. A crucial step in that procedure was the isolation of the scheme dependent terms in the anomaly, that is terms that correspond to the variation of a local functional. That allowed to write most consistency conditions as algebraic equations as opposed to differential equations. We believe this new formulation of the Weyl anomaly represents a significant simplification over the original discussion in ref. [26], providing focus on the genuinely non-trivial consistency conditions.
- Using the full set of consistency conditions, in particular those involving the background flavor gauge field strengths, we derived a general gradient flow formula for the  $\beta$ -function, Eq. (2.82). This equation implies a certain combination of anomaly coefficients  $\tilde{a} = a + w_I B^I/8$  is stationary at fixed points. It turns out this is precisely the quantity that decreases monotonically when flowing towards the IR. Therefore maxima and minima of  $\tilde{a}$  respectively correspond to UV and IR attractive fixed points. Another corollary of this result is that the  $E_4$  anomaly coefficient  $a$  is stationary on a manifold of fixed point.
- We established the monotonicity of the RG flow of  $\tilde{a}$ , under the condition that the RG trajectory is bound to a neighborhood of a CFT, where the  $\beta$ -function and the anomalous dimensions can be treated as small perturbations. These quantities are indeed the expansion parameters in all our computations. Our result evidently does not rely on the original CFT being free.

Then, in Chapter 3 we related the approach to gain insight on RG flows based on Weyl consistency conditions to the approach based on the background dilaton trick of Komargodski and Schwimmer [23, 25]. Our study consists of the following steps and results:

- We derived a formal expression for the generating functional of the correlators of the energy momentum trace  $T$ : the effective action for a background dilaton  $\tau$ . This action consists of two contributions. The first is local and determined by the Weyl anomaly. For on-shell dilaton configurations the result is fully determined by the  $E_4$  anomaly term and shown in Eq. (3.25). A consequence of our result is that, up to  $\mathcal{O}(B^2)$  in the  $\beta$ -function  $B^I$ , the forward dilaton scattering amplitude at energy  $\sqrt{s}$  is controlled by  $\tilde{a}(\lambda(\sqrt{s}))$ , the same crucial quantity describing the gradient flow equation. This result was essentially derived already in ref. [40], though, we think, without analyzing the relevance of the on-shell condition.

The second contribution to the dilaton effective action is non-local and associated with the expansion of  $T$  in terms of a complete basis of operators, also including the effects

of multiple insertions at the same point. Here the main result is that, for an on-shell dilaton, there exists a suitable “scheme” such that the action is simply generated by making the formal substitution  $\lambda(\mu)^I \rightarrow \lambda^I(\mu e^\tau)$ . On one hand the choice of scheme concerns the mixing between dimension 4-scalars  $\mathcal{O}^I$  and operators of the form  $\nabla^2 \mathcal{O}^a$ , with  $\mathcal{O}^a$  dimension 2 scalars. On the other, it concerns the systematic use of flavor Ward identities to substitute the divergence of currents  $\partial_\mu J_A^\mu$  in the correlators. That procedure corresponds to the freedom to define the Weyl operator such that  $S^A = 0$ , and such that the  $\beta$ -function is the “physical” one,  $B^I$ . We stress that, aside these technical scheme issues, the on-shellness of the background dilaton is the key to the simple result. In practice the on-shell condition beautifully filters out interactions (and related complications) associated with improvement terms. This property was already the key to the analyses in refs. [23, 39, 25].

- We used the effective action to study the forward dilaton scattering amplitude. We showed that there exists a scheme where the reduced forward amplitude  $\bar{a}(s)$ , defined in Eqs. (3.40)(3.44), equals the quantity  $\tilde{a}(\sqrt{s})$  appearing in the study of Wess-Zumino consistency conditions [32, 26]. That scheme freedom is associated with the possibility to add to the action a local and finite functional of the sources. We then applied the optical theorem to show that, within this scheme and for a unitary theory, the matrix  $\chi_{IJ}^g$  controlling the flow of  $\tilde{a}$ , essentially<sup>4</sup> coincides with a positive definite metric in coupling space  $G_{IJ}$ . The latter metric is explicitly written in terms of matrix elements involving 2, 3- and 4-point correlators of the operators  $\mathcal{O}_I$  that drive the RG flow. In practice the use of the dilaton scattering amplitude allows to identify the 4D analogue of the Zamolodchikov metric of 2D-QFT.

---

<sup>4</sup>“Essentially” is here used in the sense specified by Eq. (3.55): a possible difference  $\Delta_{IJ}$  would necessarily be “orthogonal” to the  $\beta$ -function vector  $B^I$  and not play any role.



## Chapter 4

# Constraining RG flows in six dimensions

### 4.1 Introduction

Due to the importance of the  $a$ -theorem and its consequences for the structure of QFTs, it is of great interest to continue the exploration of these ideas to higher spacetime dimensions.

In this Chapter we focus on six dimensions, where there exist non-trivial local superconformal unitary [59, 60] and non-unitary [61] CFTs. While it is believed that there are no unitary CFTs in dimensions higher than six (which has been proven rigorously in the supersymmetric case [62]), the local CS equation formalism could be applied to the local non-unitary CFTs in dimensions greater than six [61].

Let us consider a six-dimensional QFT deformed by a set of quasi-marginal operators  $\mathcal{O}_I$ ,

$$S[\Phi, \lambda] = S_{\text{CFT}}[\Phi] + \int d^6x \lambda^I \mathcal{O}_I(x), \quad (4.1)$$

and we study its RG flows through the formalism developed in Chapter 2, which can be almost straightforwardly generalized to the six-dimensional case.<sup>1</sup> However, in six dimensions the expansion of  $T$  in a set of operators takes the general form

$$T \sim \beta^I \mathcal{O}_I + S^A \partial_\mu J_A^\mu - \eta^a \square \mathcal{O}_a + d^\alpha \square \square \varphi_\alpha, \quad (4.2)$$

where  $\varphi_\alpha$  are scalar operators of dimension two, which by unitarity must satisfy the equation  $\nabla^2 \varphi_\alpha = 0$  at the fixed point.

Correspondingly, one can introduce sources  $c^\alpha$  for  $\varphi_\alpha$ , and the local CS equation is generalized

---

<sup>1</sup>Important results using other approaches have been obtained in [63, 64].

to

$$\Delta_\sigma \mathcal{W} = \int d^6x \left( 2\sigma g^{\mu\nu} \frac{\delta}{\delta g^{\mu\nu}} + \delta_\sigma \lambda \cdot \frac{\delta}{\delta \lambda} + \delta_\sigma A_\mu \cdot \frac{\delta}{\delta A_\mu} + \delta_\sigma m \cdot \frac{\delta}{\delta m} + \delta_\sigma c \cdot \frac{\delta}{\delta c} \right) = \int d^6x \mathcal{A}_\sigma \quad , \quad (4.3)$$

where the operators in (4.3) take the same form as in (2.14), apart from  $\delta_\sigma c$  which is a new term with mass dimension four.

For simplicity, in the present study we shall assume that the lower-dimensional scalar operators  $\mathcal{O}_a$  and  $\varphi_\alpha$  are absent. It would be interesting to include them in the future, also to further test results in the perturbative  $\phi^3$  theory, as initiated in [65].

By analyzing the Wess–Zumino consistency conditions, in section 4.2 we will identify a function of the coupling constants,  $\hat{a}$ , satisfying an equation analogous to (2.2), thereby proving the  $a$ -theorem in perturbation theory. In fact, we find a one-parameter family of functions,  $\hat{a} + \lambda \hat{b}$ , satisfying an equation of the form

$$\mu \frac{d}{d\mu} (\hat{a} + \lambda \hat{b}) = \chi_{IJ} \beta^I \beta^J + \mathcal{O}(\beta^3). \quad (4.4)$$

where  $\chi_{IJ}$  is positive definite at leading order by unitarity. This result dispels the concerns on the validity of the perturbative  $a$ -theorem in  $d = 6$  raised by [66], where a different function of the coupling constants was proposed as the monotonically decreasing quantity. As a direct consequence of the  $a$ -theorem we prove the equivalence SFT = CFT in our setup.

## 4.2 Wess–Zumino consistency conditions

Consistency conditions that follow from the commutativity of Weyl transformations,

$$\Delta_\sigma \mathcal{A}_{\sigma'} - \Delta_{\sigma'} \mathcal{A}_\sigma = 0 \quad (4.5)$$

impose constraints among the various terms that appear in the anomaly  $\mathcal{A}_\sigma$ . In  $d = 2, 4$  these conditions have been considered in Chapter 2 and references therein. Holographically, they have been studied in [67, 68], and in supersymmetric theories in [69, 70]. Here we derive the consistency conditions from the variation of the anomaly, as obtained in [71], and perform a detailed analysis of those. We find that some consistency conditions obtained in [71] were incorrect.

For the moment, we will neglect the contributions to equation (4.3) related to the gauge fields  $A_\mu^A$  sourcing the currents  $J_A^\mu$ . However, as it will be shown later, this will not change our conclusions. The explicit form of the anomaly functional can be found in Appendix B.2. For illustrative purposes, let us report the form of the anomaly at the fixed point, with the background couplings set to 0 [72],

$$\mathcal{A}_\sigma = \sigma (-a E_6 + c_1 I_1 + c_2 I_2 + c_3 I_3). \quad (4.6)$$

## 4.2. Wess–Zumino consistency conditions

There are other six contributions (trivial anomalies) that can be eliminated by adding local counterterms to the effective action. In (4.6)  $E_6$  is the Euler term while  $I_1, I_2, I_3$  are Weyl invariant tensors. Their explicit form can be found in Appendix B.2.

After decomposing (4.5) in a linearly-independent basis, it is possible to read off constraint equations for the anomaly coefficients. This is technically challenging, particularly due to difficulties related to integration by parts and Bianchi identities.<sup>2</sup> The consistency conditions obtained here were checked at two loops in the  $\phi^3$  theory against the results of [65].<sup>3</sup> We have also checked that they are satisfied by the general form of the trace anomaly on the conformal manifold as constructed in [53].

In this work we exploit all constraints imposed on anomaly coefficients with up to two indices. This requires us to decompose the consistency conditions and isolate the ones that stem from terms involving up to two couplings  $\lambda$ . For example, we are interested in the consistency condition arising from contributions to the left-hand side of (2.64) proportional to  $(\sigma \partial_\mu \sigma' - \sigma' \partial_\mu \sigma) \nabla^2 \lambda^I \partial^\mu \nabla^2 \lambda^J$ , but not in the one arising from contributions proportional to  $(\sigma \partial_\mu \sigma' - \sigma' \partial_\mu \sigma) \partial^\mu \lambda^I \nabla^2 \lambda^J \nabla^2 \lambda^K$ .

A particularly important equation contained in (2.64) is obtained from terms proportional to  $(\sigma \partial_\mu \sigma' - \sigma' \partial_\mu \sigma) H_1^{\mu\nu} \partial_\nu \lambda^I$ , where  $H_1^{\mu\nu}$  is a generalization of the Einstein tensor in  $d = 6$  [73] (see (B.7) for its explicit form), namely

$$\partial_I \tilde{a} = \frac{1}{6} \mathcal{H}_{IJ} \beta^J + \frac{1}{6} \mathcal{H}_I, \quad (4.7)$$

where<sup>4</sup>

$$\begin{aligned} \tilde{a} &= a + \frac{1}{6} b_1 - \frac{1}{90} b_3 + \frac{1}{6} b_{11} + \frac{1}{12} \mathcal{A}_J \beta^J + \frac{1}{6} \mathcal{H}_J^1 \beta^J, \\ \mathcal{H}_I &= -\mathcal{H}_I^5 - \frac{1}{2} \mathcal{H}_I^6 - \frac{1}{2} \mathcal{I}_I^7, \quad \mathcal{H}_{IJ} = \frac{1}{4} \mathcal{A}_{JI} + \mathcal{H}_{IJ}^1 + \partial_I \mathcal{A}_J + \partial_{[I} \mathcal{H}_{J]}^1. \end{aligned} \quad (4.8)$$

All the tensors appearing above are local functions of the couplings, and their definition can be found in Appendix B.2. Use of the consistency condition arising from  $(\sigma \nabla^\mu \nabla^\nu \partial^\rho \sigma' - \sigma' \nabla^\mu \nabla^\nu \partial^\rho \sigma) \nabla_\mu \nabla_\nu \partial_\rho \lambda^I$  allows us to put (4.7) in the simpler form

$$\partial_I \tilde{a} = \frac{1}{6} (\mathcal{H}_{IJ}^1 - \frac{1}{4} \hat{\mathcal{A}}_{IJ}^{\prime\prime}) \beta^J + \frac{1}{6} \partial_{[I} \mathcal{H}_{J]}^1 \beta^J - \frac{1}{12} \mathcal{I}_I^7, \quad \tilde{a} = a + \frac{1}{6} b_1 - \frac{1}{90} b_3 + \frac{1}{6} \mathcal{H}_I^1 \beta^I. \quad (4.9)$$

Unlike in the two and four-dimensional cases, (4.9) does not present itself in the form of (2.2), due to the presence of the vector anomaly  $\mathcal{I}_I^7$ . Notice that this contribution was missed in [71], which led to consider  $\tilde{a}$  as the candidate for a monotonically-decreasing function in [66]. However,  $\tilde{a}$  cannot be such a candidate, even more so because it is scheme-dependent<sup>5</sup> at

<sup>2</sup>All our computations were performed in *Mathematica* using the package `xAct`, and details on the derivation of the consistency conditions can be found in Appendix B.1. Due to the large number of terms appearing in (4.5) and related consistency conditions, we do not report most of them in the text. The interested reader can find them in a separate *Mathematica* file [2].

<sup>3</sup>To extend the check to higher loops it will be necessary to include the effects of the operators of dimension two and four.

<sup>4</sup>We use the notation  $X_{(IJ)} = X_{IJ} + X_{JI}$  and  $X_{[IJ]} = X_{IJ} - X_{JI}$ .

<sup>5</sup>In this Chapter, by “scheme-dependent” quantities we mean those which change under the addition of

order  $\beta$ .<sup>6</sup>

Nevertheless, we considered all possible linear combinations of the consistency conditions, to find all independent equations having the form of a gradient flow equation. Most importantly, we found the equation<sup>7</sup>

$$\partial_I \hat{a} = (\chi_{IJ} + \xi_{IJ}) \beta^J, \quad (4.10)$$

where

$$\begin{aligned} \hat{a} &= a - \frac{5}{6} b_1 + \frac{1}{10} b_2 + \frac{1}{45} b_3 + \frac{1}{10} b_4 \\ &\quad + \left( \frac{1}{10} \mathcal{B}_I + \frac{1}{24} \mathcal{C}_I + \frac{1}{20} \mathcal{E}_I + \frac{1}{24} \mathcal{F}_I + \frac{1}{6} \mathcal{H}_I^1 + \frac{1}{20} \mathcal{H}_I^2 + \frac{1}{12} \mathcal{H}_I^3 + \frac{1}{8} \mathcal{H}_I^4 - \frac{1}{40} \mathcal{H}_I^6 \right) \beta^I, \\ \chi_{IJ} &= \frac{1}{20} \partial_{[I} \mathcal{B}_{J]} - \frac{1}{40} \hat{\mathcal{B}}'_{IJ} + \frac{1}{48} \hat{\mathcal{C}}'_{IJ} + \frac{1}{20} \hat{\mathcal{E}}_{(IJ)} + \frac{1}{24} \mathcal{F}_{(IJ)} + \frac{1}{6} \mathcal{H}_{IJ}^1 \\ &\quad + \frac{1}{20} \mathcal{H}_{IJ}^2 + \frac{1}{12} \mathcal{H}_{IJ}^3 + \frac{1}{8} \mathcal{H}_{IJ}^4 - \frac{1}{40} \mathcal{H}_{IJ}^6, \\ \xi_{IJ} &= \frac{1}{20} \partial_{[I} \mathcal{B}_{J]} + \frac{1}{48} \mathcal{C}_{[IJ]} + \frac{1}{40} \hat{\mathcal{E}}_{[IJ]} + \frac{1}{48} \mathcal{F}_{[IJ]} + \frac{1}{48} \mathcal{F}'_{[IJ]} \\ &\quad + \frac{1}{6} \partial_{[I} \mathcal{H}_{J]}^1 + \frac{1}{20} \partial_{[I} \mathcal{H}_{J]}^2 + \frac{1}{12} \partial_{[I} \mathcal{H}_{J]}^3 + \frac{1}{8} \partial_{[I} \mathcal{H}_{J]}^4 - \frac{1}{40} \partial_{[I} \mathcal{H}_{J]}^6. \end{aligned} \quad (4.11)$$

$\hat{a}$  equals  $a$  at the fixed point, as the anomalies  $b_{1,\dots,7}$  are all proportional to  $\beta$ .  $\chi_{IJ}$  and  $\xi_{IJ}$  are symmetric and antisymmetric tensors, respectively.<sup>8</sup> Note that, by virtue of equation (4.10),  $\hat{a}$  is scheme independent at order  $\beta$ , while  $\chi_{IJ}$  and  $\xi_{IJ}$  are scheme-independent at order  $\beta^0$ , i.e. they are not affected to that order by adding local counterterms to the effective action.

### 4.3 Irreversibility

Consider the RG derivative of the two-point correlator of the marginal operators  $G_{IJ}(x) = \langle \mathcal{O}_I(x) \mathcal{O}_J(0) \rangle$ . Analogously to the four dimensional case studied in section 2.3,

$$\mu \frac{d}{d\mu} G_{IJ} + \gamma_I^K G_{KJ} + \gamma_J^K G_{IK} = g_{IJ} \square \square \delta^{(6)}(x) \quad (4.12)$$

where  $\delta^{(6)}(x)$  is the six-dimensional delta function, and  $g_{IJ}$  is evaluated via the anomaly in Appendix B.2,

$$g_{IJ} = -\partial_{(I} \mathcal{A}_{J)} - \hat{\mathcal{A}}_{(IJ)} + \hat{\mathcal{A}}'_{IJ} + \hat{\mathcal{A}}''_{IJ}. \quad (4.13)$$

As in section 2.3 it can be shown that  $g_{IJ}$  is proportional to the Zamolodchikov metric and is thus positive-definite by unitarity [53]. Furthermore, the consistency conditions relate the tensors  $\chi_{IJ}$  and  $g_{IJ}$  via

$$\chi_{IJ} = \frac{1}{6} g_{IJ} + \mathcal{O}(\beta). \quad (4.14)$$

---

purely background-dependent counterterms to the effective action.

<sup>6</sup>For example, the addition of a term  $\int d^6 x \sqrt{\gamma} X_I \partial_\mu \lambda^I \nabla_\nu H_4^{\mu\nu}$  in  $\mathcal{W}[\mathcal{J}]$ , with  $X_I$  arbitrary, induces, among others, the shifts  $\mathcal{I}_I^1 \rightarrow \mathcal{I}_I^1 + \mathcal{L}_\beta X_I$ , where  $\mathcal{L}_\beta$  is the Lie derivative along the beta function, and  $\mathcal{H}_I^1 \rightarrow \mathcal{H}_I^1 - \frac{1}{2} X_I$ . The shift of  $\mathcal{H}_I^1$  affects  $\hat{a}$  at order  $\beta$ .

<sup>7</sup>The linear combination of the consistency conditions leading to this equation is explicitly reported in the Mathematica file attached to the submission of [2].

<sup>8</sup>Using the consistency conditions we have checked that  $\xi_{IJ}$  cannot be written as  $\partial_{[I} X_{J]}$  for some vector  $X_J$ .



With this result, and upon contracting equation (4.10) with  $\beta^I$ , we get the desired monotonicity constraint in perturbation theory for  $\hat{a}$ ,

$$\mu \frac{d}{d\mu} \hat{a} = \beta^I \partial_I \hat{a} = \chi_{IJ} \beta^I \beta^J \geq 0, \quad (4.15)$$

where the inequality is saturated only if  $\beta^I = 0$ . This proves the  $a$ -theorem in perturbation theory (in theories with no relevant scalar operators of dimension two and four).

Additionally, we find another independent equation of the form<sup>9</sup>

$$\partial_I \hat{b} = (\chi'_{IJ} + \xi'_{IJ}) \beta^J \quad (4.16)$$

where

$$\begin{aligned} \hat{b} &= 4b_1 - \frac{4}{5}b_2 - \frac{4}{15}b_3 - \frac{4}{5}b_4 - \left( \frac{4}{5}\mathcal{B}_I + \frac{1}{2}\mathcal{C}_I + \frac{2}{5}\mathcal{E}_I + \frac{2}{5}\mathcal{H}_I^2 + \frac{2}{3}\mathcal{H}_I^3 + \frac{2}{3}\mathcal{H}_I^4 - \frac{1}{5}\mathcal{H}_I^6 \right) \beta^I, \\ \chi'_{IJ} &= -\frac{2}{5}\partial_{[I}\mathcal{B}_{J]} + \frac{1}{3}\hat{\mathcal{A}}''_{IJ} + \frac{1}{5}\hat{\mathcal{B}}'_{IJ} - \frac{1}{6}\hat{\mathcal{C}}'_{IJ} - \frac{1}{5}\hat{\mathcal{E}}_{(IJ)} - \frac{2}{5}\mathcal{H}_{IJ}^2 - \frac{2}{3}\mathcal{H}_{IJ}^3 - \frac{2}{3}\mathcal{H}_{IJ}^4 + \frac{1}{5}\mathcal{H}_{IJ}^6, \\ \xi'_{IJ} &= -\frac{2}{5}\partial_{[I}\mathcal{B}_{J]} - \frac{1}{5}\hat{\mathcal{E}}_{[IJ]} - \frac{2}{5}\partial_{[I}\mathcal{H}_{J]}^2 - \frac{2}{3}\partial_{[I}\mathcal{H}_{J]}^3 - \frac{2}{3}\partial_{[I}\mathcal{H}_{J]}^4 + \frac{1}{5}\partial_{[I}\mathcal{H}_{J]}^6. \end{aligned} \quad (4.17)$$

$\hat{b}$  is of order  $\beta$  and so vanishes at fixed points, and  $\chi'_{IJ}, \xi'_{IJ}$  are symmetric and antisymmetric respectively. The existence of the metric  $\chi'_{IJ}$  is related to the fact that in  $d = 6$  there are three rank-two conformally covariant operators one can define on the conformal manifold [53], corresponding to just as many scheme-independent rank-two tensors at the fixed point. This is in contrast with the two- and four-dimensional cases where there is only a unique rank-two tensor related to the Zamolodchikov metric. Nevertheless, we found that the consistency conditions impose an orthogonality constraint on  $\chi'_{IJ}$ ,

$$\chi'_{IJ} \beta^J = \mathcal{O}(\beta^2, \beta \partial \beta), \quad (4.18)$$

even though, in general,  $\chi'_{IJ}$  does not vanish at fixed points. Equations (4.10), (4.16), (4.18) imply that there exists a one-parameter family of monotonically decreasing functions at leading order in perturbation theory,

$$\mu \frac{d}{d\mu} (\hat{a} + \lambda \hat{b}) = \frac{1}{6} g_{IJ} \beta^I \beta^J + \mathcal{O}(\beta^3, \beta^2 \partial \beta). \quad (4.19)$$

Let us now generalize equation (4.15) in the presence of global symmetries at the fixed point, in the scheme where  $S^A = 0$ . By covariance, as in four dimensions, equation (4.15) will read

$$\partial_I \hat{a} = (\chi_{IJ} + \xi_{IJ}) B^J + P_I^A f_A, \quad (4.20)$$

where  $f_A$  is a generic combination of anomaly coefficients. Upon contracting (4.20) with  $B^I$

<sup>9</sup>As for Eq.(4.10), in the Mathematica file attached to the submission of [2] we report the explicit expression for the linear combination of consistency conditions resulting in this equation.

and using the condition  $B^I P_I^A = 0$  we get

$$B^I \partial_I \hat{a} = \mu \frac{d}{d\mu} \hat{a} = \frac{1}{6} g_{IJ} B^I B^J \geq 0. \quad (4.21)$$

Therefore, we find the same monotonicity constraint as in (4.15). Furthermore, if we are in a SFT so that  $B^I = S_A (T_A \lambda)^I$ , equation (4.21) implies that  $S^A = 0$  by  $G_F$ -covariance of  $\hat{a}$ . Therefore, we proved that scale implies conformal invariance in our setup.

## 4.4 Discussion

In this Chapter we studied the properties of RG flows originating from marginal deformations to unitary conformal field theories in six dimensions. For simplicity, we restricted the analysis to a class of CFTs where relevant scalar operators of dimension two and four are absent. Even though we work in perturbation theory, the UV CFT can in general be strongly coupled and may not admit a Lagrangian description.

The results obtained here can be summarized as follows:

- We derived all the consistency conditions with up to two powers of the coupling outside the fixed point. We solved those to find all the constraints among the anomaly coefficients which can be put in the form of a flow equation.
- We identified a one-parameter family of scheme-independent functions of the coupling constants of the theory,  $\hat{a} + \lambda \hat{b}$  with  $\lambda \in \mathbb{R}$ , equal to the  $a$ -anomaly coefficient plus  $O(\beta)$  corrections, which flow monotonically in the proximity of a fixed point thanks to unitarity. There is no parameter  $\lambda$  for which the combination  $\hat{a} + \lambda \hat{b}$ , agrees with the quantity analyzed in [66] in the context of  $\phi^3$  theory, therefore we dispel the doubts cast on the perturbative  $a$ -theorem in six dimensions.
- As a direct consequence of the  $a$ -theorem we proved, using standard arguments, that scale implies conformal invariance in our setup.

The dynamics of perturbative QFTs in six dimensions appears structurally different with respect to the four-dimensional case, due to the presence of multiple scheme-independent rank two tensors at the fixed point. Nevertheless, we were able to find a class of physical quantities whose RG flow is governed uniquely by the positive definite Zamolodchikov metric. We presume that extending our argument beyond perturbation theory would single out the monotonically-decreasing function in the one-parameter family that we found.

In the future, it will be interesting to extend our results in the presence of scalar operators of dimension two and four. First, that could highlight possible differences with the lower space-time dimensional cases, where relevant operators do not affect the monotonicity constraints [26, 55, 1].<sup>10</sup> Second, that will be necessary to test our results in the  $\phi^3$  theory, which is the only

---

<sup>10</sup>In four dimensions that is made clear by the argument employing the on-shell dilaton amplitude, which is

perturbatively calculable theory in six dimensions. It should be straightforward to generalize our computations to include those contributions, with the only difficulties arising due to the proliferation of terms in the anomaly functional and in the Weyl operator.

It would also be of interest to analyze  $\hat{a}$  and  $\hat{b}$  to higher-loop orders in  $\phi^3$  theory with the use of the consistency conditions, along the lines of [74]. The effects of dimension two and four operators as described in the previous paragraph may be necessary for such an analysis.

The question stands whether the  $a$ -theorem and the equivalence of scale and conformal invariance is valid beyond perturbation theory in six dimensions. So far no counterexamples are known. A first step towards solving this problem would be to define a physical quantity corresponding to  $\hat{a}$  close to the fixed point, such as the four-dilaton amplitude in four dimensions, as discussed in Section 3.1.4.<sup>11</sup> A fully non-perturbative argument using a six-dilaton scattering amplitude has been proposed in six dimensions with partial results [63], but it is not clear whether a different approach is needed.

---

manifestly insensitive to those effects, as explained in section 3.1.4.

<sup>11</sup>We attempted to derive a flow equation both a for four-dilaton scattering amplitude, and for the effective action on the sphere in six dimensions (as proposed originally in [20]), and we checked whether these quantities correspond to  $\hat{a}$ . We got incomplete results which we don't report in this thesis, but it is worth exploring this direction in the future.



## Part II

# Exact diagonalization methods



## Chapter 5

# Hamiltonian truncation

### 5.1 Introduction

How do we extract predictions about a strongly coupled quantum field theory (QFT) which is not exactly solvable? The lattice would be one answer, but it's not the only one. Hamiltonian truncation techniques, which generalize the Rayleigh-Ritz method familiar from quantum mechanics, are a viable deterministic alternative to the lattice Monte Carlo simulations, at least for some theories. These techniques remain insufficiently explored, compared to the lattice, and their true range of applicability may be much wider than what is currently believed. There exist several incarnations of Hamiltonian truncation, some better known than others, differing by the choice of basis and of the quantization frame. For example, Discrete Light Cone Quantization (DLCQ) [75] and Truncated Conformal Space Approach (TCSA) [76] are two representatives of this family of methods.

In Part II of this thesis we will be concerned with what is perhaps the simplest setting for the Hamiltonian truncation—the  $\phi^4$  theory in two space-time dimensions. Moreover, we will consider the most straightforward realization of the method—we will quantize at fixed time rather than on the light cone, and use the Fock space basis for the Hilbert space rather than the abstruse conformal bases.<sup>1</sup> We will expand the  $\phi^4$  Hamiltonian into ladder operators, as on the first page of every QFT textbook. We will however take this Hamiltonian more seriously than in most textbooks. Namely, we will use it to extract non-perturbative predictions, rather than as a mere starting point for the perturbative calculations. Concretely, we will (1) put the theory into a (large) finite volume, to make the spectrum discrete, (2) truncate the Hilbert space to a finite dimensional subspace of low-energy states, and (3) diagonalize the truncated Hamiltonian numerically.

In spite or perhaps because of its extreme simplicity, this concrete idea had received before our work even less attention than its more sophisticated cousins mentioned above. The only

---

<sup>1</sup>The use of a conformal basis in two dimensions requires compactifying the scalar field [77], see the discussion in section 5.4.5.

prior works known to us are [78, 79].<sup>2</sup> Here, we will follow up on these early explorations with our own detailed study. While the basic idea and the qualitative conclusions of our work will be similar to [78, 79], our implementation contains several conceptual and technical novelties. In particular, we will pay special attention to the convergence rate of the method, and will develop analytical tools allowing to accelerate the convergence, improve the accuracy, and better understand the involved systematic errors. The advances reported in this work and in other papers [83, 84], as well as the ongoing progress in developing the other variants of the Hamiltonian truncation [85, 86, 87, 88], [89, 90, 91] make us hopeful that in a not too distant future these methods will turn into precision tools for studying strongly coupled QFTs.

Concretely, our model is parametrized by the bare squared mass  $m^2$  and by the quartic coupling  $g = \bar{g}m^2$  with  $\bar{g} = O(1)$ . The physical particle mass is given by

$$m_{\text{ph}} = f(\bar{g})m \tag{5.1}$$

and the function  $f(\bar{g})$  is determined numerically. We will observe that the physical mass vanishes for  $\bar{g} = \bar{g}_c \approx 3$ , signaling the presence of a second order phase transition.

In Chapter 5 we focus mainly on the region below and around the critical coupling  $\bar{g}_c$ . In section 5.2 we present the problem and the basic methodology used to study the spectrum numerically. Section 5.3 elucidates the ideas behind the renormalization procedure, its implementations adopted in the numerical study, and provides some tests of the analytical results. The reader afraid of the technicalities may skip it. Yet it is precisely this section which is the theoretical heart of Chapter 5. Section 5.4 contains the calculation of the spectrum of the two-dimensional  $\phi^4$  theory in the  $\mathbb{Z}_2$ -unbroken phase.<sup>3</sup> The dependence of the numerical results on the physical and unphysical parameters is analyzed carefully, and an estimate of the critical coupling is provided. In section 5.5 we compare our method to the existing ones in the literature. Most of these prior studies focused in particular on the critical coupling estimates.

In Chapter 6 we will instead be interested in the complementary region  $\bar{g} > \bar{g}_c$ . In this range of couplings the theory is massive, but the  $\mathbb{Z}_2$  symmetry,  $\phi \rightarrow -\phi$ , is spontaneously broken. In infinite volume, there are therefore two degenerate vacua, and two towers of massive excitations around them. We will be able to determine the low energy spectrum as a function of  $\bar{g}$ . In finite volume the exact degeneracy is lifted, and the energy eigenstates come in pairs split by a small amount, exponentially small if the volume is large.

In the  $\mathbb{Z}_2$ -broken phase, there is also a topologically nontrivial sector of “kink” states corresponding, in the semiclassical limit, to field configurations interpolating between the two vacua. In this work we will probe the kink mass by studying the mass splittings in the topologically trivial sector.<sup>4</sup>

---

<sup>2</sup>A more extensive description of this work can be found in [80] and [81]. Another paper [82] studied the two-dimensional Yukawa model without scalar self-interaction.

<sup>3</sup> Computations were performed using a `python` code, which can be found in the `arXiv` submission of [3]

<sup>4</sup>The kink sectors has been studied directly in [84].



One interesting feature of the theory under study is that it enjoys a weak/strong coupling duality first discussed by Chang [92]. The dual description exists for all  $\bar{g} \geq \bar{g}_* \approx 2.26$ . As we review in Chapter 6, the duality relates a description in which the theory is quantized around the  $\mathbb{Z}_2$ -invariant vacuum state to an equivalent description in which it is quantized around a  $\mathbb{Z}_2$ -breaking vacuum. For  $\bar{g}$  not much above  $\bar{g}_*$  both descriptions are strongly coupled<sup>5</sup> and they can be equivalently employed as a starting point for the numerical computations. In section 6.1 we present a comparison between the numerical spectra obtained using the two descriptions, serving both as a non-trivial test of the method and as a check of the Chang duality.

On the other hand, for  $\bar{g} \gg \bar{g}_*$  the dual description becomes weakly coupled, and provides the better starting point. In section 6.2, we will explain a modification of the method which can be used, among other things, to study this regime (a weakly coupled  $\phi^4$  theory with negative  $m^2$ ) efficiently. It is based on a different treatment of the zero mode of the field. We will compare the numerical results with the predictions from perturbation theory and from semiclassical analyses.

We conclude in section 6.3. Appendix D.1 presents some technical details useful for the practical implementation of the procedure. Appendix C provides the perturbative checks of our method.

## 5.2 The problem and the method

### 5.2.1 Hamiltonian

We will be studying the two-dimensional  $\phi^4$  theory, defined by the following Euclidean action,

$$S = S_0 + g \int d^2x N_m(\phi^4), \quad (5.2)$$

$$S_0 = \frac{1}{2} \int d^2x N_m((\partial\phi)^2 + m^2\phi^2). \quad (5.3)$$

Here  $N_m$  denotes normal ordering with respect to the bare mass  $m$ . Normal ordering of the free massive scalar action  $S_0$  simply means that we set to zero the ground state energy density (*in infinite flat space, and before adding the quartic perturbation*). The quartic interaction term is then also assumed normal-ordered. In perturbation theory this simply corresponds to forbidding the diagrams with lines beginning and ending inside the same quartic vertex. In terms of operators, this means that we are adding the counterterms [93]

$$N_m(\phi^4) = \phi^4 - 6Z\phi^2 + 3Z^2. \quad (5.4)$$

Here

$$Z = \int \frac{d^2k}{(2\pi)^2} \frac{1}{k^2 + m^2} \quad (5.5)$$

---

<sup>5</sup>This explains why  $\bar{g}_*$  need not be equal, and in fact is not equal to the critical coupling  $\bar{g}_c$  mentioned above.

is a logarithmically UV-divergent quantity.

Although absent in (5.2), below we will also need to consider perturbations given by the normal-ordered  $\phi^2$  operator,

$$N_m(\phi^2) = \phi^2 - Z. \quad (5.6)$$

The above equations specify what we mean by the theory in infinite flat space, and also define the mass parameter  $m$  and the quartic coupling  $g$  in terms of which we will parametrize the theory. All physical quantities (such as particles masses and S-matrix elements) are then finite functions of  $m$  and  $g$ . Also the change of the ground state energy density due to turning on the coupling  $g$  is finite and observable in this theory. This change can be thought of as the contribution of the theory (5.2) to the cosmological constant.

Since both  $m$  and  $g$  are dimensionful, physics depends on their dimensionless ratio  $\bar{g} = g/m^2$ , while  $m$  (or  $g$ ) sets the overall mass scale. We will assume  $g > 0$  to have a stable vacuum. Both signs of  $m^2$  are interesting, but in this Chapter we will only consider the case  $m^2 > 0$ . Notice that this does not mean that we will always be in the phase of preserved  $\mathbb{Z}_2$  symmetry  $\phi \rightarrow -\phi$ , since the mass parameter undergoes renormalization. In fact, as we will see below, for  $m^2 > 0$  and  $\bar{g} > \bar{g}_c = O(1)$  the theory finds itself in the phase where the  $\mathbb{Z}_2$  symmetry is spontaneously broken. This is a non-perturbative phenomenon. For  $\bar{g} \ll 1$ , the fate of the  $\mathbb{Z}_2$  symmetry is of course determined by the sign of  $m^2$ .

In this thesis we will study the above theory not in infinite space but on a cylinder of the form  $S_L^1 \times \mathbb{R}$ , where  $S_L^1$  is the circle of length  $L$  and  $\mathbb{R}$  will be thought of as Euclidean time. We will impose the periodic boundary conditions around the circle. We will describe the theory on this geometry in the Hamiltonian formalism, taking advantage of the fact that the finite volume spectrum is discrete.

Now, what is the Hamiltonian which describes the theory (5.2) on  $S_L^1 \times \mathbb{R}$ ? The correct answer to this question involves a subtlety, so let us proceed pedagogically.

We first discuss the Hamiltonian which describes the free massive scalar. In canonical quantization, the field operator is expanded into modes:

$$\phi(x) = \sum_k \frac{1}{\sqrt{2L\omega_k}} \left( a_k e^{ikx} + a_k^\dagger e^{-ikx} \right), \quad (5.7)$$

where the momenta  $k$  take discrete values  $k = 2\pi n/L$ ,  $n \in \mathbb{Z}$ ,  $\omega_k = \sqrt{m^2 + k^2}$ , and the ladder operators satisfy the usual commutation relations:

$$[a_k, a_{k'}] = 0, \quad [a_k, a_{k'}^\dagger] = \delta_{nn'}. \quad (5.8)$$

The Hilbert space  $\mathcal{H}$  of the theory is the Fock space of these ladder operators, spanned by the states

$$|\psi\rangle = |k_1, \dots, k_m\rangle = N a_{k_1}^\dagger \dots a_{k_m}^\dagger |0\rangle, \quad (5.9)$$

where  $N$  is the normalization factor to get a unit-normalized state. The free scalar Hamiltonian is then given by

$$H_{\text{free}} = H_0 + E_0(L), \quad H_0 = \sum_k \omega_k a_k^\dagger a_k. \quad (5.10)$$

The only subtlety here is the c-number term  $E_0(L)$ . The point is that we want the oscillator part  $H_0$  of the finite volume Hamiltonian to be normal-ordered. However, the normal ordering counterterm in infinite space and for finite  $L$  is slightly different, and  $E_0(L)$  compensates for this mismatch. It is nothing but the Casimir energy of the scalar field, and is given by (see [94])

$$E_0 = -\frac{1}{\pi L} \int_0^\infty dx \frac{x^2}{\sqrt{m^2 L^2 + x^2}} \frac{1}{e^{\sqrt{m^2 L^2 + x^2}} - 1}. \quad (5.11)$$

This expression can be derived in many equivalent ways. One method is to regulate the difference of the zero-point energies,

$$\sum_n \omega_{k_n}/2 - L \int_{-\infty}^{+\infty} \frac{dk}{2\pi} \omega_k/2. \quad (5.12)$$

Another method is to compute the partition function of the theory on the torus  $S_{L_1}^1 \times S_{L_2}^1$ , which can be done from the path integral formulation of the theory. The partition function defined in this way enjoys the property of modular invariance. This method naturally produces a term in the free energy of the form  $(2\pi L_2) \times E_0(L_1)$ .

We next discuss the finite-volume Hamiltonian for the interacting theory. It will have the form

$$H = E_0(L) + H_0 + gV_4 + \dots, \quad (5.13)$$

$$V_4 = \int_0^L dx N_{m,L}(\phi^4). \quad (5.14)$$

The normal ordering here is defined on the circle of length  $L$  in the Hamiltonian sense, just putting all creation operators to the left. Thus,

$$V_4 = gL \sum_{k_1+k_2+k_3+k_4=0} \frac{1}{\prod \sqrt{2L\omega_i}} \left[ a_{k_1} a_{k_2} a_{k_3} a_{k_4} + 4a_{-k_1}^\dagger a_{k_2} a_{k_3} a_{k_4} \right. \\ \left. + 6a_{-k_1}^\dagger a_{-k_2}^\dagger a_{k_3} a_{k_4} + 4a_{-k_1}^\dagger a_{-k_2}^\dagger a_{-k_3}^\dagger a_{k_4} + a_{-k_1}^\dagger a_{-k_2}^\dagger a_{-k_3}^\dagger a_{-k_4}^\dagger \right]. \quad (5.15)$$

The origin of the  $\dots$  terms in (5.13) lies again in the fact that the normal-ordering counterterms added when defining  $V$ ,

$$N_{m,L}(\phi^4) = \phi^4 - 6Z_L \phi^2 + 3Z_L^2, \quad Z_L = \sum_n \frac{1}{2L\omega_{k_n}}, \quad (5.16)$$

are not exactly the same as in the infinite space definition (5.4). The difference is

$$N_m(\phi^4) - N_{m,L}(\phi^4) = -6(Z - Z_L)\phi^2 + 3(Z^2 - Z_L^2) = 6(Z_L - Z)N_{m,L}(\phi^2) + 3(Z_L - Z)^2, \quad (5.17)$$

where in the second equality we used  $\phi^2 = N_{m,L}(\phi^2) + Z_L$ .

To compute  $Z_L - Z$  we rewrite  $Z$  in the form adapted to the Hamiltonian quantization,

$$Z = \int \frac{dk}{4\pi} \frac{1}{\sqrt{k^2 + m^2}}. \quad (5.18)$$

The difference  $Z_L - Z$  is finite and is readily calculated using the Abel-Plana formula,

$$\zeta \equiv Z_L - Z = \frac{1}{\pi} \int_0^\infty \frac{dx}{\sqrt{m^2 L^2 + x^2}} \frac{1}{e^{\sqrt{m^2 L^2 + x^2}} - 1}. \quad (5.19)$$

This allows us to complete the ... terms in (5.13). Thus, the Hamiltonian on a circle of finite length  $L$  corresponding to the infinite space theory (5.4) is given by,

$$H = H_0 + g[V_4 + 6\zeta V_2] + [E_0 + 3\zeta^2 gL], \quad (5.20)$$

$$V_2 = \int_0^L dx : \phi^2 :_L = \sum_k \frac{1}{2\omega_k} (a_k a_{-k} + a_k^\dagger a_{-k}^\dagger + 2a_k^\dagger a_k). \quad (5.21)$$

We see that the Hamiltonian (5.20) differs from the “naive” Hamiltonian

$$H = H_0 + V, \quad V = gV_4 \quad (5.22)$$

by a “correction term”, proportional to  $E_0$  and  $\zeta$ . The presence of these terms is conceptually important. They would be also straightforward to include into numerical analysis, for any  $L$ . However, in this Chapter we will be focusing on the case  $Lm \gg 1$ . In this regime the corrections due to  $E_0$  and  $\zeta$  are exponentially suppressed, and their numerical impact is negligible. For this reason, and to simplify the discussion, we will omit the exponentially suppressed corrections in this Chapter. With this proviso, from now on we will use the “naive” Hamiltonian (5.22).

### 5.2.2 Truncation

We next explain the truncation method. We will work in the Hilbert space  $\mathcal{H}$  spanned by the free massive scalar states. The Hamiltonian  $H$  acts in this space, and the problem is to diagonalize it. We thus use the free massive scalar states as a basis into which we expand the eigenstates of the interacting theory. Let us think of the Hamiltonian as an infinite matrix  $H_{ij}$  where  $i, j$  numbers the states in  $\mathcal{H}$ ,

$$H_{ij} = \langle i | H | j \rangle. \quad (5.23)$$

Notice that the states  $|i\rangle$  as introduced above form an orthonormal basis of  $\mathcal{H}$ . To find the spectrum of the theory in finite volume, we need to diagonalize the matrix  $H_{ij}$ . This diagonalization can be done separately in sectors having fixed quantum numbers corresponding to the operators commuting with the Hamiltonian.

The first such quantum number is the momentum:  $[P, H] = 0$ . In this thesis we will be

working in the sector of states of vanishing total momentum,

$$P = k_1 + \dots + k_m = 0. \quad (5.24)$$

In a large volume, the states of nonzero momentum should correspond to boosted zero-momentum states, and their energies should be related to zero-momentum energies by the Lorentz-invariant dispersion relation. It would be interesting to check this in future work.

The second conserved quantum number is the spatial parity  $\mathbb{P}$ , which acts  $x \rightarrow -x$ . It maps the state (5.9) into  $\mathbb{P}|\psi\rangle = |-k_1, \dots, -k_m\rangle$ . In this thesis we will be working in the  $\mathbb{P}$ -invariant sector,<sup>6</sup> whose orthonormal basis consists of the states

$$|\psi^{\text{sym}}\rangle = \beta(\psi) \left( |\psi\rangle + \mathbb{P}|\psi\rangle \right), \quad (5.25)$$

where  $\beta(\psi)$  is the normalization factor,

$$\beta(\psi) = 1/\sqrt{2} \text{ if } \mathbb{P}|\psi\rangle \neq |\psi\rangle, \quad 1/2 \text{ otherwise.} \quad (5.26)$$

The restriction to the subspace  $P = 0, \mathbb{P} = 1$  will be tacitly assumed in all of the rest of this thesis.

The final conserved quantum number is the already mentioned global  $\mathbb{Z}_2$  symmetry  $\phi \rightarrow -\phi$  (the field parity). Its eigenvalue on the states (5.9) is  $(-1)^m$ . Below we will be considering both the  $\mathbb{Z}_2$ -even and  $\mathbb{Z}_2$ -odd sector.

Each of the two sectors  $\mathbb{Z}_2 = \pm 1$  still contains infinitely many states. We will thus have to truncate the Hilbert space. The truncation variable will be the  $H_0$ -eigenvalue,

$$E = \omega_{k_1} + \dots + \omega_{k_m}. \quad (5.27)$$

We will truncate by considering all states of  $E \leq E_{\text{max}}$ . The parameter  $E_{\text{max}}$  should be thought of as a UV cutoff. The truncated Hilbert space is finite-dimensional, and the matrix  $H_{ij}$  restricted to this space can be diagonalized numerically. This is what we will do.

In principle, one could imagine alternative truncation schemes. For example, one can truncate in the maximal wavenumber  $k_{\text{max}}$ . Such a truncation would be closer to the usual way one implements the UV cutoff in field theory. By itself, however, it does not render the Hilbert space finite-dimensional. One could also think of truncating in the total occupation number of the state, or in the individual occupation numbers per oscillator, and so on. Our initial exploration of such subsidiary cutoffs did not produce any dramatic gains in the performance of the method. In the end we decided to stick to the cutoff in  $E$ . As we will see in the next section, this cutoff allows for a natural implementation of the renormalization of the Hamiltonian, necessary to improve the convergence of the method. In the future it may be

---

<sup>6</sup>The extension of our method to the  $\mathbb{P}$ -odd sector is straightforward. We consider only the  $\mathbb{P}$ -even sector, because we do not expect bound states with  $\mathbb{P} = -1$ .

interesting to return to the other cutoffs, and explore them more systematically. One slightly different possibility has already been considered in [84].

## 5.3 UV cutoff dependence and renormalization

### 5.3.1 General remarks

It is not difficult to write a code which computes the  $H_{ij}$  matrix restricted to the  $E \leq E_{\max}$  subspace<sup>7</sup> and diagonalizes it. The results of these numerical calculations will be discussed below. As we will see, as the UV cutoff  $E_{\max}$  is increased, the energy levels computed using the truncated Hilbert space (‘truncated energy levels’) tend to some finite limits. These limits should be naturally identified with the exact energy levels. An interesting theoretical question then arises: *what is the convergence rate of the method?* There is also a related practical question: *how can the convergence be improved?* These questions will be discussed in this section.

By calculating the truncated energy levels we are discarding the contribution to the low-energy physics coming from the high energy states of the Hilbert space. Since the UV divergences have been already taken care of, this contribution is power-suppressed and goes to 0 as the cutoff is increased. In the standard Wilsonian approach to the renormalization group, by integrating out high-momentum (or short-distance) degrees of freedom one gets a flow in the space of Hamiltonians, along which the same physics is described in terms of low-momentum degrees of freedom with renormalized couplings. We would like to apply the same philosophy to our case, although we may expect some differences, because our cutoff prescription—cutting off in  $E$ —is different from the ones normally used in field theory. First of all, it breaks the Lorentz invariance. Second, the fact that we truncate in the *total* energy of the state, rather than in that of its individual constituents, renders our cutoff effectively non-local. Thus, we should be prepared to see non-local as well as Lorentz-violating operators generated by the flow. We will see, however, that to leading order it will be sufficient to renormalize a few local operators in the Hamiltonian. It will be possible to do this computation in perturbation theory, since the potential we add to the free Hamiltonian is a relevant deformation and becomes less important in the UV. The dimensionless parameter which sets the convergence of the truncated energy levels and the asymptotic magnitude of the counterterms will be  $g/E_{\max}^2$ . All these considerations will be made concrete in the following.

We start our analysis from the exact eigenvalue equation:

$$H.c = \mathcal{E}c, \tag{5.28}$$

where  $c$  is an infinite-dimensional vector living in the full Hilbert space  $\mathcal{H}$ . Here and below, we use curly  $\mathcal{E}$  to denote energy levels of the interacting theory, while  $E$  will be used to denote free scalar energy levels.

---

<sup>7</sup>See appendix D.1 for some tricks speeding up this computation.

### 5.3. UV cutoff dependence and renormalization

---

In our methodology the Hilbert space is divided in two subspaces:

$$\mathcal{H} = \mathcal{H}_l \oplus \mathcal{H}_h, \quad (5.29)$$

where  $\mathcal{H}_l$  is the low-energy sector of the Hilbert space, treated numerically, while  $\mathcal{H}_h$  is spanned by an infinite number of discarded high-energy states. So we have  $c = (c_l, c_h)^t$ , and Eq. (5.28) takes the following form in components:

$$H_{ll}.c_l + H_{lh}.c_h = \mathcal{E}c_l, \quad H_{hl}.c_l + H_{hh}.c_h = \mathcal{E}c_h. \quad (5.30)$$

Here we denoted

$$H_{\alpha\beta} \equiv P_\alpha H P_\beta, \quad (5.31)$$

where  $P_\alpha$  ( $\alpha = l, h$ ) is the orthogonal projector on  $\mathcal{H}_\alpha$ .

Using the second equation in (5.30) to eliminate  $c_h$  from the first one, we obtain:

$$[H_{ll} - H_{lh}.(H_{hh} - \mathcal{E})^{-1}.H_{hl}].c_l = \mathcal{E}c_l, \quad (5.32)$$

or, equivalently,

$$[H_{\text{trunc}} + \Delta H].c_l = \mathcal{E}c_l, \quad (5.33)$$

$$\Delta H = -V_{lh}.(H_0 + V_{hh} - \mathcal{E})^{-1}.V_{hl}. \quad (5.34)$$

This equation is very important. Notice that  $H_{ll} \equiv H_{\text{trunc}}$  is nothing but the Hamiltonian truncated to the low-energy Hilbert space. Notice furthermore that the mixing between the high and low-energy states is due only to  $V$ , since  $H_0$  is diagonal.

Eq. (5.33) is *exact*, yet it resembles the truncated eigenvalue equation, with a correction  $\Delta H$ . This equation will be a very convenient starting point to answer the two questions posed at the beginning of this section.

We will now start making approximations. First, we expand  $\Delta H$  in  $V_{hh}$  and keep only the zeroth term

$$\Delta H = -V_{lh}.(H_0 - \mathcal{E})^{-1}.V_{hl} + \dots \quad (5.35)$$

By dimensional reasons, we expect that the next term in the expansion,

$$V_{lh}.(H_0 - \mathcal{E})^{-1}.V_{hh}.(H_0 - \mathcal{E})^{-1}.V_{hl}, \quad (5.36)$$

will be suppressed with respect to the one we keep by  $g/E_{\text{max}}^2$ . It will be very interesting to include this term in future work, and we will comment below about how this can be done.

Equation (5.35) defines  $\Delta H$  as an operator on  $\mathcal{H}_l$ . The definition depends on the eigenvalue  $\mathcal{E}$  that we are trying to compute. This subtlety will be dealt with below, while for the moment let us replace  $\mathcal{E}$  by some reference energy  $\mathcal{E}_*$ . Even then, the definition seems impractical since it involves a sum over infinitely many states in  $\mathcal{H}_h$ . Indeed, the matrix elements of  $\Delta H$

according to this definition are given by:

$$(\Delta H)_{ij} = - \sum_{k: E_k > E_{\max}} \frac{V_{ik} V_{kj}}{E_k - \mathcal{E}_*}. \quad (5.37)$$

Fortunately, in the next section we will give a simplified approximate expression for  $\Delta H$  not involving infinite sums. As we will see, to leading order  $\Delta H$  will be approximated by a sum of local terms:

$$\Delta H \approx \sum_N \kappa_N V_N, \quad V_N = \int_0^L dx : \phi(x)^N :. \quad (5.38)$$

To this leading order, adding  $\Delta H$  to  $H_{\text{trunc}}$  results in simply renormalizing the local couplings. As we will see, a more accurate expression for  $\Delta H$  contains subleading corrections, which in general cannot be expressed as integrals of local operators. The appearance of these nonlocal corrections is due to the above-mentioned fact that truncating in total energy is not a fully local way of regulating the theory.

### 5.3.2 Computation of $\Delta H$

Consider then the matrix elements (5.37) of  $\Delta H$  for  $i, j$  in the truncated basis. We will write them in the form

$$(\Delta H)_{ij} = - \int_{E_{\max}}^{\infty} dE \frac{M(E)_{ij}}{E - \mathcal{E}_*}, \quad (5.39)$$

$$M(E)_{ij} dE \equiv \sum_{k: E \leq E_k < E+dE} V_{ik} V_{kj}. \quad (5.40)$$

We are interested in the large- $E$  asymptotics for  $M(E)_{ij}$ . Of course, for finite  $L$  the energy levels are discrete and this function should be properly thought of as a distribution (a sum of delta-functions). However, since the high-energy spectrum is dense, the fluctuations due to discreteness will tend to average out when integrating in  $E$ . Below we will find a continuous approximation for  $M(E)_{ij}$ , valid on average. Such an approximation will be good enough for computing the integral in (5.39) with reasonable accuracy. A small loss of accuracy will occur because of the sharp cutoff at  $E = E_{\max}$ ; this will be discussed below in sections 5.4.3 and 5.4.4.

Our calculation of  $M(E)_{ij}$  will follow the method introduced in [91], section 5.3. It will be based on the fact that the same quantity appears also in the following matrix element,

$$C(\tau)_{ij} = \langle i | V(\tau/2) V(-\tau/2) | j \rangle = \int_0^{\infty} dE e^{-[E - (E_i + E_j)/2]\tau} M(E)_{ij}, \quad (5.41)$$

where we inserted a completeness relation in the second step. A word about notation: the Euclidean time dependence of various operators is always meant in the interaction representation, e.g.

$$V(\tau) = e^{H_0 \tau} V e^{-H_0 \tau}. \quad (5.42)$$



### 5.3. UV cutoff dependence and renormalization

If the time dependence is not shown, it means that the operator is taken at  $\tau = 0$ .

Eq. (5.41) says that  $C(\tau)$  is basically the Laplace transform of  $M(E)$ . The leading non-analytic part of  $C(\tau)$  for  $\tau \rightarrow 0$  will come from the leading piece of  $M(E)$  as  $E \rightarrow \infty$ . Our method will proceed by first extracting the leading non-analytic part of  $C(\tau)$ , and then taking its inverse Laplace transform to get at  $M(E)$ .

We will present the computation for a general case when the potential contains both  $:\phi^2:$  and  $:\phi^4:$  terms:

$$V = g_2 V_2 + g_4 V_4. \quad (5.43)$$

Our Hamiltonian (5.22) has  $g_2 = 0$ ,  $g_4 = g$ . Turning on  $g_2 \neq 0$  corresponds to an extra contribution to the mass. Having this coupling will be useful for a check of the formalism in section 5.3.4 below.

We have

$$C(\tau) = \sum g_n g_m \int_0^L dx \int_{-L/2}^{L/2} dz : \phi(x+z, \tau/2)^n : : \phi(x, -\tau/2)^m :, \quad (5.44)$$

where we used periodicity and invariance under spatial translations. The non-analyticity of  $C(\tau)$  for  $\tau \rightarrow 0$  comes from the integration region where the product of two local operators is singular, i.e. when they are inserted at near-coinciding points. Let us focus on one term in the sum, and rewrite it using Wick's theorem as

$$g_n g_m \int_0^L dx \int_{-L/2}^{L/2} dz \sum_{0 \leq k \leq \min(n,m)} f_{nm, n+m-2k} G_L(z, \tau)^k : \phi(x+z, \tau/2)^{n-k} \phi(x, -\tau/2)^{m-k} :. \quad (5.45)$$

Here  $G_L(z, \tau)$  is the two-point function of  $\phi$  in the free theory on the circle of length  $L$ . The  $f$ 's are integer combinatorial factors (operator product expansion coefficients),

$$f_{nm, n+m-2k} = \binom{n}{k} \binom{m}{k} k!. \quad (5.46)$$

In (5.45), the leading non-analytic behavior as  $\tau \rightarrow 0$  will come from the propagator powers  $G_L(z, \tau)^k$ . The remaining normal-ordered operators can be Taylor expanded in  $z, \tau$ ,

$$g_n g_m \int_0^L dx \int_{-L/2}^{L/2} dz \sum_{0 \leq k \leq \min(n,m)} f_{nm, n+m-2k} G_L(z, \tau)^k [ : \phi(x)^{n+m-2k} : + O(\tau^2, z^2) ]. \quad (5.47)$$

The terms  $O(z)$  are not shown because they will vanish upon integration. The terms  $O(\tau^2, z^2)$  will produce a subleading singularity as  $\tau \rightarrow 0$ . The corresponding contributions to  $M(E)$  will be suppressed by  $m^2/E_{\max}^2$  compared to the leading ones. In this work these subleading contributions will be neglected, but it will be interesting and important to include them in the future.<sup>8</sup>

<sup>8</sup>The subleading contributions will give rise to new, derivative, operators in the Hamiltonian. Since our regulator breaks Lorentz invariance, the derivatives in  $\tau$  and  $z$  are not going to enter symmetrically in these subleading terms.

Eq. (5.47) means that at leading order the correction Hamiltonian  $\Delta H$  will contain terms of the form (5.38) with  $N = n + m - 2k$ . To find the couplings  $\kappa_N$ , we need to evaluate the non-analytic part of the following quantities,

$$I_k(\tau) \equiv \int_{-L/2}^{L/2} dz G_L(z, \tau)^k, \quad k = 0, 1, 2, 3, 4. \quad (5.48)$$

As we will see below, for  $k = 0, 1$  the  $\tau \rightarrow 0$  behavior will be analytic (for  $k = 0$  this is a triviality). This implies that only  $N = 0, 2, 4$  terms will be generated in (5.38).

To evaluate (5.48), we will need a few well-known facts about  $G_L(z, \tau)$ . In the infinite volume limit  $L \rightarrow \infty$  the rotation invariance is restored, and the two-point function is a modified Bessel function of the second kind, depending on the distance  $\rho = \sqrt{z^2 + \tau^2}$ ,

$$G(\rho) = \frac{1}{2\pi} K_0(m\rho) \quad (L = \infty). \quad (5.49)$$

It has a logarithmic short distance behavior and decays exponentially at long distances:<sup>9</sup>

$$G(\rho) \approx \begin{cases} -\frac{1}{2\pi} \log\left(\frac{e^\gamma}{2} m\rho\right) [1 + O(m^2\rho^2)], & \rho \ll 1/m, \\ \exp(-m\rho)/(2\sqrt{2\pi m\rho}), & \rho \gg 1/m. \end{cases} \quad (5.50)$$

For a finite  $L$ , the two-point function is obtained from the  $L = \infty$  case via periodization,

$$G_L(z, \tau) = \sum_{n \in \mathbb{Z}} G(\sqrt{(z + nL)^2 + \tau^2}). \quad (5.51)$$

The periodization corrections are exponentially small for  $Lm \gg 1$ . In the present Chapter, this condition will be always satisfied, and so we will use  $G$  in place of  $G_L$ .<sup>10</sup> This is consistent with having neglected the exponentially suppressed  $E_0(L)$  and  $\zeta$  terms when passing from (5.20) to (5.22).

So we will replace  $G_L$  by  $G(\rho)$  in (5.48). The non-analytic behavior of the integral comes from the small  $z$  region, where the short-distance logarithmic asymptotic (5.50) is applicable. To regulate spurious IR divergences, it's convenient to calculate the first derivative with respect to  $\tau$ ,

$$I'_k(\tau) = k \int_{-\infty}^{\infty} dz (dG/d\rho) G(\rho)^{k-1} \frac{\tau}{\rho} \rightarrow k \left(-\frac{1}{2\pi}\right)^k \int_{-\infty}^{\infty} dz \left[\log\left(\frac{e^\gamma}{2} m\rho\right)\right]^{k-1} \frac{\tau}{\rho^2}, \quad (5.52)$$

where we also replaced  $G$  by its short-distance asymptotics. The resulting integrals are

---

<sup>9</sup> $\gamma$  is Euler's constant.

<sup>10</sup>The induced error can be estimated by approximating  $G_L(z, \tau) \approx G(\rho) + 2G(L)$  for small  $\rho$ . This implies a shift  $\Delta I_k(\tau) \approx \alpha I_{k-1}(\tau)$ ,  $\alpha = 2kG(L)$ . For  $k = 4$  and  $L = 4/m$  ( $L = 6/m$ ) the coefficient  $\alpha = 0.01(0.002)$ .

### 5.3. UV cutoff dependence and renormalization

convergent and readily evaluated,<sup>11</sup>

$$\begin{aligned}
I_1'(\tau) &= \text{const} , \\
I_2'(\tau) &= \frac{1}{2\pi} \log m\tau + \text{const} , \\
I_3'(\tau) &= -\frac{3}{8\pi^2} (\log m\tau)^2 - \frac{3\gamma}{4\pi^2} \log m\tau + \text{const} , \\
I_4'(\tau) &= \frac{1}{4\pi^3} (\log m\tau)^3 + \frac{3\gamma}{4\pi^3} (\log m\tau)^2 + \frac{12\gamma^2 + \pi^2}{16\pi^3} \log m\tau + \text{const} ,
\end{aligned} \tag{5.53}$$

modulo errors induced by using the short-distance asymptotics of  $G$ . These errors are suppressed by  $O(m^2\tau^2)$ . The corresponding corrections to  $M(E)$  are suppressed by  $m^2/E_{\text{max}}^2$ , and will be omitted. Also, as mentioned above, we see that  $I_1'(\tau)$  is analytic.

We now have to pass from the small- $\tau$  behavior to the large- $E$  asymptotics. Differentiating Eq. (5.41) we have

$$C'(\tau) = \int_0^\infty dE e^{-E_{ij}\tau} [-E_{ij}M(E)] , \tag{5.54}$$

where we defined

$$E_{ij} \equiv E - (E_i + E_j)/2 . \tag{5.55}$$

Thus from the inverse Laplace transforms of  $I_k'(\tau)$  we should be able to determine the asymptotics of  $-E_{ij}M(E)$ . These inverse Laplace transforms are found from the following table of direct transforms,

$$\begin{aligned}
\int_\epsilon^\infty dE e^{-E\tau} \frac{1}{E} &= -\log m\tau + \text{analytic} , \\
\int_\epsilon^\infty dE e^{-E\tau} \frac{\log E/m}{E} &= \frac{1}{2} (\log m\tau)^2 + \gamma \log m\tau + \text{analytic} , \\
\int_\epsilon^\infty dE e^{-E\tau} \frac{(\log E/m)^2}{E} &= -\frac{1}{3} (\log m\tau)^3 - \gamma (\log m\tau)^2 - (\pi^2/6 + \gamma^2) \log m\tau + \text{analytic} .
\end{aligned} \tag{5.56}$$

Since we are only interested in the large- $E$  asymptotics, the IR cutoff  $\epsilon$  is not important—its value only influences the analytic parts.

Gathering everything, we obtain the following formula for the leading asymptotic behavior of  $M(E)$ ,

$$M(E) \sim [g_4^2\mu_{440} + g_2^2\mu_{220}]V_0 + [g_4^2\mu_{442} + g_2g_4\mu_{422}]V_2 + g_4^2\mu_{444}V_4 \Big|_{E \rightarrow E_{ij}} , \tag{5.57}$$

where

$$\begin{aligned}
\mu_{440}(E) &= \frac{1}{E^2} \left\{ \frac{18}{\pi^3} (\log E/m)^2 - \frac{3}{2\pi} \right\} , & \mu_{220}(E) &= \frac{1}{\pi E^2} , \\
\mu_{442}(E) &= \frac{72 \log E/m}{\pi^2 E^2} , & \mu_{422} &= \frac{12}{\pi E^2} , & \mu_{444}(E) &= \frac{36}{\pi E^2} .
\end{aligned} \tag{5.58}$$

As the notation suggests, the  $\mu$ -functions in (5.57) are evaluated at  $E = E_{ij}$ . This equation

<sup>11</sup>Mathematica's `Integrate` function sometimes gives wrong results for integrals of this type, so be careful.

is the main result of this section. We subjected it to several tests, which we are going to describe below.

Before proceeding, let us comment on the evaluation of the next-to-leading term (5.36) in the renormalization procedure, which will be important in future developments of the method. From this term we will extract the  $O(g^3/E_{\max}^4)$  contribution to the coefficients  $\kappa_N$ . This correction term is the most interesting of all  $1/E_{\max}^4$  corrections, since it dominates in the limit  $g \gg m^2$ . Technically, we should generalize  $C(\tau)$  and  $M(E)$  in Eq. (5.41) to functions of two variables ( $\tau_{1,2}$  and  $E_{1,2}$ ) and extract the leading non-analytic pieces for  $\tau_{1,2} \rightarrow 0$ . This calculation will involve Wick contractions among the operators in  $C(\tau_1, \tau_2)$ , the cyclic ones being the only nontrivial part. An alternative way to calculate the higher-order corrections has been devised in [83].

We shall now move on to the tests of Eq. (5.58).

### Test 1

Let us plug (5.57) into (5.39), and do the integral neglecting the dependence on  $\mathcal{E}_*$  and  $(E_i + E_j)/2$ .<sup>12</sup> This gives  $\Delta H$  of the form (5.38), i.e. as a sum of local counterterms with coefficients which are functions of  $E_{\max}$ . For example, the  $g_4^2$  part is given by ( $\text{Log} \equiv \log E_{\max}/m$ ),

$$\Delta H \approx -\frac{g_4^2}{E_{\max}^2} \left\{ \left[ \frac{9}{\pi^3} (\text{Log}^2 + \text{Log}) + \frac{3(6 - \pi^2)}{4\pi^3} \right] V_0 + \left( \frac{36}{\pi^2} \text{Log} + \frac{18}{\pi} \right) V_2 + \frac{18}{\pi} V_4 \right\}. \quad (5.59)$$

This expression was checked as follows. Working in infinite volume, we computed the order  $g^2$  perturbative corrections to the vacuum energy, particle mass, and  $2 \rightarrow 2$  scattering amplitude, imposing the cutoff  $E \leq E_{\max}$  on the intermediate state energy (thus working in the ‘old-fashioned’ Hamiltonian perturbation theory formalism, rather than in terms of Feynman diagrams). We then checked that the leading  $E_{\max}$  dependence of these results is precisely the one implied by (5.59). This way of arriving at (5.59) is more laborious than the one given above, and we do not report the details.

### Test 2

A direct check of the asymptotics (5.57) can be done by comparing it with the actual value of  $M(E)$  computed from its definition (5.40). One example is given in figure 5.1, where we consider the diagonal matrix elements  $\langle i|M(E)|i\rangle$ ,  $|i\rangle$  the state of  $i$  particles at rest,  $i = 0, 1, 2$ . We choose  $m = 1$ ,  $L = 6$ ,  $g_2 = 0$  and  $g_4 = 1$ . The green smooth curves are the theoretical asymptotics from (5.57). The blue irregular curves represent the moving average of  $\langle i|M(E)|i\rangle$  over the interval  $[E - \Delta E, E + \Delta E)$  with  $\Delta E = 1$ . To facilitate the comparison, both are plotted multiplied by  $E_{ii}^2$ . We see that the two curves agree quite well on average.

A third test, involving the  $g_2$  coupling, will be described in section 5.3.4.

---

<sup>12</sup>We stress that in numerical computations it will be important to retain these subleading corrections.

### 5.3. UV cutoff dependence and renormalization

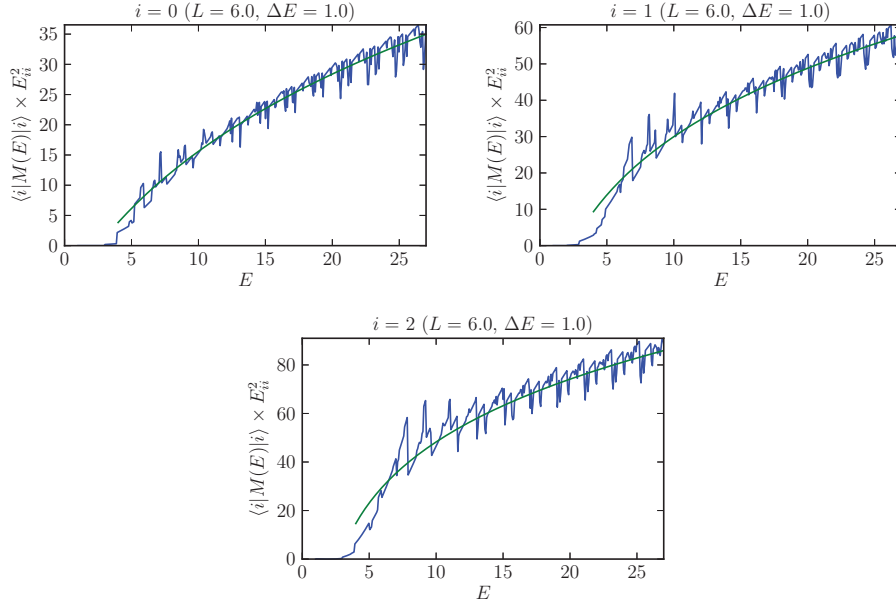


Figure 5.1: A test of the  $M(E)$  asymptotics; see the text.

#### 5.3.3 Renormalization procedures

By “renormalization”, in a broad sense, we mean adding to the truncated Hamiltonian  $H_{\text{trunc}}$  extra terms designed to compensate for the truncation effects and reduce the  $E_{\text{max}}$  dependence of the results. In this section we will describe in detail the three renormalization prescriptions used in our numerical work.

Consider thus the Hamiltonian

$$H = H_0 + V, \quad V = g_2 V_2 + g_4 V_4. \quad (5.60)$$

In the main numerical studies in section 5.4 we will set  $g_2 = 0$ . The opposite case  $g_4 = 0$ ,  $g_2 \neq 0$  will be considered in the check in section 5.3.4.

We are interested in the spectrum of  $H$  on a circle of length  $L$ . Three approximations to this spectrum, in order of increasing accuracy, can be obtained as follows.

##### 1. Raw truncation (marked ‘raw’ in plots)

In this simplest approach, we are not performing any renormalization. The truncated Hamiltonian  $H_{\text{trunc}}$  is constructed by restricting  $H$  to the subspace  $\mathcal{H}_l$  of the full Hilbert space, spanned by the states of energy  $E \leq E_{\text{max}}$ . The spectrum of  $H_{\text{trunc}}$  will be called the ‘raw spectrum’. According to Eqs. (5.57), (5.59), we expect that the raw spectrum approximates the exact spectrum with an error which scales as  $1/E_{\text{max}}^2$  (up to logarithms).

##### 2. Local renormalization (marked ‘ren.’ in plots)

## Chapter 5. Hamiltonian truncation

---

In this approach, we construct a correction Hamiltonian  $\Delta H$  by the formula (5.39). We use the asymptotics (5.57) for  $M(E)$ , in which we neglect  $(E_i + E_j)/2$  with respect to  $E_{\max}$ . This gives a local  $\Delta H$  of the form (5.38) with

$$\begin{aligned}\kappa_0 &= - \int_{E_{\max}}^{\infty} \frac{dE}{E - \mathcal{E}_*} [g_4^2 \mu_{440}(E) + g_2^2 \mu_{220}(E)], \\ \kappa_2 &= - \int_{E_{\max}}^{\infty} \frac{dE}{E - \mathcal{E}_*} [g_4^2 \mu_{442}(E) + g_2 g_4 \mu_{422}(E)], \\ \kappa_4 &= - \int_{E_{\max}}^{\infty} \frac{dE}{E - \mathcal{E}_*} g_4^2 \mu_{444}(E).\end{aligned}\tag{5.61}$$

The choice of the reference energy  $\mathcal{E}_*$  will be discussed shortly. We then construct the ‘renormalized’ Hamiltonian

$$H_{\text{ren}} = H_{\text{trunc}} + \Delta H_{\text{loc}}, \quad \Delta H_{\text{loc}} \equiv \kappa_0 V_0 + \kappa_2 V_2 + \kappa_4 V_4.\tag{5.62}$$

Thus  $\kappa_{2,4}$  correct the  $g_{2,4}$  couplings, while  $\kappa_0$  shifts the ground state energy density. Notice that the  $\kappa$ ’s scale as  $1/E_{\max}^2$  (up to logarithmic terms).

The renormalized Hamiltonian acts in the same truncated Hilbert space  $\mathcal{H}_l$  as the truncated Hamiltonian  $H_{\text{trunc}}$ . Its energy levels will be called the ‘renormalized spectrum’. This construction implements the first nontrivial approximation to the exact equation (5.33). The local coupling renormalization accounts for the leading  $1/E_{\max}^2$  error affecting the raw spectrum. Further corrections, discussed below, are suppressed by one more power of  $E_{\max}$ . So we expect that the renormalized spectrum approximates the exact spectrum with an error which scales as  $1/E_{\max}^3$ .

Let us now discuss the reference energy  $\mathcal{E}_*$  in (5.61). Recall that  $\mathcal{E}_*$  was introduced as a placeholder for the eigenstate energy  $\mathcal{E}$  in the definition (5.33) of  $\Delta H$ . Now, it’s important to realize that the eigenstate energies do *not* remain  $O(1)$  in the limit of large  $L$ . The excitations *above* the ground state,  $\mathcal{E}_I - \mathcal{E}_0$ ,<sup>13</sup> do stay  $O(1)$ , but the ground state energy itself grows linearly:

$$\mathcal{E}_0 \sim \Lambda L, \quad L \rightarrow \infty.\tag{5.63}$$

Here  $\Lambda$  is the interacting vacuum energy density (the cosmological constant), which is finite and observable in our theory.<sup>14</sup>

We will therefore use the following recipe. We will choose  $\mathcal{E}_*$  close to, although not necessarily equal, the ground state energy of the theory. The precise choice will be specified when we present the numerical results. With this choice we compute the coupling renormalization (5.61) and the renormalized spectrum. The differences  $\mathcal{E}_I - \mathcal{E}_*$  will now be  $O(1)$ , and the error induced by this mismatch will truly be  $1/E_{\max}^3$  suppressed. Moreover, even this error can be further corrected, as we discuss below.

---

<sup>13</sup>We use small roman letters  $i, j, \dots$  to number states in the Fock space, which are eigenstates of  $H_0$ , and large letters  $I, J, \dots$  to number the eigenstates of the interacting Hamiltonian.

<sup>14</sup>Recall that the free vacuum energy density was set to zero by normal ordering the free scalar Hamiltonian.

### 5.3. UV cutoff dependence and renormalization

We briefly mention here an alternative approach. One can insist that  $\mathcal{E}_*$  be adjusted, e.g. iteratively, until it exactly equals the eigenvalue  $\mathcal{E}_I$  which comes out from diagonalizing  $H_{\text{ren}}$ . This has to be done separately for each eigenstate, and so is rather expensive. We tried this method and found that it gives results in close agreement with those obtained from our simpler recipe for  $\mathcal{E}_*$ , combined with the correction procedure described below.

#### 3. Local renormalization with a subleading correction (marked ‘*subl.*’ in plots)

We will now describe the third approach which improves on the previous one by taking into account not only the renormalization of the local couplings, but also the first subleading corrections due to the eigenstate energy and  $(E_i + E_j)/2$ . As explained above, these corrections can be considered smaller than the local ones by a further  $O(1/E_{\text{max}})$  factor. They will take care of the mismatch between (5.39) and the local coupling renormalization. The corresponding correction Hamiltonian has the following matrix elements between the truncated Hilbert space states:

$$[\Delta H_{\text{subl}}(\mathcal{E})]_{ij} = (\lambda_0)_{ij}(V_0)_{ij} + (\lambda_2)_{ij}(V_2)_{ij} + (\lambda_4)_{ij}(V_4)_{ij} \quad (5.64)$$

(no summation over the repeated indexes). The  $(\lambda_N)_{ij}$  are the differences between the renormalization coefficients fully dependent on  $(E_i + E_j)/2$  and  $\mathcal{E}$  and the local ones  $\kappa_N$  defined in (5.61):

$$\begin{aligned} (\lambda_0)_{ij} &= - \int_{E_{\text{max}}}^{\infty} \frac{dE}{E - \mathcal{E}} [g_4^2 \mu_{440}(E_{ij}) + g_2^2 \mu_{220}(E_{ij})] - \kappa_0, \\ (\lambda_2)_{ij} &= - \int_{E_{\text{max}}}^{\infty} \frac{dE}{E - \mathcal{E}} [g_4^2 \mu_{442}(E_{ij}) + g_2 g_4 \mu_{422}(E_{ij})] - \kappa_2, \\ (\lambda_4)_{ij} &= - \int_{E_{\text{max}}}^{\infty} \frac{dE}{E - \mathcal{E}} g_4^2 \mu_{444}(E_{ij}) - \kappa_4. \end{aligned} \quad (5.65)$$

There is a small technical subtlety in using the given expressions. For  $(E_i + E_j)/2$  close to  $E_{\text{max}}$ , the argument  $E_{ij}$  of the  $\mu$ -functions is small in the part of the integration region close to  $E_{\text{max}}$ . In this region it makes little sense to use (5.58), valid for large  $E$ . From figure 5.1 we see that the asymptotics sets in roughly at  $E \sim 5m$ . We therefore use the following prescription in evaluating (5.65): we use (5.58) for  $E_{ij} \geq 5m$ , while we set  $\mu$ 's to zero below this threshold.

The full procedure is then as follows. We compute the local renormalized Hamiltonian (5.62) with the reference value  $\mathcal{E}_*$  fixed around the ground state energy. We diagonalize  $H_{\text{ren}}$ , determining the renormalized spectrum (in practice only a few lowest eigenvalues) and the corresponding eigenstates:

$$H_{\text{ren}}|c_I\rangle = \mathcal{E}_{\text{ren},I}|c_I\rangle \quad (5.66)$$

Every eigenvalue is then corrected by adding (5.64) at first order in perturbation theory:

$$\mathcal{E}_{\text{subl},I} = \mathcal{E}_{\text{ren},I} + \Delta\mathcal{E}_I, \quad \Delta\mathcal{E}_I = \langle c_I | \Delta H_{\text{subl}}(\mathcal{E}_{\text{ren},I}) | c_I \rangle. \quad (5.67)$$

From the computational point of view the evaluation of this correction can be considered

inexpensive, since it scales as the square of the basis dimension, whereas the matrix diagonalization typically scales as its cube. The energy levels  $\mathcal{E}_{\text{subl},I}$  will be called ‘renormalized subleading’ or simply ‘subleading’.

Second-order corrections can also be considered:

$$\Delta\mathcal{E}_I^{(2)} = \sum_{J \neq I} \frac{|\langle c_I | \Delta H_{\text{subl}}(\mathcal{E}_{\text{ren},I}) | c_J \rangle|^2}{\mathcal{E}_{\text{ren},I} - \mathcal{E}_{\text{ren},J}}. \quad (5.68)$$

These turn out to be negligible, except when there are two almost-degenerate eigenvalues.

### 5.3.4 A test for the $\phi^2$ perturbation

We will now perform a test of our method in a controlled situation when the exact answers are known.<sup>15</sup> Consider the theory described by the action (cf. (5.2))

$$S = S_0 + g_2 \int d^2x N_m(\phi^2). \quad (5.69)$$

The finite volume Hamiltonian corresponding to this problem has the form

$$H = H_0 + g_2 V_2 + C, \quad C = E_0(L) + g_2 L \zeta(L). \quad (5.70)$$

Just as in section 5.2.1, the extra constant term  $C$  appears because of the difference in the normal ordering counterterms in the infinite space and on the circle. These terms are exponentially suppressed for  $Lm \gg 1$ , but for the time being it will be instructive to keep them.

In full form, we have

$$H = C + \sum_k \omega_k a_k^\dagger a_k + \frac{g_2}{2\omega_k} (a_k a_{-k} + a_k^\dagger a_{-k}^\dagger + 2a_k^\dagger a_k), \quad \omega_k = \omega_k(m). \quad (5.71)$$

We expect, of course, that this Hamiltonian corresponds to a free scalar of a mass

$$\mu^2 = m^2 + 2g_2. \quad (5.72)$$

We will now use a Bogoliubov transformation to show this explicitly. The derivation is standard and is given here only for completeness. The transformation has the form

$$b_k = (\cosh \eta_k) a_k + (\sinh \eta_k) a_{-k}^\dagger \quad (5.73)$$

with  $\eta_k$  assumed real and depending only on  $|k|$ . The  $b$ ’s then satisfy the same oscillator commutation relations as the  $a$ ’s. We want to map (5.71) onto

$$\sum_k \Omega_k b_k^\dagger b_k + \mathcal{E}_0, \quad \Omega_k = \omega_k(\mu). \quad (5.74)$$

---

<sup>15</sup>This test is analogous to the one in [91], section 6.



### 5.3. UV cutoff dependence and renormalization

---

The conditions that the two Hamiltonians match take the form

$$\Omega_k \cosh(2\eta_k) = \omega_k + g_2/\omega_k, \quad \Omega_k \sinh(2\eta_k) = g_2/\omega_k. \quad (5.75)$$

This is indeed satisfied provided that

$$\Omega_k^2 = \omega_k^2 + 2g_2, \quad (5.76)$$

which proves the expression (5.72) for the new mass. The same derivation gives the value of the vacuum energy,

$$\mathcal{E}_0 = C - \sum \Omega_k (\sinh \eta_k)^2 = C + \frac{1}{2} \sum (\Omega_k - \omega_k - g_2/\omega_k). \quad (5.77)$$

Up to the constant  $C$ , the last expression can be intuitively understood [91] by starting from the zero-point energy  $\frac{1}{2} \sum \Omega_k$  and subtracting the terms zeroth and first order in  $g_2$ .

The series in (5.77) is convergent and can be summed using the Abel-Plana formula. We find that the final result is given by

$$\mathcal{E}_0 = E_0(L, \mu) + \Lambda L, \quad \Lambda = \frac{1}{8\pi} [\mu^2(1 - \log \mu^2/m^2) - m^2], \quad (5.78)$$

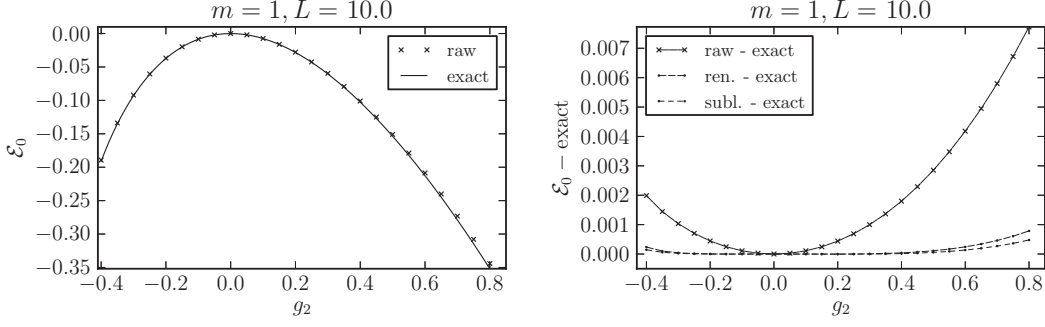
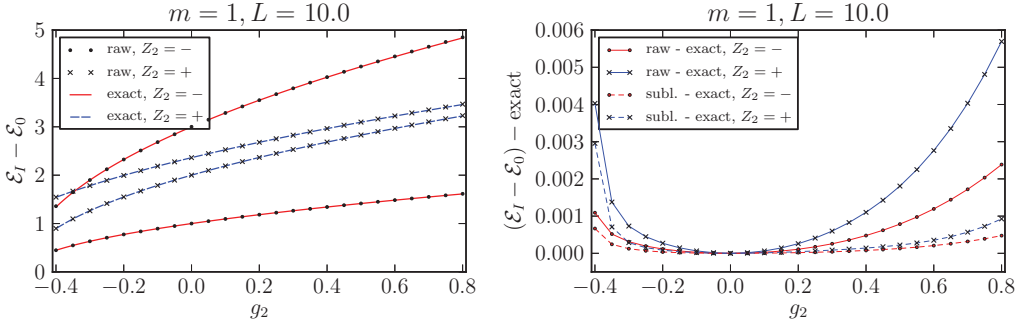
where  $E_0(L, \mu)$  is the Casimir energy of the free scalar field of mass  $\mu$ , given by (5.11) with  $m \rightarrow \mu$ .

The physical interpretation of (5.78) is clear. Apart from the usual Casimir energy term, we have an induced extensive vacuum energy, corresponding to a finite vacuum energy density  $\Lambda$ . Usually, when one studies the Casimir energy, the vacuum energy density in the infinite space limit is assumed to vanish. However, our situation here is different. We already fine-tuned to zero the vacuum energy density of the original, unperturbed, theory, i.e. the one described by the action  $S_0$ . Once this is done, the vacuum energy density of the *perturbed* theory becomes finite and observable.

We will now compare the above exact results with the numerical results obtained by using the Hamiltonian truncation. We will be considering the case  $Lm \gg 1$ , which means that we will not be sensitive to the exponentially suppressed constant term  $C$  in the initial Hamiltonian. We thus start directly from the Hamiltonian of the form (5.60) with  $g_4 = 0$ ,  $g_2 \neq 0$ . We calculate its spectrum using the three procedures from section 5.3.3. In the shown plots we chose  $m = 1$ ,  $L = 10$ , and varied  $g_2$  from  $-0.4$  to  $0.8$ .<sup>16</sup> For illustrative purposes numerics were done with a rather low cutoff  $E_{\max} = 12$ , for which the truncated Hilbert space contains about 300 states. Figure 5.2 compares the ground state energy. In the left plot, the agreement between the raw and the exact result is already pretty good. The right plot shows the difference between the numerics and the exact value. We see that the renormalization greatly reduces the discrepancy over the raw procedure, and the results are made slightly better by

---

<sup>16</sup>The reference energy  $\mathcal{E}_*$  in (5.61) was set to the value of the ground state energy given by the raw truncation procedure.


 Figure 5.2: Exact and numerical ground state energy for the  $\phi^2$  perturbation; see the text.

 Figure 5.3: Exact and numerical spectra of excitations for the  $\phi^2$  perturbation; see the text.

including the subleading correction.

In figure 5.3 we do the same comparison for the spectrum of excitations above the vacuum,  $\mathcal{E}_I - \mathcal{E}_0$ . In the left plot we pick the first two  $\mathbb{Z}_2$ -odd states (one and three particles at rest), and the first two  $\mathbb{Z}_2$ -even states (two particles at rest, and with one unit of momentum in the opposite directions). Already the raw spectrum agrees well with the exact values. In the right plot we present the differences, focusing on the first two excited levels only (one even and one odd). Notice that for  $g_4 = 0$  the difference between  $H_{\text{ren}}$  and  $H_{\text{trunc}}$  is only in the vacuum energy coefficient  $\kappa_0$ , which shifts all eigenvalues in the same way. The first non-trivial corrections for the spectrum of excitations are therefore the subleading ones. The improvement over the raw results is significant.

## 5.4 Study of the $\phi^4$ theory

In the previous sections we have developed the method and tested it in the simple setting of the  $\phi^2$  perturbation. We will now move on to the main task of this part of the thesis—to study the spectrum of the  $\phi^4$  theory described by the Hamiltonian (5.22).

The main physical parameter varied in our study will be the quartic coupling  $g$ . The physics depends on the dimensionless ratio  $\bar{g} = g/m^2$ , and we will work in the units where the mass

term  $m = 1$ .

The second parameter will be the size of the spatial circle  $L$ . This plays the role of the IR cutoff, to render the spectrum discrete. In practice one is usually interested in the infinite volume limit  $L \rightarrow \infty$ , and we will try to approach this limit. However, even a finite  $L$  is physical, in the sense that the energy levels on the circle are well-defined physical observables.

The third parameter we will vary is the cutoff on the size of the Hilbert space  $E_{\max}$  (the maximal energy of the free scalar Fock states included in the truncated Hilbert space). This parameter plays the role of the UV cutoff. It is unphysical. The continuum limit is recovered for  $E_{\max} \rightarrow \infty$ .

We will typically present the results derived using the renormalization procedures both without (marked ‘ren.’ in the plots) and with (marked ‘subl.’) subleading corrections (see section 5.3.3). These procedures are expected to converge to the exact spectrum at the rate which goes as  $1/E_{\max}^3$  and  $1/E_{\max}^4$  (modulo logarithms). We take the difference between them as a rough idea of the current error of the method.

#### 5.4.1 Varying $g$

In figure 5.4 we present the ground state energy and the low energy spectrum of excitations for  $g \leq 5$ . This extends well beyond the range  $g \lesssim 0.5 - 1$  where perturbation theory is accurate (see appendix C). In this plot we use a fixed value  $L = 10$ , and choose the UV cutoff  $E_{\max} = 20$ .<sup>17</sup> We use the two renormalization procedures explained in section 5.3.3.

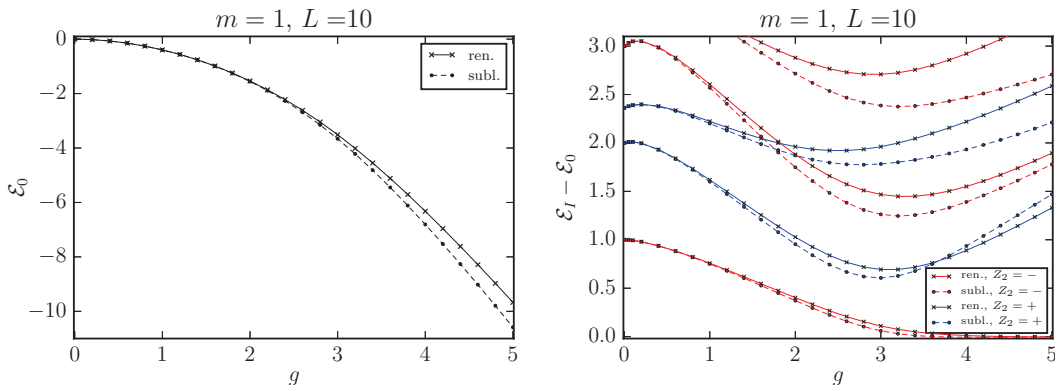


Figure 5.4: Numerical spectra as a function of  $g$  for  $m = 1$ ,  $L = 10$ ; see the text.

The left plot shows the dependence of the ground state ( $\equiv$  vacuum) energy on  $g$ . The vacuum is simply the state of the lowest energy, and it resides in the  $\mathbb{Z}_2$ -even sector. There is not much structure in this plot, except for the fact that the vacuum energy is negative and grows in absolute value as  $g$  is increased, becoming of the same order of magnitude as  $E_{\max}$  for the largest  $g$  considered here. This has a consequence for the renormalization procedure used

<sup>17</sup>This corresponds to keeping 12870(12801) states in the even(odd) sector of the Hilbert space.

in our study. Recall that in the local renormalization (the one marked ‘ren.’) the coupling are renormalized using Eqs. (5.61) which involve the reference energy  $\mathcal{E}_*$ . Everywhere in this section we set  $\mathcal{E}_*$  to the value of the vacuum energy computed using raw truncation. We already mentioned in section 5.3.3 that since the vacuum energy may become large, the integrals in (5.61) have to be evaluated without expanding in  $\mathcal{E}_*$ . We are fortunate here that the vacuum energy becomes large and *negative*, and so the renormalization corrections become smaller if nonzero  $\mathcal{E}_*$  is taken into account. A large and *positive* vacuum energy would be a big problem for the performance of our method.<sup>18</sup>

The right plot shows the 5 lowest excitations above the vacuum, with the  $\mathbb{Z}_2 = \pm$  excitations colored in blue(resp. red). As we can see the first odd level becomes almost degenerate with the vacuum for  $g \gtrsim 3$ . This is a signal of the spontaneous  $\mathbb{Z}_2$ -symmetry breaking. We therefore expect a second-order phase transition to occur at a critical point  $g = g_c \approx 3$ . For  $g = g_c$ , the theory should flow at large distances to a CFT. Since the  $\phi^4$  theory is in the same universality class as the Ising model, we expect this IR CFT to be the minimal model  $\mathcal{M}_{4,3}$ . We will analyze the region around  $g = g_c$  in more detail below. For  $g > g_c$  we are in the  $\mathbb{Z}_2$ -broken phase. In this phase, the higher excitations should also be doubly degenerate in infinite volume. For a finite  $L$  the exact degeneracy is lifted and becomes approximate. This degeneracy is not observed clearly in figure 5.4, probably because  $L = 10$  is not large enough.<sup>19</sup>

In the region of small  $g$ , it is possible to validate the numerical results by comparing them to perturbation theory. In appendix C, we do this comparison for the ground state energy and the mass of the lowest excitation. For small  $g$ , we find good agreement with the perturbative predictions computed through  $O(g^3)$ .

It is interesting to understand the sensitivity of the spectrum plot in figure 5.4 to the chosen value of  $L = 10$ . We therefore show in figure 5.5 similar plots for  $L$  equal to 6, 8, 10 and  $E_{\max}$  respectively equal to 34, 26 and 20.<sup>20</sup> To avoid clutter, only the results for the subleading renormalization (the third, most precise method in section 5.3.3) are presented.

In the left plot we show the vacuum energy *density*  $\Lambda = \mathcal{E}_0/L$ . For a sufficiently large  $L$  this is supposed to become independent of  $L$ . We see that this constancy is verified with an excellent accuracy for  $g \lesssim 2$ . In this region we are in the massive phase, and the finite  $L$  corrections are expected to be exponentially small (see section 5.4.3 below). The dependence on  $L$  becomes more pronounced around  $g = g_c$ , which is as it should be because the mass gap goes to zero here. However, in the  $\mathbb{Z}_2$ -broken phase the corrections remain significant, while theoretically they should become again exponentially suppressed. Therefore, for  $g \gtrsim 3$ , we are forced to interpret the variation with  $L$  not as a physical effect but being due to finite  $E_{\max}$  truncation

---

<sup>18</sup>In perturbation theory the vacuum energy is always negative. That it stays negative at strong coupling both here and in section 5.3.4 is probably more than just a coincidence. See the discussion in [91], note 21.

<sup>19</sup>The discussed phase diagram is the same as for the  $\phi^4$  model in  $d = 2.5$  dimensions studied in [91] using the TCSA. In that case it was possible to observe approximate degeneracy for the first and second excited states.

<sup>20</sup> $E_{\max}$  is adjusted to have roughly the same size of the Hilbert space in all three cases. Smaller  $L$  give larger energy spacings for the one-particle momentum excitations, and allow to go to larger  $E_{\max}$ .

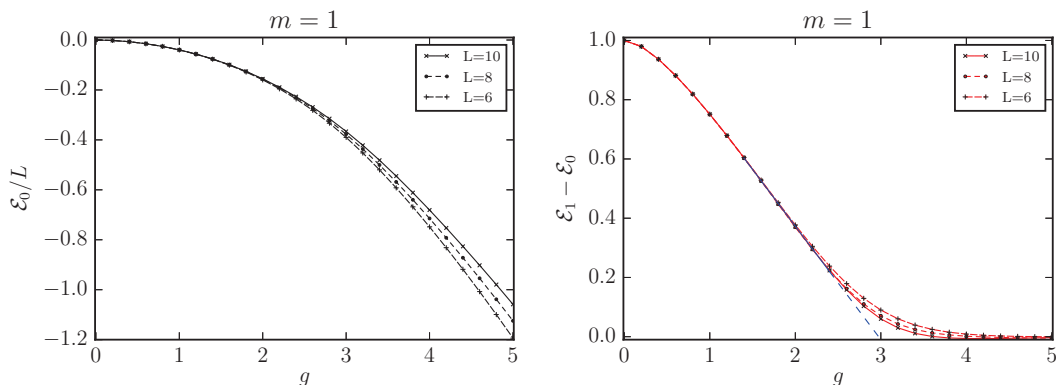


Figure 5.5: The vacuum energy (left) and the first odd excitation (right) determined numerically for  $L = 6, 8, 10$ . The blue dashed line in the right plot is the fit to determine the critical coupling; see section 5.4.2.

effects. This is consistent with the significant difference between the results obtained with the two renormalization procedures in figure 5.4.

In the right plot of figure 5.5 we show the physical particle mass  $m_{\text{ph}} = \epsilon_1 - \epsilon_0$ . Once again, in the  $\mathbb{Z}_2$  unbroken massive phase there is hardly any dependence on  $L$ , while around  $g = g_c$  there appears variation, which will be studied quantitatively in section 5.4.2 below. This plot will also be used below to extract an estimate of  $g_c$ .

Overall, the truncation effects seem to be too large for  $g \gtrsim 3$  to allow precise quantitative claims about this range of couplings (apart from the fact that the  $\mathbb{Z}_2$  symmetry appears broken). Head-on treatment of that range would require a refinement of the method, by improving the renormalization procedure. An alternative way to access this region is to use the strong/weak coupling duality due to Chang [92]. In Chapter 6 we will both test this duality, and use it to study the  $\mathbb{Z}_2$ -broken phase of the model.

### 5.4.2 The critical point

We will now try to determine with some precision the critical coupling  $g_c$ , and study the lowest operator dimensions of the CFT at the phase transition. According to the standard renormalization group theory, for  $g$  close to  $g_c$  the physical mass  $m_{\text{ph}}$  should behave as

$$m_{\text{ph}} \sim C|g - g_c|^\nu, \quad (5.79)$$

where  $C$  is a theory-dependent constant,<sup>21</sup> and  $\nu$  is a critical exponent, common for all theories in the Ising model universality class, and expressible via the dimension of the most relevant

<sup>21</sup>Which also depends on from which direction one approaches the fixed point.

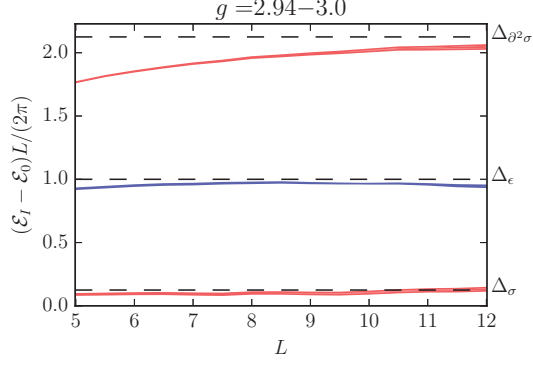


Figure 5.6: Comparison with the CFT spectrum; see the text.

$\mathbb{Z}_2$ -even scalar operator,  $\epsilon$ , of the CFT,

$$\nu = (2 - \Delta_\epsilon)^{-1}. \quad (5.80)$$

We used our numerical results obtained for  $L = 10$ ,  $E_{\max} = 20$  renormalized with subleading corrections (see figure 5.5) to perform the fit of  $m_{\text{ph}} \equiv \mathcal{E}_1 - \mathcal{E}_0$  to the formula (5.79), replacing  $\sim$  by  $=$ . Admittedly, our procedure is careless, since we do not take into account the corrections to scaling. We view the results which we will now present as preliminary; they should be validated by future studies as our method progresses. Another uncertainty concerns the range of  $g$  chosen to do the fit. On the one hand,  $g$  should be close to  $g_c$ , on the other hand right close to  $g_c$  the spectrum is modified by finite size corrections. Looking at the right plot in figure 5.5, we subjectively picked the  $g$ -interval  $[1.4, 2.4]$ , which by the eye seems to give a nice power law close to a straight line. To introduce *some* way to estimate the systematic error, we selected a few subintervals contained in the basic interval, and fitted the parameters  $\Delta_\epsilon$ ,  $g_c$  for each such subinterval.<sup>22</sup> We obtained  $g_c = 3.04(15)$  and  $\Delta_\epsilon = 1.06(13)$ . This value of  $\Delta_\epsilon$  is compatible with the two-dimensional Ising model value  $\Delta_\epsilon = 1$ , giving us confidence that the procedure is sensible. To improve the estimate of  $g_c$ , we fix  $\Delta_\epsilon$  to this theoretically known value and redo the fit. We then get  $\bar{g}_c = 2.97(3)$ .

The above error estimate may be too optimistic, because we completely ignored the error in  $m_{\text{ph}}$  induced by truncation effects. We have also performed the fit taking the  $L = 10$ ,  $E_{\max} = 20$  ‘renormalized subleading’ results as central values, and the difference  $\sigma$  between these central values and the ‘renormalized’ results without subleading correction as the error (we consider the two-sided error  $\pm\sigma$ ). Following this procedure and doing the fit in the  $[1.4, 2.4]$  interval we obtained  $\bar{g}_c = 2.97(14)$ . This is our final, conservative, estimate.

We now perform another comparison with the theoretically known CFT operator dimensions.

<sup>22</sup>In the future, the fit procedure could be refined by taking into account the value of  $\mathcal{E}_2 - \mathcal{E}_0$  at  $g = g_c$ .

Namely, for  $g = g_c$  the excitations  $\mathcal{E}_I - \mathcal{E}_0$  should go as

$$\mathcal{E}_I - \mathcal{E}_0 \sim \frac{2\pi}{L} \Delta_I, \quad (5.81)$$

where  $\Delta_I$  are the CFT dimensions. This asymptotics should be valid for  $L \gg 1$  where the theory has flown sufficiently close to the IR fixed point. To check this, in figure 5.6 we plot the three lowest excitation energies multiplied by  $L/(2\pi)$ .

In this figure, we consider  $L = 5 \dots 12$  and vary the quartic coupling within our ‘optimistic’ uncertainty range around the fixed point,  $g = 2.94 \dots 3.0$ . We have to vary the UV cutoff  $E_{\max}$  as a function of  $L$  in order to have a manageable number of basis elements in the low energy truncated Hilbert space  $\mathcal{H}_l$ . So  $E_{\max}$  decreases from 33 at  $L = 5$  to 18 at  $L = 12$ , while the truncated Hilbert space dimension stays for each  $L$  around 10000 - 15000 per  $\mathbb{Z}_2$  sector. To avoid clutter, we show only the ‘renormalized subleading’ results (but see figure 5.8 below, where the results without subleading corrections are also shown).

As figure 5.6 demonstrates, (5.81) is approximately obeyed at large  $L$ , provided that we use the 2D Ising operator dimensions  $\Delta_\sigma = 1/8$ ,  $\Delta_\epsilon = 1$ ,  $\Delta_{\partial^2\sigma} = 2 + 1/8$ , where this latter operator is a scalar descendant of  $\sigma$ .

### 5.4.3 $L$ dependence

We will now present several plots which show explicitly how the spectrum of the theory varies for increasing  $L$  while keeping  $g$  fixed. These plots are analogous to figure 5.5, but the information is presented somewhat differently.

#### $\mathbb{Z}_2$ -unbroken phase

Let us look first at the  $\mathbb{Z}_2$ -unbroken phase. We fix  $g = 1$ , which is at the outer border or the perturbativity range (see appendix C). Figure 5.7 shows then the vacuum energy density  $\mathcal{E}_0/L$  and the spectrum, for  $L = 5 \dots 12$ .

In the left plot we see that the vacuum energy density tends to a constant value. We don’t worry too much about the fluctuations around the limit which happen for some values of  $L$ , like an upward fluctuation for  $L = 8.5$  or a downward fluctuation for  $L = 11.5$ . These fluctuations, which are present also in the ‘raw’ data, are due to the sharpness of the cutoff  $E \leq E_{\max}$ . In the future it will be important to find a way to work around these fluctuations. One way would be to consider a cutoff which is not totally sharp, or to take into account the discreteness of the sequence  $M(E)$ , which in our work is calculated only on average, as figure 5.1 shows.<sup>23</sup>

Ignoring for the time being the fluctuations, let us discuss the approach of the vacuum energy

<sup>23</sup>Ref. [91], section 6.4 and appendix D, describes a method which for conformal bases used in that work allowed to perform renormalization taking into account the discreteness of the sequence  $M(E)$ . It’s not clear if that method extends to the massive Fock space bases used here.

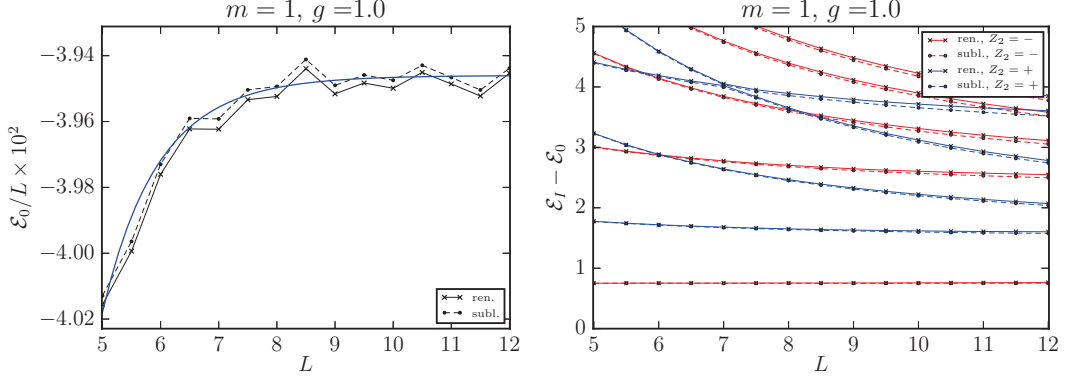


Figure 5.7: The vacuum energy density and the excitation spectrum for  $g = 1$ , as a function of  $L$ .

density to its infinite volume limit. As is well known, in a massive phase the rate of this approach is exponentially fast and is given by:

$$\begin{aligned} \mathcal{E}_0(L)/L &= \Lambda - \frac{m_{\text{ph}}}{\pi L} K_1(m_{\text{ph}}L) + O(e^{-2m_{\text{ph}}L}) \\ &\approx \Lambda - \left(\frac{m_{\text{ph}}}{2\pi L^3}\right)^{1/2} e^{-m_{\text{ph}}L} \quad (L \gg 1/m_{\text{ph}}). \end{aligned} \quad (5.82)$$

This formula can be derived by considering the partition function of the theory on a torus  $S_L^1 \times S_{L'}^1$ , where  $L$  and  $L'$  are the lengths of the circles. The  $\mathcal{E}_0(L)$  is extracted by considering the limit  $L' \gg L$ , and so it's natural to treat  $L'$  as space and  $L$  as the inverse temperature. The condition  $L \gg 1/m_{\text{ph}}$  means that we are interested in low temperatures. The deviation of the free energy can then be described in terms of thermodynamics of a gas of particles of mass  $m_{\text{ph}}$ . This type of arguments is standard in the thermodynamic Bethe ansatz calculations in integrable theories, in which case also the subleading terms in (5.82) can be determined; see e.g. [95], Eq. (3.13). However, the leading term that we show is more general. It does not require integrability nor knowing anything about how the particles interact, since it depends only on the energy of the one-particles states. In fact (5.82) can be also determined by taking the large  $L$  limit of the free scalar Casimir energy (5.11) with  $m \rightarrow m_{\text{ph}}$ .

The blue curve in the left plot is the fit of our numerical data by Eq. (5.82) with  $m_{\text{ph}}$  fixed to the value determined from the numerical spectrum (see below). We see that the rate of the approach to the infinite  $L$  limit is reasonably well described by the theoretically predicted dependence.<sup>24</sup>

The accompanying right plot shows the spectrum of excitations above the vacuum. Observe the remarkably small difference between the two renormalization procedures (we use this

<sup>24</sup>Since  $m_{\text{ph}} < m$ , the effect we are observing here is formally dominant with respect to the exponentially suppressed  $E_0(L)$  and  $\zeta(L)$  corrections, which were omitted in section 5.2.1. Still, the hierarchy  $m/m_{\text{ph}}$  is not very large, and a more careful comparison may be warranted in the future, taking also those corrections into account.



difference as an idea about the error of the method). The first excited state in the odd sector should for large  $L$  approach the infinite-volume physical mass  $m_{\text{ph}}$ . It shows hardly any variation with  $L$  in the shown range, which is consistent with the rate of approach being exponentially fast in  $m_{\text{ph}}L$  [96]. We extract  $m_{\text{ph}} = 0.751(1)$ .

The second excited state, which belongs to the even sector, for large  $L$  asymptotes to  $1.47(4)$  which within error bars coincides with  $2m_{\text{ph}}$ . This state corresponds to having two particles with opposite momentum on the circle. This momentum is non-zero due to particle interactions in finite volume.<sup>25</sup> Notice that we do not observe any states in the energy range between  $m_{\text{ph}}$  and  $2m_{\text{ph}}$ . Such states would be interpreted as two-particle bound states. As is well known, the  $\phi^4$  interaction is perturbatively repulsive, so we do not expect bound states at weak coupling. Moreover it is known rigorously that two-particle bound states are absent everywhere below the phase transition; see [97], section 17.2. What we observe here is consistent with these results.

Notice that the lowest two-particle state approaching  $2m_{\text{ph}}$ , as well as the three-particle state going to  $3m_{\text{ph}}$ , show a much larger variation with  $L$  compared to the one-particle state. That this variation is *not* exponentially suppressed is a consequence of particle-particle interactions. Since the interactions are short-ranged, their effect is expected to go like the inverse volume,  $1/L$  [98]. It is possible to use this effect to extract information about the two-particle  $S$ -matrix.<sup>26</sup>

For small  $g$ , it is easy to calculate these corrections explicitly using the first-order perturbation theory for the Hamiltonian (5.22). For the two-particle and three-particle states at rest we get<sup>27</sup>

$$\mathcal{E}_2 = 2m + \frac{3g}{Lm^2} + O(g^2), \quad \mathcal{E}_3 = 3m + \frac{9g}{Lm^2} + O(g^2). \quad (5.83)$$

The positiveness of the  $O(g)$  corrections explains the ‘‘bumps’’ at small coupling in the corresponding curves in figure 5.4 (the first  $\mathbb{Z}_2$ -even and the second  $\mathbb{Z}_2$ -odd states).

The even state just above the one asymptoting to  $2m_{\text{ph}}$  should be identified as corresponding to two particles moving in the opposite directions on the circle with approximately one unit of momentum each. Using the one-particle dispersion relation, the energy of this state should be roughly  $2 \times (m_{\text{ph}}^2 + (2\pi/L)^2)^{1/2}$  plus the corrections due to the particle interactions in finite volume. Because of the  $2\pi$  prefactor, the dispersion relation corrections are significant even at the maximal values of  $L$  that we are considering; they seem to explain most of the difference between the first two even states. At larger  $L$ , we expect the particle interaction corrections to take over, since their strength decreases only as  $1/L$ .

Our final comment about the  $g = 1$  spectrum plot concerns the pattern of level crossings. In

<sup>25</sup>This momentum is determined by the Bethe-Yang quantization condition, see [84].

<sup>26</sup>This has been done in [84]. Such analyses are standard in the TCSA approach to  $d = 2$  RG flows; see [99, 90] for previous examples.

<sup>27</sup>These formulas are valid for a fixed finite  $L$  and  $g \ll \pi^2 m/L$ . In this limit the splittings between different states with the same number of particles are sufficiently large so that we can neglect their mixing. In the opposite limit one should apply quasi-degenerate perturbation theory.

a non-integrable quantum field theory, we do not expect energy levels of the same symmetry to cross when varying the volume. In fact, the absence or presence of level crossings can be used as an empirical check of integrability (see [100] for a related recent discussion). Since the  $\phi^4$  theory is, for all we know, non-integrable, levels with the same  $\mathbb{Z}_2$  quantum number should not cross. Most levels in figure 5.7 do not cross trivially because they never come close each other. However, there is one interesting “avoided” crossing: the third and fourth  $\mathbb{Z}_2 = +$  levels head for a collision around  $L = 7$  but then repel. Many more such avoidances are present in the higher energy spectrum (not shown in figure 5.7).

### The critical point

In figure 5.8 we show analogous plots for the neighborhood of the critical point. We fix  $g = 2.97$ , i.e. the central value for our  $g_c$  estimate. One drastic change compared to figure 5.7 is that the energy differences  $\mathcal{E}_I - \mathcal{E}_0$  (plotted on the left) no longer tend to constants but scale as  $1/L$ , as expected for a CFT. This is the same plot as in figure 5.6, except that here we do not multiply by  $L/2\pi$ , and we show results for both renormalization methods, to get an idea of possible error bars. Evidently, even if  $g$  is not exactly equal to the critical coupling, the mass gap is sufficiently small so that it is not visible for the values of  $L$  shown in this plot.

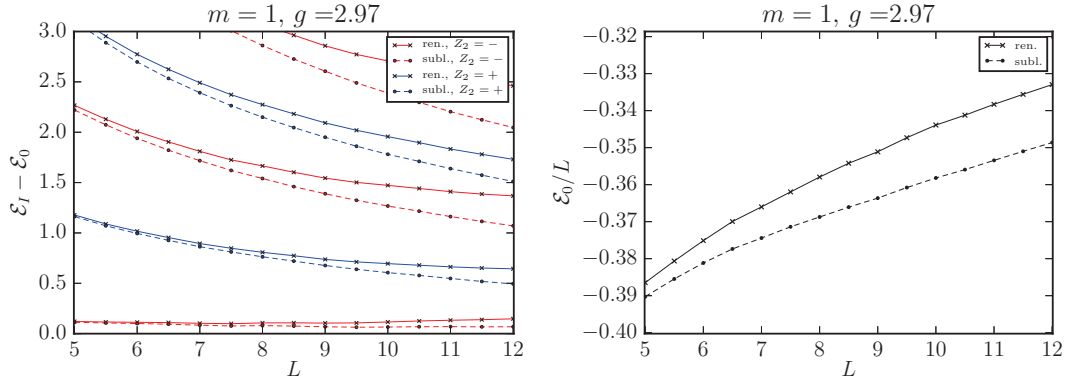
On the right we show the vacuum energy density, which, as expected, seems to approach a constant. However, the uncertainty, measured by whether or not we include the subleading corrections, remains significant. Theoretically, the asymptotics of approach to the limit should be  $-\pi c/(6L^2)$ , where  $c = 1/2$  is the central charge of the critical point. Instead, we see something like a  $1/L$  approach. Clearly, one should work to reduce the truncation errors before the agreement is achieved.

It should be remarked that the vacuum energy is always subject to larger errors than the spectrum of excitations. This is related to the fact that the unit operator, whose coefficient shifts the vacuum energy, is the most relevant operator of the theory, and gets the largest renormalization when the states above  $E_{\max}$  are integrated out. However, whichever uncertainty in the coefficient of the unit operator cancels when we compute the spectrum of excitations.

#### 5.4.4 $E_{\max}$ dependence

To get a better feel for the convergence of our method, and to demonstrate the difference between the three procedures explained in section 5.3.3, we will present here plots of the spectrum and vacuum energy as a function of  $E_{\max}$ , while keeping the other parameters fixed.

So, figure 5.9 shows the results for  $g = 1$ ,  $L = 10$ , with  $E_{\max}$  varying from 10 to 20. On the left we see that the renormalization dramatically improves the convergence of the vacuum energy with respect to the raw results, while the subsequent subleading correction is very small. The plot on the right refers to the first excited level ( $i = 1$ ). In this case we see that the further improvement due to the subleading correction is non-negligible. There are small


 Figure 5.8: Same as in figure 5.7, but for  $g = 2.97$ .

oscillations due to discretization effects, as already discussed in section 5.4.3. The higher excitations, not shown in the plot, show a similar pattern of convergence.

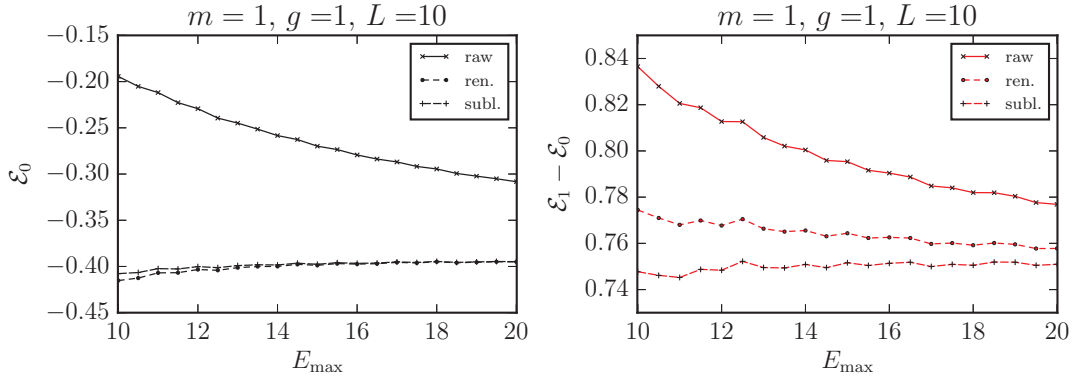
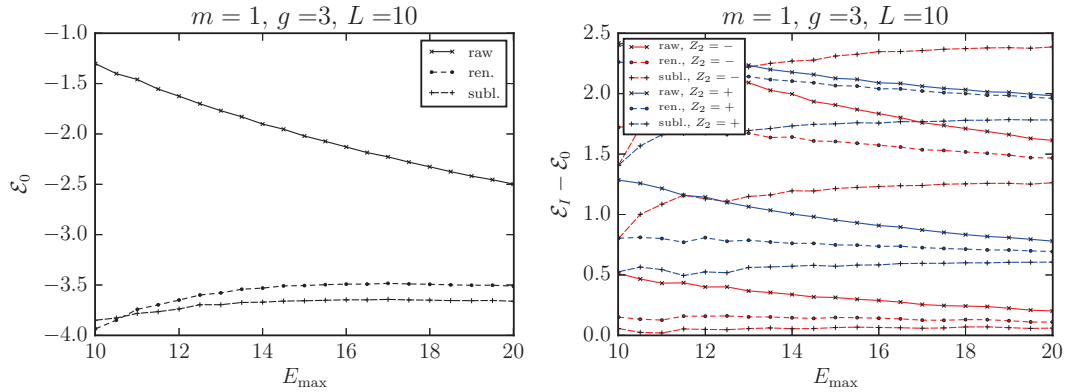

 Figure 5.9: Variation with  $E_{\max}$  and the effect of renormalization corrections for  $g = 1$ .

 Figure 5.10: Same as in figure 5.9 but for  $g = 3$ .

Figure 5.10 shows the same plots for  $g = 3$ . Once again the improvements due to renormalization are evident. For a change, here we show more states in the spectrum of excitations.

### 5.4.5 Comparison to the TCSA methods

As already mentioned, Ref. [91] studied the  $\phi^4$  theory in  $d = 2.5$  dimensions using the TCSA method. The results of that study, and in particular the phase diagram of the theory, turned out to be quite similar to the one we found here; see [91], section 7. The TCSA uses the basis of conformal operators of the free massless scalar field theory, which via the state-operator correspondence is the same as the basis of states of this theory put on the sphere  $S^{d-1}$ . In the TCSA, both the  $\phi^2$  and  $\phi^4$  perturbations are included into the  $V$  part of the Hamiltonian. This should be contrasted with our current method, where  $\phi^2$  is included into  $H_0$ . We will mention here just one advantage and one complication of working with the conformal basis and treating all potential terms as a perturbation. The advantage is that the Hamiltonian matrix  $H_{ij}$  for a general sphere radius  $R$  is related to the  $R = 1$  matrix via a simple rescaling. The complication is that the conformal basis is not orthonormal, requiring introduction of a Gram matrix or dealing with an eigenvalue problem which is not symmetric.

Naively, the conformal basis does not work in  $d = 2$ , because the scalar field dimension becomes zero, rendering the spectrum dense and numerical treatment impossible. In spite of this basic difficulty, a recent paper [77] proposed a way to use the conformal basis in  $d = 2$  dimensions. The idea of this work is to compactify the free scalar boson on a circle of a finite length  $2\pi/\beta$ . Compactification renders the CFT spectrum discrete, and the corresponding conformal basis is orthonormal. One hopes that for a sufficiently small  $\beta$  compactification effects will be negligible. It's important to realize that the procedure of [77] modifies the quantum mechanical dynamics only for the zero mode, while all higher oscillator modes don't feel it.<sup>28</sup>

On the conceptual level, the difference between our work and [77] lies in the choice of the trial wavefunction basis for the oscillator modes. They choose periodic plane waves on a circle of radius  $2\pi/\beta$  for the zero mode, and harmonic oscillator wavefunctions of frequency  $2\pi|n|/L$  for the modes with  $|n| > 0$ . We instead choose harmonic oscillator wavefunctions of frequency  $\sqrt{m^2 + (2\pi n/L)^2}$  for all modes. Of course the technique for evaluating the matrix elements is also different, since we use ladder operators, while they use the Kac-Moody algebra acting in the free scalar boson CFT.

Ref. [77] parametrizes the theory by two couplings  $G_2, G_4$  which they denote  $g_2, g_4$ ; we capitalized to avoid confusion with our notation in other parts of this thesis. Their couplings are not identical to ours; because of the different field normalization  $g = 2\pi G_4$ . More importantly, their  $\phi^4$  operator is normal-ordered differently, by subtracting the normal-ordering constants for all nonzero massless modes in finite volume  $L$  (= their  $R$ ). Going to our normal ordering prescription (in infinite volume),

$$:\phi^4:_{\text{their}} \rightarrow N_m(\phi^4) - C(mL)N_m(\phi^2) + \text{const.}, \quad C(mL) = -(3/\pi) \log[e^\gamma mL/(4\pi)], \quad (5.84)$$

---

<sup>28</sup>For example, it would be wrong to think of their procedure as considering the scalar boson in a quartic potential cut off at the boundaries of the interval  $[-\pi/\beta, \pi/\beta]$  and periodically extended to the whole real line. Such a periodized potential would not even give a UV-complete theory, because of the spikes at the cutoff points.

where  $\gamma$  is the Euler-Mascheroni constant. We don't pay attention to the ground state energy renormalization here. To put their Hamiltonian into the canonical form (6.8) one has to solve the equation

$$G_2 - 2gC(mL) = m^2 \tag{5.85}$$

for  $m$ . Keeping  $G_{2,4}$  fixed and varying  $L$  thus induces a logarithmic variation of the infinite-volume mass parameters. Although for the small quartic couplings considered in [77] this variation is not huge (order 10%), it may be problematic for extracting the spectrum by approaching the large  $L$  limit. It would seem more appropriate to vary  $G_2$  with  $L$  while keeping  $m$  or  $M$  fixed.

In the  $\mathbb{Z}_2$ -preserving phase, their strongest coupled point had  $G_2 = 0.01$  and  $G_4 = 8 \times 10^{-5}$ , which gives  $\bar{g} = g/m^2 \approx 0.05$ . From our perspective, this is an extremely weakly coupled case, where even ordinary perturbation theory would be largely adequate.

It appears that in the  $\mathbb{Z}_2$ -preserving phase our trial wavefunction basis for the zero mode is more efficient than that of [77], since it consists of wavefunctions peaked at  $\phi_0 = 0$ , as opposed to being evenly spread over a long interval. We hasten to add however that the main goal of [77] was to study the  $\mathbb{Z}_2$ -broken phase in the regime of negative  $m^2$ , something that we postpone to Chapter 6, where a careful choice of the wavefunction basis for the zero mode will play an important role.

## 5.5 Comparison with prior work

The  $\phi^4$  theory in two dimensions has been previously studied, in the strongly coupled region, with a variety of techniques. Table 5.1 summarizes the predictions for the critical coupling. Here we only mention the methods which, at least in principle, allow for a systematic improvement of the results, leaving out simple-minded variational studies. Many of these papers normalize the quartic coupling as  $\lambda/4!$ ; we translate all results to our normalization.

The clear trend in the table is that the critical coupling estimate seems to increase with time. The first two studies are rather old and do not assign an uncertainty to their results. The next result (DMRG) has the smallest claimed error, but as we will see below there are strong reasons to believe that it is grossly underestimated. The stated uncertainty of the two remaining predictions is also significantly smaller than ours. Their central values are below our result, although consistent with it at a  $2\sigma$  level if we use the conservative error estimate. As we will discuss in section 5.5.4, this slight discrepancy may be due to a subtlety in implementing the matching to a continuum limit in their procedures.

We will now review the methods in Table 5.1, following the chronological order.

Method	$\bar{g}_c$	Year, ref.
DLCQ	1.38	1988 [101]
QSE diagonalization	2.5	2000 [78]
DMRG	2.4954(4)	2004 [102]
Lattice Monte Carlo	$2.70^{+0.025}_{-0.013}$	2009 [103]
Uniform matrix product states	2.766(5)	2013 [104]
Renormalized Hamiltonian truncation	2.97(14)	This work

 Table 5.1: Estimates of  $\bar{g}_c$  from various techniques.

### 5.5.1 DLCQ

In [105, 101], the  $\phi^4$  theory was studied using the Discretized Light Cone Quantization (DLCQ). This is a Hamiltonian truncation method in which the theory is quantized in the light-cone coordinates  $x^\pm = t \pm x$ , using  $x^-$  as ‘space’ and  $x^+$  as ‘time’. The Hilbert space consists of states of several particles all moving in the  $x^+$  direction, and having a fixed total momentum  $P^+$ . This method was much touted in the past because of the apparent reduction in the number of states (since only particles moving in one direction are needed), and the simplicity of the vacuum structure, which in perturbation theory coincides with the free theory vacuum. In practical computations, one discretizes (hence *Discretized* LCQ) the momentum fraction of constituent particles with a step  $1/K$ . This is sometimes presented as a result of compactifying the  $x^-$  direction on a circle of length  $2\pi K$ .

Refs. [105, 101] used DLCQ to compute the physical particle mass as a function of  $g$ , observing that it goes to zero for a certain critical value of  $g_c$ . They find  $\bar{g}_c \approx 1.83$  for  $K = 16$  [105], and later report an even smaller value  $\bar{g}_c \approx 1.38$  based on extrapolating the  $K \leq 20$  results to  $K = \infty$  [101]. These results are in a stark disagreement with the more recent calculations by other techniques in Table 5.1. A careful repetition of these old studies is called for. It is known that DLCQ calculations are subject to severe  $1/K$  truncation effects [106], which may be the source of the discrepancy.

We would like to mention here a recent proposal to avoid the  $P^+$  discretization altogether, and instead truncate the light-cone Hilbert space by using a carefully constructed orthonormal basis of multi-particle wavefunctions. This alternative approach may be the future of the light-cone quantization. It already proved very promising in the study of 2d gauge theories [85, 86], and it has recently been applied to the  $\phi^4$  theory in two [107] and three dimensions [88].

As a final comment on the light-cone quantization, we note that the method is bound to become more complicated in the  $\mathbb{Z}_2$ -broken phase, possibly requiring a scan of the zero mode  $\langle \phi \rangle$  to find the true vacuum.

### 5.5.2 QSE diagonalization

Ref. [78] (see also [79, 80, 81]) studied the  $\phi^4$  theory using the Hamiltonian truncation in the same basic setup as ours, calling it “modal field theory”. However, the implementation details are quite different. They use a *quasi-sparse eigenvector* (QSE) method, which reduces the Hilbert space dimension by throwing out the Fock states whose contributions to the physical eigenstate one is studying are small. In a later work [79] they developed a *stochastic error correction* (SEC) method, which corrects for the resulting truncation. While the idea is similar to our renormalization, there are some differences. One difference is that their method is perturbative, unlike our basic equation (5.33) which is all-order in  $\Delta H$ . Another difference is that SEC computes infinite sums involved in the definition of  $\Delta H$  via Monte Carlo sampling, while we found an analytic approximation for this correction term.

In figure 5.11 we show their results for the finite volume spectrum [78]. These results are based on QSE with 250 states (no SEC). Using this plot, Ref. [78] estimated the critical coupling as  $\bar{g}_c \approx 2.5$ . On the same plot we overlay our results for the lowest  $\mathbb{Z}_2$ -odd state from figure 5.4. Our predictions for the physical mass are in disagreement with [78] in the range  $\bar{g} \lesssim 2$ , where the truncation errors due to finite  $E_{\max}$  are small. Notice that even though our results refer to a smaller value of  $L$  than [78], this cannot explain the differences, since the finite volume effects for the one-particle state are negligible in this range of  $\bar{g}$  (see figure 5.7). One possible explanation is that the momentum cutoff  $k_{\max} = 4m$  used in [78] is not sufficiently high to describe the continuum limit. In any case, it is this disagreement which is ultimately responsible for the difference in our estimates of  $\bar{g}_c$ .

The QSE method of [79] looks somewhat similar in spirit to the Numerical RG (NRG) method recently employed in the context of TCSCA [108, 100]. At the same time, the latter method seems to us more flexible and systematic. It would be interesting to apply the NRG method to the  $\phi^4$  theory and see if it can help resolve the above discrepancy.

### 5.5.3 DMRG

Ref. [102] studied the  $\phi^4$  theory using the Density Matrix Renormalization Group (DMRG) [109]. As a starting point of this approach, the  $x$ -direction is discretized with a spacing  $a$ , while time is kept continuous. The Hamiltonian describing such a discretized theory is

$$H = \sum_x \frac{1}{2a} \pi_x^2 + \frac{1}{2a} (\phi_x - \phi_{x+a})^2 + \frac{m^2 a}{2} \phi_x^2 + g a \phi_x^4, \quad (5.86)$$

where  $\phi_x$  are the field variables on each lattice site and  $\pi_x$  are the corresponding canonical momenta. The Hilbert space on each site is infinite, unlike in the more standard DMRG applications. Ref. [102] truncates this Hilbert space to  $N = 10$  first harmonic oscillator states. The finite-system version of the DMRG algorithm [109] is used, truncating to  $M = 10$  most dominant density matrix eigenstates. This corresponds to the superblock Hamiltonian dimension  $M^2 N = 1000$ .

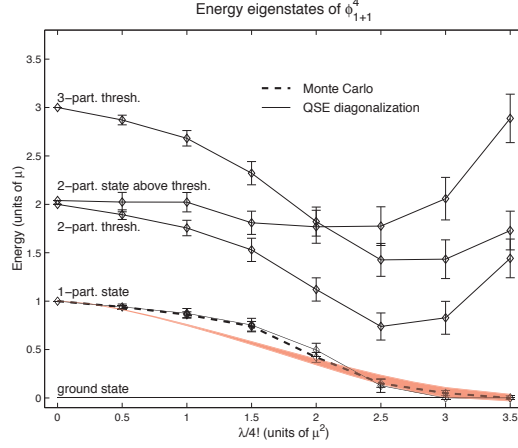


Figure 5.11: Finite volume spectrum of the  $\phi^4$  theory on a circle of length  $L = 10\pi m^{-1}$  (plot taken from [78]). In our notation  $\lambda/4! = g$ ,  $\mu = m$ . Black solid lines with error bars—the results of QSE with 250 states. Black dashed line—the results of a lattice Monte Carlo simulation. On their plot we overlay our results for the lowest  $\mathbb{Z}_2$ -odd state on a circle of a smaller length  $L = 10m^{-1}$  (red band). The central value and the width of the red band are the same as in the conservative method of determining  $\bar{g}_c$  in section 5.4.2.

The critical value of the coupling is obtained approaching the critical point from inside of the  $\mathbb{Z}_2$ -broken region, and studying how the vacuum expectation value  $\langle\phi\rangle$  approaches zero in this limit. The quoted value has an extremely small uncertainty:  $\bar{g}_c = 2.4954(4)$ . However, careful reading of the paper leaves us unconvinced that all sources of systematic error were properly taken into account. First, no attempt is made at extrapolating to  $M = \infty$ , while Figure 4 of [102] shows clearly that convergence in  $M$  is slow and the results for  $M = 10$  have not yet stabilized. Second, the value of  $\bar{g}_c$  is determined in Figure 7 of [102] by fitting a straight line through two points.

Finally, we believe that the matching to the continuum limit should have been done more carefully. In the units  $m^2 = 1$ , the smallest physical lattice spacing in [102] is  $a \approx 0.1$ .<sup>29</sup> This is factor 3 larger than the spacing used in the lattice Monte Carlo study [103] discussed in section 5.5.4 below. Since Ref. [102] used the simplest nearest-neighbor discretization of the  $x$ -derivative, the matching procedure will likely be plagued by the same basic problem as the one we will explain in section 5.5.4.

### 5.5.4 Lattice Monte Carlo

In [103] (see [110] for earlier work) the critical coupling of the  $\phi^4$  theory was determined by Monte Carlo (MC) simulations on the two-dimensional square lattice. They find  $\bar{g}_c = 2.7_{-0.01}^{+0.025}$ , somewhat below our prediction. This  $2\sigma$  discrepancy is not necessarily a reason to worry, as it may go away with further development of our method. In addition, it appears that the MC computation is subject to a subtle systematic error which was not discussed in [103].

<sup>29</sup>This is found from  $\bar{g}_c a^2 = \tilde{\lambda}/4!$  where their smallest  $\tilde{\lambda} = 0.6$ .



This error is particularly troubling because similar errors likely affect, to varying degree, all techniques involving the discretization of space, including also the DMRG and MPS methods discussed in sections 5.5.3 and 5.5.5. Below we will review the lattice computation and explain this potential error.

Ref. [103] simulated the lattice action (the subscript # stands for “lattice”)

$$S_{\#} = a^2 \sum_x \frac{1}{2} \sum_{\mu=1,2} a^{-2} (\phi_{x+ae_{\mu}} - \phi_x)^2 + \frac{1}{2} m_{\#}^2 \phi_x^2 + g_{\#} : \phi_x^4 :. \quad (5.87)$$

Here  $a$  is the lattice spacing. The normal ordering on the lattice is defined by subtracting a loop of the lattice propagator (BZ = the Brillouin zone  $|p_{\mu}| \leq \pi/a$ ),

$$: \phi_x^4 : = \phi_x^4 - \phi_x^2 \int_{\text{BZ}} \frac{dp}{(2\pi)^2} G_{\#}(p), \quad (5.88)$$

$$G_{\#}(p) = \left\{ 4a^{-2} [\sin^2(p_1 a/2) + \sin^2(p_2 a/2)] + m_{\#}^2 \right\}^{-1}. \quad (5.89)$$

So operationally, (5.88) is plugged into (5.87) and the resulting action is MC-simulated.

In the normalization in which  $m_{\#} = 1$ , Ref. [103] explored the range of lattice spacings  $a = 0.3 - 0.03$ .<sup>30</sup> Their lattices had up to  $1024 \times 1024$  sites, which corresponds to a sufficiently large physical volume varying from  $L \approx 300$  for  $a = 0.3$  to  $L \approx 30$  for  $a = 0.03$ . Depending on  $a$ , the critical quartic coupling was found to vary from  $g_{\#} \approx 2.55$  to  $2.7$ . Their final answer for  $g_c$  was obtained by fitting and extrapolating to  $a = 0$ .

The systematic error that we have in mind concerns the matching between the lattice and the continuum. Naively, the lattice theory (5.87) seems to go to the continuum limit theory as  $a \rightarrow 0$ , with  $m_{\#}$  and  $g_{\#}$  turning into  $m$  and  $g$ . However, let us try to establish this correspondence more carefully.

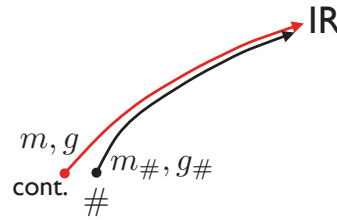


Figure 5.12: The lattice and the continuum RG flows should agree in the IR. See the text.

In figure 5.12 we show, schematically, two RG flows: the lattice flow specified by the couplings  $m_{\#}, g_{\#}$  and the continuum flow specified by  $m, g$ . The latter couplings have to be found so that the flows become the same at large distances. We can check if this is the case computing some observables at intermediate distances, when the flows are still perturbative.<sup>31</sup> If a sufficient number of observables agree at intermediate distances, the two flows have converged

<sup>30</sup>See their Table II. The value of  $a$  is computed from  $\hat{\mu}_c^2 = m_{\#}^2 a^2$ .

<sup>31</sup>We are focusing on the case when the coupling  $g$  is strong, which is relevant for the critical point. The case of small  $g$  is simpler, as the matching can be performed at  $p \lesssim m$ .

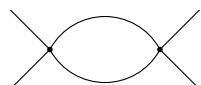
and will stay the same also at larger distances. In the language of effective field theory, this would be an example of perturbative matching (see e.g. [111]).<sup>32</sup>

At what distance scale should we do the matching? First of all, to match the continuum theory, the lattice theory should at the very least become approximately rotationally invariant. The leading deviation from rotation invariance comes from the lattice propagator (5.89), which at small momenta behaves as

$$G_{\#}^{-1}(p) = p^2 + m_{\#}^2 - \frac{1}{12}(p_1^4 + p_2^4)a^2 + \dots \quad (5.90)$$

To ensure that this is approximately rotationally invariant, we must have  $p^2 \ll a^{-2}$ .

On the other hand, the matching momentum cannot be too small since the theory is then strongly coupled. The smallest allowed matching momentum can be computed by considering the diagrams which give a correction to the quartic coupling. For momenta  $p \gg m$  these diagrams are, omitting logarithmic factors,




$$+ \text{permutations} \sim g^2/p^2, \quad (5.91)$$

which becomes comparable to the coupling  $g$  itself for  $p^2 = O(g)$ . Putting the two constraints together, we conclude that the matching must be done at momenta  $p$  such that

$$g \ll p^2 \ll a^{-2}. \quad (5.92)$$

Now, to match the mass, we have to consider the correction to the propagator, which in the considered region of momenta behaves like



$$\sim g^2/p^2[1 + O(p^2a^2)] \quad (5.93)$$

where the terms dependent on  $a^2$  indicate the schematic dependence of the correction on the lattice spacing. This suggests that

$$m^2 = m_{\#}^2 + O(g^2a^2). \quad (5.94)$$

However, such a conclusion would be on shaky grounds. The problem is that at the lowest allowed momenta  $p^2 \sim g$  the correction to the propagator due to the rotation invariance breaking has the same parametric order of magnitude,  $g^2a^2$ , as the putative mass matching correction.

The above discussion suggests that the chosen form of the lattice discretization prevents performing a controlled matching between the lattice and the continuum theory, because the

---

<sup>32</sup>In this discussion we ignore another complication arising from the fact that the two-dimensional  $\phi^4$  theory has infinitely many additional relevant couplings beyond  $m^2$  and  $g$ , since all powers of  $\phi$  are relevant. Strictly speaking establishing correspondence between the lattice and the continuum may require turning on these extra couplings.

matching corrections from loop diagrams cannot be cleanly disentangled from the rotation invariance breaking effects in the propagator. This may seem unusual to a lattice practitioner. However, the theory we are considering is a bit unusual, having a coupling constant of dimension exactly 2.

We consider it possible that this problem contributes to the mismatch between the lattice determination of  $g_c$  and our results. Our discussion also suggests the recipe to remedy the problem: one should redo the lattice simulation using an improved actions, in which the leading  $O(p^2 a^2)$  effect of rotation symmetry breaking is absent due to judiciously chosen next-to-nearest interaction terms [112]. In such a setup the matching can be done, and the correspondence between  $m_{\#}, g_{\#}$  and  $m, g$  can be established rigorously.

### 5.5.5 Uniform matrix product states

This method was applied to the  $\phi^4$  theory in [104]. The starting point of this approach is the discretized Hamiltonian (5.86). The lowest energy states are searched for in a finite variational subspace of the full Hilbert space, consisting of the so-called matrix product states (MPS), whose precise definition can be found in [104]. The MPS states are parametrized by a 3-tensor of size  $d \times D \times D$ . Here,  $d$  represents the size of the truncated Hilbert space per lattice site, while  $D$  is a parameter which bounds the degree of entanglement of the ground state across different lattice sites. The variational states are found by minimizing the energy through an imaginary-time evolution algorithm. The physical predictions are recovered in the limit  $d, D \rightarrow \infty, a \rightarrow 0$ .

As is well known, the MPS methods are essentially equivalent to DMRG (see e.g. [113]). Comparing with the DMRG study in section 5.5.5,  $d$  and  $D$  should be identified with  $N$  and  $M$ . Ref. [104] uses  $d = 16$  and  $D$  up to 128, commenting that  $N = M = 10$  used in [102] are not sufficient. They observe that an insufficiently large  $D$  shifts the critical point to lower  $\bar{g}_c$ , and provide a physical explanation for this effect. They do two measurements of  $\bar{g}_c$ , both approaching the critical point from above, one using  $\langle \phi \rangle$  and another from the lowest excitation energy. Since their two measurements differ at a  $3\sigma$  level, the value cited in Table 5.1 was obtained by expanding the error bars to include both of them.

In the units  $m^2 = 1$ , the minimal value of the lattice spacing in [104] is  $a \approx 0.04$ , about the same as in [103]. This study is thus subject to the same worries about the matching to the continuum limit as the ones brought up in section 5.5.4.



## Chapter 6

# Hamiltonian truncation in the $\mathbb{Z}_2$ -broken phase

### 6.1 The Chang duality

#### 6.1.1 Formulation and consequences

According to Chang [92], the two-dimensional  $\phi^4$  theory described by the (Euclidean) Lagrangian

$$\mathcal{L} = \frac{1}{2}(\partial\phi)^2 + \frac{1}{2}m^2\phi^2 + g N_m(\phi^4) \quad (6.1)$$

with  $m^2 > 0$ ,  $g > 0$ , admits a dual description in terms of a Lagrangian with a different, and negative, value of the squared mass,

$$\mathcal{L}' = \frac{1}{2}(\partial\phi)^2 - \frac{1}{4}M^2\phi^2 + g N_M(\phi^4). \quad (6.2)$$

The actual value of the dual mass will be given below.

Note that the duality is between quantum theories in the continuum limit, and to specify this limit one has to subtract the logarithmic divergence of the mass parameters. The divergence is removed by normal-ordering the quartic interaction with respect to the mass indicated in the subscript of the normal ordering sign  $N$ . The potential in  $\mathcal{L}'$  has two minima at  $\phi = c = \pm M/\sqrt{8g}$ . After the shift  $\phi \rightarrow \phi + c$  the dual Lagrangian becomes<sup>1</sup>

$$\mathcal{L}' \rightarrow \frac{1}{2}(\partial\phi)^2 + \frac{1}{2}M^2\phi^2 + \sqrt{2g}M N_M(\phi^3) + g N_M(\phi^4). \quad (6.3)$$

In this way of writing, interactions of both  $\mathcal{L}$  and  $\mathcal{L}'$  are normal ordered with respect to the mass appearing in the quadratic part of the Lagrangian. In perturbation theory such normal ordering means that we are simply forbidding diagrams with the lines starting and ending in the same vertex.

---

<sup>1</sup>Notice that normal ordering is a linear operation, and thus commutes with the field shift.

To find the dual mass  $M^2$ , one is instructed to solve the equation

$$F(X) = f(x), \quad (6.4)$$

where  $x = g/m^2$ ,  $X = g/M^2$  are the dimensionless quartic couplings of the two descriptions ( $x$  is given and  $X$  is an unknown) and

$$f(x) \equiv \log x - \pi/(3x), \quad F(X) \equiv \log X + \pi/(6X). \quad (6.5)$$

This equation is illustrated in Fig. 6.1. There is no solution for

$$x < x_* = \frac{\pi}{3W(2/e)} \approx 2.26149, \quad (6.6)$$

where  $W(z)$  is the Lambert  $W$  function. For  $x \geq x_*$  there are two solution branches. We are particularly interested in the lower branch  $X_1(x)$ , which for large  $x$  approaches zero,

$$X_1(x) \approx 6/(\pi \log x), \quad x \rightarrow \infty. \quad (6.7)$$

The dual description corresponding to this branch becomes weakly coupled in the limit in which the original description becomes stronger and stronger coupled. We thus have a weak/strong coupling duality.

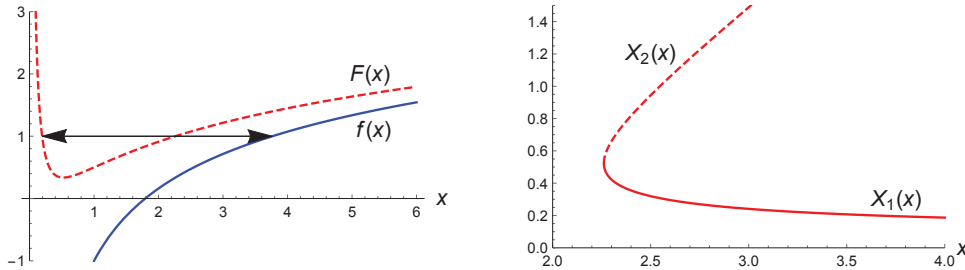


Figure 6.1: Left panel: equation  $F(X) = f(x)$  has two solutions for  $x > x_*$ . Right panel: the two solution branches  $X_{1,2}(x)$ . We are mostly interested in the lower branch  $X_1(x)$  which becomes weakly coupled as  $x \rightarrow \infty$ .

Chang [92] used this duality to show that the  $\phi^4$  theory undergoes a phase transition. Indeed, for small  $x$  we can use perturbation theory to argue that the theory is in the symmetric phase, with the  $\mathbb{Z}_2$  symmetry  $\phi \rightarrow -\phi$  unbroken. On the other hand, for large  $x$  we use the dual description. Since in that description the potential is a double well, and moreover the dual coupling is weak for  $x \gg 1$ , we conclude that for large  $x$  the  $\mathbb{Z}_2$  symmetry is spontaneously broken. By continuity, there must be a phase transition at an intermediate value of  $x$ .

This argument does not establish whether the transition is first or second order. However, as explained in [92], a first order transition is excluded by rigorous theorems due to Simon and Griffiths [114]. So the transition must be second order. This conclusion is supported by Monte Carlo simulations [110, 103, 115, 116], as well as by computations using DLCQ [105],

density matrix renormalization group [102], matrix product states [104], and the Hamiltonian truncation [78, 79].

Nor does the above argument predict the value of  $x$  at which the phase transition must happen. In particular, the fact that the dual description exists at  $x \geq x_*$  does not mean that the phase transition happens at  $x = x_*$ . Indeed, at  $x = x_*$  both the direct and the dual descriptions are strongly coupled, and the fate of the  $\mathbb{Z}_2$  symmetry is not *a priori* clear. In fact, calculations indicate a higher phase transition location at  $x_c \approx 2.75 - 3$  [115, 104, 116, 117], as also seen in section 5.4.2.

### 6.1.2 Review of the derivation

Here's a quick derivation of the Chang duality, following [92]. We will work in the Hamiltonian formalism, and consider the normal-ordered Hamiltonians corresponding to  $\mathcal{L}$  and  $\mathcal{L}'$ ,

$$H = \int dx N_m \left( \frac{1}{2} \dot{\phi}^2 + \frac{1}{2} \phi'^2 + \frac{1}{2} m^2 \phi^2 + g \phi^4 \right), \quad (6.8)$$

$$H' = \int dx N_M \left( \frac{1}{2} \dot{\phi}^2 + \frac{1}{2} \phi'^2 - \frac{1}{4} M^2 \phi^2 + g \phi^4 + \Lambda \right). \quad (6.9)$$

Notice that we are now normal ordering the full Hamiltonian, including the quadratic part. This more careful procedure will allow us to establish the correspondence also for the ground state energy. In the dual description it will receive an extra constant contribution, denoted  $\Lambda$  in (6.9).

Recall Coleman [93] relations between normal orderings with respect to different masses,

$$\begin{aligned} N_m \left( \frac{1}{2} \dot{\phi}^2 + \frac{1}{2} \phi'^2 \right) &= N_M \left( \frac{1}{2} \dot{\phi}^2 + \frac{1}{2} \phi'^2 \right) + Y, \\ N_m(\phi^2) &= N_M(\phi^2) + Z, \\ N_m(\phi^4) &= N_M(\phi^4) + 6ZN_M(\phi^2) + 3Z^2, \end{aligned} \quad (6.10)$$

where  $Y = Y(m, M)$  and  $Z = Z(m, M)$  are the differences of the normal-ordering constants,<sup>2</sup>

$$\begin{aligned} Y(m, M) &= \int \frac{dk}{8\pi} \left\{ \frac{2k^2 + M^2}{\sqrt{k^2 + M^2}} - (M \rightarrow m) \right\} = \frac{1}{8\pi} (M^2 - m^2), \\ Z(m, M) &= \int \frac{dk}{4\pi} \left\{ \frac{1}{\sqrt{k^2 + M^2}} - (M \rightarrow m) \right\} = \frac{1}{4\pi} \log \frac{m^2}{M^2}. \end{aligned} \quad (6.11)$$

Using these relations, one can see that  $H$  maps on  $H'$  as long as

$$\frac{1}{2} m^2 + 6Zg = -\frac{1}{4} M^2, \quad (6.12)$$

<sup>2</sup>The expression for  $Z$  can also be equivalently derived in the Lagrangian language as the difference of one-loop massive diagrams  $Z = \int \frac{d^2 k}{(2\pi)^2} \left( \frac{1}{k^2 + M^2} - \frac{1}{k^2 + m^2} \right)$ .

written equivalently as (6.4). We also find a constant contribution to the ground state energy

$$\Lambda = Y + \frac{1}{2}m^2Z + 3gZ^2. \quad (6.13)$$

### 6.1.3 Numerical check of the duality

We will test the Chang duality by comparing the spectra of the direct and dual theories in a finite volume—a circle of length  $L$ . The spectra will be computed using the Hamiltonian truncation. We will first describe the setup for these computations, and then present the results.

#### Direct theory

By the direct theory we mean (6.8) put on a circle of length  $L$ . This is precisely the theory we studied in Chapter 5, and we will be following the same method.

In Chapter 5 we worked at circle sizes up to  $L = 10m^{-1}$ , and it was justified to neglect the exponentially small terms proportional to  $E_0$  and  $\zeta$  in (5.20). Here, in some cases, we will work at smaller circle sizes. In the subsequent analysis we will always keep these terms, which is actually straightforward in our algorithm.

Regarding the renormalization of the couplings, we will use an identical procedure to the one described in section 5.3.2, apart from a technicality that we now explain.

We remind that the leading renormalization coefficients are calculated by extracting the leading non-analytic behavior for  $\tau \rightarrow 0$  of the quantities (5.48). In section 5.3.2 we approximated the two-point function (5.51) by its infinite-volume expression. However in the following we will encounter also the situation  $mL = O(1)$ . Our procedure will be to approximate

$$G_L(z, \tau) \simeq G(\rho) + 2 \sum_{n=1}^{\infty} G(nL), \quad (6.14)$$

which simply adds a constant to the infinite-volume two point function. This approximation is justified because the higher order Taylor expansion terms of  $G(\rho)$  around  $\rho = nL$  would result in renormalization terms suppressed by powers of  $m^2/E_{\max}^2 \ll 1$ . The short-distance asymptotics of  $G_L$  used to calculate (5.48) is modified as

$$G_L(z, \tau) \approx -\frac{1}{2\pi} \log \left( \frac{e^\gamma}{2} m' \rho \right), \quad m' \equiv m \exp \left[ -4\pi \sum_{n=1}^{\infty} G(nL) \right]. \quad (6.15)$$

It is then straightforward to generalize the renormalization procedure used in Chapter 5 to the case  $mL = O(1)$ . E.g. the Hamiltonian renormalized by local counterterms is given by

$$H(L)_{\text{ren}} = H_{\text{trunc}}(L) + \int dx N_m (\kappa_0 + \kappa_2 \phi^2 + \kappa_4 \phi^4), \quad (6.16)$$



where  $\kappa_i$  are given in (5.61) where one has to put  $g_4 = g$ ,  $g_2 = 6\zeta g$ , and replace  $m \rightarrow m'$  in the expressions for the  $\mu$ -functions in (5.58). This Hamiltonian allows to calculate the spectrum with the convergence rate of  $1/E_{\max}^3$ . In the numerical computations in section 6.1.3 we will also include subleading, non-local corrections improving the convergence rate up to  $1/E_{\max}^4$ , for which we refer the reader to section 5.3.3.

### Dual theory

The Hamiltonian for the dual theory in finite volume is easiest derived as follows. Let us rewrite  $H'$  in (6.9) by adding and subtracting  $\frac{1}{2}M^2\phi^2$ ,

$$H' = \int dx N_M \left( \frac{1}{2}\dot{\phi}^2 + \frac{1}{2}\phi'^2 + \frac{1}{2}M^2\phi^2 \right) + N_M \left( -\frac{3}{4}M^2\phi^2 + g\phi^4 + \Lambda \right). \quad (6.17)$$

This looks like the direct Hamiltonian with  $m \rightarrow M$  and an extra negative mass squared perturbation. The passage to a finite volume is then analogous to the direct theory. We get

$$H'(L) = H_0 + \left[ -\frac{3}{4}M^2 + 6\zeta g \right] V_2 + gV_4 + h, \quad (6.18)$$

$$h = \Lambda L + E_0 + 3\zeta^2 gL - \frac{3}{4}M^2\zeta L. \quad (6.19)$$

The building blocks have the same meaning as in section 6.1.3, except that we have to use  $M$  instead of  $m$  in all expressions:  $H_0 = H_0(L, M)$ ,  $\zeta = \zeta(L, M)$ , etc.

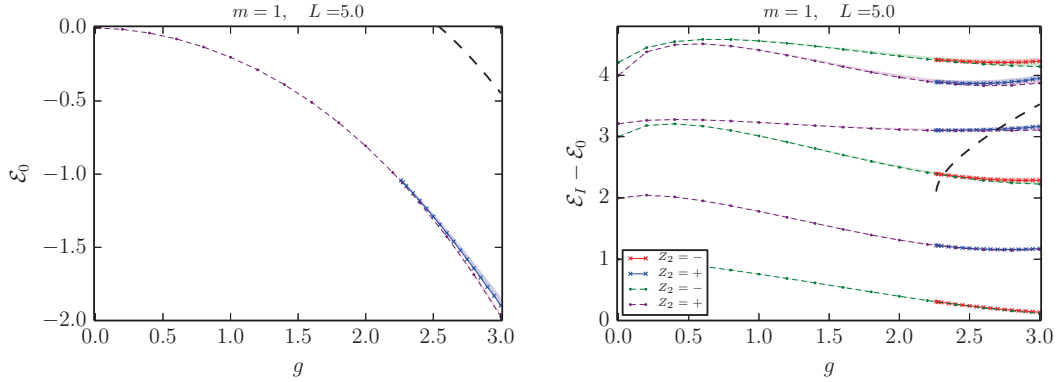


Figure 6.2: The ground state energy (left) and the spectrum of excitations (right) for the direct and the dual theory as a function of  $g$  for  $m = 1$ ,  $L = 5$ . The excitation plot shows the energies of the  $\mathbb{Z}_2$  odd and  $\mathbb{Z}_2$  even energy levels. See the text for the details.

### Comparison

In figure 6.2 we show the ground state energy  $\mathcal{E}_0$  and the spectrum of excitations  $\mathcal{E}_I - \mathcal{E}_0$  for  $m = 1$ ,  $L = 5$ . We plot them as a function of the direct coupling  $g = 0 - 3$ . The results for the direct theory are given in the full range of  $g$ , whereas for the dual theory only for  $g \geq g_c \approx 2.26$ , where the dual description exists. As in Chapter 5, the error (shaded

region) is estimated as the variation of the results upon using the “local” and “subleading” renormalization prescriptions.

We see that in the overlapping region the numerical predictions from the two descriptions agree very well. This is an explicit check of the Chang duality. This check is non-trivial, as in both descriptions the Hamiltonian is strongly coupled. To illustrate this, the black dashed lines in the plots represent the tree-level prediction for the vacuum energy and the lightest excitation in the dual description.

*Computational details:* The computation in the direct theory is carried out as described in section 6.1.3. The dual mass  $M$  for a given  $g \geq g_c$  is determined by solving Eq. (6.4) numerically. We use the solution with the smaller  $X$  (and thus the larger  $M$ ). The computation in the dual theory is then done using the Hamiltonian (6.18) with two couplings  $g_2 = -\frac{3}{4}M^2 + 6\zeta g$  and  $g_4 = g$ , i.e. by including  $-\frac{3}{4}M^2$  into the perturbation. The renormalization procedure described in 5.3.3 is applicable for such a general perturbation. It’s not a problem for the method that  $g_2$  is negative and comparable in size to the positive mass square term in  $H_0$ . There is in fact a great deal of arbitrariness in how to split the  $\phi^2$  coefficient between the zeroth-order Hamiltonian and the perturbation. What we do here is just the fastest possibility, which turns out sufficient for the purposes of this section. More sophisticated ways of dealing with the dual theory will be developed in section 6.2.

## 6.2 The $\mathbb{Z}_2$ -broken phase

In section 6.1 we reviewed the Chang duality and tested it numerically in the strongly coupled region by comparing the results obtained from the dual and the direct descriptions. We will now focus on the region  $g/m^2 \gg g_*/m^2$ , where the theory is in the  $\mathbb{Z}_2$ -broken phase. In this range of couplings the direct description is very strongly coupled and it’s difficult to achieve good numerical accuracy. On the other hand, the dual Hamiltonian becomes weakly coupled ( $g/M^2 \ll 1$ ). Therefore, we will use the dual Hamiltonian (6.9) as the starting point for the numerical calculations. It will be convenient to replace the value of  $\Lambda$  given in (6.13) by  $\Lambda = M^2/(64g)$ , which corresponds to having zero classical vacuum energy density of the dual Hamiltonian.

### 6.2.1 Modified zero mode treatment

The method employed in 6.1.3 treats all field modes on equal footing. This method is adequate in the  $\mathbb{Z}_2$ -unbroken phase and in the  $\mathbb{Z}_2$ -broken phase in moderate volumes, as in section 6.1.3. However, it becomes inefficient in the  $\mathbb{Z}_2$ -broken phase in large volume. The physical reason is that the zero mode has then very different dynamics from the rest of the modes, acquiring a VEV. It makes sense to take this into account, and to treat the zero mode separately from the rest. We will now explain how this can be done.

First of all we will rewrite (6.18) making explicit the dependence on the zero mode. We will

revert for the zero mode from using the oscillators  $a_0, a_0^\dagger$  to the field variable

$$\phi_0 = (a_0 + a_0^\dagger)/\sqrt{2LM} \quad (6.20)$$

and the corresponding conjugate momentum  $\pi_0$ ,

$$\pi_0 = i(a_0^\dagger - a_0)\sqrt{LM/2}. \quad (6.21)$$

Denoting by bar (resp. hat) all quantities involving only the nonzero (zero) modes, we have

$$H_0 = \bar{H}_0 + \frac{:\pi_0^2:}{2L} + \frac{LM^2}{2}:\phi_0^2:, \quad (6.22)$$

$$V_2 = \bar{V}_2 + L:\phi_0^2:, \quad V_4 = \bar{V}_4 + 4\bar{V}_3\phi_0 + 6\bar{V}_2:\phi_0^2: + L:\phi_0^4:. \quad (6.23)$$

Gathering everything we get

$$H'(L) = \bar{H}_0 + \hat{H} + W, \quad (6.24)$$

where  $\hat{H}$  depends only on the zero mode,

$$\hat{H} \equiv \frac{:\pi_0^2:}{2L} + L \left[ -\frac{1}{4}M^2 + 6\zeta g \right] :\phi_0^2: + Lg:\phi_0^4: + h, \quad (6.25)$$

while  $W$  involves the interactions between the zero and the nonzero modes, and among the latter,

$$W \equiv \left[ 6g:\phi_0^2: - \frac{3}{4}M^2 + 6\zeta g \right] \bar{V}_2 + 4g\phi_0\bar{V}_3 + g\bar{V}_4. \quad (6.26)$$

In a large volume and for  $g \ll M^2$ , the quantum mechanics of (6.25) predicts that the wavefunction of  $\phi_0$  is peaked around the minima of the potential at  $\phi_0^2 \approx M^2/(8g)$ , with a width scaling asymptotically as  $\langle(\Delta\phi_0)^2\rangle \sim 1/(LM)$ . For this  $\phi_0$  the coefficient of  $\bar{V}_2$  in  $W$  vanishes. Intuitively this implies that, up to small perturbative corrections induced by the  $\bar{V}_3$  and  $\bar{V}_4$  terms, the nonzero modes of the field will stay in their vacuum state. This is true in a very large volume, and it provides a good starting point for a quantitative description in finite volume.

The idea of the method will be therefore to first solve the quantum mechanics of the zero modes, by neglecting its interaction with the nonzero modes. Having done so, the full Hamiltonian will be diagonalized in a Hilbert space whose basis wavefunctions are products of the exact zero mode wavefunctions and the harmonic oscillator wavefunctions for the nonzero modes. This is expected to be more efficient than the original method which would use harmonic oscillator wavefunctions also for the zero mode.

Concretely, the procedure goes as follows. The full Hilbert space can be written as a direct product,

$$\mathcal{H} = \hat{\mathcal{H}} \otimes \bar{\mathcal{H}}, \quad (6.27)$$

where  $\hat{\mathcal{H}}$  and  $\bar{\mathcal{H}}$  are the Hilbert spaces of the zero modes and nonzero modes, respectively.

The truncated Hilbert space is then ( $l$  for low)

$$\mathcal{H}_l = \hat{\mathcal{H}}_l \otimes \bar{\mathcal{H}}_l, \quad (6.28)$$

where the basis of  $\bar{\mathcal{H}}_l$  is formed by the harmonic oscillator states for the nonzero modes with energy  $\bar{E} \leq \bar{E}_{\max}$ , while  $\hat{\mathcal{H}}_l$  is spanned by the first few low-lying eigenfunctions of  $\hat{H}$ ,

$$\hat{H}|\psi_\alpha\rangle = \hat{\mathcal{E}}_\alpha|\psi_\alpha\rangle, \quad \alpha = 1 \dots s. \quad (6.29)$$

In practice, it will be sufficient to fix  $s = 4$  or  $5$ .

A separate computation has to be done to find the  $|\psi_\alpha\rangle$ . We do this using the standard Rayleigh-Ritz method, working in the  $S$ -dimensional subspace of  $\hat{\mathcal{H}}$  spanned by the original harmonic oscillator wavefunctions  $(a_0^\dagger)^i|0\rangle$ ,  $i = 0 \dots S - 1$ . The parameter  $S \gg s$  can be chosen so large that the numerical error accumulated in this step is insignificant; in practice we choose  $S = 500$ . The eigenstates  $|\psi_\alpha\rangle$  are thus found expanding them in the harmonic oscillator wavefunctions. This facilitates the subsequent computations of the matrix elements involving these states.

One can now compute the matrix elements of  $H'(L)$  in the truncated Hilbert space and diagonalize it, finding the “raw” spectrum. As usual, we will employ a renormalization procedure to improve the precision. The necessary modifications are described in appendix D.2.

*Comparison with prior work:* The  $\mathbb{Z}_2$ -broken phase of the  $\phi^4$  model has been previously studied via a Hamiltonian truncation method in Ref. [77]. There are many similarities between our works, and some differences. The main difference lies in the treatment of the zero mode (see also the discussion in Section 5.4.5). Ref. [77] compactifies the zero mode on a circle of large radius, and uses plane waves on this target space circle as the basis of trial wavefunctions. Instead, we resolve the zero mode dynamics and pick trial wavefunctions adapted to the quartic potential. Another difference is that they use conformal, massless, basis for the nonzero modes, while we use a massive basis. Matrix elements are easier to compute in the conformal basis, while a massive basis gives, we believe, a better initial approximation.

Notice that Ref. [77] uses a different parametrization of the Hamiltonian, corresponding to a different normal-ordering prescription. Translation to our parametrization will be given in section 6.2.3.

## 6.2.2 Varying the normal-ordering mass

It turns out that in the regime we will be considering, the most important term inducing the interactions between  $\hat{\mathcal{H}}_l$  and  $\bar{\mathcal{H}}_l$  is the  $\bar{V}_2$  term in (6.26). This is because for the volumes that we will be able to consider, the localization of the  $\phi_0$  wavefunctions near the potential minimum is not very sharp, and the coefficient of  $\bar{V}_2$ , viewed as a matrix in the space of the

$\phi_0$  eigenstates, has significant matrix elements. The  $\bar{V}_3$  and  $\bar{V}_4$  terms will be suppressed at weak coupling.

Empirically, we concluded that the one-loop renormalization procedure, including the modifications to be described in appendix D.2, is insufficient to fully describe the truncation effects arising from the big  $\bar{V}_2$  term. Moreover, estimating the accuracy as the difference between the “local” and “subleading” renormalized answers was found inadequate in such a situation. Notice that the  $V_2$  term renormalizes at quadratic order only the unit operator coefficient (see section 5.3.2) and this correction does not affect the spectrum of excitations (this statement remains approximately true in the scheme with the separated zero mode discussed here). Ideally, to estimate the error one would have to compute the renormalization effects of cubic order in the problematic operator. Here we will resort to an interim alternative technique, which we now describe.<sup>3</sup>

In the modified method as described in the previous section, the trial wavefunctions of the nonzero modes are taken to be those of the free massive boson of mass  $M$ , i.e. the bare mass appearing in the Lagrangian. We will now consider the formalism in which one can vary the mass parameter  $\mu$  of the trial wavefunctions. As in [78], this will then be used to control the accuracy of our computations, since the exact spectrum should be independent of  $\mu$ . Apart from the accuracy issues, varying  $\mu$  is also natural from the point of view of searching for an optimal zeroth order approximation to the ground state, in the spirit of variational methods.

So we rewrite the infinite-volume Hamiltonian (6.17) by using the Coleman relations (6.10):

$$H' = \int dx N_\mu \left( \frac{1}{2} \dot{\phi}^2 + \frac{1}{2} \phi'^2 + \left(-\frac{1}{4}M^2 + 6gZ\right) \phi^2 + g\phi^4 + \Lambda_\mu \right), \quad (6.30)$$

$$\Lambda_\mu = \Lambda - \frac{1}{4}M^2 Z + 3gZ^2 + Y, \quad (6.31)$$

where  $Z = Z(M, \mu)$ ,  $Y = Y(M, \mu)$  are defined in (6.11) with the replacement  $M \rightarrow \mu, m \rightarrow M$ . We then pass to finite volume as in section 6.1.3,

$$H'(L) = H_0 + \left[-\frac{1}{4}M^2 - \frac{1}{2}\mu^2 + 6(Z + \zeta)g\right]V_2 + gV_4 + h_\mu, \quad (6.32)$$

$$h_\mu = \Lambda_\mu L + E_0 + 3\zeta^2 gL + \left(-\frac{1}{4}M^2 - \frac{1}{2}\mu^2 + 6gZ\right)\zeta L, \quad (6.33)$$

where  $H_0, V_2, V_4, E_0, \zeta$  are defined with respect to  $\mu$ . Finally, we separate the zero mode as in section 6.2.1. The final Hamiltonian has the form (6.24) where  $\bar{H}_0 = \bar{H}_0(L, \mu)$  while  $\hat{H}$  and  $W$  are given by

$$\hat{H} = \frac{:\pi_0^2:}{2L} + L \left[-\frac{1}{4}M^2 + 6(Z + \zeta)g\right] : \phi_0^2 : + Lg : \phi_0^4 : + h_\mu, \quad (6.34)$$

$$W = \left[6g : \phi_0^2 : - \frac{1}{4}M^2 - \frac{1}{2}\mu^2 + 6(Z + \zeta)g\right] \bar{V}_2 + 4g\phi_0 \bar{V}_3 + g\bar{V}_4. \quad (6.35)$$

This is the Hamiltonian which we use for numerical calculations, varying  $\mu$  in the range 0.9 -

<sup>3</sup>Another interesting possibility is to incorporate the coefficient of  $\bar{V}_2$  into the mass of nonzero modes, making it  $\phi_0$ -dependent. This creates technical difficulties of its own and was not tried in this work.

1.1M. This will give an idea of the systematic error due to the truncation.

### 6.2.3 Results

From the estimates in Section 5.4.2, we know that the critical point lies at  $g/m^2 \approx 2.97(14)$ ,<sup>4</sup> which by making use of the Chang duality corresponds to  $g/M^2 \approx 0.26$ . Here we will limit ourselves to values  $g/M^2 \leq 0.2$ , as beyond this value it appears difficult to reach the limit  $L \rightarrow \infty$  and get a stable spectrum.  **$M$  will be set to 1 throughout this section**, unless stated otherwise.

We are now going to present the results for the two sectors of excitations of the theory. First, we will discuss the perturbative sector, which in the  $L \rightarrow \infty$  consists of two decoupled towers of excitations around the two vacua with the opposite-sign VEV for the field. We will then turn to the non-perturbative sector of “kink” states which have topological charge, interpolating between the two vacua. Given the periodic boundary conditions imposed in our method, the kink sector will be studied here only indirectly, through the splitting of quasi-degenerate perturbative states in finite volume.

#### Perturbative sector

In figure 6.3 we plot the ground state energy density and the low-energy excitation spectrum for  $M = 1$ ,  $L = 12$ . For the ground state energy density we show both the “raw” and renormalized<sup>5</sup> results, while for the spectrum only the renormalized results, because the raw/renormalized difference is negligible. As explained above, we don’t think this difference gives a fair idea of the truncation error in the situation at hand. Instead, we estimate the error for the spectrum by varying the normal-ordering mass  $\mu = 0.9 - 1.1$ . In making these plots we fixed  $s = 4$ , while the cutoff  $\bar{E}_{\max}$  was chosen so that  $\mathcal{H}_l$  has dimension around 10000 – 15000. We checked that increasing  $s$  does not change the results significantly.

We see that the first excited level is almost degenerate with the ground state. The splittings for the higher-energy levels are larger. This is because for the higher energy states it’s easier to tunnel through the potential barrier separating the two infinite-volume vacua, which has a finite height for a finite  $L$ .

In figure 6.4 we show the same plots for  $L = 20$ . One can see that the energy splitting reduces but the truncation error increases (as one has to reduce  $\bar{E}_{\max}$  in order to keep the total number of states the same).

Finally, in figure 6.5 we plot the vacuum energy density and the spectrum for  $g = 0.1$  as a function of  $L$ . One can see how the renormalization procedure is effective for the vacuum energy density, as its renormalized value reaches a constant for sufficiently large  $L$ , while its

---

<sup>4</sup>For more precise estimates by different methods see [115, 104, 116, 117].

<sup>5</sup>In this section only local renormalization was used. Subleading nonlocal corrections were found to be totally negligible.

“raw” values does not. In the spectrum also the physical mass reaches a constant as expected.

Notice that for sufficiently small  $g/M^2$  the interaction in the considered model is attractive (the cubic vertex squared attraction overcomes the quartic vertex repulsion) [118, 77]. Therefore the second energy level pair in the spectrum in figure 6.5 is expected to asymptote to  $m_2 < 2m_{\text{ph}}$  (where  $m_{\text{ph}}$  is the single particle mass) as  $L \rightarrow \infty$ , i.e. it represents a bound state. The numerical results seem consistent with this expectation, although the precision is insufficient to extract  $m_2$  accurately. In general, it is hard to extract the perturbative bound state mass from the infinite-volume limit, as the asymptotic convergence sets in at  $L \approx (m_{\text{ph}}^2 - m_2^2/4)^{-1/2}$  [96], which diverges as  $g \rightarrow 0$ .

In Appendix C we compare the numerical results for  $\Lambda$  and  $m_{\text{ph}}$  with the predictions from perturbation theory, showing very good agreement at small couplings.

It is also interesting to analyze the higher-energy states in the spectrum. In figure 6.6 we redo the previous plot for  $g = 0.05$ , including a few more eigenvalues. Above the stable particle mass and the bound state, one can see the multiparticle states whose energy depends on  $L$  according to the dispersion relations in finite volume.<sup>6</sup> Furthermore, the horizontal line with energy  $\approx 2.5 < 3m_{\text{ph}}$  represents a resonance. Due to the non-integrability of the theory, that state is not stable, as its energy is larger than  $2m_{\text{ph}}$ . Indeed, the horizontal line does not cross the multiparticle states as could seem at first glance, thanks to the phenomenon of avoided crossing. See [119] for a discussion of how resonances should appear in the finite volume spectrum.

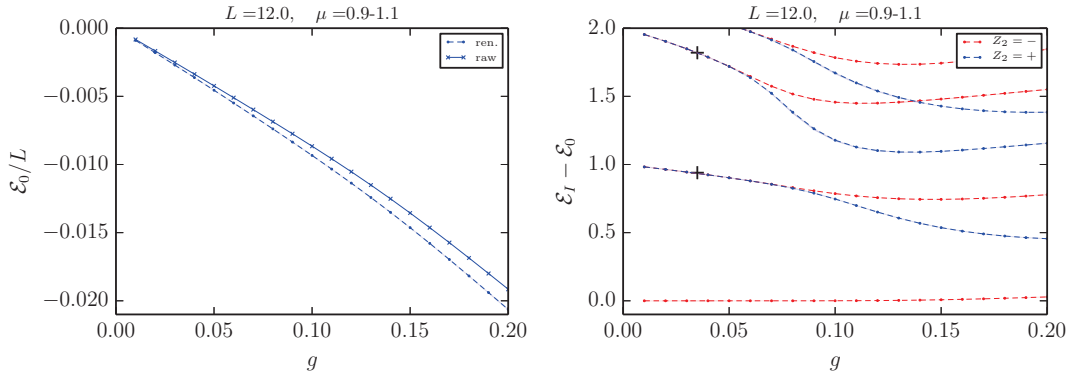
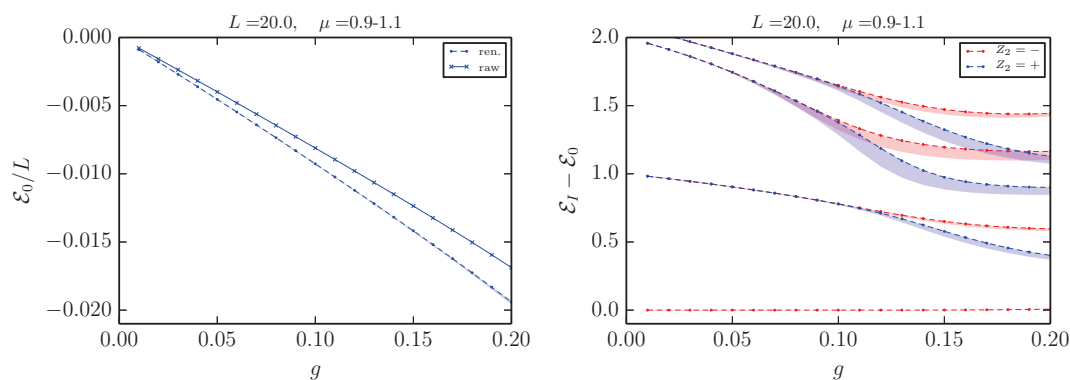
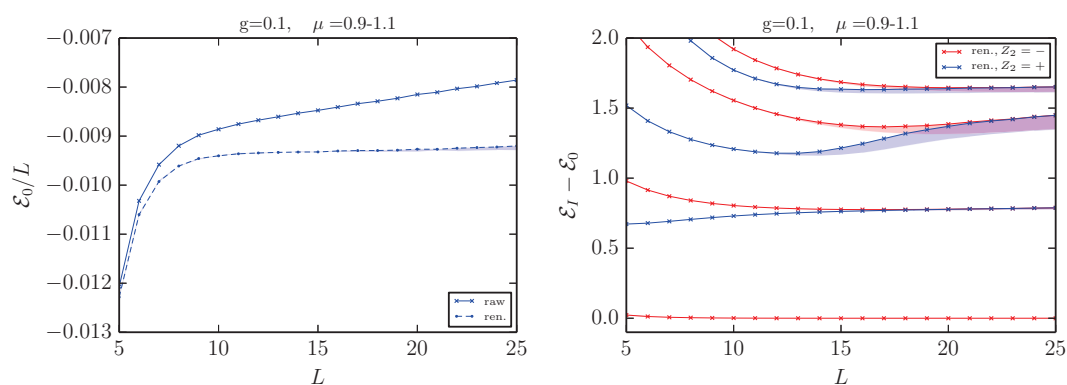
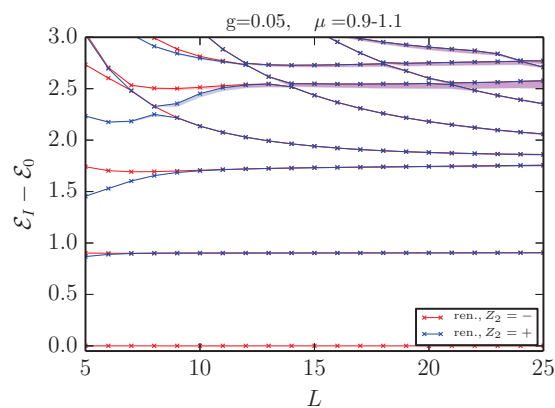


Figure 6.3: The ground state energy density and the low-energy excitation spectrum as a function of  $g$  for  $L = 12$ ; see the text. Results extracted from [77] are shown by crosses (whose size does not reflect the uncertainty), see section 6.2.3.

### Non-perturbative sector

As already mentioned, in finite volume non-perturbative effects lift the spectrum degeneracy both for the ground state and for all the excited states. For small coupling, these effects can

<sup>6</sup>See e.g. the discussion in [77], appendix B.


 Figure 6.4: Same as in figure 6.4 but for  $L = 20$ .

 Figure 6.5: Results for  $g = 0.1$  plotted as a function of  $L$ .

 Figure 6.6: Same as in the right-hand figure 6.5 but for  $g = 0.05$ .

be interpreted as tunneling due to the semiclassical field configurations interpolating between the two vacua (“kinks”). The splitting depends on the mass of the kink. Here we will need the semiclassical prediction for the splitting of the first two energy levels (the ground state,



which lives in the  $\mathbb{Z}_2$  even sector, and the  $\mathbb{Z}_2$  odd state just above it). Including the leading semiclassical results and the one-loop determinant fluctuations around it, the splitting for small  $g/M^2$  is given by (see appendix E.1),

$$\Delta\mathcal{E} = \mathcal{E}_1 - \mathcal{E}_0 \approx \sqrt{\frac{M^3}{6\pi g L}} e^{-LM_{\text{kink}} - f(ML)}, \quad M_{\text{kink}} = \frac{M^3}{12g} + M \left( \frac{1}{4\sqrt{3}} - \frac{3}{2\pi} \right), \quad (6.36)$$

where  $M_{\text{kink}}$  is the kink mass in the one-loop approximation, first computed in [120]. Corrections are suppressed by  $g/M^2$  and by  $1/(LM_{\text{kink}})$ . The function  $f(x)$ , given in (E.24), approaches zero exponentially fast for  $LM \gg 1$ . This correction can be interpreted as coming from loop corrections to the kink propagator, where virtual particles of the topologically trivial sector travel around the cylinder.

Our numerical method allows to extract  $\Delta\mathcal{E}$  with high precision and to compare with this formula. In figure 6.7 we present as an example the renormalized numerical results<sup>7</sup> for  $M = 1$ ,  $g = 0.05$ . We used  $s = 5$ , checking that its increase does not change significantly the numerics, while  $\bar{E}_{\text{max}}$  was fixed such as to have a basis dimension  $\sim 10000$  for each  $L$ . We plot  $\sqrt{L} e^{f(ML)} \Delta\mathcal{E}$  as a function of  $L$  in logarithmic scale in order to observe a linear trend, as expected from (6.36), and perform a fit in a region chosen by eye such that the data look close to a straight line,

$$\log[\sqrt{L} e^{f(ML)} \Delta\mathcal{E}] \approx \alpha - M_* L. \quad (6.37)$$

The value of  $L$  must be not too low so that the exponential law decay sets in, and not too high otherwise  $\Delta\mathcal{E}$  becomes smaller than the precision of our method. We then compare the fitted values of  $\alpha$  and  $M_*$  with the expectations from (6.36).

We carried out this analysis for several values of the coupling between 0.01 and 0.1, finding both  $\alpha$  and  $M_*$  very close to the expected values. The comparison of  $M_*$  with  $M_{\text{kink}}$  is plotted in figure 6.8 as a function of  $g$ . It turns out that in the range of points where the fit is made  $f(ML)$  is very small and does not influence the fit, except a little for the smallest considered values of  $g$ . On the other hand including  $\sqrt{L}$  is crucial for reaching the agreement. One can see that the accord with the semiclassical prediction  $M_{\text{kink}}$  (black line) is very good.

### Comparison to Ref. [77]

For comparison we included in figures 6.3,6.8 a few data points extracted from [77]. In section 5.4.5 we explained how to relate our mass and quartic coupling to their couplings  $g_2$ ,  $g_4$ . In particular,  $g = 2\pi G_4$  and, from Eq.(5.84),

$$G_2 - 2gC(ML) = -M^2/2 \quad (6.38)$$

for  $M$  in the Hamiltonian (6.9).

The two data points (crosses) in figure 6.3 were extracted from figure 10(b,d) of [77], where

<sup>7</sup>The difference between “raw” and renormalized is negligible in the present analysis.

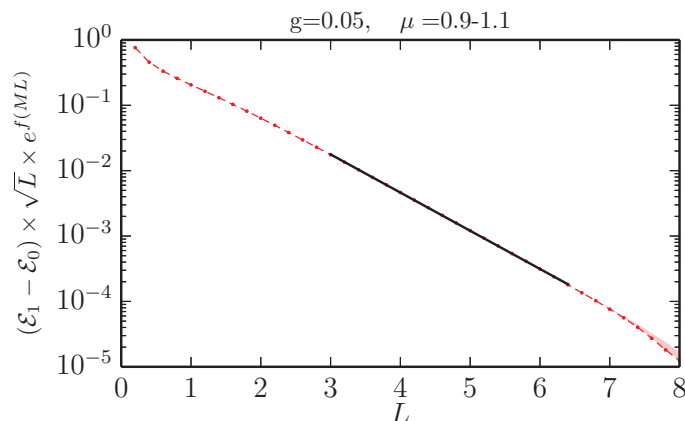


Figure 6.7: Ground state splitting as a function of  $L$  for  $g = 0.05$ ; see the text.

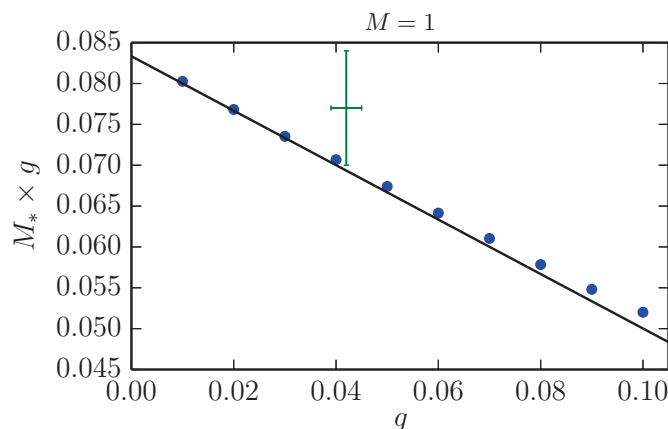


Figure 6.8: Comparison between the fitted and the theoretically predicted value of the kink mass; see the text. The green cross represents, with error bars, a result from [77] as discussed in section 6.2.3.

$G_2 = -0.1$ ,  $G_4 = 1.2 \times 10^{-3}$ . This corresponds to  $g/M^2 \approx 0.035$  at  $ML = 12$ . The agreement between their and our results is good. Their determination of the kink mass for the same  $G_{2,4}$  is shown in figure 6.8. Here  $g/M^2 = 0.042(3)$ , varying within the range of  $L$  used in their fit. The large error bars on  $M_{\text{kink}}$  may be due to this variation. Also, they did not consider the pre-exponential factor in (6.36).

### 6.3 Conclusions

In the last two chapters we revisited one of the simplest realizations of the “exact diagonalization” methods, as opposed to standard lattice Monte Carlo methods, and shown that it can be used effectively as a numerical tool to extract non-perturbative predictions about a quantum field theory. The numerical setup is relatively simple, and the error coming from

the UV regulator can be reduced by adding analytically computed correction terms to the Hamiltonian.

Our choice of the model to study here—the two-dimensional  $\phi^4$  theory—was dictated by several considerations:

- the model is not supersymmetric nor integrable, hence not amenable to analytical methods, apart from perturbation theory at small coupling ;
- the model has been studied in the past by a variety of numerical techniques, allowing for a fair comparison of the results and of the implementation difficulties ;
- the model is literally *the* textbook example of a quantum field theory. In fact we hope that our exercise also has a considerable pedagogical value, helping to bridge the conceptual gap between perturbative and non-perturbative QFT questions.

However we stress that the idea of this work is completely general, and it should be possible to apply similar techniques to any quantum field theory.

According to an exact duality, reviewed in section 6.1, the theory under consideration can be expressed via two different Lagrangian formulations. We proved that, even at strong coupling, the Hamiltonian truncation method correctly predicts the same low-energy spectrum of excitations in the two cases, despite the fact that they look totally different at the zeroth order. We regard this as a non-trivial check of the method.

The current state of the method allowed us to compute the low-energy spectrum in both the  $\mathbb{Z}_2$ -invariant and  $\mathbb{Z}_2$ -broken phases with a reasonable accuracy, and to give an estimate for the critical coupling corresponding to the phase transition. We found very good agreement with the predictions from perturbation theory and semiclassics in the perturbative and non-perturbative sectors.

We believe that the potential of “exact diagonalization” techniques, among which we have implemented a particular realization in the present work, is very large and has to be explored further. Some other representative applications to non-integrable theories to be found in the literature are [119, 121, 122, 123, 77, 124, 125, 126, 127] in  $d = 2$ . In  $d > 2$  the only works are [91] and [88].

The present analysis has been recently extended by the direct study of the topological spectrum of kink-states [84], and progress has been made towards the calculation of higher order renormalization coefficients [83]. Advancement in this direction will be necessary in order to solve higher dimensional theories, as the RG flow becomes less strongly relevant.

The hope is that exact diagonalization techniques can evolve into computationally efficient tools to address difficult problems in quantum field theory.



## Chapter 7

# Discussion and outlook

In this thesis we explored several aspects of the renormalization group in quantum field theory.

In Part I we set out to study the structure of RG flows in a large class of QFTs, namely those that are unitary and Poincaré invariant, including most of the models in particle physics. Two specific questions were addressed, which are found to be closely interrelated. Is it possible to “order” conformal field theories connected by RG flows according to monotonicity constraints? There exist (non-trivial) theories which are scale but not conformal invariant?

In our work we focused on even space-time dimensions, where the Weyl anomaly is relevant for answering these questions. In Chapter 2 we reviewed the local Callan–Symanzik equation formalism [26], which allows to treat systematically the renormalization of composite operators in curved backgrounds.

We then reconsidered the consistency conditions for the Weyl symmetry, showing that they result in only three independent non-algebraic constraints. We derived for the first time the flow equation for the coefficient  $a$  of the Weyl anomaly in a form including all the contributions from lower dimensional operators. This equation represents a formulation of the  $a$ -theorem in perturbation theory.

This methodology was then related to the “effective field theory” approach of [23] in Chapter 3, thanks to our calculation of the dilaton effective action. Additionally, we filled in some details in the proof of the equivalence SFT=CFT in perturbation theory.

In Chapter 4 we generalized the local Callan–Symanzik approach to six-dimensional QFTs. Under certain assumptions for the spectrum of relevant operators (which will be relaxed in future studies) we defined a family of functions that decrease monotonically along the RG flow. This constitutes a proof of the  $a$ -theorem and implies the equivalence SFT=CFT in perturbation theory. We would like to stress that, in general, the study of six-dimensional QFTs is not only of theoretical interest, but it can help us understand the differences between QFT in the physical four-dimensional space-time and other dimensions. Beyond perturbation

theory, ideas for a proof of the  $a$  theorem are still lacking. However, it is worth noting that in all cases studied so far no counterexample has been found [64].

In Part II of the thesis we investigated the HT method, that can be employed to solve numerically strongly-coupled RG flows in QFT. In Chapter 5 we applied the HT method to the  $\phi^4$  model in two dimensions, working in the Fock-space basis of states of the free UV Hamiltonian, and we calculated the IR spectrum with good numerical accuracy. Due to the perturbative control over the RG flow in the UV, we were able to improve the numerical convergence by constructing a low energy effective Hamiltonian. In addition, we predicted the value of the coupling where the theory flows to the critical Ising model, pointing out a significant disagreement with previous lattice determinations, which has been later resolved [116].

In Chapter 6 we studied the broken phase of the same model at strong coupling, which required a modification of the Hilbert space basis. We were able to calculate purely non-perturbative quantities, including the mass of the lightest topologically non-trivial state, which was found in agreement with the semiclassical prediction.

One obvious advantage of the exact diagonalization over lattice Monte Carlo methods is that the low-energy spectrum is found all at once by a direct diagonalization of the Hamiltonian, without any statistical error. One drawback is that manifest locality of the original QFT is lost after the truncation. Consequently, along the RG flow non-local operators are generated and have to be taken into account in the renormalization procedure.

One of the next steps to advance exact diagonalization methods will consist in improving the renormalization procedure, whose study has already started [83]. It is also worth exploring other truncation prescriptions, such as those already employed in the light-cone quantization schemes in two and three dimensions [107][88], where the wave-functional in the sectors with fixed number of particles are approximated by polynomials.

Thanks to this research program, exact diagonalization methods will hopefully evolve into an efficient tool to perform precision calculations in three and four-dimensional QFTs.

## Part III

# Appendix





# Appendix A

## Local CS equation in $d = 4$

### A.1 Definitions and useful equations

#### A.1.1 Notations

The generator of the local CS symmetry:

$$\Delta_\sigma = \Delta_\sigma^g - \Delta_\sigma^\beta \quad (\text{A.1})$$

where

$$\begin{aligned} \Delta_\sigma^g &= \int d^4x \left[ 2\sigma g^{\mu\nu} \frac{\delta}{\delta g^{\mu\nu}(x)} \right] \\ \Delta_\sigma^\beta(x) &= \int d^4x \left[ \sigma \left( \beta^I \frac{\delta}{\delta \lambda^I(x)} + \rho_I^A \nabla_\mu \lambda^I \frac{\delta}{\delta A_\mu^A(x)} \right) - \nabla_\mu \sigma \left( S^A \frac{\delta}{\delta A_\mu^A(x)} \right) \right. \\ &\quad \left. - \sigma \left( m^b (2\delta_b^a - \bar{\gamma}_b^a) + C^a R + D_I^a \nabla^2 \lambda^I + \frac{1}{2} E_{IJ}^a \nabla_\mu \lambda^I \nabla^\mu \lambda^J \right) \frac{\delta}{\delta m^a(x)} \right. \\ &\quad \left. + \nabla_\mu \sigma \left( \theta_I^a \nabla^\mu \lambda^I \frac{\delta}{\delta m^a(x)} \right) - \nabla^2 \sigma \left( \eta^a \frac{\delta}{\delta m^a(x)} \right) \right] \quad (\text{A.2}) \end{aligned}$$

Non-ambiguous functions in the local CS equation

$$B^I = \beta^I - (S^A T^A \lambda)^I \quad \gamma_b^a = \bar{\gamma}_b^a - (S^A T^A)^a_b \quad P_I^A = \rho_I^A + \partial_I S^A \quad (\text{A.3})$$

Notations appearing in the dilaton effective action

$$\tilde{B}^I = (U^{-1})^I_J B^J \quad \tilde{\eta}^a = \eta^a + \frac{1}{2} \theta_I^a \tilde{B}^I \quad (\text{A.4})$$

Useful anomalous dimension matrices

$$\begin{aligned}
\gamma_J^I &= \partial_J B^I + P_I^A (T_A \lambda^J) \\
\gamma_{IJ}^K &= \left( U^{-1} \right)_L^K \left( \partial_{(I} \gamma_{J)}^L + P_{(I}^A (T_A)_{J)}^L \right) \\
\gamma_{IJ}^a &= \frac{1}{2} \left( E_{IJ}^a + \theta_K^a \gamma_{IJ}^K \right) \\
\gamma_{IJ}^{KL} &= B^{(K} \gamma_{IJ)}^L \\
\gamma_A^B &= P_J^B (T_A \lambda)^J \\
U_J^I &= \delta_J^I + \partial_J B^I + \frac{1}{2} P_I^A (T_A \lambda^J)
\end{aligned} \tag{A.5}$$

Useful functions of the sources

$$\begin{aligned}
\Lambda^I &= \left( U^{-1} \right)_J^I \left( \nabla^2 \lambda^J + \frac{1}{6} B^J R \right) \\
\Pi^{IJ} &= \nabla_\mu \lambda^I \nabla^\mu \lambda^J - B^{(I} \Lambda^{J)} \\
\Pi^a &= m^a - \eta^a \frac{R}{6} - \frac{1}{2} \theta_I^a \Lambda^I \\
\Gamma^{\mu\nu} &= G^{\mu\nu} + \frac{R}{6} g^{\mu\nu} \\
\Omega^{IJK} &= \left( \Pi^{IJ} + \frac{1}{2} B^{(I} \Lambda^{J)} \right) \Lambda^K \\
\Xi_\sigma^{IJ} &= \Lambda^I \left( 2 \nabla_\mu \sigma \nabla^\mu \lambda^J - \sigma \gamma_{KL}^J \Pi^{KL} \right) .
\end{aligned} \tag{A.6}$$

### A.1.2 Lie derivatives

We use  $\mathcal{L}$  to denote a Lie derivative along a direction in parameter space defined by the RG flow. This derivative satisfies the following definitions and relations:

$$\begin{aligned}
\mathcal{L}[Y] &= B^I \partial_I Y \\
\mathcal{L}[Y_I^J] &= B^K \partial_K Y_I^J + \gamma_I^K Y_K^J - \gamma_K^J Y_I^K \\
\mathcal{L}[Y_{AI}] &= B^J \partial_J Y_{AI} + \gamma_I^J Y_{AJ} + \gamma_A^B Y_{BI} \\
B^I \mathcal{L}[Y_{IJ\dots}] &= \mathcal{L}[B^I Y_{IJ\dots}] \\
(T_B \lambda)^I \mathcal{L}[Y_{AI\dots}] &= \mathcal{L}[(T_B \lambda)^I Y_{AI\dots}] \\
\mathcal{L}[U_J^I] &= \gamma_{KL}^I B^K U_J^L \\
\mathcal{L}[\tilde{B}^I] &= -\gamma_{JK}^I B^J \tilde{B}^K
\end{aligned} \tag{A.7}$$

where  $Y_{\dots}$  stands for an arbitrary covariant function of  $\lambda^I$ , and  $U_J^I$  is defined in (A.5).

### A.1.3 Gravitational terms and their Weyl variations

$$\begin{aligned}
W^2 &= R^{\mu\nu\rho\sigma} R_{\mu\nu\rho\sigma} - 2R^{\mu\nu} R_{\mu\nu} + \frac{1}{3}R^2 \\
E_4 &= R^{\mu\nu\rho\sigma} R_{\mu\nu\rho\sigma} - 4R^{\mu\nu} R_{\mu\nu} + R^2 \\
G_{\mu\nu} &= R_{\mu\nu} - \frac{1}{2}g_{\mu\nu}R
\end{aligned} \tag{A.8}$$

$$\begin{aligned}
\Delta_\sigma^g g^{\mu\nu} &= 2\sigma g^{\mu\nu} \\
\Delta_\sigma^g \sqrt{-g} &= -4\sigma \sqrt{-g} \\
\Delta_\sigma^g \nabla_\mu \nabla_\nu f &= 2\partial_{(\mu} \sigma \partial_{\nu)} f - g_{\mu\nu} \partial^\rho \sigma \partial_\rho f \\
\Delta_\sigma^g \nabla^2 f &= 2\sigma \nabla^2 f - 2\partial_\mu \sigma \partial^\mu f \\
\Delta_\sigma^g R &= 2\sigma R + 6\nabla^2 \sigma \\
\Delta_\sigma^g G_{\mu\nu} &= 2\nabla_{(\mu} \nabla_{\nu)} \sigma - 2g_{\mu\nu} \nabla^2 \sigma \\
\Delta_\sigma^g \sqrt{-g} W^2 &= 0 \\
\Delta_\sigma^g \sqrt{-g} E_4 &= -8\sqrt{-g} G^{\mu\nu} \nabla_\mu \nabla_\nu \sigma
\end{aligned} \tag{A.9}$$

### A.1.4 Weyl Variations of dimensionful functions of the sources

$$\begin{aligned}
\Delta_\sigma (Y_I \Lambda^I) &= \sigma (2Y_I \Lambda^I - \mathcal{L}[Y_I] \Lambda^I - Y_I \gamma_{JK}^I \Pi^{JK}) - 2\nabla_\mu \sigma (Y_I \nabla^\mu \lambda^I) \\
\Delta_\sigma (Y_{IJ} \Pi^{IJ}) &= \sigma (2Y_{IJ} \Pi^{IJ} - \mathcal{L}[Y_{IJ}] \Pi^{IJ} + Y_{IJ} \gamma_{KL}^{IJ} \Pi^{KL}) \\
\Delta_\sigma (Y_a \Pi^a) &= \sigma (2Y_a \Pi^a - \mathcal{L}[Y_a] \Pi^a + \gamma_{IJ}^a \Pi^{IJ}) \\
\Delta_\sigma (Y_A F_{\mu\nu}^A) &= \sigma (-\mathcal{L}[Y_A] F_{\mu\nu}^A - 2Y_A \partial_{[J} P_{I]}^A \nabla_\mu \lambda^J \nabla_\nu \lambda^I) - \nabla_{[\mu} \sigma (2Y_A P_I^A \nabla_{\nu]} \lambda^I) \\
\Delta_\sigma (Y_{IJK} \Omega^{IJK}) &= \sigma (4Y_{IJK} \Omega^{IJK} - \mathcal{L}[Y_{IJK}] \Omega^{IJK} + Y_{IJK} \gamma_{MN}^{IJK} \Pi^{IJ} \Pi^{MN}) \\
&\quad + \nabla_\mu \sigma (-2Y_{IJK} \nabla_\nu \lambda^I \nabla^\nu \lambda^J \nabla^\mu \lambda^K) - B^I Y_{I[JK]} \Xi_\sigma^{JK}
\end{aligned} \tag{A.10}$$

where the  $Y$ 's are arbitrary covariant functions of  $\lambda^I$ .

## A.2 Weyl symmetry in a regulated theory

In this appendix we shall give more details concerning the local CS equation. In particular we shall outline its derivation in dimensional regularization in weakly coupled 4D field theory and explicitly derive the structure of the anomaly and its consistency condition in 2D field theory.

First of all we want to explain how to find the Weyl transformation for the sources  $\mathcal{J}$ . An explicit way to do that is by a variant of the dilaton trick [25]. In order to see how that works, let us focus for the moment on a classical bare action  $S^{(1)}[\Phi, g_{\mu\nu}, \mathcal{I}_0]$ , where  $\mathcal{I}_0$  indicates the general set of bare sources, the metric excluded, that can couple to non-trivial local functions of  $\Phi$  and of its derivatives. In the case of a theory regulated with a momentum cut-off such as

## Appendix A. Local CS equation in $d = 4$

---

Pauli-Villars one should add to the set  $\mathcal{I}_0$  also the regulator mass  $\Lambda$ . Now, the trick is to write the metric in a redundant way by introducing a dilaton field  $\tau$ :  $S^{(1)} \equiv S^{(1)}[\Phi, e^{2\tau} g_{\mu\nu}, \mathcal{I}_0]$ . The action so written is trivially invariant under a Weyl transformation under which  $\tau \rightarrow \tau + \sigma$ ,  $g_{\mu\nu} \rightarrow g_{\mu\nu} e^{-2\sigma}$ , while  $\Phi, \mathcal{I}_0$  (and the regulator mass) do not transform. Now, if, and only if,  $\mathcal{I}_0$  includes *all* the sources that can couple to the fields  $\Phi$ , we can certainly absorb  $\tau$  in the fields and in the sources (and regulator if needed):  $S^{(1)}[\Phi, e^{2\tau} g_{\mu\nu}, \mathcal{I}_0] = S^{(1)}[\Phi^\tau, g_{\mu\nu}, \mathcal{I}_0^\tau]$ . Now, the redefined fields and sources, via their  $\tau$  dependence, transform in a definite way under Weyl so as to compensate the transformation of the metric, and ensure formal invariance of the action. That is most easily understood by working around  $\tau = 0$  which gives

$$\delta_\sigma \mathcal{I}_0 \equiv \mathcal{I}_0^\sigma - \mathcal{I}_0. \quad (\text{A.11})$$

The situation is particularly neat when dimensional regularization (DR) can be used. In DR, the regulator itself is Weyl invariant and only the bare sources transform non-trivially. On the other hand, in the case of a momentum regulator, such as Pauli-Villars, things are a bit more involved as one must also consider a  $\tau$  dependent, and consequent Weyl transforming, regulator mass:  $\delta_\sigma \Lambda = \sigma \Lambda$ . An obvious generalization of RG invariance then ensures that the combination of the transformation in Eq. (A.11) together with  $\delta_\sigma \Lambda = \sigma \Lambda$  has the same effect on the partition function as a certain transformation  $\delta_\sigma \mathcal{I}$  of the renormalized sources  $\mathcal{I}$ . The latter combined with  $\delta_\sigma g_{\mu\nu} = -2\sigma g_{\mu\nu}$ , defines the transformation of renormalized sources  $\mathcal{J}$ . According to the discussion at the end of section 2.2.1, the local Callan Symanzik equation then follows.

Consider now a 4D renormalizable field theory based on a gauge group  $G$ , and involving scalars and fermion transforming in a representation of  $G$ . In addition to the metric  $g_{\mu\nu}$ , the set of sources  $\mathcal{J}$  consists of

- the marginal couplings  $\lambda^I \equiv$  gauge, Yukawa and scalar quartic couplings
- the gauge fields  $A_\mu^A$  of the flavor symmetry group  $G_F$  of the kinetic term; this symmetry is in general broken by the Yukawa and quartic couplings<sup>1</sup>.
- mass terms  $m^a$  for the scalar bilinears.

The general relation between the bare and the renormalized sources is obtained by considering all the terms allowed by symmetry and power counting

$$\begin{aligned} \lambda_0^I(x) &= \mu^{k^I \epsilon} \left( \lambda^I(x, \mu) + L^I \right) \\ A_{0\mu}^A(x) &= A_\mu^A(x, \mu) + N_I^A \nabla_\mu \lambda^I \\ m_0^a(x) &= \left( (\delta_b^a + Z_b^a) m^b(x, \mu) + Z^a R(g) + Z_I^a \nabla^2 \lambda^I + Z_{IJ}^a \nabla_\mu \lambda^I \nabla^\mu \lambda^J \right) \end{aligned} \quad (\text{A.12})$$

where  $L^I, N_I^A, Z_b^a, Z^a, Z_I^a, Z_{IJ}^a$  are series of poles in  $\epsilon$  whose coefficients are polynomial series in  $\lambda$ . The coefficients  $k^I$  (understood not to be part of the summation convention) correspond

---

<sup>1</sup>As we assume our theory respects parity we just need to focus on the maximal vector-like subgroup of  $G_F$ .

---

## A.2. Weyl symmetry in a regulated theory

to the dimensionality of the bare couplings in  $4+\epsilon$ . The  $k^I$  equal  $-1$ ,  $-1$ ,  $-1/2$  for respectively gauge, scalar quartic and Yukawa couplings. Notice that the dimensionality of  $A_{0\mu}^A$  and  $m_0^a$  is not affected by dimensional continuation. Notice also that the bare and the renormalized metric can be taken to coincide. The effective action is renormalized by adding the most general set of diffeomorphism invariant counterterms: these can be absorbed in redefinitions of the fields and sources in Eq. (A.12), with no need to redefine  $g_{\mu\nu}$ . By inspection of the most general dimensionally continued bare action  $S^{(1)}$ , the Weyl transformation of the bare sources is simply given by

$$(g^{\mu\nu}, \lambda_0^I, A_{0\mu}^A, m_0^a) \longrightarrow (e^{2\sigma} g^{\mu\nu}, e^{k_I \epsilon \sigma} \lambda_0^I, A_{0\mu}^A, e^{2\sigma} m_0^a) \quad (\text{A.13})$$

By Eq. (A.12) this can be univocally translated into the, generally more involved, transformation law for the renormalized sources

$$\delta_\sigma \mathcal{J} \equiv (2\sigma g^{\mu\nu}, \delta_\sigma \lambda^I, \delta_\sigma A_\mu^A, \delta_\sigma m^a). \quad (\text{A.14})$$

In practice, the first of Eqs. (A.12) fixes  $\delta_\sigma \lambda^I$ , and once that is fixed the second equation fixes  $\delta_\sigma A_\mu^A$ . Finally, once all other transformations are fixed, the third equation can be used to deduce  $\delta_\sigma m^a$ . By applying the logic described in section 2.2.1, we thus conclude the renormalized action must satisfy an equation of the form

$$\int d^D x \left( \delta_\sigma \mathcal{J} \frac{\delta}{\delta \mathcal{J}} \right) \mathcal{W} = \int d^D x \delta_\sigma S^{(2)}[\mathcal{J}] \equiv \int d^D x \mathcal{A}_\sigma \quad (\text{A.15})$$

By this equation, given the finiteness of  $g^{\mu\nu} \frac{\delta}{\delta g^{\mu\nu}} \mathcal{W}$  and the finiteness of derivatives with respect to the renormalized sources, one deduces that  $(\delta_\sigma \lambda^I, \delta_\sigma A_\mu^A, \delta_\sigma m^a)$  and  $\mathcal{A}(x)$  must also be finite. In other words: given  $T$  is finite, then the coefficients of its expansion in terms of renormalized operators must be finite, along with the contact terms associated with the anomaly. The condition of  $T$  finiteness is at the basis of the derivation of consistency conditions given in ref. [32]. Finiteness then allows us to safely take the  $n \rightarrow 4$  limit in the above equation. This is the formal derivation of the local CS equation. In the following sections we shall describe in detail the structure of  $(\delta_\sigma \lambda^I, \delta_\sigma A_\mu^A, \delta_\sigma m^a)$ .

### A.2.1 The variation of $\lambda^I$

$\delta_\sigma \lambda^I$  can be found using the following manipulation

$$\begin{aligned} e^{\sigma \epsilon k^I} \lambda_0^I(x) &= e^{\sigma \epsilon k^I} \mu^{k^I \epsilon} \left( \lambda^I(x, \mu) + L^I(\lambda(x, \mu), \epsilon) \right) \\ &= \mu^{k^I \epsilon} \left( \lambda^I(x, e^{-\sigma} \mu) + L^I(\lambda(x, e^{-\sigma} \mu), \epsilon) \right) \end{aligned} \quad (\text{A.16})$$

where we used the  $\mu$  independence of the bare sources. In other words, a Weyl transformation for the bare sources is equivalent to a change in the renormalization scale:

$$\lambda_0^I \rightarrow e^{\sigma \epsilon k^I} \lambda_0^I \quad \Longrightarrow \quad \lambda^I(x, \mu) \rightarrow \lambda^I(x, e^{-\sigma} \mu) \quad (\text{A.17})$$

## Appendix A. Local CS equation in $d = 4$

---

In assigning these transformation properties it was essential that the sources are  $x$  dependent by definition. This can be translated into the following infinitesimal transformation law for the renormalized sources

$$\delta_\sigma \lambda^I(x, \mu) = -\sigma(x) \frac{d}{d \log \mu} \lambda^I(x, \mu) \equiv -\sigma \hat{\beta}^I \quad (\text{A.18})$$

In agreement with the local CS equation.

The last step is to relate the  $\hat{\beta}$ -function to the poles in the counterterm. This is done by using the invariance of the bare parameters under change of renormalization scale:

$$\mu \frac{d\lambda_0}{d\mu} = 0 \Rightarrow \quad \left( \delta_J^I + \partial_J L^I \right) \mu \frac{d\lambda^J}{d\mu} = -\epsilon k^I \left( \lambda^I + L^I \right) \quad (\text{A.19})$$

Using the finiteness of  $\lambda_I$  we find in the  $\epsilon \rightarrow 0$  limit

$$\hat{\beta}^I \rightarrow \beta^I = -k^I L_1^I + k^J \lambda^J \partial_J L_1^I \quad (\text{A.20})$$

### A.2.2 The variation of $A_\mu^A$

Unlike  $\lambda_0^I$ ,  $A_{0\mu}^A$  is invariant under the local scale transformation. Using this in Eq. (A.12) we find

$$\left( \delta_B^A + \left( N_I^A (T_B)^I_J \lambda^J \right) \right) \delta_\sigma A_\mu^B = \sigma \left( \hat{\beta}^J \partial_J N_I^A + N_J^A \partial_I \hat{\beta}^J \right) \nabla_\mu \lambda^I + N_I^A \hat{\beta}^I \nabla_\mu \sigma \quad (\text{A.21})$$

and we can identify the functions  $\rho$  and  $S$  from the local CS equation:

$$\begin{aligned} \left( \delta_B^A + \left( N^A T_B \lambda \right) \right) \rho_I^A &= -\hat{\beta}^J \partial_J N_I^A - N_J^A \partial_I \hat{\beta}^J \\ \left( \delta_B^A + \left( N^A T_B \lambda \right) \right) S^B &= N_I^A \hat{\beta}^I. \end{aligned} \quad (\text{A.22})$$

Focusing on the  $\epsilon$  independent terms in these equations, and using the finiteness of the renormalized sources, we find

$$\begin{aligned} S^A &= -k^I \lambda^I N_{I,1}^A \\ \rho_I^A &= k^J \left( \lambda^J \partial_J N_{I,1}^A + N_{I,1}^A \right) \\ P_I^A &= k^J \lambda^J \left( \partial_J N_{I,1}^A - \partial_I N_{J,1}^A \right) \end{aligned} \quad (\text{A.23})$$

where  $L_{I,1}^I$  and  $N_{I,1}^A$  are the coefficients of the simple poles in  $L^I$  and  $N_I^A$ .

Let us now derive the consistency condition  $B \cdot P = 0$ . First, we multiply the first line of (A.22) by  $\hat{B}^I = \hat{\beta}^I - (S^A T_A \lambda)^I$

$$\left( \delta_B^A + \left( N^A T_B \lambda \right) \right) \hat{B}^I \rho_I^A = -\hat{\beta}^I \partial_I \left( N_J^A \hat{\beta}^J \right) + S^B \hat{\beta}^I \partial_I \left( \delta_B^A + N^A T_B \lambda \right) \quad (\text{A.24})$$

where we used the covariance of  $\hat{\beta}$ , namely  $(T\lambda)^I \partial_I \hat{\beta}^J = (T\hat{\beta})^J$ . Next, we substitute the

---

## A.2. Weyl symmetry in a regulated theory

second line of Eq. (A.22) and find

$$\left(\delta_B^A + (N^A T_B \lambda)\right) \left(\hat{B}^I \rho_I^A + \hat{\beta}^I \partial_I S\right) = 0. \quad (\text{A.25})$$

We conclude that

$$\hat{B}^I P_I^A \equiv \hat{B}^I \left(\rho_I^A + \partial_I S^A\right) = 0 \quad (\text{A.26})$$

where we used the covariance of  $S^A$  to show that  $(ST\lambda)^I \partial_I S = 0$  and hence  $\hat{B}^I \partial_I S^A = \hat{\beta}^I \partial_I S^A$ .

### A.2.3 Dim 2 operators

Once the Weyl transformations of  $g^{\mu\nu}$ ,  $\lambda^I$  and  $A_\mu^A$  are fixed the expression for the bare source

$$m_0^a = \left( (\delta_b^a + Z_b^a) m^b(\mu) + Z^a R + Z_I^a \nabla^2 \lambda^I + Z_{IJ}^a \nabla_\mu \lambda^I \nabla^\mu \lambda^J \right), \quad (\text{A.27})$$

as well as its Weyl transformation equation  $m_0^a \rightarrow e^{2\sigma} m_0^a$ , fix the coefficients functions in  $\delta_\sigma m^a$ .

$$\begin{aligned} (2\delta_c^a + Z_c^a) \bar{\gamma}_b^c &= \mathcal{L}[Z_b^a] \\ (2\delta_b^a + Z_b^a) C^b &= \mathcal{L}[Z^a] \\ (2\delta_b^a + Z_b^a) D_I^b &= \mathcal{L}[Z_I^a] \\ (2\delta_b^a + Z_b^a) E_{IJ}^b &= 2Z_K^a \partial_I \partial_J \hat{\beta}^K + 2\mathcal{L}[Z_{IJ}^a] \\ (2\delta_b^a + Z_b^a) \theta_I^b &= -2Z_I^a - 2Z_J^a \partial_I \hat{\beta}^J - 2\hat{\beta}^J Z_{IJ}^a \\ (2\delta_b^a + Z_b^a) \eta^b &= \hat{\beta}^I Z_I^a - 6Z^a \end{aligned} \quad (\text{A.28})$$

(for brevity we have ignored the contributions in the transformation related to global symmetries). From these expressions it is possible to derive the remaining consistency conditions (2.50).

### A.2.4 Consistency conditions for the anomaly coefficients

As an example for the derivation of the consistency conditions for the anomaly coefficients we present the computation for the 2d case where the anomaly is given by (see [26]):

$$\frac{1}{\sqrt{-g}} \mathcal{A}_\sigma = \sigma \left( -\frac{1}{2} \beta_\Phi R + \frac{1}{2} \chi_{IJ} \nabla_\mu \lambda^I \nabla^\mu \lambda^J \right) + \nabla^\mu \sigma \left( w_I \nabla^\mu \lambda^I \right) \quad (\text{A.29})$$

For simplicity we will ignore the contributions from dimensionful sources. The coefficients in this anomaly satisfy the consistency condition

$$\partial_I \beta_\Phi - \chi_{IJ} \beta^J + \mathcal{L}[w_I] = 0 \quad (\text{A.30})$$

## Appendix A. Local CS equation in $d = 4$

---

In dimensional regularization this anomaly can be understood as the result of the non-invariance of the following counterterms in the effective action

$$\mathcal{W} \supset \int d^D y \sqrt{-g} \mu^\epsilon \left( \frac{1}{2} b R + \frac{1}{2} c_{IJ} \nabla_\mu \lambda^I \nabla^\mu \lambda^J \right) \quad (\text{A.31})$$

where  $b$  and  $c_{IJ}$  are understood as a series of poles in  $\epsilon = D - 2$ , where the finite part is assumed to vanish.

Defining the symmetry generator of the regulated theory as

$$\Delta_\sigma = \int d^D x \sigma(x) \left( \frac{\delta}{\delta \tau(x)} - \hat{\beta}^I \frac{\delta}{\delta \lambda^I(x)} \right) \quad (\text{A.32})$$

where  $\hat{\beta}^I = -\epsilon \lambda^I + \beta^I$ , we find

$$\begin{aligned} \Delta_\sigma & \int d^D y \sqrt{-g} \mu^\epsilon \left( \frac{1}{2} b R + \frac{1}{2} c_{IJ} \nabla_\mu \lambda^I \nabla^\mu \lambda^J \right) \\ & = \int \sqrt{-g} d^D x \left( \sigma \left( -\frac{1}{2} \hat{\beta}_\Phi + \frac{1}{2} \hat{\chi}_{IJ} \nabla_\mu \lambda^I \nabla^\mu \lambda^J \right) + \nabla_\mu \sigma \left( \hat{w}_I \nabla^\mu \lambda^I \right) \right) \end{aligned} \quad (\text{A.33})$$

where

$$\begin{aligned} \hat{\beta}_\Phi & = \hat{\beta}^K \partial_K b - \epsilon b \\ \hat{\chi}_{IJ} & = -\mathcal{L}_{\hat{\beta}}[c_{IJ}] + \epsilon c_{IJ} \\ \hat{w}_I & = -(1 + \epsilon) \partial_I b - c_{IJ} \hat{\beta}^J. \end{aligned} \quad (\text{A.34})$$

The finiteness of  $T$  ensures that these specific combinations are necessarily finite. In other words, in the  $\epsilon = 0$  limit we find  $\hat{\beta}_\Phi \rightarrow \beta_\Phi$ ,  $\hat{\chi}_{IJ} \rightarrow \chi_{IJ}$  and  $\hat{w}_I \rightarrow w_I$ . Moreover, these coefficients satisfy the relation

$$\partial_I \hat{\beta}_\Phi - \hat{\chi}_{IJ} \hat{\beta}^J + \mathcal{L}_{\hat{\beta}}[\hat{w}_I] = \epsilon \left( -\partial_I \hat{\beta}_\Phi + \hat{w}_I \right) \quad (\text{A.35})$$

which, in the  $\epsilon = 0$  limit, gives Eq. (A.30).

### A.3 Unitarity and anomalous dimensions of currents

In this appendix we would like to study in more detail the scale and conformal transformations of the operators, Eq. (2.31), at a conformal fixed point. In particular, we would like to distinguish the primary scalar operators from the descendants of the non-conserved currents. Let us suppose the background couplings  $\lambda^I$  break the flavor group  $G_F$  down to a subgroup  $H$ . Let us to parametrize the coset  $G_F/H$  with indices  $A = 1, \dots, m$ , while the remaining indices  $A = m + 1, \dots, \dim_{G_F}$  parametrize the generators of  $H$ . Using the notation  $v_A^I \equiv (T_A \lambda^I)$ , we thus have that for  $A = 1, \dots, m$ ,  $v_A^I \neq 0$  are  $m$  linearly independent vectors, while  $v_A^I = 0$  for



### A.3. Unitarity and anomalous dimensions of currents

$A > m$ . In block matrix notation we can write

$$v = \begin{pmatrix} \hat{v} & a \\ 0 & 0 \end{pmatrix} \quad (\text{A.36})$$

where  $\hat{v}$  is a  $m \times m$  matrix. The rows of  $v$  run over the indices  $A$ , while its columns run over the indices  $I = 1, \dots, N$ :  $v$  is a rectangular  $\dim_{G_F} \times N$  matrix. Since  $v_A^I$  are  $m$  linearly-independent vectors,  $\hat{v}$  can be taken invertible by a proper linear transformation in  $I$ -space.

The anomalous dimension matrix for  $J_A^\mu$  is:

$$\gamma_A^B = v_A^I P_I^B. \quad (\text{A.37})$$

By the properties of unitary representation of the conformal group it must vanish for the conserved currents and take the form

$$\gamma = \begin{pmatrix} \hat{\gamma} & 0 \\ 0 & 0 \end{pmatrix} \quad (\text{A.38})$$

with  $\hat{\gamma}$  a diagonal and strictly positive definite (thus invertible) matrix acting on the subspace of broken generators. Now, using Eqs. (A.36-A.38)  $P$  is constrained to have the form

$$P = \begin{pmatrix} \hat{v}^{-1}(\hat{\gamma} - ab) & -\hat{v}^{-1}ap \\ b & p \end{pmatrix} \quad (\text{A.39})$$

with  $b$  an  $(N - m) \times m$  matrix and  $p$  is an  $(N - m) \times (\dim_{G_F} - m)$  matrix. Notice that  $P$  is a transposed rectangular matrix with respect to  $v$ : rows run over  $I$  and columns over  $A$ . We can now go to a basis in  $I$  space such that  $v$  and  $P$  are block-diagonal:

$$v \rightarrow v' = vS^{-1} = \begin{pmatrix} 1 & 0 \\ 0 & 0 \end{pmatrix} \quad (\text{A.40})$$

$$P \rightarrow P' = SP = \begin{pmatrix} \hat{\gamma} & 0 \\ 0 & p \end{pmatrix} \quad (\text{A.41})$$

$$S = \begin{pmatrix} \hat{v} & a \\ -b\hat{\gamma}^{-1}\hat{v} & (1 - b\hat{\gamma}^{-1}a) \end{pmatrix} \quad (\text{A.42})$$

In the new basis, by Eq. (2.33) the operators  $\mathcal{O}_I$ ,  $I = 1, \dots, m$  are the descendants of the broken currents  $J_A^\mu$ ,  $A = 1, \dots, m$ . On the broken generator subspace  $P$  equals the anomalous dimension matrix  $\hat{\gamma}$ . Correspondingly Eq. (2.31) gives, as expected,  $K^\mu \mathcal{O}_\alpha = -\hat{\gamma}_\alpha^\beta J_\beta^\mu$  for  $\alpha, \beta = 1, \dots, m$ . However, as long as  $p \neq 0$ , Eq. (2.31) also implies  $K^\mu \mathcal{O}_I = \sum_{A>m} p_i^A J_A^\mu \neq 0$  for the supposedly primary operators described by  $I > m$  (notice the sum is over the conserved currents). We thus expect  $p$  should vanish. The proof comes by using unitarity as follows.

## Appendix A. Local CS equation in $d = 4$

---

Let us consider the 2-point correlator of a scalar field and an unbroken current:

$$\langle J_A^\mu(p) O_I(-p) \rangle = f(p^2) p^\mu \quad (\text{A.43})$$

The conservation of the current  $p_\mu J_A^\mu(p)$  implies  $f(p^2) p^2 = 0$ , thus  $f(p^2) = 0$ .

$$\langle J_A^\mu(x) O_I(0) \rangle = 0 \quad (\text{A.44})$$

If we act with a conformal transformation:

$$0 = \langle [K^\nu, J_A^\mu(x)] O_I(0) \rangle + \langle J_A^\mu(x) [K^\nu, O_I(0)] \rangle = p_I^B \langle J_A^\mu(x) J_B^\nu(0) \rangle \quad (\text{A.45})$$

where the  $B$  runs only over the non-conserved currents, since otherwise the 2-point function vanishes. In a unitary theory  $\langle J_A^\mu(x) J_B^\nu(0) \rangle$  is invertible, thus  $p_I^B = 0$ .

### A.4 The consistency conditions for the Weyl anomaly

The most general parameterization of the Weyl anomaly given in Eq. (2.63) can be reduced by a change of scheme. More specifically, the terms proportional to  $d$ ,  $U_I$ ,  $V_{IJ}$ ,  $\tilde{S}_{(IJ)}$ ,  $T_{IJK}$ ,  $k_a$ , and  $j_{aI}$  can be eliminated by adding to the generating functional  $\mathcal{W}$  a local functional

$$\mathcal{F}_{\nabla^2 R} = \int d^4x \sqrt{g} \mathcal{L}_{\nabla^2 R} \quad (\text{A.46})$$

with

$$\begin{aligned} \mathcal{L}_{\nabla^2 R} = & \left( d + \frac{1}{2} B^I U_I \right) \frac{R^2}{36} + U_I \frac{R}{6} \nabla^2 \lambda^I + \frac{1}{2} V_{IJ} \frac{R}{6} \nabla_\mu \lambda^I \nabla^\mu \lambda^J + \hat{m}^a k_a \frac{R}{6} \\ & + \frac{1}{4} T_{IJK} \Pi^{IJ} \Lambda^K + \frac{1}{2} j_{aI} \Pi^a \Lambda^I + \frac{1}{4} \left( \tilde{S}_{(IJ)} + \frac{1}{2} T_{IJK} B^K + \frac{1}{2} j_{aI} \theta_J^a \right) \Lambda^I \Lambda^J \end{aligned} \quad (\text{A.47})$$

In addition to eliminating the mentioned terms, this operation also changes the remaining anomaly coefficients (the specific expressions are not particularly illuminating). In the following equations we assume that all the coefficients are given in the scheme where these terms are indeed vanishing.

A key observation is that in this scheme the consistency conditions can be written as algebraic constraints. Here we list the equations, and the terms in the l.h.s. of (2.60) to which they are related:

#### A.4. The consistency conditions for the Weyl anomaly

$$\begin{aligned}
\sigma_{[1}\nabla_{\mu}\sigma_{2]}\nabla^{\mu}R &: \beta_c = -\frac{1}{4}\chi_I^e B^I \\
\sigma_{[1}\nabla_{\mu}\sigma_{2]}\nabla^{\mu}\nabla^2\lambda^I &: \chi_I^e = -\frac{1}{2}\chi_{IJ}^a B^J \\
\nabla^2\sigma_{[1}\nabla_{\mu}\sigma_{2]}\nabla^{\mu}\lambda^I &: Y_I - \chi_I^e = -\frac{1}{2}\tilde{S}_{[IJ]}B^J \\
\sigma_{[1}\nabla^2\sigma_{2]}\nabla_{\mu}\lambda^I\nabla^{\mu}\lambda^J &: \chi_{IJ}^f = \frac{1}{2}\chi_{IJ}^g + \frac{1}{2}\chi_{IJK}^b B^K - \partial_{(J}(\chi_{I)K}^a B^K) \\
\sigma_{[1}\nabla^2\sigma_{2]}\hat{m}^a &: q_a = \frac{1}{2}r_{aI}B^I \\
\sigma_{[1}\nabla_{\mu}\sigma_{2]}\nabla^{\mu}\lambda^I\hat{m}^a &: r_{aJ}U_I^J = -\frac{1}{2}s_{aIJ}B^J - \frac{1}{2}p_{ab}\theta_I^b \\
\sigma_{[1}\nabla_{\mu}\sigma_{2]}\nabla^{\mu}\lambda^{(I}\Lambda^{J)} &: \chi_{KL}^a U_I^K U_J^L = \frac{1}{4}p_{ab}\theta_I^a\theta_J^b + \frac{1}{2}s_{a(JK}\theta_I^a)B^K \\
&\quad -\frac{1}{2}B^K\chi_{K(IL}U_J^L) - \frac{1}{2}\chi_{(IK}^g U_J^K) \\
\sigma_{[1}\nabla_{\mu}\sigma_{2]}\nabla^{\mu}\lambda^K\nabla_{\nu}\lambda^I\nabla^{\nu}\lambda^J &: \chi_{IJL}^B U_K^L = -\frac{1}{2}s_{aIJ}\theta_K^a + \bar{\chi}_{IJK}^g - \chi_{IJKL}^c B^L + \tilde{S}_{[KM]}\gamma_{IJ}^M \\
&\quad -\frac{1}{2}(\zeta_{AJK}P_I^A + \zeta_{AIK}P_J^A) - (\eta_{AJ}\partial_{[K}P_{I]}^A + \eta_{AI}\partial_{[K}P_{J]}^A) \\
\nabla_{\mu}\sigma_{[1}\nabla_{\nu}\sigma_{2]}\nabla^{\mu}\lambda^I\nabla^{\nu}\lambda^J &: \tilde{S}_{[IJ]} = \partial_{[J}w_{I]} + \eta_{A[J}P_{I]}^A \tag{A.48}
\end{aligned}$$

The three non-trivial consistency conditions and the corresponding terms in the commutator are

$$\begin{aligned}
\sigma_{[1}\nabla_{\mu}\sigma_{2]}G^{\mu\nu}\nabla_{\nu}\lambda^I &: \mathcal{L}[w_I] = -8\partial_I\beta_b + \chi_{IJ}^g B^J \\
\sigma_{[1}\nabla^{\mu}\sigma_{2]}F_{\mu\nu}^A\nabla^{\nu}\lambda^I &: \mathcal{L}[\eta_{AI}] = \kappa_{AB}P_I^B + \zeta_{AIJ}B^J - \chi_{IJ}^g(T_A\lambda)^J \\
\nabla^{\mu}\sigma_{[1}\nabla^{\nu}\sigma_{2]}F_{\mu\nu}^A &: \eta_{AI}B^I = -w_I(T_A\lambda)^I
\end{aligned}$$

The coefficient of the last term in the commutator,  $\sigma_{[1}\nabla_{\mu}\sigma_{2]}\nabla^{\mu}\lambda^{[I}\Lambda^{J]}$ , vanishes by imposing the three unresolved consistency conditions, without introducing new constraints.

The anomaly coefficients appearing in 2.2.3 are related to the ones appearing in the original formulation of the anomaly via

$$\begin{aligned}
a &= \beta_b, \quad c = -\beta_a, \\
b_{ab} &= p_{ab} \\
b_{aIJ} &= s_{aIJ} - j_{aK}\gamma_{IJ}^K, \\
b_{IJKL} &= \chi_{IJKL}^c - \frac{1}{2}T_{IJM}\gamma_{KL}^M - \frac{1}{2}T_{KLM}\gamma_{IJ}^M. \tag{A.49}
\end{aligned}$$



# Appendix B

## Local CS equation in $d = 6$

### B.1 Derivation of the consistency conditions

In this work, in order to derive the consistency conditions it was necessary to write the variation (2.64) in a linearly independent basis. This was technically nontrivial due to the large number of terms ( $\sim O(100)$ ) and redundancies related to integration by parts. Our approach is outlined in this appendix. First, by integrating by parts, we took all the derivatives off either  $\sigma$  or  $\sigma'$ . As a result, we ended up with terms such as

$$(\sigma \partial_\mu \sigma' - \sigma' \partial_\mu \sigma) f_I(\lambda) \partial^\mu \lambda^I R^2, \quad (\sigma \nabla_\mu \partial_\nu \sigma' - \sigma' \nabla_\mu \partial_\nu \sigma) f(\lambda) H_1^{\mu\nu}. \quad (\text{B.1})$$

However, there are still redundancies related to anti-symmetrization with respect to  $\sigma, \sigma'$ . For example, consider the trivial equation

$$(\partial_\mu \sigma \partial_\nu \sigma' - \partial_\mu \sigma' \partial_\nu \sigma) f(\lambda) H_1^{\mu\nu} = 0, \quad (\text{B.2})$$

where  $H_1^{\mu\nu}$  is symmetric. Upon integrating by parts and writing this equation in the same basis as (B.1), we get

$$(\sigma \nabla_\mu \partial_\nu \sigma' - \sigma' \nabla_\mu \partial_\nu \sigma) f(\lambda) H_1^{\mu\nu} + (\sigma \partial_\nu \sigma' - \sigma' \partial_\nu \sigma) \partial_I f(\lambda) \partial_\mu \lambda^I H_1^{\mu\nu} = 0, \quad (\text{B.3})$$

since  $\nabla_\mu H_1^{\mu\nu} = 0$  in this example. This allows to eliminate the second term in (B.1). Similarly one can get rid of all the terms with an even number of derivatives on  $\sigma, \sigma'$ . This prescription fixes unambiguously a complete basis for (2.64).

### B.2 Conventions and basis for the anomaly

We define the Riemann tensor via

$$[\nabla_\mu, \nabla_\nu] A^\rho = R^\rho_{\sigma\mu\nu} A^\sigma, \quad (\text{B.4})$$

## Appendix B. Local CS equation in $d = 6$

and the Ricci tensor and Ricci scalar as  $R_{\mu\nu} = R^\rho{}_{\mu\rho\nu}$  and  $R = g^{\mu\nu}R_{\mu\nu}$ . The Einstein tensor is defined in  $d \geq 2$  by

$$G_{\mu\nu} = \frac{2}{d-2}(R_{\mu\nu} - \frac{1}{2}g_{\mu\nu}R), \quad (\text{B.5})$$

while the Weyl tensor is defined in  $d \geq 3$  by

$$W_{\mu\nu\rho\sigma} = R_{\mu\nu\rho\sigma} + \frac{2}{d-2}(g_{\mu[\sigma}R_{\rho]\nu} + g_{\nu[\rho}R_{\sigma]\mu}) + \frac{2}{(d-1)(d-2)}g_{\mu[\rho}g_{\sigma]\nu}R. \quad (\text{B.6})$$

At dimension four we consider the tensors

$$\begin{aligned} E_4 &= \frac{2}{(d-2)(d-3)}(R^{\mu\nu\rho\sigma}R_{\mu\nu\rho\sigma} - 4R^{\mu\nu}R_{\mu\nu} + R^2), & I &= W^{\mu\nu\rho\sigma}W_{\mu\nu\rho\sigma}, \\ H_{1\mu\nu} &= \frac{(d-2)(d-3)}{2}E_4g_{\mu\nu} - 4(d-1)H_{2\mu\nu} + 8H_{3\mu\nu} + 8H_{4\mu\nu} - 4R^{\rho\sigma\tau}{}_{\mu}R_{\rho\sigma\tau\nu}, \\ H_{2\mu\nu} &= \frac{1}{d-1}RR_{\mu\nu}, & H_{3\mu\nu} &= R_{\mu}{}^{\rho}R_{\rho\nu}, & H_{4\mu\nu} &= R^{\rho\sigma}R_{\rho\mu\sigma\nu}, \\ H_{5\mu\nu} &= \nabla^2R_{\mu\nu}, & H_{6\mu\nu} &= \frac{1}{d-1}\nabla_{\mu}\partial_{\nu}R. \end{aligned} \quad (\text{B.7})$$

A complete basis of scalar dimension-six curvature terms consists of [72]

$$\begin{aligned} K_1 &= R^3, & K_2 &= RR^{\mu\nu}R_{\mu\nu}, & K_3 &= RR^{\mu\nu\rho\sigma}R_{\mu\nu\rho\sigma}, & K_4 &= R^{\mu\nu}R_{\nu\rho}R_{\mu}{}^{\rho}, \\ K_5 &= R^{\mu\nu}R^{\rho\sigma}R_{\mu\rho\sigma\nu}, & K_6 &= R^{\mu\nu}R_{\mu\rho\sigma\tau}R_{\nu}{}^{\rho\sigma\tau}, & K_7 &= R^{\mu\nu\rho\sigma}R_{\rho\sigma\tau\omega}R^{\tau\omega}{}_{\mu\nu}, \\ K_8 &= R^{\mu\nu\rho\sigma}R_{\tau\nu\rho\omega}R_{\mu}{}^{\tau\omega}{}_{\sigma}, & K_9 &= R\nabla^2R, & K_{10} &= R^{\mu\nu}\nabla^2R_{\mu\nu}, & K_{11} &= R^{\mu\nu\rho\sigma}\nabla^2R_{\mu\nu\rho\sigma}, \\ K_{12} &= R^{\mu\nu}\nabla_{\mu}\partial_{\nu}R, & K_{13} &= \nabla^{\mu}R^{\nu\rho}\nabla_{\mu}R_{\nu\rho}, & K_{14} &= \nabla^{\mu}R^{\nu\rho}\nabla_{\nu}R_{\mu\rho}, \\ K_{15} &= \nabla^{\mu}R^{\nu\rho\sigma\tau}\nabla_{\mu}R_{\nu\rho\sigma\tau}, & K_{16} &= \nabla^2R^2, & K_{17} &= (\nabla^2)^2R. \end{aligned} \quad (\text{B.8})$$

In  $d = 6$  a convenient basis is given by

$$\begin{aligned} I_1 &= \frac{19}{800}K_1 - \frac{57}{160}K_2 + \frac{3}{40}K_3 + \frac{7}{16}K_4 - \frac{9}{8}K_5 - \frac{3}{4}K_6 + K_8, \\ I_2 &= \frac{9}{200}K_1 - \frac{27}{40}K_2 + \frac{3}{10}K_3 + \frac{5}{4}K_4 - \frac{3}{2}K_5 - 3K_6 + K_7, \\ I_3 &= -\frac{11}{50}K_1 + \frac{27}{10}K_2 - \frac{6}{5}K_3 - K_4 + 6K_5 + 2K_7 - 8K_8 \\ &\quad + \frac{3}{5}K_9 - 6K_{10} + 6K_{11} + 3K_{13} - 6K_{14} + 3K_{15}, \\ E_6 &= K_1 - 12K_2 + 3K_3 + 16K_4 - 24K_5 - 24K_6 + 4K_7 + 8K_8, \\ J_1 &= 6K_6 - 3K_7 + 12K_8 + K_{10} - 7K_{11} - 11K_{13} + 12K_{14} - 4K_{15}, \\ J_2 &= -\frac{1}{5}K_9 + K_{10} + \frac{2}{5}K_{12} + K_{13}, & J_3 &= K_4 + K_5 - \frac{3}{20}K_9 + \frac{4}{5}K_{12} + K_{14}, \\ J_4 &= -\frac{1}{5}K_9 + K_{11} + \frac{2}{5}K_{12} + K_{15}, & J_5 &= K_{16}, & J_6 &= K_{17}, \\ L_1 &= -\frac{1}{30}K_1 + \frac{1}{4}K_2 - K_6, & L_2 &= -\frac{1}{100}K_1 + \frac{1}{20}K_2, \\ L_3 &= -\frac{37}{6000}K_1 + \frac{7}{150}K_2 - \frac{1}{75}K_3 + \frac{1}{10}K_5 + \frac{1}{15}K_6, & L_4 &= -\frac{1}{150}K_1 + \frac{1}{20}K_3, \\ L_5 &= \frac{1}{30}K_1, & L_6 &= -\frac{1}{300}K_1 + \frac{1}{20}K_9, & L_7 &= K_{15}, \end{aligned} \quad (\text{B.9})$$

where the first three transform covariantly under Weyl variations, and  $E_6$  is the Euler term in  $d = 6$ . The  $J$ 's are trivial anomalies in a six-dimensional CFT defined in curved space, and the first six  $L$ 's are constructed based on the relation  $\delta_{\sigma} \int d^6x \sqrt{-g} L_{1,\dots,6} = \int d^6x \sqrt{-g} \sigma J_{1,\dots,6}$ .

In six space-time dimensions there are ninety four independent terms that can contribute to

## B.2. Conventions and basis for the anomaly

the anomaly [71]. In general, we can write

$$\int d^6x \sqrt{-g} \mathcal{A}_\sigma = \sum_{p=1}^{65} \int d^6x \sqrt{-g} \sigma \mathcal{T}_p + \sum_{q=1}^{30} \int d^6x \sqrt{-g} \partial_\mu \sigma \mathcal{Z}_q^\mu, \quad (\text{B.10})$$

where  $\mathcal{T}_p$  and  $\mathcal{Z}_q^\mu$  are dimension-six and dimension-five terms respectively, that can involve curvatures as well as derivatives on the couplings  $\lambda^I$ . In writing down the various terms below, we neglect total derivatives.

If only curvatures are included, then we have the terms

$$\mathcal{T}_1 = -c_1 I_1, \quad \mathcal{T}_2 = -c_2 I_2, \quad \mathcal{T}_3 = -c_3 I_3, \quad \mathcal{T}_4 = -a E_6, \quad \mathcal{T}_{5,\dots,11} = -b_{1,\dots,7} L_{1,\dots,7}. \quad (\text{B.11})$$

We also have the terms

$$\begin{aligned} \mathcal{Z}_1^\mu &= -b_8 \partial^\mu E_4, & \mathcal{Z}_2^\mu &= -b_9 \partial^\mu I, & \mathcal{Z}_3^\mu &= -\frac{1}{25} b_{10} R \partial^\mu R, \\ \mathcal{Z}_4^\mu &= -\frac{1}{5} b_{11} \partial^\mu \nabla^2 R, & \mathcal{Z}_{5,6,7}^\mu &= -b_{12,13,14} \nabla_\nu H_{2,3,4}^{\mu\nu}. \end{aligned} \quad (\text{B.12})$$

Actually, the terms in (B.12) overcomplete the basis of trivial anomalies. This is because there are six trivial anomalies, but seven terms in (B.12). If we integrate the (B.12) terms by parts, then we may require that  $\nabla_\mu \mathcal{Z}_{1,\dots,7}^\mu$  do not affect the coefficients of  $L_{1,\dots,7}$ . This forces us to impose

$$b_{13} = -\frac{24}{d^2 - 5d + 6} b_8 + \frac{4(d-6)}{d-2} b_9 - \frac{5}{d-1} b_{12}. \quad (\text{B.13})$$

With (B.13) it is guaranteed that  $L_{1,\dots,7}$  are vanishing anomalies<sup>1</sup>, and we also see that the coefficients of  $E_6, I_{1,2,3}$  are unaffected by  $\nabla_\mu \mathcal{Z}_{1,\dots,7}^\mu$ . Thus, with the condition (B.13) the terms  $\mathcal{Z}_{1,\dots,7}^\mu$  substitute exactly the trivial anomalies  $J_{1,\dots,6}$ .

Next, we have

$$\begin{aligned} \mathcal{T}_{12} &= \mathcal{I}_I^1 \partial_\mu \lambda^I \partial^\mu E_4, & \mathcal{T}_{13} &= \mathcal{I}_I^2 \partial_\mu \lambda^I \partial^\mu I, & \mathcal{T}_{14} &= \frac{1}{25} \mathcal{I}_I^3 \partial_\mu \lambda^I R \partial^\mu R, \\ \mathcal{T}_{15} &= \frac{1}{5} \mathcal{I}_I^4 \partial_\mu \lambda^I \partial^\mu \nabla^2 R, & \mathcal{T}_{16,17,18} &= \mathcal{I}_I^{5,6,7} \partial_\mu \lambda^I \nabla_\nu H_{2,3,4}^{\mu\nu}, \end{aligned} \quad (\text{B.14})$$

and

$$\begin{aligned} \mathcal{Z}_8^\mu &= \mathcal{G}_I^1 \partial^\mu \lambda^I E_4, & \mathcal{Z}_9^\mu &= \mathcal{G}_I^2 \partial^\mu \lambda^I I, & \mathcal{Z}_{10}^\mu &= \frac{1}{25} \mathcal{G}_I^3 \partial^\mu \lambda^I R^2, \\ \mathcal{Z}_{11}^\mu &= \frac{1}{5} \mathcal{G}_I^4 \partial^\mu \lambda^I \nabla^2 R, & \mathcal{Z}_{12,\dots,17}^\mu &= \mathcal{H}_I^{1,\dots,6} \partial_\nu \lambda^I H_{1,\dots,6}^{\mu\nu}, \\ \mathcal{Z}_{18}^\mu &= \mathcal{F}_I \nabla_\kappa \partial_\lambda \lambda^I \nabla^\mu G^{\kappa\lambda}, & \mathcal{Z}_{19}^\mu &= \frac{1}{5} \mathcal{E}_I \nabla^2 \lambda^I \partial^\mu R. \end{aligned} \quad (\text{B.15})$$

<sup>1</sup>By ‘‘vanishing’’ anomalies we mean those which are set to 0 at the fixed point by the consistency conditions.

## Appendix B. Local CS equation in $d = 6$

With more  $\partial\lambda$ 's we have

$$\begin{aligned}
\mathcal{T}_{19} &= \frac{1}{2}\mathcal{G}_{IJ}^1 \partial_\mu \lambda^I \partial^\mu \lambda^J E_4, & \mathcal{T}_{20} &= \frac{1}{2}\mathcal{G}_{IJ}^2 \partial_\mu \lambda^I \partial^\mu \lambda^J I, & \mathcal{T}_{21} &= \frac{1}{50}\mathcal{G}_{IJ}^3 \partial_\mu \lambda^I \partial^\mu \lambda^J R^2, \\
\mathcal{T}_{22} &= \frac{1}{10}\mathcal{G}_{IJ}^4 \partial_\mu \lambda^I \partial^\mu \lambda^J \nabla^2 R, & \mathcal{T}_{23,\dots,28} &= \frac{1}{2}\mathcal{H}_{IJ}^{1,\dots,6} \partial_\mu \lambda^I \partial_\nu \lambda^J H_{1,\dots,6}^{\mu\nu}, \\
\mathcal{T}_{29} &= \mathcal{F}_{IJ} \partial_\kappa \lambda^I \nabla_\lambda \partial_\mu \lambda^J \nabla^\kappa G^{\lambda\mu}, & \mathcal{T}_{30} &= \mathcal{F}'_{IJ} \partial_\kappa \lambda^I \nabla_\lambda \partial_\mu \lambda^J \nabla^\lambda G^{\kappa\mu},
\end{aligned} \tag{B.16}$$

and

$$\begin{aligned}
\mathcal{Z}_{20}^\mu &= \frac{1}{5}\mathcal{E}_{IJ} \partial^\mu \lambda^I \partial_\nu \lambda^J \partial^\nu R, & \mathcal{Z}_{21}^\mu &= \mathcal{D}_{IJ} \partial_\kappa \lambda^I \nabla_\lambda \partial_\nu \lambda^J R^{\mu\lambda\nu}, \\
\mathcal{Z}_{22}^\mu &= \mathcal{C}_I \partial_\nu \nabla^2 \lambda^I G^{\mu\nu}, & \mathcal{Z}_{23}^\mu &= \mathcal{C}_{IJ} \partial_\kappa \lambda^I \nabla_\nu \partial^\kappa \lambda^J G^{\mu\nu}, & \mathcal{Z}_{24}^\mu &= \mathcal{C}'_{IJ} \partial_\nu \lambda^I \nabla^2 \lambda^J G^{\mu\nu}, \\
\mathcal{Z}_{25}^\mu &= \frac{1}{5}\mathcal{B}_{IJ} \partial^\mu \lambda^I \nabla^2 \lambda^J R & \mathcal{Z}_{26}^\mu &= \mathcal{A}_{IJ} \partial_\nu \nabla^2 \lambda^I \nabla^\mu \partial^\nu \lambda^J, & \mathcal{Z}_{27}^\mu &= \mathcal{A}'_{IJ} \partial^\mu \lambda^I (\nabla^2)^2 \lambda^J.
\end{aligned} \tag{B.17}$$

Furthermore, we have

$$\begin{aligned}
\mathcal{T}_{31} &= \frac{1}{2}\mathcal{F}_{IJK} \partial_\kappa \lambda^I \partial_\lambda \lambda^J \partial_\mu \lambda^K \nabla^\kappa G^{\lambda\mu}, & \mathcal{T}_{32} &= \frac{1}{5}\hat{\mathcal{E}}_{IJ} \partial_\mu \lambda^I \nabla^2 \lambda^J \partial^\mu R, \\
\mathcal{T}_{33} &= \frac{1}{10}\mathcal{E}_{IJK} \partial_\mu \lambda^I \partial_\nu \lambda^J \partial^\nu \lambda^K \partial^\mu R, & \mathcal{T}_{34} &= \mathcal{D}_{IJK} \partial_\kappa \lambda^I \partial_\mu \lambda^J \nabla_\lambda \partial_\nu \lambda^K R^{\kappa\lambda\mu\nu}, \\
\mathcal{T}_{35} &= \frac{1}{4}\mathcal{D}_{IJKL} \partial_\kappa \lambda^I \partial_\lambda \lambda^J \partial_\mu \lambda^K \partial_\nu \lambda^L R^{\kappa\lambda\mu\nu}, & \mathcal{T}_{36} &= \hat{\mathcal{C}}_{IJ} \nabla_\mu \partial_\nu \lambda^I \nabla^2 \lambda^J G^{\mu\nu}, \\
\mathcal{T}_{37} &= \frac{1}{2}\hat{\mathcal{C}}'_{IJ} \nabla_\kappa \partial_\mu \lambda^I \nabla^\kappa \partial_\nu \lambda^J G^{\mu\nu}, & \mathcal{T}_{38} &= \frac{1}{2}\mathcal{C}_{IJK} \partial_\mu \lambda^I \partial_\nu \lambda^J \nabla^2 \lambda^K G^{\mu\nu}, \\
\mathcal{T}_{39} &= \mathcal{C}'_{IJK} \partial_\mu \lambda^I \partial_\nu \lambda^J \nabla^\kappa \partial_\nu \lambda^K G^{\mu\nu}, & \mathcal{T}_{40} &= \frac{1}{2}\mathcal{C}''_{IJK} \partial_\kappa \lambda^I \partial^\kappa \lambda^J \nabla_\mu \partial_\nu \lambda^K G^{\mu\nu}, \\
\mathcal{T}_{41} &= \frac{1}{4}\mathcal{C}_{IJKL} \partial_\mu \lambda^I \partial_\nu \lambda^J \partial_\kappa \lambda^K \partial^\kappa \lambda^L G^{\mu\nu}, & \mathcal{T}_{42} &= \frac{1}{5}\mathcal{B}_I (\nabla^2)^2 \lambda^I R, \\
\mathcal{T}_{43} &= \frac{1}{10}\hat{\mathcal{B}}_{IJ} \nabla^2 \lambda^I \nabla^2 \lambda^J R, & \mathcal{T}_{44} &= \frac{1}{10}\hat{\mathcal{B}}'_{IJ} \nabla_\mu \partial_\nu \lambda^I \nabla^\mu \partial^\nu \lambda^J R, \\
\mathcal{T}_{45} &= \frac{1}{10}\mathcal{B}_{IJK} \partial_\mu \lambda^I \partial^\mu \lambda^J \nabla^2 \lambda^K R, & \mathcal{T}_{46} &= \frac{1}{10}\mathcal{B}'_{IJK} \partial_\mu \lambda^I \partial_\nu \lambda^J \nabla^\mu \partial^\nu \lambda^K R, \\
\mathcal{T}_{47} &= \frac{1}{20}\mathcal{B}_{IJKL} \partial_\mu \lambda^I \partial^\mu \lambda^J \partial_\nu \lambda^K \partial^\nu \lambda^L R,
\end{aligned} \tag{B.18}$$

and

$$\begin{aligned}
\mathcal{Z}_{28}^\mu &= \mathcal{A}_{IJK} \partial_\nu \lambda^I \nabla^\mu \partial^\nu \lambda^J \nabla^2 \lambda^K, & \mathcal{Z}_{29}^\mu &= \mathcal{A}'_{IJK} \partial_\kappa \lambda^I \nabla^\mu \partial_\lambda \lambda^J \nabla^\kappa \partial^\lambda \lambda^K, \\
\mathcal{Z}_{30}^\mu &= \frac{1}{2}\mathcal{A}_{IJKL} \partial_\nu \lambda^I \partial^\nu \lambda^J \partial^\mu \lambda^K \nabla^2 \lambda^L.
\end{aligned} \tag{B.19}$$

Finally, we also have the terms

$$\begin{aligned}
\mathcal{T}_{48} &= \mathcal{A}_I (\nabla^2)^3 \lambda^I, & \mathcal{T}_{49} &= \hat{\mathcal{A}}_{IJ} (\nabla^2)^2 \lambda^I \nabla^2 \lambda^J, & \mathcal{T}_{50} &= \frac{1}{2}\hat{\mathcal{A}}'_{IJ} \partial_\mu \nabla^2 \lambda^I \partial^\mu \nabla^2 \lambda^J, \\
\mathcal{T}_{51} &= \frac{1}{2}\hat{\mathcal{A}}''_{IJ} \nabla_\kappa \nabla_\lambda \partial_\mu \lambda^I \nabla^\kappa \nabla^\lambda \partial^\mu \lambda^J, & \mathcal{T}_{52} &= \frac{1}{8}\hat{\mathcal{A}}_{IJK} \nabla^2 \lambda^I \nabla^2 \lambda^J \nabla^2 \lambda^K, \\
\mathcal{T}_{53} &= \frac{1}{2}\hat{\mathcal{A}}'_{IJK} \nabla_\kappa \partial_\mu \lambda^I \nabla^\kappa \partial_\nu \lambda^J \nabla^\mu \partial^\nu \lambda^K, & \mathcal{T}_{54} &= \hat{\mathcal{A}}''_{IJK} \partial_\mu \lambda^I \nabla^2 \lambda^J \partial^\mu \nabla^2 \lambda^K, \\
\mathcal{T}_{55} &= \check{\mathcal{A}}_{IJK} \partial_\mu \lambda^I \nabla^\mu \partial_\nu \lambda^J \partial^\nu \nabla^2 \lambda^K, & \mathcal{T}_{56} &= \frac{1}{2}\check{\mathcal{A}}'_{IJK} \partial_\mu \lambda^I \partial^\mu \lambda^J (\nabla^2)^2 \lambda^K, \\
\mathcal{T}_{57} &= \frac{1}{2}\check{\mathcal{A}}''_{IJK} \partial_\mu \lambda^I \partial_\nu \lambda^J \nabla^\mu \partial^\nu \nabla^2 \lambda^K, & \mathcal{T}_{58} &= \frac{1}{4}\hat{\mathcal{A}}_{IJKL} \partial_\mu \lambda^I \partial^\mu \lambda^J \nabla^2 \lambda^K \nabla^2 \lambda^L, \\
\mathcal{T}_{59} &= \frac{1}{4}\hat{\mathcal{A}}'_{IJKL} \partial_\kappa \lambda^I \partial^\kappa \lambda^J \nabla_\mu \partial_\nu \lambda^K \nabla^\mu \partial^\nu \lambda^L, & \mathcal{T}_{60} &= \frac{1}{2}\hat{\mathcal{A}}''_{IJKL} \partial_\kappa \lambda^I \partial_\lambda \lambda^J \nabla^\kappa \partial_\mu \lambda^K \nabla^\lambda \partial^\mu \lambda^L, \\
\mathcal{T}_{61} &= \frac{1}{2}\check{\mathcal{A}}_{IJKL} \partial_\mu \lambda^I \partial_\nu \lambda^J \nabla^\mu \partial^\nu \lambda^K \nabla^2 \lambda^L, & \mathcal{T}_{62} &= \frac{1}{2}\check{\mathcal{A}}'_{IJKL} \partial_\kappa \lambda^I \partial_\lambda \lambda^J \partial_\mu \lambda^K \nabla^\kappa \nabla^\lambda \partial^\mu \lambda^L, \\
\mathcal{T}_{63} &= \frac{1}{4}\mathcal{A}_{IJKLM} \partial_\mu \lambda^I \partial^\mu \lambda^J \partial_\nu \lambda^K \partial^\nu \lambda^L \nabla^2 \lambda^M, & \mathcal{T}_{64} &= \frac{1}{4}\mathcal{A}'_{IJKLM} \partial_\kappa \lambda^I \partial^\kappa \lambda^J \partial_\lambda \lambda^K \partial_\mu \lambda^L \nabla^\lambda \partial^\mu \lambda^M, \\
\mathcal{T}_{65} &= \frac{1}{8}\mathcal{A}_{IJKLMN} \partial_\kappa \lambda^I \partial^\kappa \lambda^J \partial_\lambda \lambda^K \partial^\lambda \lambda^L \partial_\mu \lambda^M \partial^\mu \lambda^N.
\end{aligned} \tag{B.20}$$



# Appendix C

## Perturbative checks of Hamiltonian truncation

### C.1 $\mathbb{Z}_2$ -unbroken phase

We computed the first two perturbative corrections to the ground state energy density  $\Lambda$  and the physical particle mass for the  $\phi^4$  theory defined by the action (5.2)

$$\begin{aligned}\Lambda/m^2 &= -\frac{21\zeta(3)}{16\pi^3}\bar{g}^2 + 0.0416485\bar{g}^3 + \dots, \\ \Delta m^2/m^2 \equiv (m_{\text{ph}}^2 - m^2)/m^2 &= -\frac{3}{2}\bar{g}^2 + 2.86460(20)\bar{g}^3 + \dots\end{aligned}\tag{C.1}$$

( $\bar{g} \equiv g/m^2$ ). Recall that  $\Lambda$  at  $g = 0$  is set to zero. Because the interaction is normal ordered the  $O(\bar{g})$  contributions are absent. The  $O(\bar{g}^3)$  coefficients are numerical with a shown number of significant digits and an error estimate if needed.<sup>1</sup> The size of the coefficients suggests that the series are perturbative for  $\bar{g} \lesssim 1$ .

The coefficients were obtained by numerical integration of Feynman diagrams. It is much easier to perform this integration in the coordinate space, since the propagator (5.49) is exponentially decreasing at large distances, and also because parallel lines in multi-loop diagrams correspond in the  $x$ -space to trivially raising the propagator to a power. For example, the  $O(g^3)$  correction to  $\Delta m^2$  comes from the diagram

(C.2)

evaluated at the (Euclidean) external momentum  $p^2 = -m^2$ . In the  $x$ -space this gives the

---

<sup>1</sup>It's likely that exact expressions for these coefficients can be found, but since this is not the focus of our work, we have not invested the effort.

## Appendix C. Perturbative checks of Hamiltonian truncation

integral (we omit the combinatorial factors)

$$\int d^2x \int d^2y e^{ip \cdot x} G(|x-y|)^2 G(|y|)^2 G(|x|). \quad (\text{C.3})$$

We pick  $p = (im, 0)$ , introduce the polar coordinates and evaluate the integral via Monte Carlo.

In figure C.1 we compare the above perturbative results with the numerical spectra obtained with our method for  $m = 1$ ,  $L = 10$ . Perturbative computations refer to the infinite volume, but  $L = 10$  is sufficiently large so that the expected exponentially small corrections should not disturb the comparison. We use the cutoff  $E_{\max} = 20$ . Notice that  $m_{\text{ph}}$  is extracted as  $\mathcal{E}_1 - \mathcal{E}_0$ , where  $\mathcal{E}_1$  is the lowest  $\mathbb{Z}_2$ -odd eigenstate, while  $\Lambda$  is extracted as  $\mathcal{E}_0/L$ .

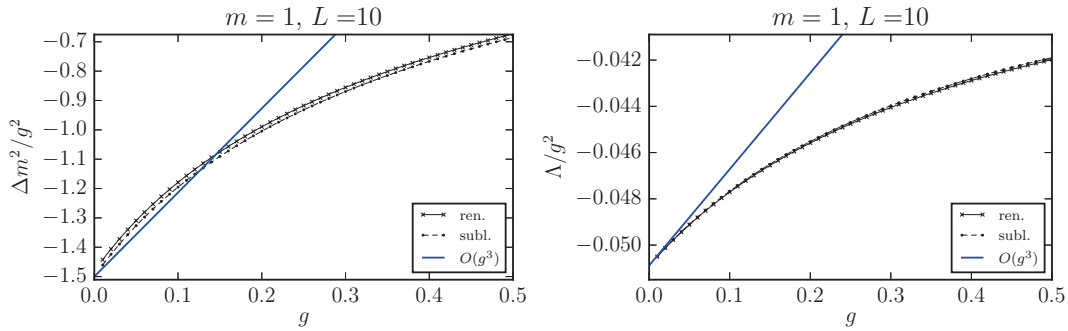


Figure C.1: Comparing perturbative and numerical predictions; see the text.

To facilitate the comparison, we plot  $\Lambda$  and  $\Delta m^2$  divided by  $g^2$ . The reasonably good match in the region of small  $g \lesssim 0.1$  shows that our numerical method agrees with both  $O(\bar{g}^2)$  and  $O(\bar{g}^3)$  coefficients of the perturbative expansion. At the same time, higher order corrections are clearly non-negligible—they would become comparable to the  $O(\bar{g}^3)$  correction at  $\bar{g} \sim 0.5$ .

### C.2 $\mathbb{Z}_2$ -broken phase

We repeated the perturbative computation performed in the previous chapter in the presence of a cubic coupling, corresponding to the potential density

$$\mathcal{V} = \frac{1}{2} M^2 N_M(\phi^2) + g_3 N_M(\phi^3) + g_4 N_M(\phi^4) \quad (\text{C.4})$$

The symmetric double-well case of Eq. (6.3) can be recovered by setting  $g_4 = g$ ,  $g_3 = \sqrt{2g_4}M$ , but we will keep the couplings independent for the sake of generality.

For comparison with numerics, we will need results for  $\Delta m^2 = m_{\text{ph}}^2 - M^2$  and  $\Lambda$  up to the second order in  $g$ . In terms of  $g_3, g_4$ , we need to include all diagrams up to order  $O(g_4^2)$ ,  $O(g_3^2)$ ,

$O(g_3^2 g_4)$  and  $O(g_3^4)$ . The results are<sup>2</sup> ( $\bar{g}_3 \equiv g_3/M^2$ ,  $\bar{g}_4 \equiv g_4/M^2$ ):

$$\Lambda/M^2 = \text{[diagram 1]} + \text{[diagram 2]} + \text{[diagram 3]} + \text{[diagram 4]} + \text{[diagram 5]} + \dots \quad (\text{C.5})$$

$$\begin{aligned} &= -0.0445289\bar{g}_3^2 - \frac{21\zeta(3)}{16\pi^3}\bar{g}_4^2 \\ &\quad - (0.0109030(51) + 0.026854(32))\bar{g}_3^4 + 0.0799586(41)\bar{g}_3^2\bar{g}_4 + \dots \end{aligned} \quad (\text{C.6})$$

and

$$\begin{aligned} \Delta m^2/M^2 &= \text{[diagram 1]} + \text{[diagram 2]} + \text{[diagram 3]} + \text{[diagram 4]} \\ &\quad + \text{[diagram 5]} + \text{[diagram 6]} + \text{[diagram 7]} + \dots \\ &= -\sqrt{3}\bar{g}_3^2 - 1.5\bar{g}_4^2 - (2.2492(37) + 2.8020(70))\bar{g}_3^4 \\ &\quad + (1.06864(15) + 1.9998(10) + 5.50025(91))\bar{g}_3^2\bar{g}_4 + \dots \end{aligned} \quad (\text{C.7})$$

In figure C.2 we compare the above predictions for  $g_4 = g$ ,  $g_3 = \sqrt{2g_4}M$  with the numerical spectra obtained with our method for  $M = 1$ ,  $L = 12$ . We use the zero-mode cutoff  $s = 4$  and adjust  $\bar{E}_{\max}$  so that the basis dimension is  $\sim 10000$  in each sector.

In the left plot we show the renormalized results for  $\Delta m^2$ , computed both in the  $\mathbb{Z}_2$ -even and  $\mathbb{Z}_2$ -odd spectra, with an error estimate given by variation of the normal ordering mass. We observe a reasonably good agreement for  $g \lesssim 0.04$ .<sup>3</sup> For larger  $g$ , the deviation may be attributed to higher-order perturbative effects and to the finite-volume splitting affecting the numerics.

In the right plot we show instead both the “raw” and renormalized results for the ground state energy density, extracted from both  $\mathbb{Z}_2$ -even and  $\mathbb{Z}_2$ -odd spectra. Again, an error estimate for the renormalized values is attributed by varying the normal ordering mass. We see a perfect agreement with the perturbative prediction until the finite-volume splitting between the eigenvalues kicks in.

<sup>2</sup>We do not report explicitly the symmetry factors for the diagrams. Most of them were evaluated numerically by Monte Carlo integration using coordinate space propagators. We did not invest much effort in analytic results.

<sup>3</sup>We haven’t investigated the reasons behind a small residual deviation visible in this region. One possible reason is that we may be underestimating the renormalization corrections by including contributions only from the  $\hat{\mathcal{H}}_l \otimes \bar{\mathcal{H}}_h$  part of the high energy Hilbert space. See appendix D.2.

## Appendix C. Perturbative checks of Hamiltonian truncation

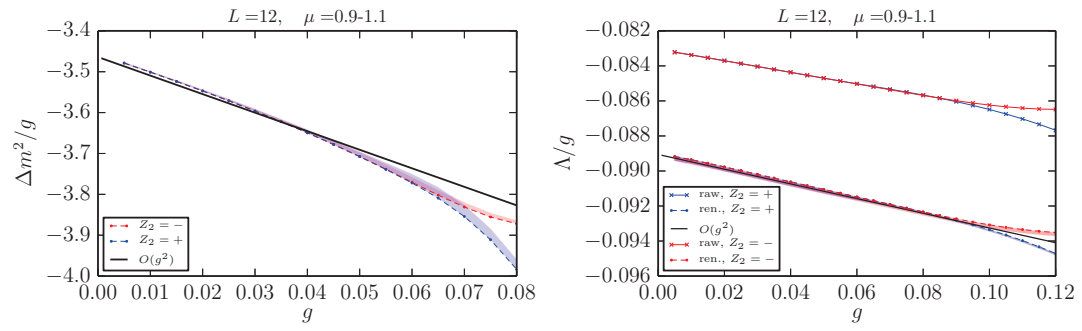


Figure C.2: Comparing perturbative and numerical predictions; see the text.

## Appendix D

# Computational details for the Hamiltonian truncation

### D.1 Speeding up the Hamiltonian matrix computation

In our computations, most time is spent in matrix diagonalization. Still, matrix evaluation should also be organized efficiently. Here we list some tricks useful to speed it up. These tricks are realized in our `python` code, included with the `arXiv` submission.

#### Diagonal/offdiagonal decomposition

Let's split  $H$  into three parts,

$$H = H_{\text{diag}} + H_{\text{offdiag}} + H_{\text{offdiag}}^\dagger \quad (\text{D.1})$$

where  $H_{\text{diag/offdiag}}$  have only diagonal/off-diagonal matrix elements.  $H_{\text{diag}}$  includes  $H_0$  and the terms in  $V$  of the form<sup>1</sup>

$$a_{k_1}^\dagger a_{k_2}^\dagger a_{k_3} a_{k_4}, \quad \{k_1, k_2\} = \{k_3, k_4\}. \quad (\text{D.2})$$

The rest of the terms in  $V$  get assigned to  $H_{\text{offdiag}}$  and  $H_{\text{offdiag}}^\dagger$ . Only the matrix elements of  $H_{\text{offdiag}}$  need to be evaluated, while those of  $H_{\text{offdiag}}^\dagger$  are obtained by transposition. We include into  $H_{\text{offdiag}}$  the  $a^\dagger a^\dagger a^\dagger a^\dagger$ ,  $a^\dagger a^\dagger a^\dagger a$  terms in  $V$ , as well as the operators

$$a_{k_1}^\dagger a_{k_2}^\dagger a_{k_3} a_{k_4}, \quad \{k_1, k_2\} \neq \{k_3, k_4\}, \quad (\text{D.3})$$

satisfying the following lexicographic ordering condition,<sup>2</sup>

$$\text{sort}(|k_1|, |k_2|) \prec \text{sort}(|k_3|, |k_4|) \quad (\text{D.4})$$

---

<sup>1</sup>Here and below  $\{x_1, x_2, \dots\}$  denotes an unordered set.

<sup>2</sup>It's not hard to see that  $\text{sort}(|k_1|, |k_2|) = \text{sort}(|k_3|, |k_4|)$  is impossible given  $\{k_1, k_2\} \neq \{k_3, k_4\}$  and  $k_1 + k_2 = k_3 + k_4$ . So any operator (D.3) gets assigned either to  $H_{\text{offdiag}}$  or to  $H_{\text{offdiag}}^\dagger$ .

## Appendix D. Computational details for the Hamiltonian truncation

---

Notice that this condition depends only on the absolute values of momenta, hence it is  $\mathbb{P}$ -invariant. This ensures that all three terms in the decomposition (D.1) are separately  $\mathbb{P}$ -invariant. This will be important below, when we describe our method to evaluate the matrix elements.

### Keeping track of the energy

Each elementary operator  $\mathcal{O} \in V$ , a product of ladder operators, increases/decreases energy of any basis vector it acts upon by a fixed amount  $\Delta E_{\mathcal{O}}$ . Since we will be working in the space of low-energy states  $\mathcal{H}_l$  of energies  $0 \leq E \leq E_{\max}$ , we can drop from  $V$  all operators for which

$$|\Delta E_{\mathcal{O}}| > E_{\max}. \quad (\text{D.5})$$

Moreover, when acting on a basis state  $|\psi\rangle$  the result is guaranteed to be zero in  $\mathcal{H}_l$  unless

$$0 \leq E(\psi) + \Delta E_{\mathcal{O}} \leq E_{\max}. \quad (\text{D.6})$$

### Combinatorial factors for oscillator ordering

To reduce the number of elementary operators in  $V$ , it's worth ordering them. We have

$$\sum_{k_1, k_2, k_3, k_4} a_{k_1} a_{k_2} a_{k_3} a_{k_4} = \sum_{k_1 \leq k_2 \leq k_3 \leq k_4} f_4(k_1, k_2, k_3, k_4) a_{k_1} a_{k_2} a_{k_3} a_{k_4} \quad (\text{D.7})$$

where the symmetry factor

$$f_4(a \leq b \leq c \leq d) = \begin{cases} 24 & a < b < c < d, \\ 12 & a = b < c < d \text{ or } a < b = c < d \text{ or } a < b < c = d, \\ 6 & a = b < c = d, \\ 4 & a = b = c < d \text{ or } a < b = c = d, \\ 1 & a = b = c = d. \end{cases} \quad (\text{D.8})$$

### $\mathbb{P}$ -conservation

In this paper we work in the Hilbert space of  $P = 0$  states of energies  $E \leq E_{\max}$ . Internally we represent a state  $|\psi\rangle$ , see (5.9), as a sequence of occupation numbers  $Z_n$  for each momentum mode,

$$|\psi\rangle \leftrightarrow [Z_n : -n_{\max} \leq n \leq n_{\max}], \quad (\text{D.9})$$

where  $n_{\max}$  is the maximal possible mode number for the given  $L$  and  $E_{\max}$ .

The matrix  $H_{ij}$  is then computed as follows. The diagonal part from  $H_0$  is trivial so we do not discuss it. For the rest, we take a particular state  $|\psi_j\rangle$  and act on it with elementary operators  $\mathcal{O} \in V$ , one by one. Each operator gives one particular state  $|\psi_i\rangle$  times a numerical coefficient. We accumulate this coefficient in the matrix element  $H_{ij}$ . Thus the matrix is

---

## D.2. Renormalization in the $\mathbb{Z}_2$ -broken phase

generated column by column. As discussed above, we can do this computation for  $H_{\text{offdiag}}$  and get  $H_{\text{offdiag}}^\dagger$  by transposition. We generate the matrix separately in each of the  $\mathbb{Z}_2 = \pm$  sectors.

The computation we just discussed produces the matrix  $H$  in the full Hilbert space of  $P = 0$ ,  $E \leq E_{\text{max}}$  states. However, in this paper we are interested in the  $\mathbb{P} = +1$  subspace of this space. The basis of this subspace consists of symmetrized linear combinations (5.25) of the basic  $P = 0$  Fock states. In principle, the matrix in the  $\mathbb{P} = +1$  subspace could be obtained once the full matrix is computed, but this is wasteful. We will now describe a method which generates the matrix in the  $\mathbb{P} = +1$  subspace directly.

When we store the symmetrized state  $|\psi^{\text{sym}}\rangle$  internally, we only store  $|\psi\rangle$ . If  $|\psi\rangle \neq \mathbb{P}|\psi\rangle$ , then we keep only one of these two vectors (no matter which one), since they give rise to the same  $|\psi^{\text{sym}}\rangle$ .

We have to compute the matrix with respect to the symmetrized basis, which we will call  $S_{ij}$ ,

$$H|\psi_j^{\text{sym}}\rangle = S_{ij}|\psi_i^{\text{sym}}\rangle. \quad (\text{D.10})$$

Consider also the matrix  $H_{ij}$  with respect to the Fock basis, whose computation was discussed above. Let's split it into three pieces,

$$H|\psi_i\rangle = H_{ji}^a|\psi_j\rangle + H_{ki}^b|\psi_k\rangle + H_{ki}^c\mathbb{P}|\psi_k\rangle, \quad (\text{D.11})$$

where the index  $j$  runs over  $\mathbb{P}$ -invariant  $|\psi_j\rangle$ , and the rest of the Fock basis is split into  $|\psi_k\rangle$ 's and  $\mathbb{P}|\psi_k\rangle$ 's. Since  $[\mathbb{P}, H] = 0$ , we have

$$H\mathbb{P}|\psi_i\rangle = \mathbb{P}(H|\psi_i\rangle) = H_{ji}^a|\psi_j\rangle + H_{ki}^b\mathbb{P}|\psi_k\rangle + H_{ki}^c|\psi_k\rangle, \quad (\text{D.12})$$

and finally

$$\begin{aligned} H|\psi_i^{\text{sym}}\rangle &= \beta(\psi_i)(H|\psi_i\rangle + H\mathbb{P}|\psi_i\rangle) = \beta(\psi_i)[2H_{ji}^a|\psi_j\rangle + (H_{ki}^b + H_{ki}^c)(|\psi_k\rangle + \mathbb{P}|\psi_k\rangle)] \\ &= \beta(\psi_i)[2H_{ji}^a|\psi_j^{\text{sym}}\rangle + \sqrt{2}(H_{ki}^b + H_{ki}^c)|\psi_k^{\text{sym}}\rangle] \end{aligned} \quad (\text{D.13})$$

From here we obtain a recipe for an economic way to compute  $S_{ji}$ . Namely, we compute  $H|\psi_i\rangle$  and accumulate the coefficients  $2H_{ji}^a$  and  $\sqrt{2}(H_{ki}^b + H_{ki}^c)$ , and then multiply by  $\beta(\psi_i)$ .

Notice that we used the  $\mathbb{P}$ -invariance of the Hamiltonian in the first step of (D.12). When this method is combined with splitting  $H$  into the diagonal/off-diagonal parts, it's important that every part be  $\mathbb{P}$ -invariant by itself. As mentioned above, condition (D.4) ensures this.

## D.2 Renormalization in the $\mathbb{Z}_2$ -broken phase

The following discussion extends the renormalization procedure introduced in Section 5.3 to the basis presented in Section 6.2.1 for the  $\mathbb{Z}_2$ -broken phase.

## Appendix D. Computational details for the Hamiltonian truncation

---

Let us start from the full eigenvalue problem,

$$H.c = \mathcal{E}c. \quad (\text{D.14})$$

The full Hilbert space can be split into “low” energy and “high” energy subspaces,

$$H_l = \hat{\mathcal{H}}_l \otimes \bar{\mathcal{H}}_l, \quad (\text{D.15})$$

$$H_h = (\hat{\mathcal{H}}_h \otimes \bar{\mathcal{H}}_l) \oplus (\hat{\mathcal{H}}_l \otimes \bar{\mathcal{H}}_h) \oplus (\hat{\mathcal{H}}_h \otimes \bar{\mathcal{H}}_h). \quad (\text{D.16})$$

Accordingly, (D.14) can be projected onto these subspaces,

$$H_{ll}.c_l + H_{lh}.c_h = \mathcal{E}c_l, \quad (\text{D.17})$$

$$H_{hl}.c_l + H_{hh}.c_h = \mathcal{E}c_h. \quad (\text{D.18})$$

“Integrating out”  $c_h$  via the second equation, we get

$$(H_{ll} + \Delta H)c_l = \mathcal{E}c_l, \quad (\text{D.19})$$

$$\Delta H = -H_{lh} \frac{1}{H_{hh} - \mathcal{E}} H_{hl} = -W_{lh} \frac{1}{H_{hh} - \mathcal{E}} W_{hl}, \quad (\text{D.20})$$

where we used that in the Hamiltonian (6.24) only  $W$  will mix the low and high subspaces. At leading order one can neglect  $W$  in the denominator, which gives

$$\Delta H \approx -W_{lh} \frac{1}{\hat{H} + \bar{H}_0 - \mathcal{E}} W_{hl} = - \sum_{i \in \mathcal{H}_h} \frac{1}{E_i - \mathcal{E}} P_l W |i\rangle \langle i| W P_l \quad (\text{D.21})$$

where a summation over all the states in  $\mathcal{H}_h$  appears.

It turns out that the effect induced by the truncation of  $\hat{\mathcal{H}}$  is less significant than for  $\bar{\mathcal{H}}$ . It’s also less expensive to control. We found that fixing the corresponding cutoff  $s$  to 4 or 5 basically stabilizes the results. For this reason we will only take into account the renormalization effect coming from the nonzero field modes. This means that we will restrict the sum in (D.21) to go only over the  $\hat{\mathcal{H}}_l \otimes \bar{\mathcal{H}}_h$  part of  $\mathcal{H}_h$ . Therefore, we approximate

$$\Delta H \approx - \sum_{\psi_\alpha \in \hat{\mathcal{H}}_l} \sum_{k \in \bar{\mathcal{H}}_h} \frac{1}{\hat{\mathcal{E}}_\alpha + \bar{E}_k - \mathcal{E}} W |\psi_\alpha, k\rangle \langle \psi_\alpha, k| W \quad (\text{D.22})$$

where we dropped the projectors  $P_l$  to avoid cluttering. The potential matrix  $W$  can be schematically written as

$$W = \sum_{a=2,3,4} \hat{m}_a \otimes \bar{V}_a, \quad (\text{D.23})$$

where  $\hat{m}_a$  and  $\bar{V}_a$  are matrices in the  $\hat{\mathcal{H}}$  and  $\bar{\mathcal{H}}$ , respectively. Therefore,

$$\Delta H \approx - \sum_{a,b} \sum_{\psi_\alpha \in \hat{\mathcal{H}}_l} \left( \hat{m}_a |\psi_\alpha\rangle \langle \psi_\alpha| \hat{m}_b \right) \otimes \left( \sum_{k \in \bar{\mathcal{H}}_h} \frac{1}{\hat{\mathcal{E}}_\alpha + \bar{E}_k - \mathcal{E}} \bar{V}_a |k\rangle \langle k| \bar{V}_b \right). \quad (\text{D.24})$$



The matrix elements  $\left(\hat{m}_a|\psi_\alpha\rangle\langle\psi_\alpha|\hat{m}_b\right)$  can be computed explicitly, while the second factor in (D.24) is evaluated with the same technique developed in [3]:

$$\sum_{k \in \mathcal{H}_h} \frac{1}{\hat{\mathcal{E}}_\alpha + \bar{E}_k - \mathcal{E}} \bar{V}_a |k\rangle \langle k| \bar{V}_b = \int_{\bar{E}_{\max}}^{\infty} dE \frac{1}{\hat{\mathcal{E}}_\alpha + E - \mathcal{E}} M^{ab}(E), \quad (\text{D.25})$$

$$M^{ab}(E)_{ij} dE \equiv \sum_{k: E \leq \bar{E}_k \leq E+dE} (\bar{V}_a)_{ik} (\bar{V}_b)_{kj}, \quad (\text{D.26})$$

where the matrix elements  $M_{ij}^{ab}$  can be related to the non-analytic behavior of two-point functions of the potential operators,

$$C^{ab}(\tau)_{ij} = \langle i | \bar{V}_a(\tau/2) \bar{V}_b(-\tau/2) | j \rangle = \int_0^\infty e^{-[E - (E_i + E_j)/2]} M_{ij}^{ab}(E) dE, \quad (\text{D.27})$$

$$\bar{V}_a(\tau) \equiv e^{H_0 \tau} \bar{V}_a e^{-H_0 \tau}. \quad (\text{D.28})$$

The quantities  $C^{ab}(\tau)_{ij}$  are computed as in [3] using the Wick theorem. The only difference is that the boson two point function  $\bar{G}(\rho)$  in the present case does not include the contribution from the zero mode,

$$\bar{G}(\rho) = G(\rho) - \frac{1}{2LM}. \quad (\text{D.29})$$



# Appendix E

## Semiclassical ground state splitting

### E.1 Ground state splitting

We will review here the derivation of Eq. (6.36).<sup>1</sup> We start from the Euclidean action

$$S = \int d^2x \left[ \frac{1}{2}(\partial\phi)^2 + g(\phi^2 - c^2)^2 \right], \quad (\text{E.1})$$

which entails the perturbative particle mass  $m^2 = 8gc^2$ . The normal ordering prescription for renormalization adopted in this work is equivalent to the mass renormalization<sup>2</sup>

$$S \rightarrow S - \frac{\delta m^2}{4} \int d^2x \phi^2, \quad \delta m^2 = \frac{6g}{\pi} \int_{-\infty}^{\infty} dk \frac{1}{\sqrt{k^2 + m^2}}. \quad (\text{E.2})$$

We will compute the matrix elements

$$\mathcal{A}_{\pm} = \langle \phi = \pm c | e^{-H\tau_0} | \phi = c \rangle = \mathcal{N} \int \mathcal{D}\phi e^{-S[\phi]}, \quad (\text{E.3})$$

where the path integral in the r.h.s. is defined with the boundary conditions  $\phi(x, \tau_0/2) = \pm c$ ,  $\phi(x, -\tau_0/2) = c$ . The path integral measure normalization factor  $\mathcal{N}$  will be fixed below. The results for the matrix elements will then be translated into the energy splitting.

Consider first the transition amplitude from  $c$  to  $-c$  in the one-instanton approximation. The instanton takes the form

$$\phi_0(x, \tau) = c \tanh \frac{m(\tau - \tau_c)}{2}, \quad (\text{E.4})$$

where the center  $\tau_c$  is arbitrary. This solution has action

$$S_0 + \delta S_0 = L \frac{m^3}{12g} - L \delta m^2 \frac{c^2}{4} \int_{-\infty}^{\infty} d\tau \left( \tanh^2 \frac{m\tau}{2} - 1 \right) = L \frac{m^3}{12g} + L \frac{\delta m^2}{8g} m, \quad (\text{E.5})$$

---

<sup>1</sup>See [128] for a pedagogical discussion in quantum mechanics, and [129] for an analogous computation for the partition function at finite temperature, which can be interpreted as a computation of the coefficient  $\kappa$  in (E.10).

<sup>2</sup>Let us neglect the cosmological constant renormalization as it does not affect the energy splitting.

## Appendix E. Semiclassical ground state splitting

---

where we included the contribution due to the mass counterterm. We need  $S_0 \gg 1$  for the validity of the semiclassical approximation.

At the one-loop order, (E.3) can be approximated by

$$\mathcal{N} \int \mathcal{D}\phi e^{-S[\phi]} \approx e^{-S_0} \mathcal{N} \int \mathcal{D}\eta e^{-\int \eta \frac{\delta^2 S}{\delta \phi^2} \eta}. \quad (\text{E.6})$$

Taking into account the presence of the zero mode of the quadratic fluctuation operator  $\frac{\delta^2 S}{\delta \phi^2}$  due to the invariance of  $S$  under a shift of  $\tau_c$ , this results in

$$\sqrt{\frac{S_0}{2\pi}} e^{-S_0} \mathcal{N} [\det'(-\square + V'')]^{-1/2} \tau_0, \quad (\text{E.7})$$

where the prime indicates that the zero mode has been removed from the determinant, and we replaced the integral over the zero mode with [128]

$$\int dc_0 = \sqrt{\frac{S_0}{2\pi}} \int_{-\tau_0/2}^{\tau_0/2} d\tau. \quad (\text{E.8})$$

To fix  $\mathcal{N}$ , consider the  $0 \rightarrow 0$  transition amplitude in the free massive theory, given simply by

$$\mathcal{A}_0 = \langle \phi = 0 | e^{-H_0 \tau_0} | \phi = 0 \rangle = \mathcal{N} [\det(-\square + m^2)]^{-1/2}. \quad (\text{E.9})$$

In the ratio of the two amplitudes the normalization factor cancels,

$$\mathcal{A}_- / \mathcal{A}_0 \approx \kappa \tau_0, \quad \kappa = \sqrt{\frac{S_0}{2\pi}} e^{-S_0} \left[ \frac{\det'(-\square + V'')}{m^{-2} \det(-\square + m^2)} \right]^{-1/2} m. \quad (\text{E.10})$$

Now, let us calculate the determinant ratio. We need to solve the eigenvalue equation

$$\left( -\frac{d^2}{dx^2} - \frac{d^2}{d\tau^2} + 12g\phi_0^2 - 4gc^2 \right) \psi = \left( -\frac{d^2}{dx^2} - \frac{d^2}{d\tau^2} + m^2 - \frac{3}{2}m^2 \frac{1}{\cosh^2 \frac{m\tau}{2}} \right) \psi = \epsilon \psi. \quad (\text{E.11})$$

The eigenstates are of the form  $\psi(x, \tau) = e^{-ik_n x} \psi_n(\tau)$ , where  $k_n = \frac{2\pi n}{L}$  due to periodic boundary condition on the cylinder, and

$$\left( -\frac{d^2}{d\tau^2} + \omega_n^2 - \frac{3}{2}m^2 \frac{1}{\cosh^2 \frac{m\tau}{2}} \right) \psi_n = \epsilon_n \psi_n, \quad (\text{E.12})$$

where we defined  $\omega_n^2 \equiv k_n^2 + m^2$ . The eigenvalues of (E.12) comprise two bound states,

$$\epsilon_{n,0} = k_n^2, \quad \epsilon_{n,1} = \frac{3}{4}m^2 + k_n^2 \quad (\text{E.13})$$

and a continuum (for infinite  $\tau_0$ ) of states with  $\epsilon_n \geq \omega_n^2$  [130], which can be parametrized by

the “momentum”

$$p = \sqrt{\epsilon_n} - \omega_n \geq 0. \quad (\text{E.14})$$

We consider  $\tau_0 \gg m^{-1}$  large but finite (but not too large—see below). Imposing the boundary conditions  $\psi_n(\pm\tau_0/2) = 0$ , the  $p$ 's take discrete values,

$$p\tau_0 - \delta_p = \pi l = \tilde{p}_l \tau_0, \quad l = 0, 1, \dots \quad (\text{E.15})$$

where the  $\tilde{p}_l$  represent the eigenvalues in the free theory, and the phase shift is [130]

$$\delta_p = -2\pi + 2 \arctan \frac{2p}{m} + 2 \arctan \frac{p}{m} \quad (\text{E.16})$$

Here the  $-2\pi$  term is added so that  $\delta_p$  vanishes for  $p \rightarrow \infty$ , corresponding to the fact that the effects of the potential disappear at high energies. In fact only  $l \geq 2$  gives  $p \geq 0$ , while for  $\tilde{p}$  we have  $l \geq 0$ . Taking into account the two bound states, we have the same number of eigenstates with and without the kink. The determinant ratio in (E.7) at large  $\tau_0$  evaluates to

$$\frac{\det'(-\square + V'')}{m^{-2} \det(-\square + m^2)} = \prod_{n=-\infty}^{\infty} \left\{ \left( \frac{k_n^2}{\omega_n^2} \right)^{1-\delta_{n0}} \frac{k_n^2 + \frac{3}{4}m^2}{\omega_n^2} \prod_{l=2}^{\infty} \frac{p_l^2 + \omega_n^2}{\tilde{p}_l^2 + \omega_n^2} \right\}. \quad (\text{E.17})$$

We took into account that for  $n = 0$  the first bound state of the kink theory is the zero mode which has been already factored out.

Performing the product over  $n$  by means of the identity

$$\frac{\sinh z}{z} = \prod_{n=1}^{\infty} \left( 1 + \frac{z^2}{\pi^2 n^2} \right), \quad (\text{E.18})$$

we can write the result in the form

$$\frac{\det'(-\square + V'')}{m^{-2} \det(-\square + m^2)} = (mL)^2 e^{mL \left( \frac{\sqrt{3}}{2} - 2 \right) + L\Sigma + 2b}, \quad (\text{E.19})$$

$$\Sigma = \sum_{l=2}^{\infty} (p_l^2 + m^2)^{1/2} - (\tilde{p}_l^2 + m^2)^{1/2}, \quad (\text{E.20})$$

$$b = \log \frac{1 - e^{-\frac{\sqrt{3}}{2}mL}}{(1 - e^{-mL})^2} + \sum_{l=2}^{\infty} \log(1 - e^{-(p_l^2 + m^2)^{1/2}L}) - \log(1 - e^{-(\tilde{p}_l^2 + m^2)^{1/2}L}). \quad (\text{E.21})$$

For  $\tau_0 m \gg 1$  we can approximate the sums by integrals,

$$\Sigma = \int_0^{\infty} \frac{dp}{\pi} \delta_p \frac{d}{dp} (p^2 + m^2)^{1/2} = m(2 - 3/\pi - 1/\sqrt{3}) + \log.\text{div.}, \quad (\text{E.22})$$

where the logarithmic UV divergence is canceled in the final answer by the counterterm in (E.5).

## Appendix E. Semiclassical ground state splitting

---

Analogously

$$b = \log \frac{1 - e^{-\frac{\sqrt{3}}{2}mL}}{(1 - e^{-mL})^2} + \int_0^\infty \frac{dp}{\pi} \delta_p \frac{d}{dp} \log(1 - e^{-(p^2+m^2)^{1/2}L}) = f(mL), \quad (\text{E.23})$$

$$f(x) = \log(1 - e^{-\frac{\sqrt{3}}{2}x}) - \frac{2}{\pi} \int_0^\infty dq \left( \frac{1}{1+q^2} + \frac{2}{1+4q^2} \right) \log(1 - e^{-(q^2+1)^{1/2}x}). \quad (\text{E.24})$$

The function  $f(x)$  tends to zero exponentially fast for  $x \gg 1$ , whereas for intermediate  $x$  it has to be computed numerically, see figure E.1.

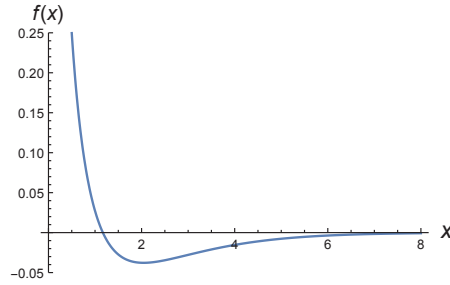


Figure E.1: The function  $f(x)$  defined in Eq. (E.24).

Gathering everything, the coefficient  $\kappa$  in (E.10) is given by (cf. [129], (3.27))

$$\kappa = \sqrt{\frac{m^3}{24\pi gL}} e^{-LM_{\text{kink}} - f(mL)}, \quad M_{\text{kink}} = \frac{m^3}{12g} + m \left( \frac{1}{4\sqrt{3}} - \frac{3}{2\pi} \right). \quad (\text{E.25})$$

Not surprisingly, the leading exponential dependence of this result is governed by the kink mass  $M_{\text{kink}}$  in the one-loop approximation, first computed in [120].

The one-instanton approximation for  $\mathcal{A}_-$  will break down for  $\tau_0$  so large that  $\kappa\tau_0 = O(1)$ . In this extreme  $\tau_0 \rightarrow \infty$  limit, both amplitudes  $\mathcal{A}_\pm$  receive contributions from multi-instanton configurations in the path integral, which are approximate solutions of the equation of motion. We can use the instanton-gas approximations, where the centers of the instantons are far apart, and resum all these contributions, to give

$$\mathcal{A}_+ = \mathcal{A}_0 \cosh \kappa\tau_0, \quad \mathcal{A}_- = \mathcal{A}_0 \sinh \kappa\tau_0. \quad (\text{E.26})$$

We did not consider the purely perturbative corrections to these amplitudes, as they are the same for the quasi-degenerate states and therefore do not interest us.

Taking the  $\tau_0 \rightarrow \infty$  limit in (E.26), one can infer the presence of two exchanged states split in energy by  $\Delta\mathcal{E} = 2\kappa$ , which is our final result.

# Bibliography

- [1] F. Baume, B. Keren-Zur, R. Rattazzi, and L. Vitale, “The local Callan-Symanzik equation: structure and applications,” *JHEP* **08** (2014) 152, [arXiv:1401.5983 \[hep-th\]](#).
- [2] A. Stergiou, D. Stone, and L. G. Vitale, “Constraints on Perturbative RG Flows in Six Dimensions,” *JHEP* **08** (2016) 010, [arXiv:1604.01782 \[hep-th\]](#).
- [3] S. Rychkov and L. G. Vitale, “Hamiltonian truncation study of the  $\phi^4$  theory in two dimensions,” *Phys. Rev.* **D91** no. 8, (2015) 085011, [arXiv:1412.3460 \[hep-th\]](#).
- [4] S. Rychkov and L. G. Vitale, “Hamiltonian truncation study of the  $\phi^4$  theory in two dimensions. II. The  $\mathbb{Z}_2$  -broken phase and the Chang duality,” *Phys. Rev.* **D93** no. 6, (2016) 065014, [arXiv:1512.00493 \[hep-th\]](#).
- [5] K. G. Wilson, “The Renormalization Group: Critical Phenomena and the Kondo Problem,” *Rev. Mod. Phys.* **47** (1975) 773.
- [6] J. L. Cardy, “Operator content and modular properties of higher dimensional conformal field theories,” *Nucl.Phys.* **B366** (1991) 403–419.
- [7] P. Di Francesco, P. Mathieu, and D. Senechal, *Conformal Field Theory*. Graduate Texts in Contemporary Physics. Springer-Verlag, New York, 1997.  
<http://www-spines.fnal.gov/spines/find/books/www?cl=QC174.52.C66D5::1997>.
- [8] K. G. Wilson, “Confinement of Quarks,” *Phys. Rev.* **D10** (1974) 2445–2459. [,45(1974)].
- [9] A. B. Zamolodchikov, “Irreversibility of the Flux of the Renormalization Group in a 2D Field Theory,” *JETP Lett.* **43** (1986) 730–732. [Pisma Zh. Eksp. Teor. Fiz.43,565(1986)].
- [10] Y. Nakayama, “Scale invariance vs conformal invariance,” *Phys. Rept.* **569** (2015) 1–93, [arXiv:1302.0884 \[hep-th\]](#).
- [11] S. El-Showk, M. F. Paulos, D. Poland, S. Rychkov, D. Simmons-Duffin, *et al.*, “Solving the 3D Ising Model with the Conformal Bootstrap,” [arXiv:1203.6064 \[hep-th\]](#).
- [12] S. El-Showk, M. F. Paulos, D. Poland, S. Rychkov, D. Simmons-Duffin, and A. Vichi, “Solving the 3d Ising Model with the Conformal Bootstrap II. c-Minimization and Precise Critical Exponents,” *J. Stat. Phys* (2014) , [arXiv:1403.4545 \[hep-th\]](#).

## Bibliography

---

- [13] F. Kos, D. Poland, D. Simmons-Duffin, and A. Vichi, “Precision Islands in the Ising and  $O(N)$  Models,” arXiv:1603.04436 [hep-th].
- [14] J. Polchinski, “Scale and Conformal Invariance in Quantum Field Theory,” *Nucl. Phys.* **B303** (1988) 226.
- [15] D. L. Jafferis, I. R. Klebanov, S. S. Pufu, and B. R. Safdi, “Towards the F-Theorem:  $N=2$  Field Theories on the Three-Sphere,” *JHEP* **06** (2011) 102, arXiv:1103.1181 [hep-th].
- [16] I. R. Klebanov, S. S. Pufu, and B. R. Safdi, “F-Theorem without Supersymmetry,” *JHEP* **10** (2011) 038, arXiv:1105.4598 [hep-th].
- [17] L. Fei, S. Giombi, I. R. Klebanov, and G. Tarnopolsky, “Generalized  $F$ -Theorem and the  $\epsilon$  Expansion,” *JHEP* **12** (2015) 155, arXiv:1507.01960 [hep-th].
- [18] H. Casini, M. Huerta, and R. C. Myers, “Towards a derivation of holographic entanglement entropy,” *JHEP* **05** (2011) 036, arXiv:1102.0440 [hep-th].
- [19] H. Casini and M. Huerta, “On the RG running of the entanglement entropy of a circle,” *Phys. Rev.* **D85** (2012) 125016, arXiv:1202.5650 [hep-th].
- [20] J. L. Cardy, “Is There a  $c$  Theorem in Four-Dimensions?,” *Phys. Lett.* **B215** (1988) 749–752.
- [21] M. J. Duff, “Twenty years of the Weyl anomaly,” *Class. Quant. Grav.* **11** (1994) 1387–1404, arXiv:hep-th/9308075 [hep-th].
- [22] D. J. Gross and F. Wilczek, “Ultraviolet Behavior of Nonabelian Gauge Theories,” *Phys. Rev. Lett.* **30** (1973) 1343–1346.
- [23] Z. Komargodski and A. Schwimmer, “On Renormalization Group Flows in Four Dimensions,” *JHEP* **1112** (2011) 099, arXiv:1107.3987 [hep-th].
- [24] G. 't Hooft, *Recent Developments in Gauge Theories*. Plenum Press, 1980.
- [25] M. A. Luty, J. Polchinski, and R. Rattazzi, “The  $a$ -theorem and the Asymptotics of 4D Quantum Field Theory,” *JHEP* **1301** (2013) 152, arXiv:1204.5221 [hep-th].
- [26] H. Osborn, “Weyl consistency conditions and a local renormalization group equation for general renormalizable field theories,” *Nucl. Phys.* **B363** (1991) 486–526.
- [27] J. Gasser and H. Leutwyler, “Chiral Perturbation Theory to One Loop,” *Annals Phys.* **158** (1984) 142.
- [28] N. Seiberg, “The Power of holomorphy: Exact results in 4-D SUSY field theories,” in *PASCOS '94: Proceedings, 4th International Symposium on Particles, Strings and Cosmology, Syracuse, New York, USA, May 19-24, 1994*. 1994. arXiv:hep-th/9408013 [hep-th].



- 
- [29] L. Girardello and M. T. Grisaru, “Soft Breaking of Supersymmetry,” *Nucl. Phys.* **B194** (1982) 65.
- [30] N. Arkani-Hamed and R. Rattazzi, “Exact results for nonholomorphic masses in softly broken supersymmetric gauge theories,” *Phys. Lett.* **B454** (1999) 290–296, [arXiv:hep-th/9804068](#) [hep-th].
- [31] H. Osborn, “Derivation of a Four-dimensional  $c$  Theorem,” *Phys. Lett.* **B222** (1989) 97.
- [32] I. Jack and H. Osborn, “Analogues for the  $c$  Theorem for Four-dimensional Renormalizable Field Theories,” *Nucl. Phys.* **B343** (1990) 647–688.
- [33] I. T. Drummond and G. M. Shore, “Conformal Anomalies for Interacting Scalar Fields in Curved Space-Time,” *Phys. Rev.* **D19** (1979) 1134.
- [34] D. M. Capper and M. J. Duff, “Trace anomalies in dimensional regularization,” *Nuovo Cim.* **A23** (1974) 173–183.
- [35] L. S. Brown and J. C. Collins, “Dimensional Renormalization of Scalar Field Theory in Curved Space-time,” *Annals Phys.* **130** (1980) 215.
- [36] S. J. Hathrell, “Trace Anomalies and  $\lambda\phi^4$  Theory in Curved Space,” *Annals Phys.* **139** (1982) 136.
- [37] D. J. Wallace and R. K. P. Zia, “Gradient Properties of the Renormalization Group Equations in Multicomponent Systems,” *Annals Phys.* **92** (1975) 142.
- [38] D. Anselmi, J. Erlich, D. Z. Freedman, and A. A. Johansen, “Positivity constraints on anomalies in supersymmetric gauge theories,” *Phys. Rev.* **D57** (1998) 7570–7588, [arXiv:hep-th/9711035](#) [hep-th].
- [39] Z. Komargodski, “The Constraints of Conformal Symmetry on RG Flows,” *JHEP* **07** (2012) 069, [arXiv:1112.4538](#) [hep-th].
- [40] J.-F. Fortin, B. Grinstein, and A. Stergiou, “Limit Cycles and Conformal Invariance,” *JHEP* **01** (2013) 184, [arXiv:1208.3674](#) [hep-th].
- [41] A. Dymarsky, Z. Komargodski, A. Schwimmer, and S. Theisen, “On Scale and Conformal Invariance in Four Dimensions,” *JHEP* **10** (2015) 171, [arXiv:1309.2921](#) [hep-th].
- [42] A. Dymarsky, K. Farnsworth, Z. Komargodski, M. A. Luty, and V. Prilepina, “Scale Invariance, Conformality, and Generalized Free Fields,” *JHEP* **02** (2016) 099, [arXiv:1402.6322](#) [hep-th].
- [43] A. A. Belavin and A. A. Migdal, “Calculation of anomalous dimensions in non-abelian gauge field theories,” *Pisma Zh. Eksp. Teor. Fiz.* **19** (1974) 317–320.
- [44] T. Banks and A. Zaks, “On the Phase Structure of Vector-Like Gauge Theories with Massless Fermions,” *Nucl. Phys.* **B196** (1982) 189.

## Bibliography

---

- [45] R. G. Leigh and M. J. Strassler, “Exactly marginal operators and duality in four-dimensional  $N=1$  supersymmetric gauge theory,” *Nucl. Phys.* **B447** (1995) 95–136, arXiv:hep-th/9503121 [hep-th].
- [46] B. Keren-Zur, “The local RG equation and chiral anomalies,” *JHEP* **09** (2014) 011, arXiv:1406.0869 [hep-th].
- [47] Y. Nakayama, “Vector Beta function,” *Int. J. Mod. Phys.* **A28** (2013) 1350166, arXiv:1310.0574 [hep-th].
- [48] Y. Nakayama, “Consistency of local renormalization group in  $d=3$ ,” *Nucl. Phys.* **B879** (2014) 37–64, arXiv:1307.8048 [hep-th].
- [49] A. A. Tseytlin, “Conformal Anomaly in Two-Dimensional Sigma Model on Curved Background and Strings,” *Phys. Lett.* **B178** (1986) 34.
- [50] S. Deser, M. J. Duff, and C. J. Isham, “Nonlocal Conformal Anomalies,” *Nucl. Phys.* **B111** (1976) 45.
- [51] J. Wess and B. Zumino, “Consequences of anomalous Ward identities,” *Phys. Lett.* **B37** (1971) 95.
- [52] S. Deser and A. Schwimmer, “Geometric classification of conformal anomalies in arbitrary dimensions,” *Phys. Lett.* **B309** (1993) 279–284, arXiv:hep-th/9302047 [hep-th].
- [53] H. Osborn and A. Stergiou, “Structures on the Conformal Manifold in Six Dimensional Theories,” *JHEP* **1504** (2015) 157, arXiv:1501.01308 [hep-th].
- [54] D. Z. Freedman, K. Johnson, and J. I. Latorre, “Differential regularization and renormalization: A New method of calculation in quantum field theory,” *Nucl. Phys.* **B371** (1992) 353–414.
- [55] I. Jack and H. Osborn, “Constraints on RG Flow for Four Dimensional Quantum Field Theories,” *Nucl. Phys.* **B883** (2014) 425–500, arXiv:1312.0428 [hep-th].
- [56] H. Osborn and A. C. Petkou, “Implications of conformal invariance in field theories for general dimensions,” *Annals Phys.* **231** (1994) 311–362, arXiv:hep-th/9307010 [hep-th].
- [57] A. Bzowski, P. McFadden, and K. Skenderis, “Implications of conformal invariance in momentum space,” *JHEP* **03** (2014) 111, arXiv:1304.7760 [hep-th].
- [58] H. Osborn. Private communication.
- [59] J. J. Heckman, D. R. Morrison, and C. Vafa, “On the Classification of 6D SCFTs and Generalized ADE Orbifolds,” *JHEP* **05** (2014) 028, arXiv:1312.5746 [hep-th]. [Erratum: JHEP06,017(2015)].

- 
- [60] J. J. Heckman, D. R. Morrison, T. Rudelius, and C. Vafa, “Atomic Classification of 6D SCFTs,” *Fortsch. Phys.* **63** (2015) 468–530, arXiv:1502.05405 [hep-th].
- [61] H. Osborn and A. Stergiou, “ $C_T$  for non-unitary CFTs in higher dimensions,” *JHEP* **06** (2016) 079, arXiv:1603.07307 [hep-th].
- [62] W. Nahm, “Supersymmetries and their Representations,” *Nucl. Phys.* **B135** (1978) 149.
- [63] H. Elvang, D. Z. Freedman, L.-Y. Hung, M. Kiermaier, R. C. Myers, *et al.*, “On renormalization group flows and the a-theorem in 6d,” *JHEP* **1210** (2012) 011, arXiv:1205.3994 [hep-th].
- [64] C. Cordova, T. T. Dumitrescu, and K. Intriligator, “Anomalies, Renormalization Group Flows, and the a-Theorem in Six-Dimensional (1,0) Theories,” arXiv:1506.03807 [hep-th].
- [65] B. Grinstein, A. Stergiou, D. Stone, and M. Zhong, “Two-loop renormalization of multiflavor  $\phi^3$  theory in six dimensions and the trace anomaly,” *Phys. Rev.* **D92** no. 4, (2015) 045013, arXiv:1504.05959 [hep-th].
- [66] B. Grinstein, D. Stone, A. Stergiou, and M. Zhong, “Challenge to the  $a$  Theorem in Six Dimensions,” *Phys. Rev. Lett.* **113** no. 23, (2014) 231602, arXiv:1406.3626 [hep-th].
- [67] S. Rajagopal, A. Stergiou, and Y. Zhu, “Holographic Trace Anomaly and Local Renormalization Group,” *JHEP* **11** (2015) 216, arXiv:1508.01210 [hep-th].
- [68] K. Kikuchi and T. Sakai, “AdS/CFT and local renormalization group with gauge fields,” arXiv:1511.00403 [hep-th].
- [69] R. Auzzi and B. Keren-Zur, “Superspace formulation of the local RG equation,” *JHEP* **05** (2015) 150, arXiv:1502.05962 [hep-th].
- [70] M. Gillioz, “The local renormalization of super-Yang-Mills theories,” arXiv:1602.03875 [hep-th].
- [71] B. Grinstein, A. Stergiou, and D. Stone, “Consequences of Weyl Consistency Conditions,” *JHEP* **1311** (2013) 195, arXiv:1308.1096 [hep-th].
- [72] L. Bonora, P. Pasti, and M. Bregola, “Weyl cocycles,” *Class.Quant.Grav.* **3** (1986) 635.
- [73] D. Lovelock, “The Einstein tensor and its generalizations,” *J.Math.Phys.* **12** (1971) 498–501.
- [74] J. A. Gracey, I. Jack, and C. Poole, “The a-function in six dimensions,” *JHEP* **01** (2016) 174, arXiv:1507.02174 [hep-th].
- [75] S. J. Brodsky, H.-C. Pauli, and S. S. Pinsky, “Quantum chromodynamics and other field theories on the light cone,” *Phys.Rept.* **301** (1998) 299–486, arXiv:hep-ph/9705477 [hep-ph].

## Bibliography

---

- [76] V. P. Yurov and Al. B. Zamolodchikov, “Truncated Conformal Space Approach to Scaling Lee-Yang Model,” *Int.J.Mod.Phys.* **A5** (1990) 3221–3246.
- [77] A. Coser, M. Beria, G. P. Brandino, R. M. Konik, and G. Mussardo, “Truncated Conformal Space Approach for 2D Landau-Ginzburg Theories,” *J. Stat. Mech.* **1412** (2014) P12010, [arXiv:1409.1494](#) [hep-th].
- [78] D. Lee, N. Salwen, and D. Lee, “The Diagonalization of quantum field Hamiltonians,” *Phys.Lett.* **B503** (2001) 223–235, [arXiv:hep-th/0002251](#) [hep-th].
- [79] D. Lee, N. Salwen, and M. Windolowski, “Introduction to stochastic error correction methods,” *Phys.Lett.* **B502** (2001) 329–337, [arXiv:hep-lat/0010039](#) [hep-lat].
- [80] N. Salwen, *Non-perturbative methods in modal field theory*. [arXiv:hep-lat/0212035](#) [hep-lat]. Ph.D. thesis, Harvard University, 2001.
- [81] M. Windolowski, *A Non-perturbative Study of Three-Dimensional Quartic Scalar Field Theory Using Modal Field Theory*. Ph.D. thesis, University of Massachusetts Amherst, 2000.
- [82] I. Brooks, E.D. and S. C. Frautschi, “Scalars Coupled to Fermions in (1+1)-dimensions,” *Z.Phys.* **C23** (1984) 263.
- [83] J. Elias-Miro, M. Montull, and M. Riemann, “The renormalized Hamiltonian truncation method in the large  $E_T$  expansion,” *JHEP* **04** (2016) 144, [arXiv:1512.05746](#) [hep-th].
- [84] Z. Bajnok and M. Lajer, “Truncated Hilbert space approach to the 2d  $\phi^4$  theory,” [arXiv:1512.06901](#) [hep-th].
- [85] E. Katz, G. M. Tavares, and Y. Xu, “Solving 2D QCD with an adjoint fermion analytically,” *JHEP* **1405** (2014) 143, [arXiv:1308.4980](#) [hep-th].
- [86] E. Katz, G. M. Tavares, and Y. Xu, “A solution of 2D QCD at Finite  $N$  using a conformal basis,” [arXiv:1405.6727](#) [hep-th].
- [87] S. Chabysheva and J. Hiller, “Basis of symmetric polynomials for many-boson light-front wave functions,” [arXiv:1409.6333](#) [hep-ph].
- [88] E. Katz, Z. U. Khandker, and M. T. Walters, “A Conformal Truncation Framework for Infinite-Volume Dynamics,” [arXiv:1604.01766](#) [hep-th].
- [89] P. Giokas and G. Watts, “The renormalisation group for the truncated conformal space approach on the cylinder,” [arXiv:1106.2448](#) [hep-th].
- [90] M. Lencses and G. Takacs, “Excited state TBA and renormalized TCSA in the scaling Potts model,” *JHEP* **09** (2014) 052, [arXiv:1405.3157](#) [hep-th].

- 
- [91] M. Hogervorst, S. Rychkov, and B. C. van Rees, “Truncated conformal space approach in  $d$  dimensions: A cheap alternative to lattice field theory?,” *Phys. Rev.* **D91** (2015) 025005, arXiv:1409.1581 [hep-th].
- [92] S.-J. Chang, “The Existence of a Second Order Phase Transition in the Two-Dimensional  $\phi^4$  Field Theory,” *Phys.Rev.* **D13** (1976) 2778.
- [93] S. R. Coleman, “The Quantum Sine-Gordon Equation as the Massive Thirring Model,” *Phys.Rev.* **D11** (1975) 2088.
- [94] M. Bordag, G. L. Klimchitskaya, U. Mohideen, and V. M. Mostepanenko, “Advances in the Casimir effect,” *Int. Ser. Monogr. Phys.* **145** (2009) 1–768.
- [95] A. Zamolodchikov, “Thermodynamic Bethe Ansatz in Relativistic Models. Scaling Three State Potts and Lee-Yang Models,” *Nucl.Phys.* **B342** (1990) 695–720.
- [96] M. Lüscher, “Volume Dependence of the Energy Spectrum in Massive Quantum Field Theories. 1. Stable Particle States,” *Commun.Math.Phys.* **104** (1986) 177.
- [97] J. Glimm and A. M. Jaffe, *Quantum Physics. A Functional Integral Point Of View*. Springer, 1987.
- [98] M. Lüscher, “Volume Dependence of the Energy Spectrum in Massive Quantum Field Theories. 2. Scattering States,” *Commun.Math.Phys.* **105** (1986) 153–188.
- [99] V. Yurov and Al. B. Zamolodchikov, “Truncated fermionic space approach to the critical 2-D Ising model with magnetic field,” *Int.J.Mod.Phys.* **A6** (1991) 4557–4578.
- [100] G. Brandino, R. Konik, and G. Mussardo, “Energy Level Distribution of Perturbed Conformal Field Theories,” *J.Stat.Mech.* **1007** (2010) P07013, arXiv:1004.4844 [cond-mat.stat-mech].
- [101] A. Harindranath and J. Vary, “Stability of the Vacuum in Scalar Field Models in  $1 + 1$  Dimensions,” *Phys.Rev.* **D37** (1988) 1076–1078.
- [102] T. Sugihara, “Density matrix renormalization group in a two-dimensional lambda  $\phi^4$  Hamiltonian lattice model,” *JHEP* **0405** (2004) 007, arXiv:hep-lat/0403008 [hep-lat].
- [103] D. Schaich and W. Loinaz, “An improved lattice measurement of the critical coupling in  $\phi_2^4$  theory,” *Phys.Rev.* **D79** (2009) 056008, arXiv:0902.0045 [hep-lat].
- [104] A. Milsted, J. Haegeman, and T. J. Osborne, “Matrix product states and variational methods applied to critical quantum field theory,” *Phys.Rev.* **D88** (2013) 085030, arXiv:1302.5582 [hep-lat].
- [105] A. Harindranath and J. Vary, “Solving Two-Dimensional  $\phi^4$  Theory By Discretized Light Front Quantization,” *Phys.Rev.* **D36** (1987) 1141–1147.

## Bibliography

---

- [106] B. van de Sande, “Convergence of discretized light cone quantization in the small mass limit,” *Phys.Rev.* **D54** (1996) 6347–6350, arXiv:hep-ph/9605409 [hep-ph].
- [107] M. Burkardt, S. S. Chabysheva, and J. R. Hiller, “Two-dimensional light-front  $\phi^4$  theory in a symmetric polynomial basis,” arXiv:1607.00026 [hep-th].
- [108] R. M. Konik and Y. Adamov, “Numerical renormalization group for continuum one-dimensional systems,” *Phys. Rev. Lett.* **98** (2007) 147205, arXiv:cond-mat/0701605 [cond-mat.str-el].
- [109] S. R. White, “Density-matrix algorithms for quantum renormalization groups,” *Phys. Rev. B* **48** (1993) 10345.
- [110] W. Loinaz and R. Willey, “Monte Carlo simulation calculation of critical coupling constant for continuum  $\phi^4$  in two-dimensions,” *Phys.Rev.* **D58** (1998) 076003, arXiv:hep-lat/9712008 [hep-lat].
- [111] I. Z. Rothstein, “TASI lectures on effective field theories,” arXiv:hep-ph/0308266 [hep-ph].
- [112] K. Symanzik, “Continuum Limit and Improved Action in Lattice Theories. 1. Principles and  $\phi^4$  Theory,” *Nucl.Phys.* **B226** (1983) 187.
- [113] U. Schollwöck, “The density-matrix renormalization group in the age of matrix product states,” *Annals of Physics* **326** (2011) 96.
- [114] B. Simon, *The  $P(\phi)_2$  Euclidean (Quantum) Field Theory*. 1974.
- [115] C. Wozar and A. Wipf, “Supersymmetry Breaking in Low Dimensional Models,” *Annals Phys.* **327** (2012) 774–807, arXiv:1107.3324 [hep-lat].
- [116] P. Bosetti, B. De Palma, and M. Guagnelli, “Monte Carlo determination of the critical coupling in  $\phi_2^4$  theory,” *Phys. Rev.* **D92** no. 3, (2015) 034509, arXiv:1506.08587 [hep-lat].
- [117] A. Pelissetto and E. Vicari, “Critical mass renormalization in renormalized  $\phi^4$  theories in two and three dimensions,” *Phys. Lett.* **B751** (2015) 532–534, arXiv:1508.00989 [hep-th].
- [118] M. Caselle, M. Hasenbusch, P. Provero, and K. Zarembo, “Bound states in the three-dimensional  $\phi^4$  model,” *Phys.Rev.* **D62** (2000) 017901, arXiv:hep-th/0001181 [hep-th].
- [119] G. Delfino, G. Mussardo, and P. Simonetti, “Nonintegrable quantum field theories as perturbations of certain integrable models,” *Nucl. Phys.* **B473** (1996) 469–508, arXiv:hep-th/9603011 [hep-th].
- [120] R. F. Dashen, B. Hasslacher, and A. Neveu, “Nonperturbative Methods and Extended Hadron Models in Field Theory. 2. Two-Dimensional Models and Extended Hadrons,” *Phys. Rev.* **D10** (1974) 4130–4138.

- 
- [121] Z. Bajnok, L. Palla, G. Takács, and F. Wagner, “Nonperturbative study of the two frequency sine-Gordon model,” *Nucl.Phys.* **B601** (2001) 503–538, arXiv:hep-th/0008066 [hep-th].
- [122] P. Fonseca and A. Zamolodchikov, “Ising spectroscopy. I. Mesons at  $T < T_c$ ,” arXiv:hep-th/0612304 [hep-th].
- [123] J.-S. Caux and R. M. Konik, “Constructing the generalized Gibbs ensemble after a quantum quench,” *Phys. Rev. Lett.* **109** (2012) 175301, arXiv:1203.0901 [cond-mat.quant-gas].
- [124] G. P. Brandino, J.-S. Caux, and R. M. Konik, “Glimmers of a Quantum KAM Theorem: Insights from Quantum Quenches in One Dimensional Bose Gases,” arXiv:1407.7167 [cond-mat.str-el].
- [125] R. M. Konik, T. Pálmai, G. Takács, and A. M. Tsvetik, “Studying the perturbed Wess-Zumino-Novikov-Witten  $SU(2)_k$  theory using the truncated conformal spectrum approach,” *Nucl. Phys.* **B899** (2015) 547–569, arXiv:1505.03860 [cond-mat.str-el].
- [126] L. Lepori, G. Z. Toth, and G. Delfino, “Particle spectrum of the 3-state Potts field theory: A Numerical study,” *J. Stat. Mech.* **0911** (2009) P11007, arXiv:0909.2192 [hep-th].
- [127] M. Lencsés and G. Takács, “Confinement in the  $q$ -state Potts model: an RG-TCSA study,” *JHEP* **09** (2015) 146, arXiv:1506.06477 [hep-th].
- [128] A. I. Vainshtein, V. I. Zakharov, V. A. Novikov, and M. A. Shifman, “ABC of Instantons,” *Sov. Phys. Usp.* **25** (1982) 195. [Usp. Fiz. Nauk 136, 553 (1982)].
- [129] H. Osborn, “Partition Function For Two-Dimensional Solitons,” *Nucl. Phys.* **B143** (1978) 327.
- [130] P. M. Morse and H. Feshbach, *Methods of Theoretical Physics*. McGraw-Hill, New York, 1953. part II, ch.12, p.1651.

# Lorenzo Vitale – Curriculum vitae

---

<b>Address</b>	Route de la Maladière 28, Chavannes-pres-Renens, CH-1022	<b>Mobile Phone</b>	+41 76 720 1210
<b>Date of Birth</b>	16 <sup>th</sup> February 1989	<b>Email</b>	lorenzovitale89@gmail.com
<b>Nationality</b>	Italian		

## Education

**2012-2016** Ph.D. in Theoretical particle physics, EPFL, Switzerland

*Thesis title* Perturbative and non-perturbative aspects of RG flows  
in quantum field theory

*Supervisor* Prof. Riccardo Rattazzi

*Co-supervisor* Prof. Vyacheslav Rychkov

**2012-2016** Visiting scientist at CERN

**2010-2012** M.Sc. in theoretical physics at University of Padova

*Thesis title* Discrete symmetries and mixing angles for neutrinos

*Final grade* 110/110 with honors

*Supervisor* Prof. Ferruccio Feruglio

*Co-supervisor* Dr. Claudia Hagedorn

**2007-2010** B.Sc. in physics at University of Bari

*Final grade* 110/110 with honors

## Invited presentations

**01/12/15** Johannes Gutenberg-Universität, Mainz, theoretical physics seminar

**09/03/15** Universitat de Barcelona, theoretical physics seminar

**06/03/15** IFAE, UAB, Barcelona, theoretical physics seminar

**23/12/13** Bari Theory Xmas Workshop 2013, Italy

## Schools and workshops attended

**30/05/16-10/06/16**

*Conformal Field Theories and Renormalization Group Flows in Dimensions  $d > 2$ ,*  
Galileo Institute for Theoretical Physics, Florence

**07/02/16-13/02/16**

*Lectures on Statistical Field Theories,*  
Galileo Institute for Theoretical Physics, Florence



**01/06/15-26/06/15**

*New Frontiers in Fields and Strings* TASI summer school, Boulder, Colorado

**30/06/14-11/07/14**

*Back to the Bootstrap IV* workshop, Porto

**02/06/14-14/06/14**

*String theory and holography*, Cargese Summer School

**07/01/2014-24/01/14**

*GGI lectures on the theory of fundamental interactions*,  
Galileo Institute for Theoretical Physics, Florence

**02/09/13-13/09/13**

*Foundations and New Methods in Theoretical Physics*,  
“Saalburg” Summer School for Graduate Students

**02/04/13-06/04/13**

*Introduction to string theory*, String Steilkurs - Part I, DESY, Hamburg

**07/01/13-09/01/13**

*Particle Physics in the LHC era*, Zurich Phenomenology Workshop

## Publications

- A. Stergiou, D. Stone, and L. G. Vitale, “Constraints on Perturbative RG Flows in Six Dimensions,” [arXiv:1604.01782](#) [[hep-th](#)]
- S. Rychkov and L. G. Vitale, “Hamiltonian truncation study of the  $\phi^4$  theory in two dimensions. II. The  $Z_2$ -broken phase and the Chang duality,” *Phys. Rev.* **D93** no. 6, (2016) 065014, [arXiv:1512.00493](#) [[hep-th](#)]
- S. Rychkov and L. G. Vitale, “Hamiltonian truncation study of the  $\phi^4$  theory in two dimensions,” *Phys. Rev.* **D91** no. 8, (2015) 085011, [arXiv:1412.3460](#) [[hep-th](#)]
- F. Baume, B. Keren-Zur, R. Rattazzi, and L. Vitale, “The local Callan-Symanzik equation: structure and applications,” *JHEP* **1408** (2014) 152, [arXiv:1401.5983](#) [[hep-th](#)]
- F. Coradeschi, P. Lodone, D. Pappadopulo, R. Rattazzi, and L. Vitale, “A naturally light dilaton,” *JHEP* **1311** (2013) 057, [arXiv:1306.4601](#) [[hep-th](#)]
- C. Hagedorn, A. Meroni, and L. Vitale, “Mixing patterns from the groups  $\Sigma(n\phi)$ ,” *J.Phys.* **A47** (2014) 055201, [arXiv:1307.5308](#) [[hep-ph](#)]

## Teaching activities

Teaching assistant at EPFL for the duration of six semesters, for the Bachelor and Master courses of *Champs quantiques relativistes I, II* and *Electrodynamique*

## Software Skills

- **Programming Languages**

*Python*

*C, C++*

*Mathematica*

*Mathlab*

- **Miscellaneous**

*Scipy, matplotlib*

*Linux, shell scripting*

*Vim, git*

*Latex*

## Languages

- **Italian** - Native or bilingual proficiency
- **English** - Full professional proficiency
- **French** - Limited working proficiency

